The Tangihua complex, New Zealand : implications for cretaceous - oligocène convergent margin processes in the Sw Pacific from comparison with the Poya terrane, new Caledonia

Kirsten Nicholson

▶ **To cite this version:**

Kirsten Nicholson. The Tangihua complex, New Zealand : implications for cretaceous - oligocène convergent margin processes in the Sw Pacific from comparison with the Poya terrane, new Caledonia. Petrography. Université Joseph-Fourier - Grenoble I, 1999. English. NNT : . tel-00760055

HAL Id: tel-00760055

https://theses.hal.science/tel-00760055

Submitted on 3 Dec 2012

HAL is a multi-disciplinary open access archive for the deposit and dissemination of scientific research documents, whether they are published or not. The documents may come from teaching and research institutions in France or abroad, or from public or private research centers.

L'archive ouverte pluridisciplinaire **HAL**, est destinée au dépôt et à la diffusion de documents scientifiques de niveau recherche, publiés ou non, émanant des établissements d'enseignement et de recherche français ou étrangers, des laboratoires publics ou privés.

TS 99/GRE1/0266/D
double
558

UNIVERSITE JOSEPH FOURIER - GRENOBLE 1
SCIENCES - GEOGRAPHIE

B.U.S. GRENOBLE
D 052 137431 5

THESE

pour obtenir le grade de

DOCTEUR DE L'UNIVERSITE JOSEPH FOURIER

En Co-Tutelle avec l'Université d'Auckland - Nouvelle Zélande

Discipline : Sciences de la Terre

Présentée et soutenue publiquement

par

NICHOLSON, Kirsten Ngaire
le 10 décembre 1999

THE TANGIHUA COMPLEX, NEW ZEALAND :
IMPLICATIONS FOR CRETACEOUS - OLIGOCENE CONVERGENT MARGIN PROCESSES IN THE SW PACIFIC FROM COMPARISON WITH THE POYA TERRANE, NEW CALEDONIA.

LE COMPLEXE DE TANGIHUA, NOUVELLE ZELANDE ET SES RELATIONS AVEC L'UNITE DE POYA, NOUVELLE CALEDONIE :
IMPLICATIONS SUR LES PROCESSUS DE CONVERGENCE AU CRETACE-OLIGOCENE DANS LE PACIFIQUE SW.

BIBLIOTHÈQUE SCIENCES GRENOBLE UNIVERSITAIRE

Directeurs de thèse :

M. P.M. BLACK, Professeur, University of Auckland, New Zealand
M. C. PICARD, Professeur Université de Nouvelle Calédonie, Chercheur LGCA - Grenoble

COMPOSITION DU JURY

M. Jean MASCLE	Directeur de Recherche CNRS, UMR Géosciences Azur, Nice	Président
M. John GAMBLE	Professeur, Victoria University, Wellington, NZ	Rapporteur
M. Philippa BLACK	Professeur, University of Auckland, N.Z	Directeur de Thèse
M. Christian PICARD	Professeur, LGCA, Grenoble, Université N. Calédonie	Directeur de Thèse

Invités

M. Dominique Cluzel, Professeur, UMR 6530, Université d'Orléans
M. Henriette Lapierre, Professeur, LGCA - Université Joseph Fourier, Grenoble
M. Arnaud Pêcher, Professeur, LGCA, Université Josph Fourier, Grenoble

TS 99/GRE1/0266
DOUBLE

UNIVERSITE JOSEPH FOURIER - GRENOBLE 1
SCIENCES - GEOGRAPHIE

THESE

pour obtenir le grade de

DOCTEUR DE L'UNIVERSITE JOSEPH FOURIER

En Co-Tutelle avec l'Université d'Auckland - Nouvelle Zélande

Discipline : Sciences de la Terre

Présentée et soutenue publiquement

par

NICHOLSON, Kirsten Ngaire
le 10 décembre 1999

THE TANGIHUA COMPLEX, NEW ZEALAND : IMPLICATIONS FOR CRETACEOUS - OLIGOCENE CONVERGENT MARGIN PROCESSES IN THE SW PACIFIC FROM COMPARISON WITH THE POYA TERRANE, NEW CALEDONIA.

LE COMPLEXE DE TANGIHUA, NOUVELLE ZELANDE ET SES RELATIONS AVEC L'UNITE DE POYA, NOUVELLE CALEDONIE : IMPLICATIONS SUR LES PROCESSUS DE CONVERGENCE AU CRETACE-OLIGOCENE DANS LE PACIFIQUE SW.

BIBLIOTHÈQUE SCIENCES GRENOBLE UNIVERSITAIRE

Directeurs de thèse :

M. P.M. BLACK, Professeur, University of Auckland, New Zealand
M. C. PICARD, Professeur Université de Nouvelle Calédonie, Chercheur LGCA - Grenoble

COMPOSITION DU JURY

M. Jean MASCLE	Directeur de Recherche CNRS, UMR Géosciences Azur, Nice	Président
M. John GAMBLE	Professeur, Victoria University, Wellington, NZ	Rapporteur
M. Philippa BLACK	Professeur, University of Auckland, N.Z	Directeur de Thèse
M. Christian PICARD	Professeur, LGCA, Grenoble, Université N. Calédonie	Directeur de Thèse

Invités

M. Dominique Cluzel, Professeur, UMR 6530, Université d'Orléans
M. Henriette Lapierre, Professeur, LGCA - Université Joseph Fourier, Grenoble
M. Arnaud Pêcher, Professeur, LGCA, Université Josph Fourier, Grenoble

102 146 84

ABSTRACT

New major oxide, trace element and isotopic analyses of basaltic lavas from the Tangihua Complex, Northland, New Zealand, have led to the development of a new model explaining the generation of the Tangihua Complex ophiolite and a new interpretation of the tectonic setting of New Zealand during the Cretaceous. New $^{40}Ar/^{39}Ar$ dates from the Tangihua Complex confirm their age of formation is most likley ±100Ma and they have suffered a major episode of alteration at ±30Ma, which most likely corresponds to the age of emplacement of the Northland Allochthon.

The Tangihua Complex basalts are relatively homogeneous, differentiated (Mg#<45) and dominantly tholeiitic with lesser calc-alkaline and minor alkaline affinities. The primary phenocryst assemblage is dominated by plagioclase (An_{66-87}) with lesser amounts of clinopyroxene ($En_{31-52}Fs_{10-33}Wo_{28-45}$; Mg# ≈ 61), orthopyroxene and magnetite whereas olivine, biotite and hornblende are rare. Unusually, the lavas reveal a continuum between arc and back-arc chemistries, with a depletion of Nb and HFSE suggesting derivation from a depleted mantle source. Geochemical modelling shows the back-arc lavas have undergone ≈ 35% fractional crystallisation of a source depleted by ≈ 2-3% and the arc lavas have undergone ≈ 30% fractional crystallisation of a source depleted by less than 5%. High LILE/HFSE and LILE/LREE ratios suggest LILE enrichment by a slab-related aqueous fluid and possibly small amounts of a slab-derived silicic melt.

The pervasive, low-temperature alteration assemblage can be divided into three main phases based primarily on temperature but also influenced by the water/rock ratios: an initial phase of Na-rich zeolite precipitation, followed by a transitional cooling phase, characterised by K-, Na- and Ca-rich zeolites, and finally, at <50°C, a period of K- and Ca-dominated alteration. The alteration patterns in the Tangihua Complex suggests that little or no tectonic activity occurred between formation and obduction, enabling a classic seafloor alteration sequence to develop.

The trace element contents and $^{87}Sr/^{86}Sr$ and $^{143}Nd/^{144}Nd$ ratios of the Tangihua Complex are typical of arc and back-arc systems found within the SW Pacific. The Poya terrane ophiolite of New Caledonia is the geographically closest ophiolite complex of a similar age to the Tangihua Complex but despite many similarities between the systems, close inspection of the alteration and geochemistry show that the systems are unrelated.

The combined geochemistry and tectonic constraints suggest that the Tangihua Complex formed either in a transitional zone between an arc and a back-arc setting, or in a zone of migration from arc to back-arc volcanism. The end of the Late Cretaceous, and the break-up of the eastern and southern Gondwana margin, saw the approach and incipient collision of the spreading ridge between the Phoenix and Pacific plates. Initially subducted, the small, buoyant, Phoenix plate was captured by the Pacific plate, which led to the initiation of rifting between the newly formed Phoenix-Pacific plate and West Antarctica. Stalling of the Phoenix-Pacific ridge and associated subduction system, in combination with the initiation of rifting in the Tasman Sea, resulted in the partial subduction and dehydration of portions of the Phoenix Plate, which then reacted with the previously depleted mantle wedge. Remnants of the ensuing volcanism include the obducted Tangihua Complex of Northland, New Zealand.

RESUME

Le complexe de Tangihua, Nouvelle Zélande et ses relations avec l'unité de Poya, Nouvelle Calédonie: Implications sur les processus de convergence au Crétacé-Oligocène dans le Pacifique SW. De nouvelles données analytiques en éléments majeurs, en éléments traces et en isotopes des laves basaltiques du Complexe de Tangihua (Nouvelle Zélande) sont présentées afin de développer un nouveau modèle sur la genèse de ce complexe ophiolitique et une nouvelle interprétation de l'évolution tectonique de la Nouvelle Zélande au cours du Crétacé. De nouvelles datations par la méthode 40Ar/39Ar ont confirmé l'âge de formation de l'ophiolite vers 100 Ma et révélé un épisode majeur d'altération vers 30 Ma, qui probablement correspond à l'âge de mise en place de l'allochtone du Northland.

L'essentiel du complexe de Tangihua est constitué par des formations volcaniques relativement homogènes et évoluées (Mg#<45) d'affinité le plus souvent tholéiitique, parfois calco-alcaline et çà et là alcaline. Le plagioclase (An_{66-87}) est le minéral primaire le plus fréquent avec en moindre quantité des phénocristaux de clinopyroxène (En_{31-52} Fs10-33 Wo_{28-45}, Mg# = 61), d'orthopyroxène et de magnétite, alors que l'olivine, la biotite et la hornblende sont rares. Les laves montrent un continuum entre des affinités d'arc et d'arrière-arc, marquées par des teneurs déprimées en Nb et éléments HFS suggérant qu'elles proviennent d'une partie appauvrie du manteau. Les modélisations montrent que les laves arrière-arc résultent d'une source déprimée et de liquides ayant subit au moins 35% de cristallisation fractionnée, tandis que les laves d'arc résulteraient d'une source davantage déprimée et de liquides ayant subit au moins 30% cristallisation fractionnée. Les rapports élevés LILE/HFSE, et LILE/REE suggèrent un enrichissement en LILE par un fluide acqueux lié à la croûte subductée et peut être aussi à des matériaux siliceux partiellement fondus.
Les assemblages minéralogiques issus des altérations de basse température correspondent à trois phases principales en fonction des températures et du rapport eau/roche : une phase initiale marquée par la précipitation de zéolites sodiques, une phase transitoire riche en zéolites potasiques, sodiques et calciques, et finalement une phase de très basse température (T<50°C) essentiellement potassique et calcique. Les schémas d'altération dans le complexe de Tangihua suggèrent qu'entre la formation de l'ophiolite et son obduction, l'activité tectonique était faible ou inexistante, ce qui a permis le développement de l'altération océanique.

Les teneurs en éléments traces et les rapports isotopiques $^{87}Sr/^{86}Sr$ et $^{143}Nd/^{144}Nd$ du complexe de Tangihua sont typiques des systèmes d'arcs et d'arrière-arcs rencontrés dans le Pacifique SW. En Nouvelle Calédonie, l'Unité de Poya qui a longtemps été considérée comme de même origine (mêmes caractéristiques lithologiques, même âge de formation 80-85 Ma) est en réalité différente du point de vue géochimique révélant une histoire tectonique non identique pour ces deux complexes.

La combinaison des contraintes géochimiques et tectoniques suggèrent que le complexe de Tangihua s'est formé soit dans une zone transitionnelle arc - bassin arrière-arc, soit dans une zone de passage entre un volcanisme d'arc
et un volcanisme arrière arc. La fin du Crétacé-supérieur, marqué par la fragmentation des marges Est et Sud du Gondwana, a vu le rapprochement et la collision naissante de la dorsale en expansion entre les plaques de Phoenix et du Pacifique. La plaque de Phoenix, petite, légère et ayant à l'origine subi une subduction, a été capturée par la plaque Pacifique, initiant ainsi le rifting entre la plaque Phoenix-Pacifique nouvellement formée, et celle de l'Antarctique W. La mise en place de la dorsale Phoenix-Pacifique et du système de subduction associé, conjugués à l'initiation du rifting dans la mer de Tasman, ont eu pour effet la subduction et la déshydratation partielles de portions de la plaque de Phoenix, qui alors ont réagi avec le coin mantellique précédemment déprimé. Le complexe de Tangihua est une des conséquences de tels processus.

Acknowledgements

This thesis would not have been possible without the love and support of my family and friends. I would especially like to thank Charlotte, Jeff, Natalie and Philippa. Without them I would never have finished what I started.

The Department of Conservation and Muriwhenua Incorperation both provided field advice and access to land.

My research has been supported by the University of Auckland: University of Auckland Doctoral Scholarship, University of Auckland Graduate Research Fund and the R.N. Brothers Memorial Award (Geology), by a French Embassy Research Grant, Wellington, NZ, by a French Government Scholarship, by the Université Joseph Fourier and by the University of New Caledonia.

Merci pour tout.

TABLE OF CONTENTS

LIST OF FIGURES

CHAPTER ONE

CHAPTER TWO

CHAPTER THREE

CHAPTER FOUR

CHAPTER FIVE

CHAPTER SIX

CHAPTER SEVEN

LIST OF TABLES

CHAPTER TWO

CHAPTER THREE

CHAPTER FOUR

CHAPTER FIVE

CHAPTER ONE: INTRODUCTION

SECTION 1.1

Introduction

The most significant contribution to the volume of continental crust since the Archean has been the accretion of island arcs and associated sediments along convergent plate boundaries but an analogous cross-section of island arc crust has only recently been widely accepted (Conrad and Kay, 1984). Scientists agree that ophiolites are obducted fragments of the oceanic lithosphere, which includes hotspot chains, leaky fracture zones, back-arc basins and island arcs (Stern *et al.*, 1989), along with crust and upper most mantle generated at mid-ocean ridge spreading centres.

Our knowledge about igneous processes, related to the magmatism generated at divergent and convergent plate boundaries, is fundamental to an understanding of crustal growth. With the Benioff Zone dipping beneath it and the production of primarily mafic to intermediate magmas, the upper lithospheric crust produced at convergent margins is especially well suited to be preserved as an ophiolite. This warm, moderately low density, crust is exceptionally buoyant. As it enters the subduction zone it clogs the system causing plate convergence to stop. The arc material on top will then be in an excellent position to be preserved by obduction. In contrast, old denser crust on the subducting plate is in a tectonic setting that invariably places this material on the downgoing slab, and therefore it is unlikely to be preserved by obduction (Stern *et al.*, 1989).

Ophiolites are now more commonly being interpreted as fragments of island arc or back-arc basin crust. The involvement of subduction related processes is fundamental during the formation of these ophiolitic complexes, that are better known today as suprasubduction zone (SSZ) ophiolites (Pearce *et al.*, 1984). Consideration of trace element variations in tandem with other lines of geologic evidence has permitted more confident identification of SSZ ophiolites as forming in either a back-arc or island arc environment (Pearce *et al.*, 1984; Taylor and Nesbitt, 1988; Shervias, 1990; Jones *et al.*, 1991; Hawkins and Florendo, 1992). Other geochemical studies of ophiolites have revealed the presence of volcanic and hypabyssal rock suites exhibiting a combination of both mid-ocean ridge basalt and island arc tholeiite affinities (e.g. Alabaster *et al.*, 1982; Coleman, 1984; Shervias and Kimbrough, 1985; Ishiwatari *et al.*, 1990, Pedersen and Furnes, 1991).

Magmatic arcs (Figure 1.1.1), which develop above subduction zones, evolve in tensional tectonic settings because trenches tend to retreat oceanwards as the subducting lithosphere sinks into the mantle (Monlar and Atwater, 1978; Hamilton, 1979; Seno and Maruyama, 1984). In many cases, extension ultimately results in the arc splitting along its axis and the formation of a back-arc basin (Knittel and Oles, 1995). If this portion of the oceanic lithosphere is preserved as an ophiolite then subsequent geochemical analyses will reveal two distinctly different chemical affinities.

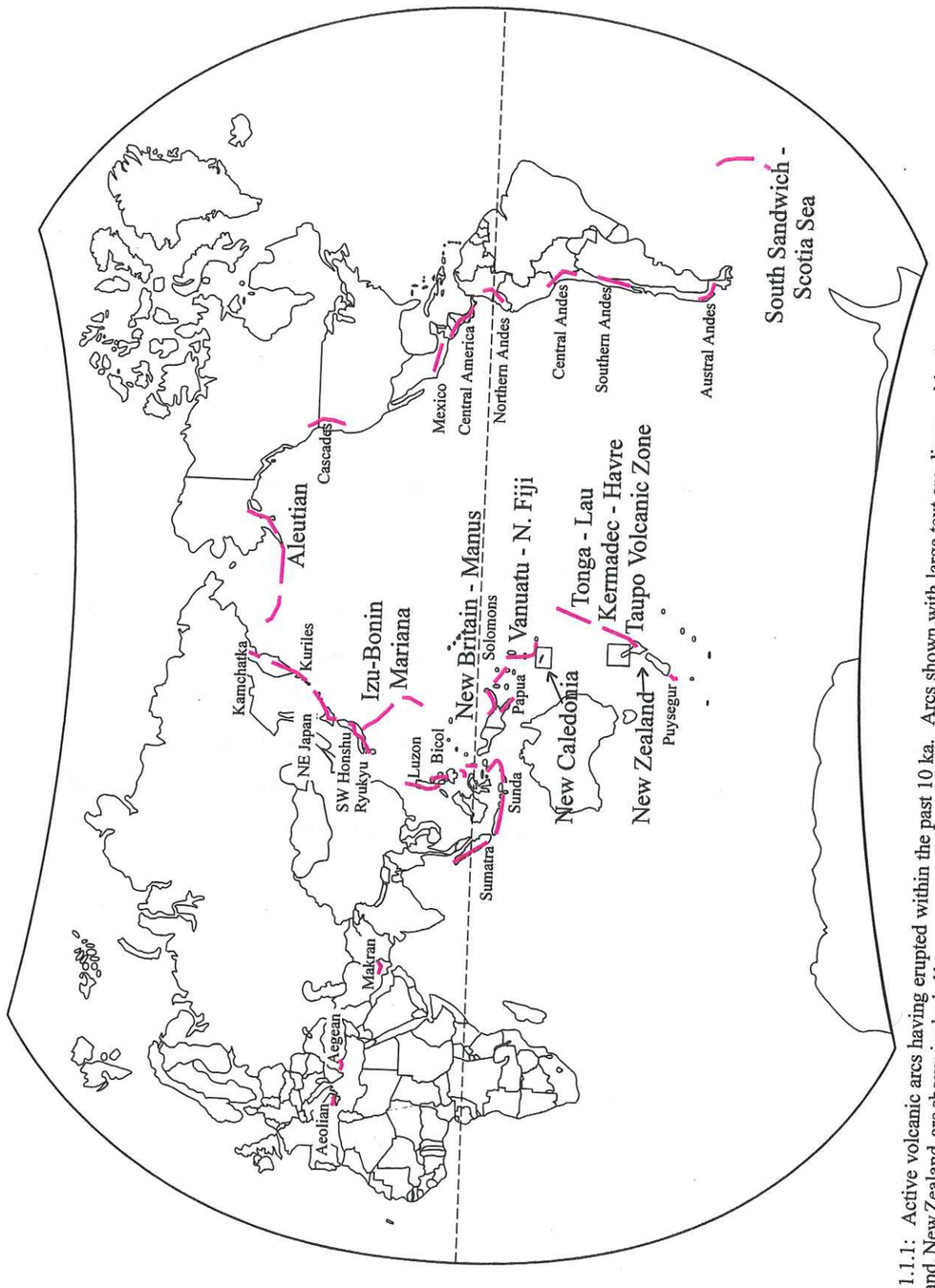

Figure 1.1.1: Active volcanic arcs having erupted within the past 10 ka. Arcs shown with large text are discussed in the text (specifically in Chapter 7). New Caledonia and Northland, New Zealand, are shown in shaded boxes.

Volcanic arc magmas are characterised by enrichment in LILE and depletion of HFSE relative to MORB (e.g. Pearce, 1983) whereas back-arc basin (BAB) basalts have HFSE abundances similar to MORB and show only moderate LILE enrichment. The varying geochemistry of these rock suites can be attributed to differing degrees of interaction with subduction-related fluids. However, other differences may be attributed to evolving mantle sources, different degrees of partial melting, crystallisation or other processes operative during magma generation, ascent and extrusion (Arculus, 1987; Furnes *et al.*, 1992, Taylor *et al.*, 1992). Woodhead *et al.* (1993) interpreted the HFSE systematics of island arc basalts (IAB) and BAB to indicate that the BAB are derived from sources similar to MORB whereas IAB are derived from more depleted sources. McCulloch and Gamble (1991) suggested that the depletion in the IAB sources might be due to the withdrawal of the BAB lavas.

In recent years, the formation of several ophiolite complexes have been re-examined and re-evaluated. The results of these studies show that while some fragmented ophiolites may have petrologic and geochemical signatures similar to crust generated at MORs, most do not (Alt *et al.*, 1998). Perhaps the most outstanding example of such re-interpretation is that of the Troodos Ophiolite. This was originally considered to be a fragment of typical oceanic crust produced at a mid-ocean ridge spreading center (Moores and Vine, 1971; Gass and Smewing, 1973), but has since been convincingly re-interpreted as a SSZ ophiolites (McCulloch and Cameron, 1983; Rautenschlein *et al.*, 1985). Many other ophiolites are being interpreted for the first time or being re-interpreted as SSZ ophiolites. Other ophiolites, which have been re-evaluated include the large, relatively intact Tethyan Semail ophiolite in Oman and relatively large and well-studied ophiolites in California and Newfoundland. These formed in suprasubduction settings, as evidenced by trace element compositions of the rocks and the presence of boninites (high-Mg, low-Ti andesites) and differentiated calc-alkaline rocks and basalts, rather than MOR tholeiites (Pearce *et al.*, 1984; Rautenschlein *et al.*, 1985; Harper *et al.*, 1988; Schiffman *et al.*, 1991; Bloomer *et al.*, 1994).

The SW Pacific has been a dynamic zone of tectonic activity since the end of the Palaeozoic, involving the margins of the Pacific, Phoenix and Indian-Australian Plates (Aitchison *et al.*, 1995). During the time frame, Late Cretaceous to recent, the entire region was characterised by the successive openings of marginal basins that isolated ridges of a continental, oceanic or intermediate nature. Consequently ophiolitic rocks occur throughout the SW Pacific region. Two such ophiolites are the Tangihua Ophiolitic Complex of New Zealand and the Poya terrane ophiolite of New Caledonia. These ophiolites formed during the late Cretaceous on the SW Pacific rim and were emplaced during the lower Tertiary onto a variably thinned continental crust of Palaeocene - Palaeozoic age. However, due to the complex nature of this region our understanding of the tectonic evolution of the SW Pacific between the Cretaceous and the Miocene is incomplete.

The resolution of the paleotectonic environment of ophiolite formation can be extremely difficult, but the development of regional tectonic and obduction models depends on the nature of the ophiolite; i.e. whether the ophiolite represents marginal basin crust or a fragment of a crust from a major oceanic spreading centre. This, the most recent study of the Tangihua Ophiolite in Northland, New Zealand, is a comprehensive compilation of new analyses and previous work. In the past studies have concentrated on structural aspects (i.e. Spörli and Aita, 1994), paleontological features (i.e. Hayward *et al.*, 1989) and/or cumulate and intrusive petrology (Hopper and Smith, 1996; Thompson *et al.*, 1997). In recent years the idea that the Northland ophiolites were influenced by suprasubduction processes has come to the fore (Malpas *et al.*, 1992; Hopper and Smith, 1996; Thompson *et al.*, 1997). Each individual piece of research, although not conclusive, has suggested magma generation at or near a back-arc environment. The development of a definitive model for the formation of the Tangihua Complex has been hindered by its wide variety of rock types, low-grade but pervasive alteration, and relatively limited exposures. By concentrating on the geochemistry of the basaltic rocks within the Tangihua Complex, this study is able to characterise the most primitive magmas within the complex and hence has yielded a better understanding of the formation of these magmas. The following Chapters have then combined the geochemical results with petrographic analyses to generate a new, more comprehensive model for the formation and emplacement of the Tangihua ophiolite, which conforms to the tectonic and chronological constraints.

SECTION 1.2

Background: The Tangihua Complex

The ophiolitic igneous complexes in the northern regions of the North Island of New Zealand are collectively called the Tangihua Complex and informally known as the Northland Ophiolite (Figure 1.2.1). The complex is part of the Northland Allochthon, which was emplaced, as a series of thrust sheets from the NE, over a very short time period in the late Oligocene (Ballance and Spörli, 1979; Brook *et al.*, 1988; Malpas *et al.*, 1992; Hopper and Smith, 1996; Brothers and Delaloye, 1982; Brothers, 1983; Spörli, 1989; Malpas *et al.*, 1992).

The massifs occur as 25 structurally discrete, rootless, bodies, which range in area from a few square meters to high standing massifs of up to 900 km^2, and extend for at least 50 km NW along the Reinga Ridge (Mortimer *et al.*, 1998; Quennell and Hay, 1964; Cassidy and Locke, 1987; Sharpe *et al.*, 1989). Geophysical data indicates a maximum depth to the metagreywacke basement of 4 to 5 km (Woodward, 1970; Stern *et al.*, 1987). In general the complex consists of massive and pillowed basaltic lava sequences with intercalated siliceous mudstone and micritic limestone. Gabbro, microgabbro and basaltic intrusives form a subordinate component (Brothers, 1974; Brothers and Delaloye, 1982; Hayward *et al.*, 1989; Malpas *et al.*, 1992). Previous work suggests that the lavas of the Tangihua Complex are dominantly tholeiitic basalts with N-MORB affinities (Malpas *et al.*, 1992; Thompson *et al.*, 1997). The complex also includes minor felsic derivatives, such as plagiogranites, younger alkalic intrusives which exhibit within plate characteristics (Malpas *et al.*, 1992), and ultramafic rocks in the North Cape area (Bennett, 1976).

Inoceramus and formaminiferal fossils in intercalated siliceous mudstone and micritic limestone units indicate mostly late Cretaceous ages for the Tangihua Complex (Brothers and Delaloye, 1982; Hayward *et al.*, 1989). Further studies by Farnell (1973), Brook *et al.* (1988) and Hollis and Hanson (1991) of fossils in incorporated sediments give upper ages of Early Tertiary extending back to mid-Cretaceous.

Radiometric K-Ar dating on whole rock and mineral separates from various massifs yield a bimodal age distribution of *ca.* 100 Ma and *ca.* 42 Ma (Brothers and Delaloye, 1982). Similarly, K-Ar ages within individual massifs range from about mid-Tertiary to mid-Cretaceous (Brothers and Delaloye, 1982). However, as all of the massifs have been altered to some extent, by low-temperature hydrothermal alteration and/or greenschist metamorphism alteration (Black, 1989; Nicholson and Black, 1998; Nicholson *et al.*, (a) in review), the rocks may have undergone some amount of argon leakage or argon homogenisation rendering a degree of uncertainty to the radiometric ages (Brothers and Delaloye, 1982).

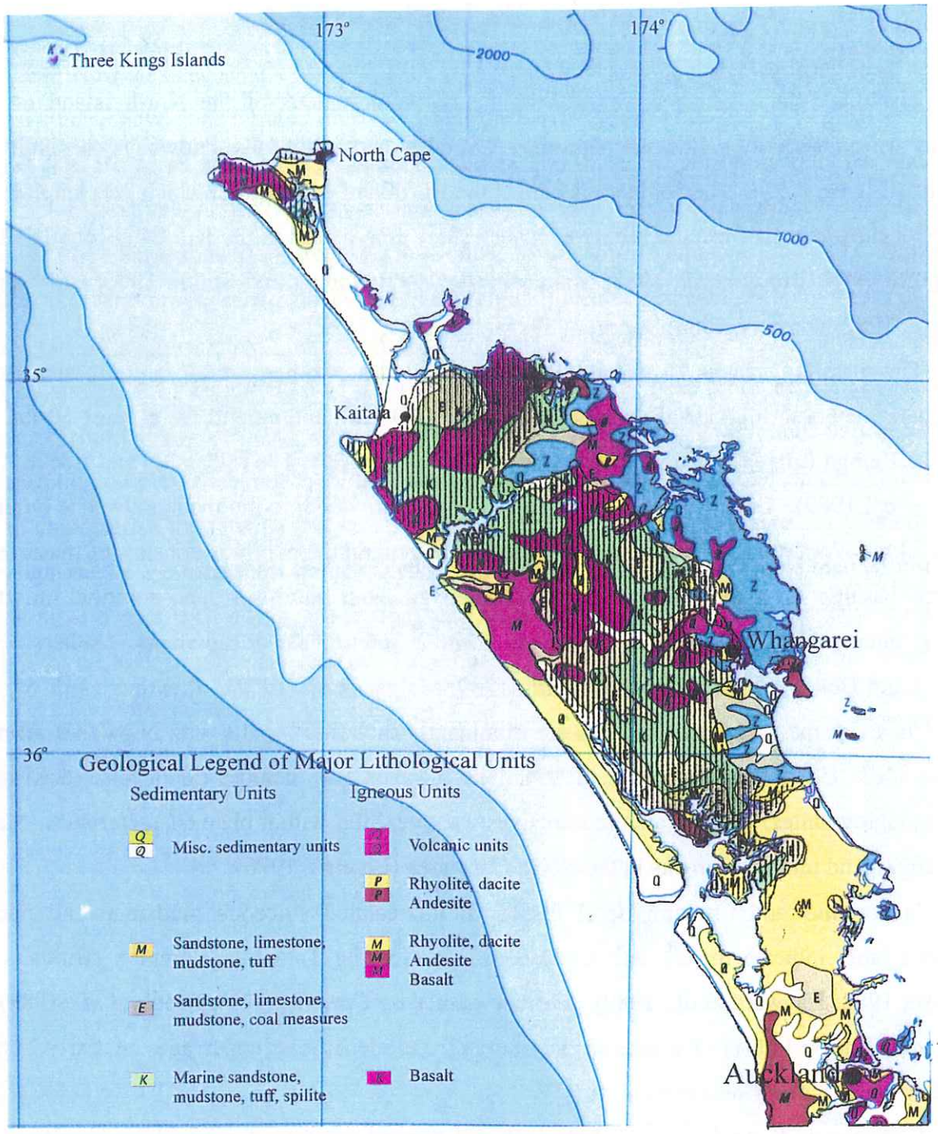

Figure 1.2.1: Simplified geological map of Northland, New Zealand, including Auckland and North Auckland.

The deformational characteristics are similar throughout the Tangihua Complex. Locally the rocks may be intensely sheared but on an outcrop scale such rocks are often associated with relatively undeformed pillows or rocks exhibiting small scale structures. Shear sense indicators within younger, brittle, low-angle fault zones in the ophiolite indicate emplacement from the north-east (Hanson, 1991) with the position of the generating spreading ridge, if still preserved, lying to the north-east and trending north to north-west (Malpas *et al.*, 1994). The consistent north to north-west trends of the dykes, including those in the sheeted dyke complexes at North Cape and Ahipara, indicate that the massifs have not rotated much relative to each other.

Early interpretations regarding the formation of the Tangihua Complex were formulated before the acceptance of plate tectonic theory (Quennell and Hay, 1964; Hughes, 1966). Briggs (1969) was possibly the first to suggest that the Tangihua Complex might be allochthonous, with a northerly emplacement direction, but due to the lack of evidence he rejected this hypothesis. Brothers (1974) was the first to describe the Tangihua Complex as ophiolites, as a result, Brothers and Delaloye (1982) placed the rocks found in the Tangihua Complex into a stylised section through the ocean crust. By the mid 1980's the allochthonous model was generally accepted by several MSc studies (from the University of Auckland) and the entire complex was thought to be analogous to a spreading ridge system (e.g. Larsen, 1987; Arden, 1988; Martin, 1988; Malpas *et al.*, 1992) and by the early 1990's there was thought to be some subduction zone influence with the system (Hopper and Smith, 1996; Thompson *et al.*, 1997).

SECTION 1.3

Why New Caledonia?

The similarities between New Zealand and New Caledonia are numerous, spanning late Paleozoic and Mesozoic faunas and strata (Figure 1.3.1). According to Stevens (1977) New Zealand and New Caledonia can be regarded as a single biogeographical unit during those times (Lillie and Brothers, 1973). Both countries are missing faunas representing the Oxfordian and Kimmeridgian stages, however, Fleming (1970, 1979) stresses the existence of an endemic fauna and a Tethyan element, which are found in both countries.

Lithological similarities include the Permian "tufs polycolores" (Avias, 1953) of New Caledonia which resembles the Lower Permian Te Anau breccias and sandstones of Southland, New Zealand. The Triassic and Jurassic fossiliferous strata of the Mondou - Baie de St Vincent areas closely resembles the Murihiku Supergroup of both the South and North Islands of New Zealand. The Mesozoic strata, of the Central Chain, contains volcanoclastic beds which closely resemble the Morrinsville facies of the North Island, New Zealand (Paris and Bradshaw, 1977; Lillie and Brothers, 1973). Both countries are missing the Neocomian strata, following the Rangitata orogeny, although rocks of Aptian - Albian age are found in New Zealand but not in New Caledonia. Following the Aptian - Albian, are sandstones and shales which are found in both countries, most notably the coal bearing units. The marine Cretaceous shales of the east coast geosyncline of New Zealand, is the shale units of the Northern region in New Caledonia and both countries record the transition from marine Cretaceous to Tertiary strata.

There are fewer similarities within the Tertiary sequences. After the Miocene the landmass of New Caledonia appears to have become consolidated and to have reached a period of relative quiescence, while in New Zealand the Miocene marked the beginning of a continuous period of arc volcanism and seismic activity which continues today. However, during the Eocene, ophiolitic complexes were emplaced in both countries. These ophiolites have remarkably similar chemistries and were formed at approximately the same time during the late Cretaceous. Both the Tangihua Complex of New Zealand and the Poya terrane of New Caledonia (Cluzel *et al.*, 1997; Essien *et al.*, 1998; Aitchison *et al.*, 1999) contain rocks from only the uppermost levels of the crust and are dominated by tholeiitic basaltic lavas. Because of the apparent similarities in age, setting and lithologies between New Zealand and New Caledonia, the ophiolites have been genetically linked. Consequently, this study also includes new data on the Poya terrane and a number of discussions regarding the similarities and differences between the two systems, which show that although there are many general similarities between the two systems, they are very different.

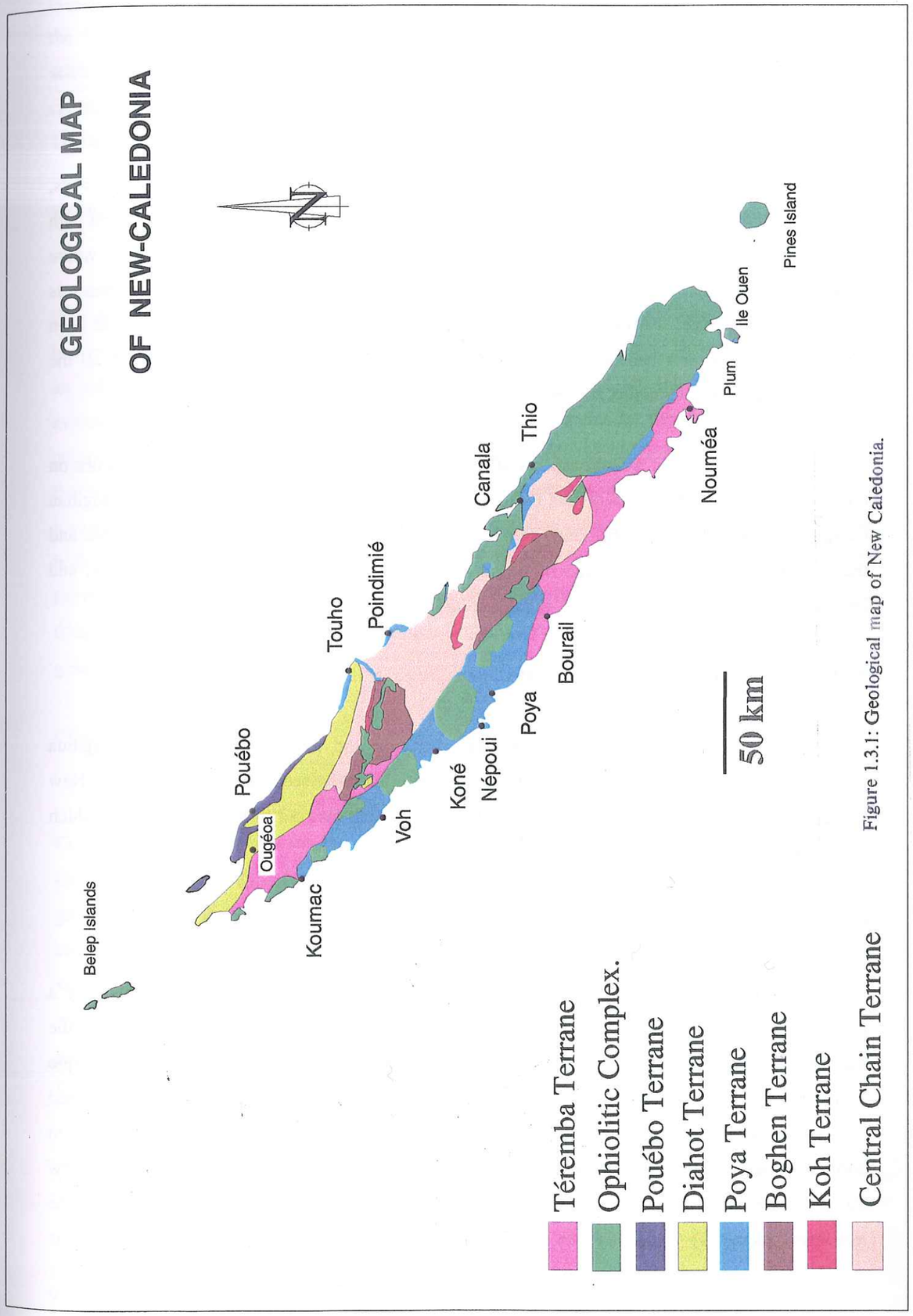

Figure 1.3.1: Geological map of New Caledonia.

SECTION 1.4

Thesis Outline

This thesis is in the format of a thesis by publications, i.e. a series of written manuscripts, following the convention of the Université Joseph Fourier, Grenoble, France, and in agreement with the University of Auckland, New Zealand. Background material has been provided where necessary. However due to the inclusion of the intact submitted manuscripts, the thesis is occasionally repetitive. At the time of completion of this thesis, one of the manuscripts had been published and another 4 had been submitted. Unless otherwise specified and referenced, all the work on the Tangihua Complex and the Poya terrane is new to this study.

Detailed studies of 4 main aspects of the Tangihua Complex combined with new work on the Poya terrane are the focus of this thesis. In addition to the 4 main aspects of the Tangihua Complex, a detailed petrographic study of over 250 samples from both the Tangihua Complex and the Poya terrane (Figure 1.4.1) can be found in Chapter 2. Much of the following work, and interpretation is based or aided by the initial petrographic work.

ALTERATION AND METAMORPHISM

Chapter 3 encompasses a study of the alteration and metamorphism in the Tangihua Complex, followed by a comparison with the alteration patterns seen in the Poya terrane, New Caledonia. The nature of the alteration has yielded insight into the post formation processes, which may have effected the ophiolite complex.

GEOCHEMISTRY

The geochemistry of the Tangihua Complex can be found in Chapter 4, followed by a geochemical comparison with the Poya terrane, New Caledonia. Over 120 samples from the Tangihua Complex were analysed for major oxides and selected trace elements using XRF, 50 were analysed from trace elements (including the rare earth elements) using ICP-MS, 10 were analysed for oxygen isotopes and 12 were analysed for Sr and Nd isotopes. A further 40 samples from northern New Zealand were analysed using XRF for comparative purposes. 40 samples from New Caledonia were analysed using XRF, of these 17 were analysed for trace elements (including the rare earth elements) using ICP-MS. The samples from the Poya terrane were classified as

dominantly N- and P- MORB samples. From the geochemical analyses of the Tangihua samples, the lavas were subdivided into arc-type and back-arc-type lavas and classified into standard schemes for subduction related rocks. The findings of this study contradict earlier work which classifies the Tangihua Complex as a MORB-type ophiolite complex (Malpas *et al.*, 1992; Thompson *et al.*, 1997).

PETROGENESIS AND TECTONIC SETTING

The new geochemical finding for the Tangihua Complex brought forth new problems as to their genesis. Little is known about the region north of New Zealand during the late Cretaceous, however there is little evidence for a well developed arc/back-arc system. Hence the generation of an ophiolitic complex with chemistries indicating an arc and back-arc setting has required a re-evaluation of the local tectonic regime combined with constraints on the source and subduction component in the lavas. Chapter 5 deals specifically with the generation of the lavas, using fractional crystallisation to account for some of the characteristics, a depleted N-MORB source and a variable slab-related component. The question of constraining the tectonic setting is handled in both Chapters 4 and 5 where the aborted subduction of the small Phoenix Plate is used to account for the generation of the Tangihua lavas without the development of a mature arc/back-arc system. Chapter 6 contains new Ar/Ar age data, which helps to further constrain the tectonic model for the generation of the Tangihua Complex.

COMPARISONS

Chapter 7, and parts of Chapters 3 and 4, deal with the relationship between the Tangihua Complex and other ophiolites and arc/back-arc systems within the SW Pacific. The Tangihua Complex has previously been compared to the Poya terrane of New Caledonia. However, both the geochemical and the alteration studies have shown that although there are similarities between the two systems, these similarities are superficial only. Once the Poya terrane is analysed in detail the similarities disappear (Chapter 3 and 4). The Tangihua Complex is then further compared with arc/back-arc systems currently active within the SW Pacific. The petrography, mineral chemistry, geochemistry and new Ar/Ar dates (Chapter 6) are used in the comparisons. Data for the Tangihua Complex compares favourably with oceanic arc/back-arc systems such as the Marianas' but is dissimilar to continental arc systems, such as the Taupo Volcanic Zone.

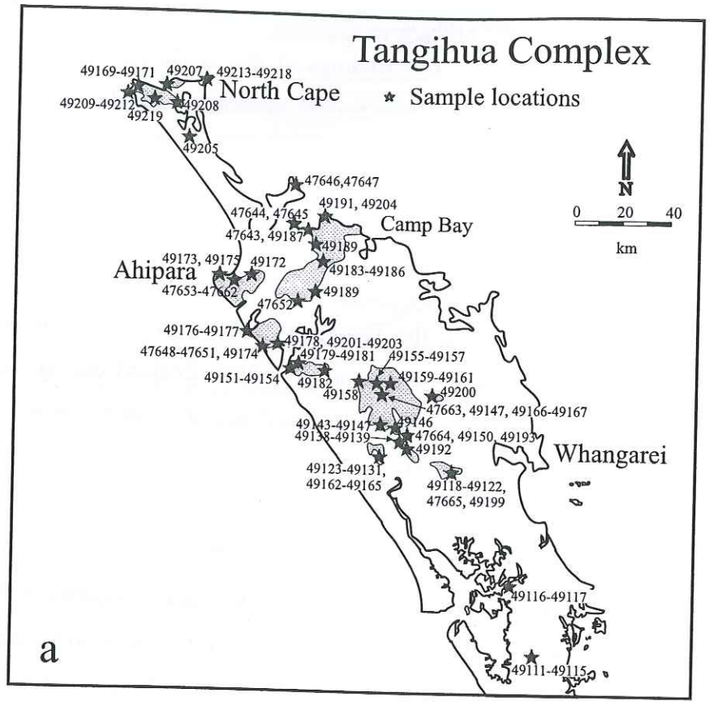

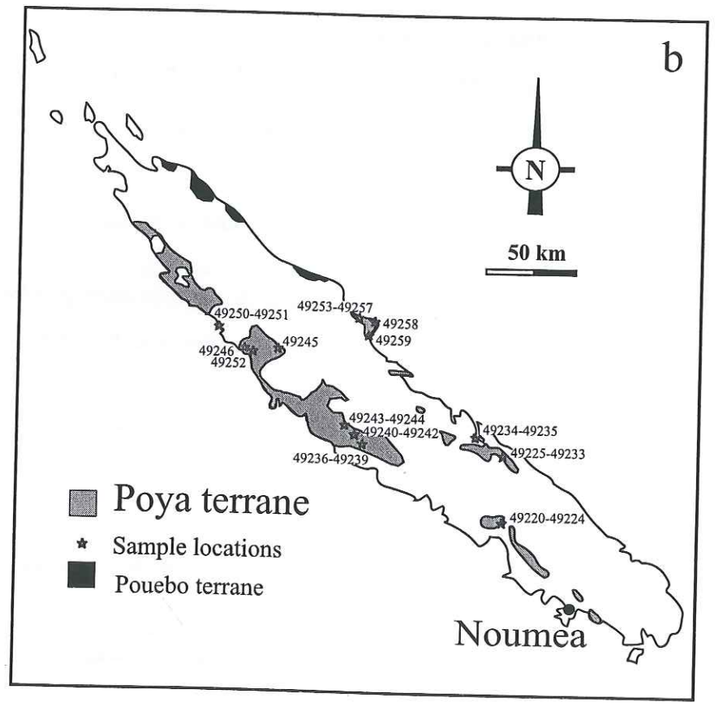

Figure 1.4.1: Sample location maps for (a) the Tangihua Complex, Northland, New Zealand and(b) the Poya terrane, New Caledonia.

CHAPTER TWO: PETROGRAPHY

SECTION 2.1

Introduction

The mafic volcanic rocks integral to this study belong to the Tangihua Ophiolite Complex, which is part of the Northland Allochthon. In general the complex consists of massive and pillowed basaltic lava sequences with intercalated sediments and lesser gabbro, microgabbro and basaltic intrusions (Figure 2.2.1). Chemically the lavas are dominantly tholeiitic basalts with either arc or back-arc affinities. The complex also includes minor felsic derivatives, younger alkalic intrusions and rare ultramafic rocks.

This study has concentrated on the basalt rocks within the Tangihua Complex, however a basic overview of the petrography of the intrusive rocks is also given. Unlike many geochemical studies of igneous rocks, this study has concentrated on both the fresh basalts and the alteration mineralogy throughout the complex. The alteration mineralogy is discussed in further detail in Chapter 3. Since the early 1960's, there have been several studies on the Tangihua Complex. In much of the early work there are petrographic descriptions of individual massifs including: McDonald (1951), Leitch (1966), Le Couteur (1967), Cooper (1968), Fortune (1968), Maxwell (1968), Briggs (1969), Hughes (1969), Baskett (1970), Mason (1973), Bennett (1976), Soffee (1986), Larsen (1987), Martin (1988) and Arden (1988). A list of sample location and field descriptions can be found in Appendix 1.

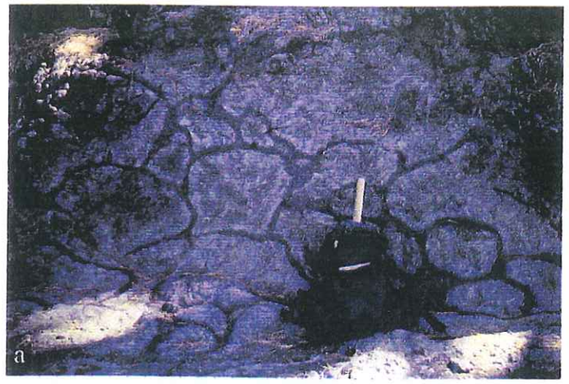

Figure 2.1.1: (a) Pillow basalts at Whangapei Harbour, Northland. Pillow rims are glass and moderately fresh, whereas the pillow cores are completely altered. (b) Sheeted dykes on Ahipara Beach, Northland. The dykes trend in a north-east/south-west direction.

SECTION 2.2

Petrography

TANGIHUA COMPLEX, NEW ZEALAND

BASALT PETROGRAPHY

Primary features:

The basaltic rocks within the Tangihua Complex are generally porphyritic with a cryptocrystalline - microcrystalline groundmass. Fresh glass is also present, as are courser grained intrusive equivalents. The primary phenocryst assemblage is dominated by plagioclase (<45 % by volume) with lesser amounts of clinopyroxene (<40% by volume; Figure 2.2.1). The average phenocryst content in these lavas is approximately 45% by volume, however there is a wide range from <2% to ±80% by volume. Orthopyroxene (<15 % by volume) and magnetite (<5% by volume) are also common but in much lesser amounts, while olivine, biotite and hornblende are rare. Primary biotite and hornblende appear to be stable in only a few of the samples and olivine, where present, is often resorbed or psuedomorphed by alteration minerals.

The groundmass mineral assemblage is dominated plagioclase and clinopyroxene with lesser amounts of orthopyroxene and magnetite. Groundmass phases are generally cryptocrystalline. Plagioclase also occurs as microlites and as inclusions in clinopyroxene. Glass generally occurs as small, <10cm, balls or as the chilled margins of pillow basalts.

Plagioclase phenocrysts are found ranging in size up to 4 mm. It is generally euhedral and often glomerophyric with or without clinopyroxene. Both twinning and zoning are common in plagioclase phenocrysts, which often contain inclusions of pyroxene, glass and/or magnetite.

Clinopyroxene phenocrysts are generally smaller, ranging in size up to 1 mm, although generally less than 0.5 mm. Clinopyroxene is euhedral to subhedral and is often glomerophyric. Clinopyroxene grains show signs of minor oscillatory and sector zoning which is typical of pyroxenes formed in submarine pillow lavas and is indicative of rapid cooling (e.g. Bryan, 1972). Titanomagnetite grains occur disseminated throughout the groundmass. Titanomagnetite ranges in size up to 5 mm and is almost always euhedral.

Alteration:

Alteration within the Tangihua Basalts varies from weak to moderate and is very pervasive. Secondary minerals include chlorite, pumpellyite, actinolite, epidote, calcite, prehnite, mixed layer

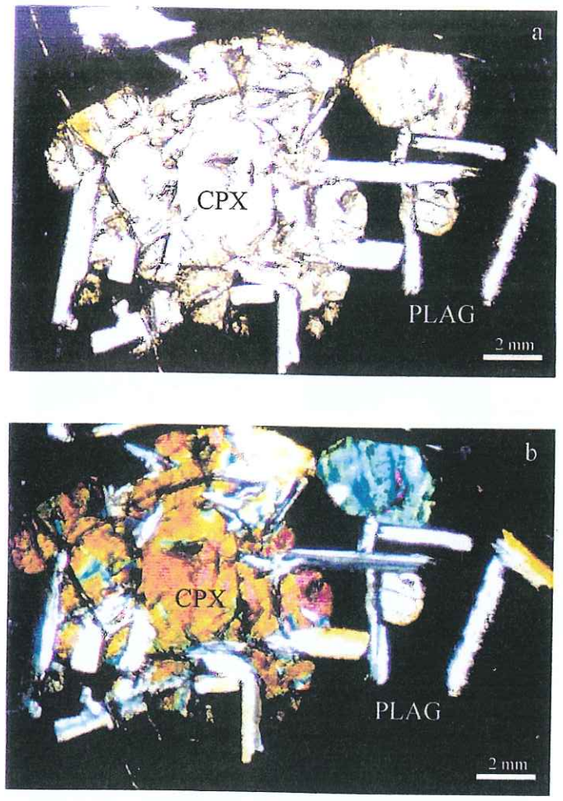

Figure 2.2.1: Photo of fresh glomerophyric clinopyroxene and plagioclase in a microcrystalline groundmass. (a) Transmitted light (b) Crossed polars. Sample #KN115 from North Cape, Northland, New Zealand.

chlorite-smectite, quartz and late stage zeolites (Figure 2.2.2a,b) which are found throughout the groundmass, while pumpellyite, actinolite, epidote, quartz, zeolites, clay minerals and calcite are seen replacing phenocrysts. Alteration by smectite and lesser amounts of both calcite and chlorite – smectite is prevalent throughout the groundmass. Plagioclase phenocrysts are often etched, pitted and embayed. In places plagioclase is partially replaced varying amounts of chlorite, pumpellyite, actinolite, rare epidote and quartz while in some samples plagioclase phenocrysts are almost totally replaced by smectite, zeolites and/or calcite. Alteration of clinopyroxene is less severe with prevalent rim alteration by chlorite and chlorite-smectite. Clinopyroxene cores are generally unaltered, however, rarely they are partially replaced by zeolites and/or clay minerals. Orthopyroxene phenocrysts have been partially altered to smectite and lesser amounts of calcite, zeolites and chlorite - smectite. Where present olivine is almost totally replaced by clay minerals. Primary biotite and hornblende appear to be replaced by clay minerals, zeolites and in some places, by secondary biotite. Magnetite is commonly being oxidised to hematite, or other iron oxides, and may be associated with secondary pyrite.

Veining:

Throughout most of the Tangihua Complex samples, there appears to be only one major generation of veining, however, in some localities there are up to three different generations of veining (Figure 2.2.2c). The major vein sets are crosscutting, sinuous, discontinuous and bifurcating. They range in size from less than 0.1 mm, up to several cm in diameter. Mineral precipitation within the veins is initially dominated by precipitation of sodic zeolites, such as analcime, stilbite and thomsonite. Later phases of vein filling are dominated by calcite and apophyllite precipitation. In places the veins appear to be infilled by multiple precipitation events.

Primary minerals:	plagioclase, clinopyroxene, orthopyroxene, magnetite
Rare:	olivine, biotite, hornblende
Secondary minerals:	analcime, actinolite, mesolite, chlorite, natrolite, epidote, stilbite, pumpellyite, thomsonite, chabazite, clinoptilolite, chlorite-smectite and/or smectite, heulandite, prehnite, laumontite, apophyllite, calcite, pyrite, iron oxides

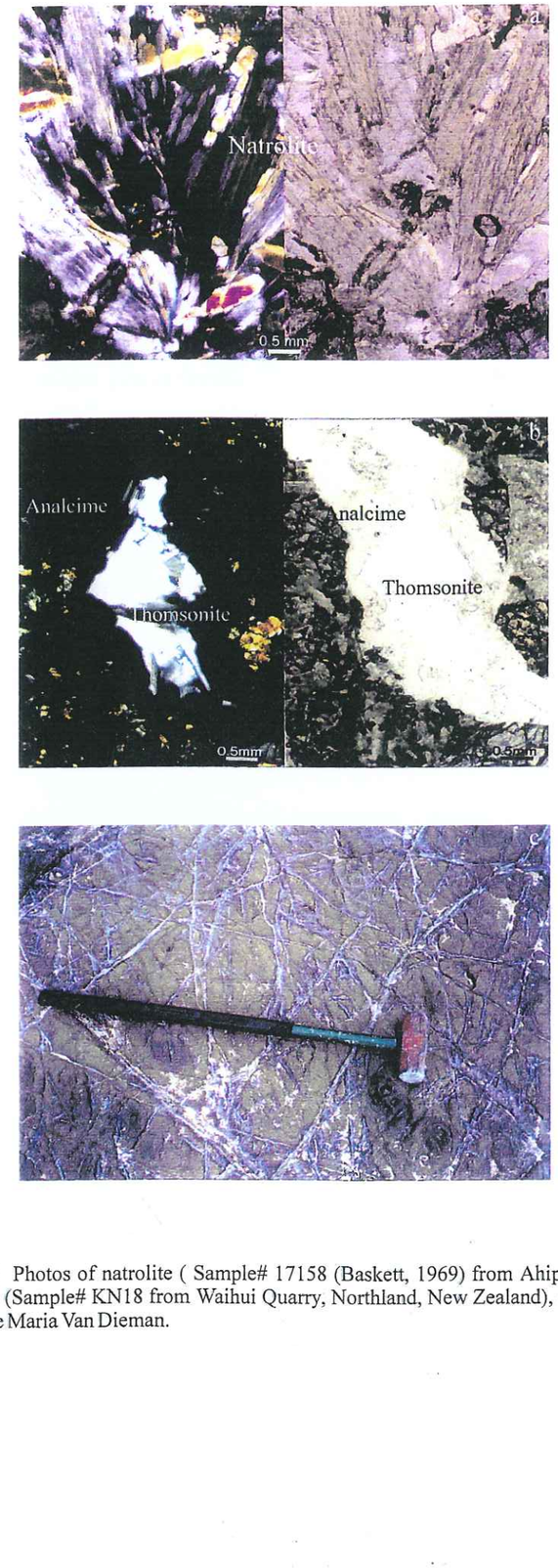

Figure 2.2.2: (a) and (b) Photos of natrolite (Sample# 17158 (Baskett, 1969) from Ahipara, Northland, New Zealand) and thomsonite with analcime (Sample# KN18 from Waihui Quarry, Northland, New Zealand), in veins, respectively. (c) Photo of cross cutting veins at Cape Maria Van Dieman.

GABBRO PETROGRAPHY

Primary features:

Primary features in the plutonic units within the Tangihua Complex vary significantly. Grain size varies from fine (< 1mm) to very course (>15mm) with rare individual crystals reaching 30mm, however, the average grain size is fine (<1mm). The fine grained units are equigranular and ophitic to subophitic. In places layering may be well developed with both felsic and mafic layers present. Layers can be traced for several meters and range in width up to 30cm, although, the average layer width is approximately 1 cm. Felsic schlieren and stringers of felsic gabbro form small lensoidal pods and rare pegmatitic gabbro veins may also occur.

Clinopyroxene and plagioclase dominate the primary mineral assemblages with lesser amounts of iron oxides, orthopyroxene, hornblende and rare olivine (Figure 2.2.3a,b). Alkali gabbros have a high proportion of mafic minerals including titanaugite and hornblende. They are medium to course grained and slightly porphyritic.

Alteration:

As with the basaltic rocks, alteration within the Tangihua gabbros varies from weak to moderate and is very pervasive. Secondary minerals include chlorite, actinolite, epidote, calcite, prehnite, sphene, mixed layer chlorite-smectite, quartz and late stage zeolites which are found throughout the gabbros.

Primary minerals:	plagioclase, clinopyroxene, magnetite
Rare:	orthopyroxene, olivine, hornblende
Secondary minerals:	analcime, actinolite, chlorite, natrolite, epidote, thomsonite, chabazite, chlorite-smectite and/or smectite, prehnite, apophyllite, calcite, pyrite, iron oxides

INTRUSIVE (DYKES AND SILLS) PETROGRAPHY

Primary features:

Primary features in the intrusive units within the Tangihua Complex vary significantly. Both sills and dykes are aphyric to moderately porphyritic and range from quartz-diorite and microgabbro in composition. The units are commonly ophitic to subophitic and equilgranular with grain size varying from very fine (<0.5mm) to medium (<5mm). Centimetre wide chilled margins are common. Narrow stringers extend from s ills/dykes into the surrounding volcanic rocks.

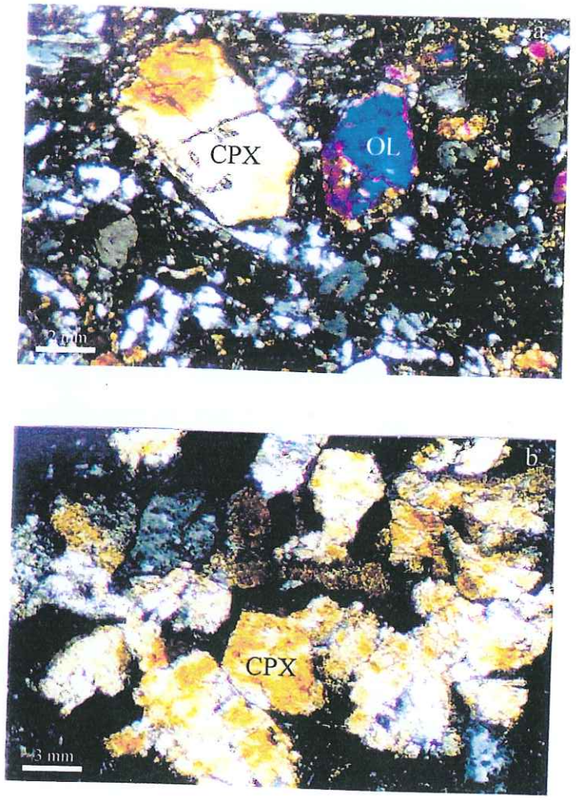

Figure 2.2.3: (a) Photo of medium grained clinopyroxene and olivine in a crystalline groundmass. Sample# KN15 from Waihui Quarry, Northland, New Zealand. (b) Photo of medium grained glomerophyric clinopyroxene in cryptocrystalline groundmass. Sample# KN27 from Houto, Northland, New Zealand.

Plagioclase is the dominate primary mineral with lesser amounts of hornblende, iron oxides, clinopyroxene, olivine and rare quartz.

Alteration:

As with the basaltic rocks, alteration within the intrusive units in the Tangihua complex varies from weak to intense and can be very pervasive. Clinopyroxene is found with reaction rims of hornblende while plagioclase is altered to clays, zeolites and/or quartz. Secondary minerals include chlorite, actinolite, epidote, calcite, prehnite, sphene, mixed layer chlorite-smectite, quartz and late stage zeolites which are found throughout the gabbros.

Primary minerals:	plagioclase, clinopyroxene, Fe-Ti oxides
Rare:	olivine, hornblende, quartz
Secondary minerals:	analcime, hornblende, mesolite, chlorite, natrolite, epidote, stilbite, pumpellyite, thomsonite, chabazite, clinoptilolite, chlorite-smectite and/or smectite, heulandite, prehnite, laumontite, apophyllite, calcite, pyrite, iron oxides

POYA TERRANE, NEW CALEDONIA
BASALT PETROGRAPHY

The Late Cretaceous basaltic volcanic rocks from New Caledonia belong to the Poya terrane. The Poya terrane is a complex set of submarine mafic volcanic rocks, dolerites, gabbros and associated abyssal sediments, which appear to have formed as part of a marginal basin. Geochemically the Poya terrane basalts are dominantly N- and P-MORB in character, however the complex also contains minor alkaline basalts (Parat, 1996; Cluzel *et al.*, 1997; Eissen *et al.*, 1998; Picard *et al.*, 1999; Chapter 4, this study). As with the Tangihua Complex, this study has concentrated on the basalt rocks within the Poya terrane.

Primary features:

The basaltic rocks within the Poya terrane range from almost aphyric massive flows, through to intergranular and intersertial textured basalts with >10 modal % plagioclase and clinopyroxene phenocrysts (Figure 2.2.4a,b). Less commonly the terrane contains plagioclase + clinopyroxene phyric or rare olivine + plagioclase phyric pillow basalts with largely devitrified glassy rims. Phenocryst content is sometimes as high as 60% and is dominated by clinopyroxene

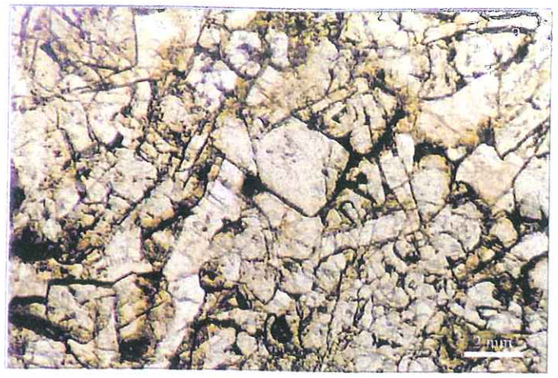

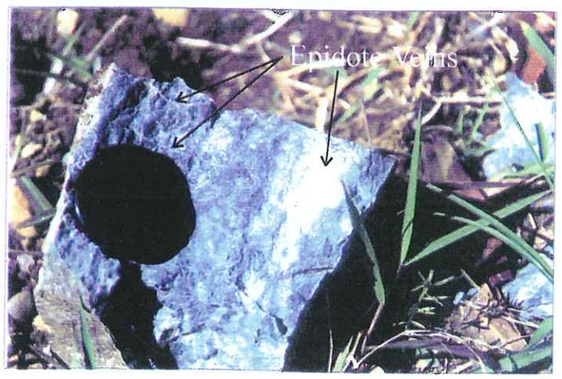

Figure 2.2.4: Photos (a) and (b) of clinopyroxene and plagioclase in a slightly chloritised groundmass, under transmitted light and crossed polars respectively. Sample# NC 3 from near Nassirah, New Caledonia. (c) Photo of macro-scale epidote veining in basalt. Sample# NC7 from NW of Thio, New Caledonia.

and plagioclase. Primary phenocryst are: plagioclase + clinopyroxene >> orthopyroxene, magnetite and sphene. Several samples contain primary hornblende, in some cases up to 35%, and both rare olivine and biotite bearing basaltic rocks are present within the Poya terrane.

Plagioclase occurs as euhedral to subhedral grains, generally tabular in form, and ranging in size from microcrystalline to 4mm in length, although larger crystals are seen. Both simple and multiple twins are common as is zoning.

The clinopyroxene present in the PTB basalts occurs as pale green, subhedral to euhedral, crystals up to 2mm in length. Clinopyroxene phenocrysts are generally calcic augite (Figure 2.2.4b), however, in the alkaline basalts the pyroxene is dominantly diopside. Clinopyroxene crystals are often embayed and may contain exsolution lamellae of orthopyroxene. Orthopyroxene is colourless to pale greenish brown, anhedral to subhedral, grains which are found up to 1mm in length. Both clinopyroxene and orthopyroxene are being altered to clay minerals.

Hornblende, where present, occurs as euhedral to subhedral crystals ranging in size up to 2mm in length. Hornblende is generally dark green and commonly twinned. Olivine is very rarely fresh and is more commonly resorbed or altered to chlorite and/or calcite. Primary biotite is very rare and may in fact be secondary. It occurs as very small platelets and is generally associated with chlorite and hornblende. Magnetite grains range in size up to 5 mm, are generally euhedral and are commonly found disseminated throughout the groundmass.

Alteration:

Low grade metamorphism is uniform throughout the PTB with virtually all samples containing mineral assemblages reflecting both the prehnite-pumpellyite and the greenschist metamorphic facies (Nicholson and Black, 1998). Secondary minerals include; prehnite, pumpellyite, epidote, chlorite, albite and titanite (200-400°C), which generally correspond with the prehnite-pumpellyite metamorphic facies (Figure 2.2.5a). In most areas minor actinolite and K-feldspar also occur as secondary mineral phases, suggesting that the temperatures associated with metamorphism were upwards of 300°C which corresponds with greenschist facies.

Throughout the groundmass, the secondary minerals include chlorite, pumpellyite, albite, lawsonite, stipnomelane, actinolite, epidote, calcite, prehnite, and mixed layer chlorite-smectite. Pumpellyite and chlorite are the most abundant secondary minerals found throughout the groundmass, in cases 40-60% of the groundmass is replaced by secondary minerals.

Relict primary minerals are common and in many cases primary textures are preserved. Both chlorite and pumpellyite occur as alteration minerals of plagioclase and pyroxene. Albite and K-feldspar occur as a recrystallised phase of plagioclase whereas titanite usually occurs as an

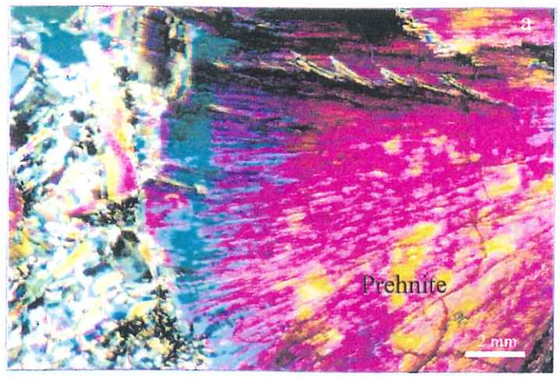

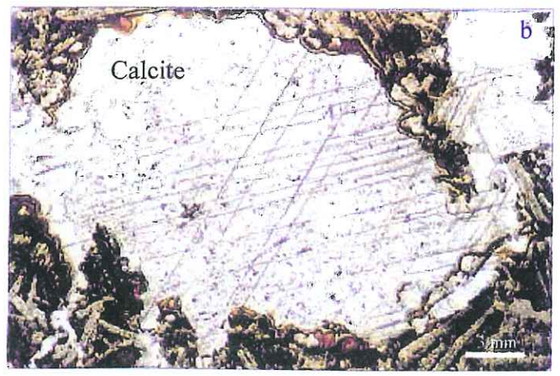

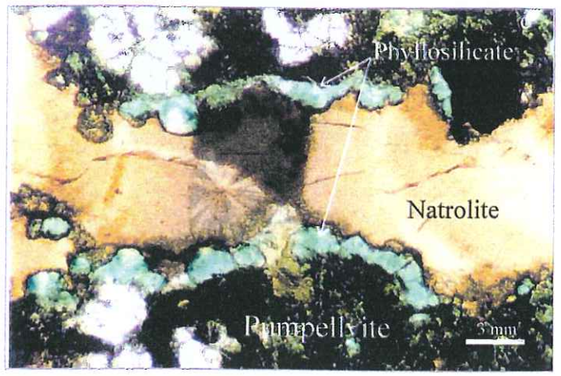

Figure 2.2.5: (a) Photo of macrocrystalline and microcrystalline prehnite in a vein under crossed polars. Sample# NC38 from Poindimie Beach, New Caledonia. (b) Photo of calcite infilling a vesicle in transmitted light. Sample# NC17 from near Nandai, New Caledonia. (c) Photo of natrolite surrounded by an apple green phyllosilicate and pumpellyite in a vein under crossed polars. Sample# NC40 from Pambou, New Caledonia.

alteration phase of pyroxene and oxide minerals. Relict primary pyroxenes are rimmed by more sodic pyroxene, amphibole or pumpellyite, where as primary amphiboles are rimmed by riebeckite or actinolite. Fine needles of actinolite are found in patches of chlorite and pumpellyite, whereas epidote occurs in association with prehnite, both minerals are scattered throughout the groundmass as an uncommon, patchy secondary phase. Rare oxychlorite occurs as small grains associated with chlorite. Opaque minerals are replaced by titanite and to a lesser extend by pyrite and/or hematite.

Zeolite minerals, in association with chlorite and calcite, are found in veins and open space (Figure 2.2.5b,c). They include analcime, apophyllite, thomsonite, natrolite and chabasite. No zeolites are found within the groundmass.

Late stage smectite and chlorite-smectite clays are found throughout the samples, altering phenocryst and groundmass minerals, which have already undergone some amount of alteration. In places most of the previously precipitated clay minerals have been altered further to smectite clays.

Veining:

Several generations of veins are present within the Poya terrane. The major vein sets are crosscutting and may be either sinuous or straight, discontinuous and are commonly bifurcating. Veins range in size from less than 0.1 mm, up to 15 cm, and possibly wider, in diameter. Vein mineralogy includes pumpellyite, calcite, stipnomelane, albite, actinolite, riebeckite, epidote, titanite, phengite, chlorite, apophyllite and quartz (Figure 2.2.4c). Veins containing epidote and riebeckite are younger than the pumpellyite bearing veins. In general the veining is thought to post date the highest temperature and pressure phase of blueschist metamorphism. Mineral precipitation within the veins in dominated by calcite, especially as a later phase.

Primary minerals:	plagioclase, clinopyroxene, orthopyroxene, magnetite
Rare:	olivine, biotite, hornblende
Secondary minerals:	actinolite, albite, analcime, apophyllite, biotite, calcite, chabazite, chlorite:, epidote, k-feldspar, lawsonite, Na-pyroxene:, natrolite, phengite, prehnite, pumpellyite:, quartz, riebeckite:, smectite and/or smectite-chlorite, stipnomelane, thomsonite, titanite, pyrite, iron oxides.

SECTION 2.3

Mineral Chemistry

Mineral compositions for the Tangihua Complex and the Poya terrane were determined from carbon-coated polished thin sections by energy dispersive (EDS) methods using the JOEL JXA-5A electron microprobe housed in the Department of Geology, University of Auckland. As previously stated, this study has concentrated on the Tangihua Complex. Analyses of clinopyroxene and plagioclase from the Poya terrane have been used for comparative purposes and are included here. Where necessary, data from other studies has been included and referenced.

TANGIHUA COMPLEX, NEW ZEALAND

Plagioclase

Plagioclase dominates the mineral assemblage in all the rock types found in the Tangihua Complex. The modal proportions of plagioclase phenocrysts varies from <5% in the glass samples up to 45% in the more crystalline basalts. In general plagioclase forms euhedral crystals which may occur as isolated grains or glomerophyric clusters. Often plagioclase phenocrysts contain micro-inclusions of pyroxene, magnetite and/or glass, which appear to occupy growth zones.

Representative analyses of plagioclase phenocrysts are given in Table 2.3.1 and Figure 2.3.1, the remainder of the data can be found in Appendix 2. The majority of the plagioclase phenocrysts have compositions in the range of An_{66-87} with an average of An_{74}. There appears to be little variation between the composition of phenocryst rims and cores, although rim compositions are more sodic, averaging An_{60}. Plagioclase groundmass microlites are common in all samples except the glasses. Again groundmass plagioclase is more sodic than the phenocryst phase, An_{63}. It is likely that the groundmass plagioclase and rim compositions may be slightly hydrated. In general there appears to be only a small difference between the phenocryst plagioclase, microlite plagioclase and the groundmass plagioclase compositions.

Of the plagioclase phenocrysts analysed, few reported values of K_2O above the detection limit. Where K_2O is present it occurs in a limited range of 1-3 mol.% Or. It is likely that the raised K_2O content in some of the lavas is the result of alteration and the consequential replacement by K_2O within the plagioclase grains. Almost all plagioclase analyses show a small amount of FeO^{total}, average 1 wt.% FeO^{total}. The maximum Fe content approached 4 wt.% in the phenocrysts and is probably associated with magnetite inclusions.

	New Zealand									
Sample#	49172	49172	49172	49172	49172	49123	49123	49123	49123	49123
Affinity	Arc	Arc	Arc	Arc	Arc	Back-arc	Back-arc	Back-arc rim	Back-arc rim	Back-arc rim
SiO2	47.70	50.37	49.07	48.46	49.62	46.13	46.23	50.51	54.17	60.36
TiO2	0.17	0.00	0.00	0.00	0.00	0.00	0.00	0.00	0.00	0.00
Al2O3	32.36	30.71	31.41	32.17	31.59	34.34	34.09	30.30	28.20	24.24
FeO	0.81	0.65	0.74	0.89	0.80	0.47	0.41	0.83	1.31	1.51
MnO	0.00	0.00	0.00	0.00	0.00	0.00	0.00	0.00	0.00	0.00
MgO	0.29	0.29	0.40	0.31	0.49	0.00	0.00	0.00	0.44	0.00
CaO	16.25	13.89	15.15	15.93	15.04	18.01	17.67	13.71	11.64	6.53
Na2O	2.35	3.71	3.12	2.66	3.10	1.46	1.44	3.62	4.87	7.12
K2O	0.00	0.00	0.00	0.00	0.00	0.00	0.00	0.00	0.00	0.15
Cl	0.00	0.00	0.00	0.00	0.00	0.00	0.00	0.00	0.00	0.00
P2O5	0.00	0.00	0.00	0.00	0.00	0.00	0.00	0.00	0.00	0.00
Cr2O3	0.00	0.00	0.00	0.00	0.00	0.00	0.00	0.00	0.00	0.00
Total	99.9	99.6	99.9	100.4	100.6	100.4	99.8	99.0	100.6	101.0
Sample#	47643	47643	47643	47643	47643	47648	47648	47648	47648	47648
Affinity	Arc	Arc rim	Arc rim	Arc	Arc	Back-arc	Back-arc	Back-arc rim	Back-arc rim	Back-arc
SiO_2	46.91	53.66	56.89	74.83	59.27	49.99	50.19	50.72	50.37	51.26
TiO_2	0.00	0.00	0.00	0.00	0.00	0.00	0.00	0.00	0.00	0.00
Al_2O_3	33.24	28.82	26.61	15.70	25.19	31.09	31.34	30.96	30.78	30.83
FeO	0.73	1.49	0.67	0.00	0.45	0.57	0.46	0.59	0.59	0.56
MnO	0.00	0.00	0.00	0.00	0.00	0.00	0.00	0.00	0.00	0.00
MgO	0.00	0.43	0.00	0.00	0.00	0.00	0.00	0.00	0.00	0.00
CaO	17.15	11.42	8.85	2.20	7.17	14.81	14.63	14.36	14.49	14.28
Na_2O	1.94	4.66	4.86	7.01	7.37	3.19	3.15	3.38	3.47	3.71
K2O	0.00	0.10	2.64	0.12	0.00	0.00	0.00	0.00	0.00	0.00
Cl	0.00	0.00	0.00	0.00	0.00	0.00	0.00	0.00	0.00	0.00
P_2O_5	0.00	0.00	0.00	0.00	0.00	0.00	0.00	0.00	0.00	0.00
Cr_2O_3	0.00	0.00	0.00	0.00	0.00	0.00	0.00	0.00	0.00	0.00
Total	100.0	100.6	100.5	99.9	99.5	99.7	99.8	100.0	99.7	100.6
	New Caledonia									
Sample#	49225	49225	49225	49225	49225	49225	49225	49251	49251	49251
SiO_2	52.41	52.12	54.10	52.35	50.87	53.69	51.39	48.99	49.89	51.21
TiO_2	0.14	0.05	0.08	0.03	0.06	0.03	0.12	0.00	0.04	0.04
Al_2O_3	29.40	29.82	28.60	29.10	29.93	29.08	29.74	31.60	30.16	30.60
FeO	0.85	0.96	0.57	1.35	1.03	0.93	0.92	0.57	0.65	1.03
MnO	0.02	0.04	0.00	0.00	0.01	0.00	0.04	0.06	0.04	0.03
MgO	0.29	0.37	0.19	0.21	0.27	0.25	0.25	0.40	0.41	0.30
CaO	12.10	12.71	10.91	11.85	13.18	11.52	12.71	14.95	13.77	13.47
Na_2O	4.66	4.41	5.32	4.71	4.21	5.06	4.20	3.14	3.64	3.99
K2O	0.08	0.01	0.07	0.01	0.03	0.04	0.03	0.00	0.05	0.06
Cl	0.02	0.00	0.02	0.01	0.00	0.02	0.03	0.01	0.04	0.00
P_2O_5	0.08	0.10	0.10	0.07	0.07	0.12	0.06	0.05	0.05	0.03
Cr_2O_3	0.00	0.00	0.00	0.09	0.00	0.00	0.00	0.03	0.08	0.00
Total	100.0	100.5	99.9	99.7	99.6	100.7	99.5	99.7	98.8	100.7

Table 2.3.1: Representative plagioclase analyses from the Tangihua Complex and the Poya terrane. Geochemical affinities explained in Chapter 4.

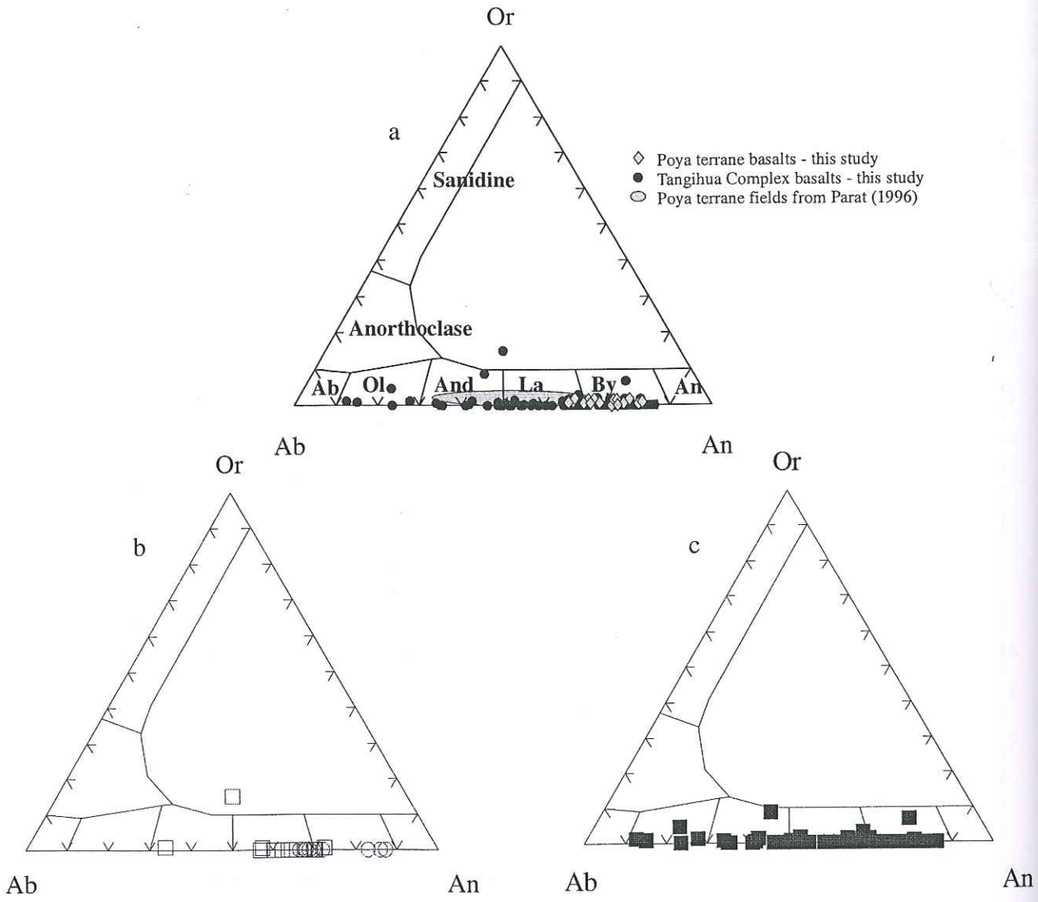

Figure 2.3.1: (a) Feldspar compositions in basaltic lavas from the Tangihua Complex and the Poya terrane. Feldspar compositions for the Poya terrane are from this study and from Parat (1996). (b) Representative plagioclase core (circles) and rim (squares) compositions for the Tangihua Complex. (c) Representative plagioclase groundmass (solid squares) compositions from the Tangihua Complex. Plagioclase composition calculated on the basis of 20 oxygens. .

Clinopyroxene

The second most common phenocryst phase within the Tangihua basalts is clinopyroxene. The modal proportion of clinopyroxene phenocrysts ranges from < 2 % in the glasses to 40% in some of the basalts. However, in general the average modal proportion of clinopyroxene is between 25-30%. Clinopyroxene phenocrysts occur in a variety of forms. It is commonly found as euhedral grains, which are often glomerophyric. In places clinopyroxene grains are subrounded, they occasionally have alteration rims and sometimes show minor oscillatory and sector zoning. The size of the clinopyroxene phenocrysts ranges from microcrystalline groundmass grains up to 1mm long crystals. On average clinopyroxene phenocrysts are <0.5mm in diameter. Both solitary and glomerphyric clinopyroxene is often found in association with plagioclase clusters.

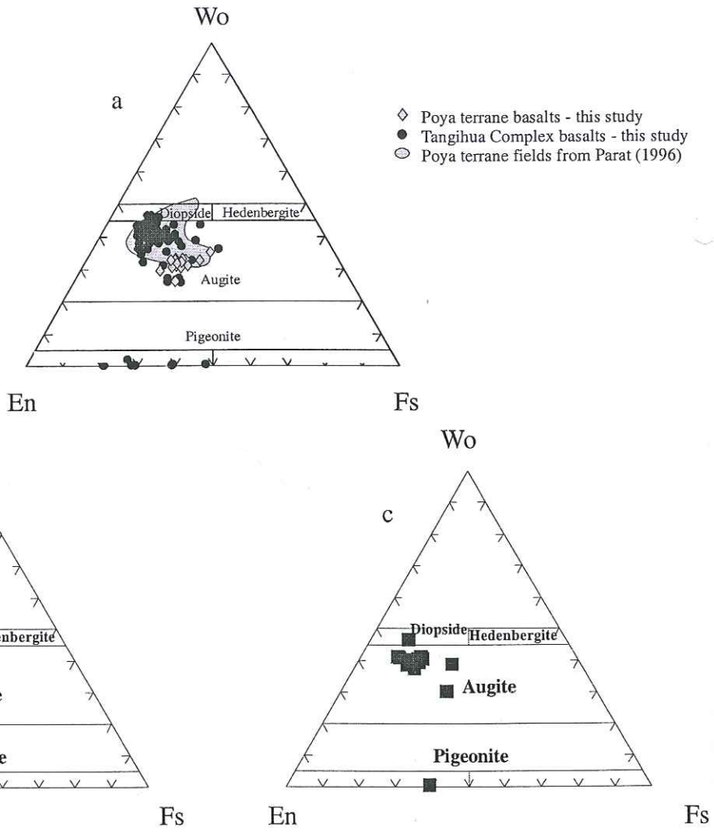

Figure 2.3.2: (a) Representative clinopyroxene and orthopyroxene analyses from basaltic lavas in the Tangihua Complex and the Poya terrane. Poya terrane data from this study and from Parat (1996). (b) Representative core (circles) and rim (squares) compositions from the Tangihua Complex. (c) Representative groundmass (solid squares) pyroxene compositions from the Tangihua Complex. Pyroxene compositions calculated on the basis of 6 oxygens.

Representative analyses of clinopyroxene phenocrysts are given in Table 2.3.2 and Figure 2.3.2, the remainder of the data can be found in Appendix 3. Clinopyroxene phenocrysts are predominately calcic augite, although they range between diopside and augite. Both diopside and calcic augite occur in most of the lavas analysed. Some of the scatter in Figure 2.3.2 is due to alteration of clinopyroxene rims even though analyses with totals of less than 98.5% were discarded. The composition of the clinopyroxene varies widely with a range of $En_{31-52}Fs_{10-33}Wo_{28-45}$. Clinopyroxene phenocrysts cores have an average of $En_{47}Fs_{15}Wo_{38}$. Mg#s fall between 34 and 73 with an average of 61 for core compositions and a standard deviation of 6.25 (Mg# = Mg/(Mg+Fe)). Rim compositions are similar with an average composition of $En_{42}Fs_{20}Wo_{38}$ and lower Mg#, average = 56. Groundmass clinopyroxene also is similar in composition to the cores with $En_{44}Fs_{16}Wo_{40}$. Rare grains of pigeonite are present in three of the samples analysed. The pigeonite phenocrysts have an average composition of $En_{60}Fs_{33}Wo_{7}$ and Mg# =52. In places pyroxene analyses with 15-25 mol.% Wo are found. These have been interpreted as an intergrowth between

more calcic augite and less calcic pigeonite (Morimoto *et al.*, 1988). As with the zoning, the crystal intergrowths are most likely the result of rapid groundmass crystallisation during pillow formation.

Clinopyroxene phenocrysts contain up to 2.68 wt.% TiO_2 with an average of 0.66 wt.% and a standard deviation of 0.24 wt.% TiO_2. The higher values are comparable to MORB whereas the lower values are characteristic of arc systems. Al_2O_3 ranges from 0 to 6.88 wt.% with and average of 2.94 wt.%, MnO is always less than 0.78 wt.% and averages 0.2 wt.% and Cr_2O_3 contents are between 0 and 1.16, averaging 0.19 wt.%. Both the Mn and Cr contents rarely exceed 0.2 wt.%. The Ti:Al ratio in the clinopyroxene phenocrysts is approximately 7:1. According to Stewart *et al.* (1996), who express crystallising pressures in terms of the Ti:Al cation ratios for MORB, a 7:1 Ti:Al ratio for clinopyroxene suggests crystallisation at pressures of approximately 0.1GPa.

New Zealand										
Sample#	47660	47660	47660	47660	47660	49172	49172	49172	49172	49172
Affinity	Back-arc	Back-arc	Back-arc	Back-arc	Back-arc	ARC	ARC	ARC	ARC	ARC
	rim	rim	core	core	Core	core	core	core	Rim	rim
SiO_2	51.15	49.35	49.55	51.69	50.22	48.83	50.89	50.93	49.47	50.83
TiO_2	0.74	1.03	0.84	0.46	0.89	0	0.64	0.71	0.97	0.83
Al_2O_3	6.88	3.37	3.81	2.59	3.77	31.52	2.83	2.32	3.31	2.72
FeO	10.37	12.95	11.9	7.85	10.51	0.85	9.77	9.94	10.6	10.39
MnO	0.24	0.4	0.38	0.25	0.21	0	0.35	0	0.24	0.24
MgO	11.88	13.6	13.8	16.45	14.75	0.38	14.7	14.94	14.56	15.37
CaO	17.24	18.46	19.28	19.91	19.63	15.25	19.6	19.97	19.4	19.33
Na_2O	1.05	0	0	0	0	3.06	0.48	0.66	0.68	0.92
K2O	0.25	0	0	0	0	0	0	0	0	0
Cl	0	0	0	0	0	0	0	0	0	0
P_2O_5	0	0	0	0	0	0	0	0	0	0.25
Cr_2O_3	0	0	0	0	0	0	0	0	0	0
Total	99.81	99.16	99.57	99.22	99.97	99.88	99.26	99.46	99.22	100.87
En	43.7	41.0	42.9	45.0	43.7	92.5	44.5	44.5	43.5	42.9
Fs	26.3	28.8	26.5	17.8	23.4	5.2	22.2	22.2	23.8	23.0
Wo	30.1	30.2	30.7	37.2	32.9	2.3	33.4	33.3	32.7	34.1
Sample#	49123	49123	49123	49123	49123	47643	47643	47643	47643	47643
	Back-arc	Back-arc	Back-arc	Back-arc	Back-arc	ARC	ARC	ARC	ARC	ARC
	core	core	rim	rim	Rim	rim	rim	core	core	core
SiO_2	50.92	51.87	51.69	50.16	52.59	51.07	52.92	50.39	52.96	52.41
TiO_2	0.74	0.57	0.72	1.36	0.67	0.69	0.40	0.71	0.33	0.49
Al_2O_3	2.65	2.22	1.92	3.37	1.86	2.90	2.09	4.07	1.95	2.25
FeO	9.71	9.66	15.04	16.42	13.24	6.30	7.20	7.60	7.41	6.84
MnO	0.25	0.28	0.41	0.50	0.37	0.00	0.21	0.23	0.32	0.24
MgO	15.62	16.24	17.11	15.71	15.98	15.98	17.93	16.35	18.42	17.66
CaO	19.20	19.06	13.24	13.33	14.99	21.01	18.75	19.84	18.73	19.59
Na_2O	0.00	0.00	0.00	0.00	0.00	0.00	0.00	0.00	0.00	0.00
K2O	0.00	0.00	0.00	0.00	0.00	0.00	0.00	0.00	0.00	0.00
Cl	0.00	0.00	0.00	0.00	0.00	0.00	0.00	0.00	0.00	0.00
P_2O_5	0.00	0.00	0.00	0.00	0.00	0.00	0.00	0.00	0.00	0.00
Cr_2O_3	0.00	0.00	0.00	0.00	0.00	0.61	0.37	0.23	0.23	0.31
Total	99.1	99.9	100.1	100.8	99.7	98.6	99.9	99.4	100.4	99.8
En	43.1	42.4	29.2	29.3	33.9	48.5	42.7	45.3	42.0	44.4
Fs	21.8	21.5	33.1	36.1	29.9	14.6	16.4	17.4	16.6	15.5
Wo	35.1	36.1	37.7	34.6	36.1	36.9	40.9	37.3	41.3	40.1

New Caledonia										
Sample#	49225	49225	49225	49225	49225	49251	49251	49251	49251	49251
	core	core	core	core	core	core	core	core	core	core
SiO_2	51.30	49.97	50.34	50.93	50.30	50.09	52.16	50.47	52.36	49.95
TiO_2	0.51	0.80	0.73	0.63	0.80	0.81	0.37	0.68	0.50	0.71
Al_2O_3	2.58	2.29	2.15	2.46	1.75	3.80	2.23	3.58	1.92	3.45
FeO	7.00	12.12	12.60	8.66	14.26	6.98	8.31	7.26	6.63	6.20
MnO	0.16	0.35	0.32	0.22	0.36	0.10	0.21	0.17	0.17	0.08
MgO	16.37	14.32	14.25	15.25	13.46	15.89	18.11	16.06	17.00	15.59
CaO	20.84	18.98	18.74	20.42	17.92	20.31	17.52	20.05	19.97	21.40
Na_2O	0.61	0.69	0.87	0.60	0.54	0.81	0.59	0.73	0.63	0.58
K2O	0.00	0.00	0.00	0.03	0.00	0.01	0.00	0.00	0.00	0.00
Cl	0.01	0.01	0.01	0.02	0.00	0.00	0.00	0.01	0.00	0.04
P_2O_5	0.13	0.08	0.12	0.14	0.15	0.07	0.12	0.03	0.06	0.13
Cr_2O_3	0.43	0.02	0.25	0.19	0.00	0.58	0.17	0.22	0.33	0.85
Total	99.9	99.6	100.3	99.5	99.5	99.4	99.7	99.2	99.5	99.0
En	47.1	41.8	41.1	46.1	39.3	47.0	39.9	46.2	45.8	49.5
Fs	15.8	26.7	27.6	19.5	31.2	16.2	18.9	16.7	15.2	14.4
Wo	37.0	31.5	31.3	34.4	29.5	36.8	41.2	37.0	39.0	36.1

Table 2.3.2: Representative clinopyroxene analyses from the Tangihua Complex and the Poya terrane.

In Figure 2.3.3 the cations Ti, Ca, Na and Cr are used to discriminate between calc-akali, tholeiitic and alkali clinopyroxenes (Figure 2.3.3a) and clinopyroxenes formed in orogenic or non-orogenic settings (Figure 2.3.3b). These diagrams show that basalts from the Tangihua Complex are predominately calc-alkali and tholeiitic and formed in a predominately orogenic setting (Leterrier *et al.*, 1982). However there is a great deal of overlap between the fields for orogenic and

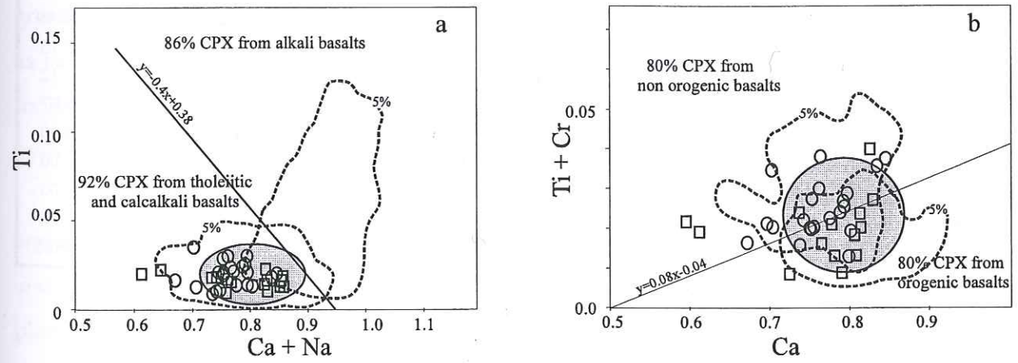

Figure 2.3.3: (a) Discrimination diagram of the cations Ca + Na versus Al for clinopyroxene from the Tangihua Complex basalts. Fields for alkali and calc-alkali-tholeiitic basalts are from Leterrier *et al.* (1982). In both diagrams the dashed lines represent the 5% level of confidence for a given field, the shaded grey field represents >80% of the analyses from the Tangihua Complex, the squares = back-arc basalts and the circles = arc basalts as defined in Chapter 4. (b) Discrimination diagram of the cations Ca versus Ti + Cr for clinopyroxene from the Tangihua Complex basalts. Fields for orogenic and non-orogenic basalts are from Leterrier *et al.* (1982).

non-orogenic clinopyroxenes (Figure 2.3.3b), which hinders interpretation of the diagram unless the conclusions are supported by other geological evidence. In this case the interpretation can be supported by geochemical evidence as seen in Chapters 4 and 5.

Orthopyroxene

Orthopyroxene is found in most of the Tangihua basalts although the modal proportion rarely exceeds 5%. Representative analyses of orthopyroxene phenocrysts are given in Table 2.3.3, the remainder of the data can be found in Appendix 4. Orthopyroxene phenocrysts occur as solitary euhedral grains but are often subrounded with alteration rims. In some samples orthopyroxene grains are pitted and sieved. Zoning is not apparent in orthopyroxene phenocrysts. The size of the orthopyroxene phenocrysts ranges from microcrystalline groundmass grains up to 0.5 mm in diameter, but rarely exceed 0.25mm. Samples which have a modal proportion of orthopyroxene greater than %5, may contain orthopyroxene clusters. The average orthopyroxene composition is $En_{58}Fs_{38}Wo_4$ with Mg# = 46.

Mineral	OPX	OPX	OPX	OPX	OPX	OPX	OPX	OPX	OPX	OPX	OPX
Sample	49158	47649	47649	49186	49186	49186	47663	47663	47663	47663	49201
SiO_2	52.61	53.64	51.09	52.56	52.03	49.04	53.26	51.85	53.67	53.41	41.33
TiO_2	0.87	0.53	1.15	0.43	0.68	1.44	0.29	0.54	0.31	0.48	5.71
Al_2O_3	1.84	1.58	1.25	0.97	1.86	4.38	0.43	0.74	0.13	1.04	11.40
FeO	13.90	14.33	13.63	13.50	10.66	10.28	23.12	23.39	20.23	19.79	16.31
MnO	0.30	0.38	0.32	0.38	0.31	0.25	0.75	0.72	0.71	0.65	0.16
MgO	17.29	19.26	15.60	19.04	18.55	14.30	20.94	19.76	21.66	20.97	11.01
CaO	13.45	11.18	16.13	12.44	14.65	19.62	1.95	2.30	3.27	3.60	10.89
Na_2O	0.00	0.00	0.00	0.00	0.26	0.15	0.00	0.00	0.00	0.00	2.76
K2O	0.02	0.00	0.12	0.04	0.05	0.02	0.03	0.03	0.05	0.09	0.12
Cl	0.02	0.00	0.01	0.05	0.01	0.00	0.00	0.04	0.02	0.00	0.07
P_2O_5	0.00	0.00	0.00	0.00	0.00	0.00	0.00	0.00	0.00	0.00	0.00
SO_3	0.00	0.00	0.00	0.00	0.01	0.05	0.10	0.07	0.13	0.00	0.00
Cr_2O_3	0.09	0.01	0.09	0.13	0.08	0.05	0.02	0.01	0.01	0.00	0.05
NiO	0.04	0.09	0.05	0.06	0.09	0.00	0.08	0.00	0.02	0.05	0.18
TOTAL	100.4	101.0	99.4	99.6	99.3	99.6	101.0	99.5	100.2	100.1	100.0

Table 2.3.3: Representative orthopyroxene compositions from basaltic lavas of the Tangihua Complex.

Olivine

Olivine is rare in the Tangihua Complex basalts and hence was analysed in only three samples. Representative analyses of olivine phenocrysts are given in Table 2.3.4 and Figure 2.3.4, the remainder of the data can be found in Appendix 5. The modal proportion of olivine ranges from 0 to 2% and averages <<1%. No olivine has been found in the glass samples. Olivine phenocrysts occur as discrete grains with subhedral to anhedral crystal faces and are <0.2mm in diameter. Olivine phenocrysts are often found being replaced by clay minerals and are occasionally rimmed

by clinopyroxene, such that it is rare for more than the core compositions to be preserved. Due to the alteration in the olivine grains it is difficult to distinguish zoning. The average composition of olivine phenocrysts is Fo_{76} with Mg#s ranging from 38 to 77 with an average of 65.

Sample	49182	49182	49182	47666	47666	47666	49143	49143	49143
SiO_2	37.7	37.09	35.77	39.15	38.98	39.51	37.22	37.79	40.55
TiO_2	0	0	0	0	0	0	0.03	0.01	0
Al_2O_3	0	0	0	0.29	0	0.36	0	0	0
FeO	25	25.52	33.1	19.04	19.1	19.13	28.93	27.89	13.67
MnO	0.39	0.51	0.67	0.2	0.32	0.28	0.58	0.51	0.17
MgO	36.26	35.44	29.45	41.05	41.1	41	32.37	33.73	45.98
CaO	0.28	0.31	0.32	0.24	0.23	0.35	0.34	0.37	0.37
Na_2O	0.91	0.85	0.98	0	0	0	0	0	0
K_2O	0	0	0	0	0	0	0.08	0.08	0
Cl	0	0	0	0	0	0	0	0.03	0
P_2O_5	0	0	0	0	0	0	0	0	0
Cr_2O_3	0	0	0	0	0	0	0	0	0
Total	100.54	99.72	100.29	99.98	99.72	100.63	99.62	100.46	100.89

Table 2.3.4: Representative olivine compositions from basaltic lavas of the Tangihua Complex.

POYA TERRANE, NEW CALEDONIA

Plagioclase

Plagioclase is the dominant phenocryst phase in the Poya terrane. The modal proportions of plagioclase phenocrysts varies from <20% in the samples with a micro-cryptocrystalline groundmass up to 55% in crystalline basalts. Plagioclase forms euhedral crystals which may occur as isolated grains or as glomerophyric clusters in a micro-cryptocrystalline groundmass. It is also found as interstitial anhedral infillings. Often plagioclase phenocrysts contain micro-inclusions of pyroxene and opaques (magnetite or titanomagnetite) which appear to occupy growth zones.

The majority of the plagioclase phenocrysts have compositions in the range of $An_{53\text{-}73}$ with and average of An_{62}. Representative analyses of plagioclase phenocrysts are given in Table 2.3.1 and Figure 2.3.1, the remainder of the data can be found in Appendix 2. Of the plagioclase phenocrysts analysed, none reported values of K_2O above the detection limit. Almost all plagioclase analyses show a small amount of FeO^{total}, average <1 wt.% FeO^{total}.

Clinopyroxene

Clinopyroxene is the second most common phenocryst phase within Poya terrane basalts with modal proportions ranging from between 15 % to 40%, although, in many samples clinopyroxene is the dominant phase. Clinopyroxene phenocrysts are commonly found as solitary euhedral grains and as glomerophyric euhedral clusters. In places clinopyroxene grains are

subrounded with alteration rims and have been pitted and/or sieved and may show minor oscillatory and sector zoning. The size of the clinopyroxene phenocrysts ranges from microcrystalline groundmass grains up to 1.5 mm in diameter.

Representative analyses of clinopyroxene phenocrysts are given in Table 2.3.2 and Figure 2.3.2, the remainder of the data can be found in Appendix 3. Clinopyroxene phenocrysts are predominately calcic augite, although they range between diopside and augite. The composition of the clinopyroxene phenocrysts is very consistent with a range of $En_{39-51}Fs_{10-24}Wo_{35-45}$ and an average of $En_{44}Fs_{13}Wo_{41}$. Mg#s fall between 30 and 76 with an average of 57 and a standard deviation of 7.5 (Mg# = Mg/(Mg+Fe).

Clinopyroxene phenocrysts contain up to 0.8 wt.% TiO_2 with an average of 0.6 wt.%. These values are comparable to clinopyroxene phenocrysts from other arc systems. Al_2O_3 ranges from 1.75 to 3.80 wt.% with and average of 2.65 wt.%, MnO is always less than 0.4 wt.% and Cr_2O_3 contents are between 0 and 0.88, averaging 0.29 wt.%. Both the Mn and Cr contents rarely exceed 0.2 wt.%. The Ti:Al ratio in the clinopyroxene phenocrysts is approximately 7:1. Using the method of Stewart *et al.* (1996), which expresses the crystallising pressures in terms of the Ti:Al cation ratios for MORB, the clinopyroxene may have crystallised at pressures nearing 0.1GPa.

Olivine

Olivine phenocrysts are often completely altered. However, where fresh, olivine has a composition of Fo83-85 (Eissen *et al.*, 1998).

SECTION 2.4

Mineral Geothermometry - Tangihua Complex

According to the stable mineral assemblages observed in the Tangihua Complex, two geothermometers can be used to constrain the crystallisation history of the TCB. These geothermometers are based on the diopside-enstatite miscibility gap in coexisting pyroxene pairs (Wells, 1977) and on clinopyroxene-orthopyroxene pairs (Wood and Banno, 1973). Starting with the solvus data presented by Davis and Boyd (1966), Wood and Banno (1973) derived an empirical equation which adapts binary En-Di solvus reactions to multicomponent systems behaviour by assuming an ideal solid solution model, and correcting the activities of $Mg_2Si_2O_6$ in both orthorhombic and monoclinic phases for dilution by all other constituents. Nominal temperatures of formation for diopsidic pyroxenes in equilibrium with orthopyroxenes, employing the Wood and Banno (1973) equation, yielded temperature ranges of 1143 to 1187°C and 1222 to 1301°C.

Another method involves projecting the pyroxene analyses within the enstatite-diopside-hedenbergite-ferrosilite quadrilateral after all non-quadrilateral end-member compositions have been removed (Lindsley, 1983). No allowance was made for Fe^{+3}. Estimates of Fe^{+3} could be obtained from the charge balance equation Al(IV) + Fe^{+3} + Cr + 2*Ti = Al(IV) + Na, where Al=Al(IV) + Al(VI) and Al(IV) = 2 – Si (Papike *et al.*, 1974). However, these estimates are sensitive to error in SiO2 determinations, which for pyroxenes $2\sigma = \pm 0.02$ cations per 6 O. Crystallisation temperatures were then read from a series of graphs calibrated for different pressures where the crystallisation temperature decreases by <8°C per pressure reduction of 0.1GPa (Lindsley, 1983). At high pressures, typical of the base of an island arc (0.08 – 0.1GPa), the stable assemblage for a basaltic composition is clinopyroxene + orthopyroxene + plagioclase + spinel (Kushiro and Yoder, 1966; Presnall *et al.*, 1979). Therefore, given the observed mineralogy, clinopyroxene compositions and the estimated crustal thickness for the SW Pacific region (Shor *et al.*, 1971) a pressure of 0.1GPa was assumed, however a range of temperatures is given in Table 2.4.1 to indicate a possible pressure range of 0.1GPa to 0.5GPa.

Inferred crystallisation temperatures for clinopyroxene rims using the method of Lindsley (1983) are listed in Table 2.4.1. Temperatures were also estimated for orthopyroxene and are good in agreement with the clinopyroxene rims. However co-existing clinopyroxene-orthopyroxene pairs in other samples did not yield useable temperature estimates, regardless of their apparent equilibrium conditions.

AU No.	Clinopyroxene				Orthopyroxene				Accepted
	En	Fs	Wo	T(°C)	En	Fs	Wo	T(°C)	T(°C)
47663	49	16	35	1115	60	36	4	1060	**1088**
47663	44	17	39	950	57	38	4	1095	**1023**
47663	48	17	35	1115	62	34	4	1100	**1108**
49172	48	14	38	1035	57	39	5	1075	**1055**
Average temperature = 1068°C at 0.1GPa									
Up to approximately = 1108°C at 0.5GPa									

Table 2.4.1: Crystallisation temperatures calculated from co-existing clinopyroxene-orthopyroxene rims using the method of Lindsley (1983). Clinopyroxene temperatures were estimated to the nearest 5°C and orthopyroxene was estimated to the nearest 10°C.

The validity of the Wood and Banno (1973) geothermometer has been questioned (Hawke, 1983). The Wood and Banno (1973) geothermometer yielded an average temperature of 1229°C ± 80°C which is higher than the temperatures estimated from Lindsley (1983), 1055-1095°C ± 10°C. The highest temperature estimate from Lindsley (1983) was 1115 ± 10°C, which is in good agreement with the lowest temperature estimates from Wood and Banno (1973) of 1143 ± 67°C. However, as the average temperature using the Wood and Banno (1973) method appears to be high for arc and back-arc basalts (Wilson, 1989) it is thought that pyroxene in the Tangihua Complex crystallised at temperatures of approximately 1068°C ± 80°C.

SECTION 2.5

Summary

The Tangihua Complex is dominated by porphyritic basaltic lavas with a cryptocrystalline - microcrystalline groundmass, which formed at pressures of 0.1GPa to 0.5GPa and temperatures of approximately 1068°C ± 80°C. The primary phenocryst assemblage is plagioclase with lesser amounts of clinopyroxene, orthopyroxene and magnetite and rare olivine, biotite and hornblende. Groundmass minerals are plagioclase and clinopyroxene with lesser amounts of orthopyroxene and magnetite.

Plagioclase phenocrysts have compositions in the range of An_{66-87} with an average of An_{74}, although rim and groundmass compositions are slightly more sodic. Clinopyroxene phenocrysts have an average of $En_{47}Fs_{15}Wo_{38}$ and Mg# of 61, whereas orthopyroxene composition average $En_{58}Fs_{38}Wo_4$ with Mg# = 46.

Alteration varies from weak to moderate and is very pervasive. Secondary minerals are chlorite, pumpellyite, actinolite, epidote, calcite, prehnite, mixed layer chlorite-smectite, quartz and zeolites. There appears to be only one major generation of veining. Mineral precipitation within the veins in dominated by calcite, however, sodic zeolites, such as analcime, stilbite and thomsonite, opaque minerals (pyrite and hematite) and apophyllite also occur.

The Poya terrane is dominated by porphyritic basalts, with 2-20 modal % plagioclase and clinopyroxene phenocrysts. The primary phenocryst assemblage is plagioclase + clinopyroxene >> orthopyroxene, magnetite and sphene. Plagioclase composition ranges from An_{30} to An_{85} with an average of An_{55}. Clinopyroxene phenocrysts are generally calcic augite, with an average composition of $En_{44}Fs_{13}Wo_{41}$. Fresh olivine, although rare, has a composition of Fo_{83-85} (Eissen *et al.*, 1998)

Low grade metamorphism is uniform throughout the PTB with virtually all samples containing mineral assemblages reflecting both the prehnite-pumpellyite and the greenschist metamorphic facies. Secondary minerals include; prehnite, pumpellyite, epidote, chlorite, albite and titanite (200-400°C), which correspond with the prehnite-pumpellyite metamorphic facies. In most areas minor actinolite and K-feldspar also occur as secondary mineral phases, suggesting that the temperatures associated with metamorphism were upwards of 300°C, indicating greenschist facies.

CHAPTER THREE: ALTERATION AND METAMORPHISM

SECTION 3.1

Introduction

Much of the data regarding mechanisms operating at low temperatures, in either arc or MOR environments, are derived from experimental studies, although more recently there have been several studies of MOR drill core from both the DSDP and ODP (Freyer *et al.*, 1990; Alt *et al.*, 1998). Hence, ophiolites, which are accessible fragments of oceanic crust exposed on land, are commonly studied as analogues for magmatic, tectonic and hydrothermal processes occurring at modern mid-ocean ridges. As these processes are more difficult to sample and examine directly, data from ophiolites have been used to model chemical and isotopic fluxes between seawater and the ocean crust during hydrothermal alteration (e.g. Gregory and Taylor, 1981; Bickle and Teagle, 1992; Alt, 1994). The same basic logic is also applied to mineralisation and massive sulfide deposits in ophiolites, which are also cited as analogues of black smokers and massive sulfide deposits actively forming at modern mid-ocean ridges (Hannington *et al.*, 1995).

Although the general structure and the processes of hydrothermal alteration appears to be very similar in both oceanic crust and ophiolites, some important differences exist. For example: the amount of seawater that has interacted with rocks in ophiolites is much greater than that in the oceanic crust; rock compositions are different, ophiolites generally contain more glassy rocks, mafic phases, and volatiles; there are variations in tectonic setting, and other effects. These differences all contribute to variations in hydrothermal alteration between ophiolitic and oceanic crust (Gillis and Robinson, 1990; Gillis and Thompson, 1993; Gillis, 1995; Pflumio, 1991; Schiffmann *et al.*, 1991; Bickle and Teagle., 1992; Alt, 1994; 1995; Alt *et al.*, 1996; Alt *et al.*, 1998). As such, it is important to remember these factors when examining the alteration and low temperature metamorphism of ophiolitic rocks in hopes of constraining their tectonic history. It is also important to remember that many other factors contribute to the alteration and/or metamorphism of ophiolitic basalts, such as interaction with seawater, burial diagenesis, and obduction or tectonically related metamorphism. When all these factors are accounted for and included in the study, it is often possible to make concise estimates regarding the tectonic history of a given ophiolite and, in this instance, the regional tectonic setting in which it formed.

The Tangihua Complex and Poya terrane ophiolites have been subjected to many different forms of alteration and/or metamorphism. By studying the alteration in these two systems we hope to be able to make observations regarding tectonism active in the Southwest Pacific during the Cretaceous - Oligocene. While the ophiolites of the Tangihua Complex provide an excellent opportunity to study the effects of low-temperature hydrothermal alteration on basalts, the

metamorphism of the Poya terrane basalts give further insight on the tectonic evolution of New Caledonia during ophiolite emplacement. As such, the alteration and metamorphism in each of these ophiolites provides information regarding specific local tectonic conditions and more general information regarding the entire region.

SECTION 3.2

Low-temperature alteration of basalts from the Tangihua Complex, New Zealand.

Nicholson, K.N. and Black, P.M., 1998, Low-temperature alteration of basalts from the Tangihua Complex, New Zealand, Proceedings of the 9th International Water/Rock Conference, 675-678.

ABSTRACT

Low-temperature hydrothermal alteration of the Tangihua Complex of Northland, New Zealand, is characterised by the zeolite minerals in veins, filling open spaces and in the rock. The alteration assemblages can be divided into three main phases based primarily on temperature but also influenced by the water/rock ratios. The initial phase of alteration is characterised by the Na-rich zeolites: analcime, stilbite and thomsonite with lesser amounts of natrolite and mesolite, while the groundmass and phenocryst alteration minerals include chlorite, actinolite, epidote and pumpellyite. Cooling of the system results in the transitional phase of alteration which is characterised by lower temperature minerals including mixed layer chlorite-smectite clays and Ca-rich zeolites with minor precipitation of both Na- and K-rich end members. Finally the system reaches temperatures <50°C with high water/rock ratios. During this stage of alteration both K^+ and Ca^{2+} start to precipitate as apophyllite and calcite in veins and open spaces and as calcite, smectite and smectite-chlorite in the groundmass. Eventually the Ca^{2+} becomes dominant resulting in the overprinting of earlier phases by secondary calcite.

INTRODUCTION

The interaction between seawater and basalt occurs under conditions ranging from low-temperature seafloor alteration (≈2°) to hydrothermal alteration within the oceanic crust (≤350°). There have been many studies of the high-temperature hydrothermal alteration processes of basalts which include the Ocean Drilling Project (e.g. Jeffery *et al.*, 1986) and oceanic ridge hot springs (e.g. Edmonds *et al.*, 1979 a,b; Campbell *et al.*, 1988; Bowers *et al.*, 1988; Massoth *et al.*, 1989). In contrast there is little data available on either the fluid or the solid phases involved in low-temperature alteration processes.

Most data regarding mechanisms operating at low temperatures is derived from experimental studies which show that low-temperature basalt alteration produces a slight but continuous loss of Mg^{2+}, Na^+ and K^+ and an enrichment of Ca^{2+} and SiO_2 in seawater while pH decreases slowly

(Seyfried and Bischoff, 1979). More recent studies based on field relations and mineral assemblages (i.e. Bednarz and Schmincke,1989; Guy *et al.*, 1992) support earlier results. Bednarz and Schmincke (1989) reported an increase in K^+ and Mg^{2+} and a decrease in Na in rocks in a cold seawater alteration zone (<20°C) while in their low-temperature hydrothermal alteration zone (<170°C) only Ca^{2+} is depleted and both Na^+ and K^+ are enriched.

Similar results were obtained by Guy *et al.* (1992) who show that low-temperature alteration of basalts by seawater is a function of the rock/water ratio (R/W). As R/W increases (up to 70g/l) there is an almost total removal of Mg^{2+} and K^+ and an enrichment of Ca^{2+}, Sr^{2+} and Si^{4+} from the interstitial waters. This process is accompanied by a decrease in pH and Eh and a depletion of ^{18}O and D. Increasing the R/W above 70 g/l results in a reversal of the Mg-Ca exchange and an enrichment of both ^{18}O and D. Their study attributes the chemical and isotopic reversals to the transformation of early precipitated Mg-rich saponite to a Ca-Na-rich saponite.

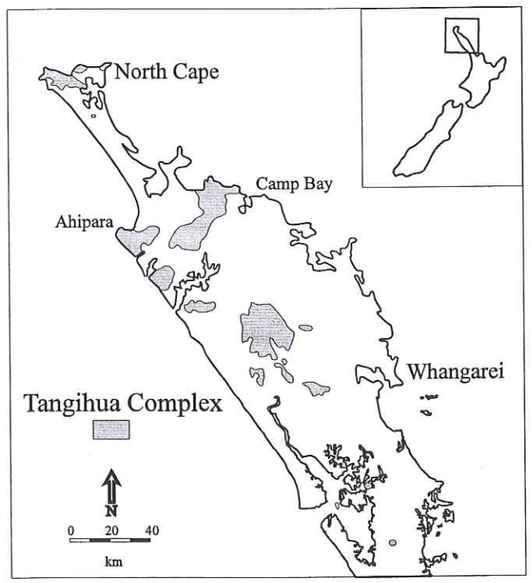

Figure 3.2.1: Outline map showing the relative location of Northland, New Zealand and the distribution of the ophiolite massifs of the Tangihua Complex, Northland, New Zealand.

The ophiolites of the Tangihua Complex (Figure 1) provide an excellent opportunity to study the effects of low-temperature hydrothermal alteration on basalts. The present study is based on new sampling and analyses and the reinterpretation of previous work. The findings of this study have been used in combination with other investigations of low-temperature alteration of basalts in order to determine the alteration history of the Tangihua Complex.

GEOLOGICAL SETTING

The ophiolitic igneous complexes in the northern regions of the North Island are collectively called the Tangihua Complex and informally known as the Northland Ophiolite. It is one of a number of ophiolites on the SW Pacific rim with a lower Tertiary emplacement age. The others include the Papuan Ultramafic Belt and the Massif du Sud ultramafics and the Poya terrane basalts of New Caledonia. The ophiolites in New Caledonia and Papua New Guinea include major belts of ultramafic and plutonic rocks which represent deep levels of oceanic lithosphere while the Tangihua Complex is dominated by rocks from the uppermost levels of the oceanic crust.

Tangihua Complex ophiolites occur as structurally discrete, rootless bodies which range in area from a few square metres to high standing massifs of up to 900 km^2. In general the complex consists of massive and pillowed basaltic lava sequences with intercalated sediments and lesser gabbro, microgabbro and basaltic intrusions. Chemically the lavas are dominantly tholeiitic basalts with N-MORB* affinities (* the interpretation of geochemical data has changed since the publication of this manuscript: see Chapters 4 and 5). The complex also includes minor felsic derivatives, younger alkalic intrusions (which exhibit within plate characteristics) and rare ultramafic rocks.

MINERALOGY OF SECONDARY PHASES

There are two distinct phases of alteration found in the Tangihua massifs. The majority of the massifs contain low-temperature hydrothermal/diagenetic minerals such as zeolites. Some of the massifs exhibit mineral assemblages characteristic of higher temperature hydrothermal alteration. In places the higher temperature assemblages have obscured the low-temperature alteration, however, in some massifs there is no evidence that the low-temperature assemblages were ever present. The massifs containing the higher temperature assemblages are associated with either cogenetic intrusive processes or much younger intrusive rocks which have been responsible for the higher grade of alteration. The secondary phases produced by high-temperature hydrothermal alteration in the Tangihua Complex are described by Leitch (1966), Mason (1973) and Farnell (1973).

The lower temperature alteration mineral assemblages in the Tangihua basalts can be divided into three phases: an early higher temperature phase, a transitional phase and late stage alteration (Tables 3.2.1, 3.2.2 and 3.2.3). The early higher-temperature phase of alteration is accompanied by the formation of chlorite, pumpellyite, actinolite, epidote and quartz both in the groundmass and replacing phenocrysts while in the later alteration phases only chlorite-smectite, smectite and rare

actinolite are found in the groundmass. Most of the secondary minerals are found only in veins and filling open spaces reflecting both the chemistry of the fluids and the lack of fracture related permeability which restricts the pervasive nature of the alteration.

Initially the alteration is characterised by Na^+ enrichment of the fluids with the precipitation of sodic zeolites, such as analcime, stilbite and thomsonite, in veins and open spaces. This phase is similar to the type I, high-temperature hydrothermal alteration zone, of Bednarz and Schmincke (1989) and to the transitional zone of Gillis and Robinson (1988).

Table 3.2.1

Early high-temperature alteration minerals	
Vein and open space filling	*Groundmass and phenocryst alteration*
analcime: $Na_{16}(Al_{16}Si_{32}O_{96}) \cdot 16H_2O$	Chlorite: $(Mg,Al,Fe)_3(Si,Al)_4O_{10}(OH)_2 \cdot (Mg,Al,Fe)_3(OH)_6$
stilbite: $NaCa_4(Al_9Si_{27}O_{72})$	Actinolite: $Ca_2(Mg,Fe^{2+})_5Si_8O_{22}(OH)_2$
thomsonite: $Na_4Ca_8(Al_{20}Si_{20}O_{80}) \cdot 24H_2O$	Epidote: $Ca_2Fe^{3+}Al_2O(Si_2O_7)(SiO_4)OH$
natrolite: $Na_{16}(Al_{16}Si_{24}O_{80}) \cdot 16H_2O$	Pumpellyite: $Ca_2MgAl_2(SiO_4)(Si_2O_7)(OH)_2 \cdot H_2O$
mesolite: $Na_{16}Ca_{16}(Al_{48}Si_{72}O_{240}) \cdot 64H_2O$	

During the reaction between seawater and basalts, at temperatures ranging from 70° to 425°C and a variety of water/rock ratios, Mg^{2+} is highly reactive. The precipitation of Mg-bearing clays (such as chlorite) and Mg-bearing minerals results in the depletion of Mg^{2+} in the fluids (Bischoff and Dickson, 1975; Seyfried and Mottl, 1982) which generates high acidity. This generally results in the leaching of Ca^{2+} and K^+ from the rocks. The enrichment of Na in the fluids is thought to be the result of a combination of decreased water/rock ratios and the higher temperatures. These findings are in agreement with Bednarz and Schmincke (1989). They believe that the marked up take of K^+ accompanied by a characteristic change from Na_2O loss to Na_2O uptake in the fluids, indicates increasing temperature and/or lower water/rock ratios (e.g. Mottl *et al.*, 1979; Seyfried and Bischoff, 1981; Mottl 1983).

Secondary minerals in the groundmass and phenocrysts suggest a temperature for hydrothermal alteration of approximately 250°-300°C: given that chlorite forms at temperatures up to 275°C, actinolite at >250°C and epidote at >260°C. Precipitation of the cogenetic zeolite assemblage in veins and open spaces is possible within this temperature range. Thomsonite has a moderately well constrained temperature of formation of between 150° and 275°C while stilbite generally precipitates at temperatures between 70° and 200°C.

During the transitional alteration phase the water/rock ratio remained low. At low water/rock ratios the pH of the fluids is reduced to near-neutral conditions and the fluids become enriched in Mg^{2+}, while Ca^{2+} and to a lesser extend K^+ is removed (Guy *et al.*, 1992). The transitional phase of alteration also represents the result of cooling within the system. The secondary phases seen in the groundmass are minor and include calcite, mixed layer chlorite-smectite (150°-180°C) and lesser amounts of prehnite while the precipitating zeolites range from Ca-rich to K-rich end members. In other words, a cooler system with low water/rock ratios resulted in a Ca-rich fluid which precipitated predominantly Ca-rich zeolites, while the formation of clay minerals (such as chlorite-smectite) depleted the fluid of what little Mg^{2+} it contained.

Table 3.2.2

Transitional phase alteration minerals	
Vein and open space filling	*Groundmass and phenocryst alteration*
chabazite: $Ca_2(Al_4Si_8O_{24}) \cdot 12H_2O$	chlorite-smectite and/or smectite
Heulandite: $(Na,K)Ca_4(Al_9Si_{27}O_{72}) \cdot 24H_2O$	calcite: $CaCO_3$
Clinoptilolite: $(Na,K)_6(Al_6Si_{30}O_{72}) \cdot 20H_2O$	prehnite: $Ca_2Al(AlSi_3O_{10})(OH)_2$
Laumontite: $Ca_4(Al_8Si_{16}O_{48}) \cdot 16H_2O$	

The latest phase of alteration in these rocks is a low-temperature (<50°C) phase characterised by the precipitation of Ca- and minor K-rich minerals in the veins and open spaces. Plagioclase phenocrysts are almost totally replaced by smectite and calcite which may overprint earlier alteration of plagioclase to K-feldspar. Calcite and apophyllite are found in veins and open spaces.

Most other primary phenocrysts and groundmass assemblages have been altered to smectite and lesser amounts of both calcite and smectite-chlorite.

Table 3.2.3

Late phase alteration minerals	
Vein and open space filling	*Groundmass and phenocryst alteration*
apophyllite: $KCa_4Si_8O_{20}(F,OH) \cdot 8H_2O$ calcite: $CaCO_3$	smectite and/or smectite-chlorite calcite: $CaCO_3$

This secondary mineral assemblage suggests alteration temperatures of less than 50°C and high water/rock ratios such that the rock becomes enriched in K^+ while the fluids are enriched in Na^+ and Ca^+ (Gillis and Robinson, 1988; Guy *et al.*, 1992). This phase of alteration corresponds to the cold seawater alteration zone of Bednarz and Schmincke (1989). At some stage the fluids become oversaturated with respect to Ca^+ resulting in the precipitation of calcite as the final mineral phase in the paragenetic sequence. Calcite precipitation may have overprinted an earlier K-rich assemblages which are typically characteristic of this type of alteration (Gillis and Robinson, 1988; Guy *et al.*, 1992), however, there is little evidence that this phase was present.

CONCLUSIONS

Alteration in the Tangihua Complex of Northland, New Zealand, can be divided into three main phases based primarily on temperature but is also influenced by the water/rock ratios. The earliest phase of alteration occurs at high temperatures (250°-300°C) and low water/rock ratios and is characterised by Na-rich zeolites, such as analcime, stilbite and thomsonite, which are found filling veins and open spaces. Cooling of the system results in a transitional phase of alteration which is characterised by lower temperature minerals including mixed layer chlorite-smectite clays and Ca-rich zeolites with minor precipitation of both Na- and K-rich end members. The water/rock ratio remains low during the transitional phase. The last phase of alteration in the system occurs at temperatures <50°C with high water/rock ratios. While both K^+ and Ca^{2+} start to precipitate, the system must have become Ca-oversaturated as Ca^{2+} is the late precipitating phase.

The zeolite minerals appear to be the most responsive to changes in the water/rock ratio, fluid chemistries and temperature. The lack of characteristic groundmass alteration minerals may be due

to low permeability in the rock. Hence the precipitating zeolite assemblages are, in part, used to characterise each phase of alteration.

SECTION 3.3

Alteration/low grade metamorphism and its tectonic significance in ophiolitic basalts from the Poya terrane, New Caledonia, and Tangihua Complex, New Zealand

Nicholson, K.N., Black, P.M. and Picard, C., Submitted in July, 1999, to *Journal of Metamorphic Geology.*

ABSTRACT

The evolution and the tectonic history of the Southwest Pacific are poorly constrained between the Cretaceous and the Miocene. However, during this period several ophiolitic complexes formed and were emplaced, including the Tangihua Complex of New Zealand and the Poya terrane of New Caledonia.

A varied tectonic history is suggested for New Caledonia, based on patterns of alteration and low grade metamorphism. The first mineral assemblage precipitated in the Poya terrane basalts represents greenschist facies metamorphism. The greenschist event is thought to result from alteration by mixed hydrothermal fluids and seawater. Following the greenschist event was a period of lower temperature and pressure when zeolites formed. These were then partially overprinted by a higher temperature and pressure event. In the north-eastern regions of New Caledonia, this stage of metamorphism reached blueschist facies metamorphism. It has been proposed that blueschist metamorphism was caused by either partial subduction of the oceanic crust or the obduction of the overlying ultramafics.

In contrast the alteration patterns in the Tangihua Complex of New Zealand suggests that little or no tectonic activity occurred between the formation and obduction of the ophiolite. A classic, low temperature, seafloor alteration sequence was developed. This alteration assemblage can be divided into three main phases based primarily on temperature: an initial phase of Na-rich zeolite precipitation, followed by a transitional cooling phase, characterised by K-, Na- and Ca-rich zeolites, and finally, at <50°C. a period of K- and Ca-dominated mineralisation. The alteration mineral assemblages also indicate that the emplacement event itself was cold as the vein mineral assemblage associated with obduction primarily contains Ca-bearing phases, suggesting temperatures of less than <50°C, and at low pressures as there are no overprinting by either high temperature or high pressure phases.

INTRODUCTION

Many factors contribute to the alteration and/or metamorphism of ophiolitic basalts; these include interaction with seawater, burial diagenesis and obduction or tectonically related metamorphism. The interaction between seawater and basalt occurs under conditions ranging from low-temperature seafloor alteration (<20°C) to hydrothermal alteration within the oceanic crust (~350°). Burial diagenesis usually occurs at temperatures ranging from 100 to 300°C and pressures ranging up to 1 kbar, whereas tectonically related metamorphism can occur over a wide range of temperatures and pressures.

There are many similarities between the Tangihua Complex, New Zealand, and the Poya terrane, New Caledonia, ophiolites, including their age of formation and emplacement (Figure 3.3.1). Consequently, it has been proposed that the two systems are somehow related (Parrot and Dugas, 1980; Aitchison *et al.*, 1995). As a result, a program has been started to compare the formation and emplacement of the two ophiolitic complexes and to determine the tectonic history of the SW Pacific during the early Tertiary. One of the most compelling differences between the two ophiolite systems is the different alteration, metamorphism and, hence, tectonic history of the two regions.

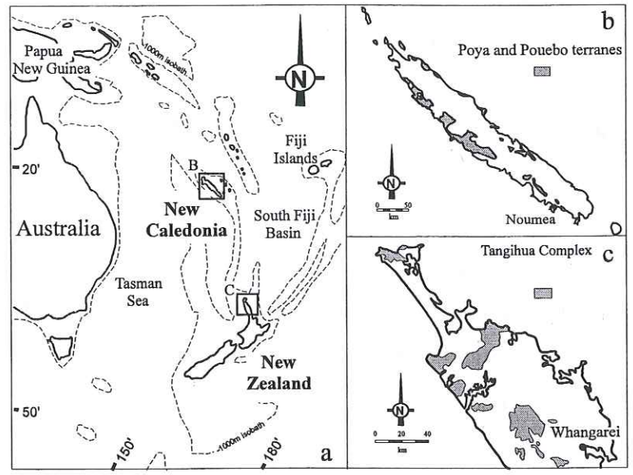

Figure 3.3.1. Location map of the SW Pacific region showing the position of New Zealand and New Caledonia, and showing the distribution of the ophiolite massifs in (b) the Tangihua Complex, Northland, New Zealand, and (c) the Poya terrane (including the Pouebo terrane), New Caledonia.

The Poya terrane, of New Caledonia, is a major geological unit, which is exposed along both the west and east coasts (Figure 3.3.1c). It is a tectonically complex set of submarine mafic volcanic rocks, dolerites, gabbros and associated abyssal sediments. In this paper the Poya terrane includes the Pouébo terrane, which is thought to have formed with the Poya terrane but was dismembered, forming an ophiolitic melange, and subjected to a higher degree of post-emplacement metamorphism (Picard *et al.*, 1999). The ophiolitic igneous complexes in the northern regions of

the North Island, New Zealand, are collectively called the Tangihua Complex (Ferrar, 1934). In general, the complex consists of massive and pillowed basaltic lava sequences with intercalated sediments and lesser gabbro, microgabbro and basaltic intrusives.

MINERALOGY OF SECONDARY PHASES

New Caledonia

There have been four distinct stages of alteration and/or metamorphism, throughout the Poya terrane (Table 3.3.1). The two early stages of alteration occurred before obduction began and are the result of ocean floor metamorphism, which, in this case, ranged from prehnite-pumpellyite to greenschist facies. Following these initial stages was a blueschist event (stage 3; Table 3.3.1), apparently associated with subduction of limited regional extent (Cluzel *et al.*, 1997; D. Cluzel and C. Picard, pers. comm.) and found only in the northeastern regions of New Caledonia. The final stage of alteration was simple, post obduction, weathering.

Low grade metamorphism is uniform throughout the Poya basalts , on both the east and west coasts, with almost all samples containing mineral assemblages reflecting both prehnite-pumpellyite and greenschist metamorphic facies. Secondary minerals include; prehnite, pumpellyite, (formed at 200-400°C), epidote (>230-260°C; Bird *et al.*, 1984), chlorite (>230-275°C; Kristmannsdottir, 1975; Schifman and Fridleifsson, 1991), albite and titanite (200-400°C; Bird *et al.*, 1984), and minor actinolite (>250-300°C; Kristmannsdottir, 1975), and K-feldspar (>300°C; greenschist facies). It is possible that the distribution of prehnite-pumpellyite versus greenschist metamorphic facies may relate to minor changes in permeability whereby the thermal gradient was suppressed (~230°C for the prehnite-pumpellyite facies) by the circulation of cold seawater whereas in zones of lower permeability restricted seawater circulation resulted in slightly higher temperatures (approximately 300°C for the greenschist facies).

Prehnite, pumpellyite and chlorite occur throughout the groundmass and in veins. Both chlorite and pumpellyite occur as alteration products of plagioclase and pyroxene. Albite generally occurs as a recrystallised phase of plagioclase whereas titanite usually occurs as an alteration phase of pyroxene and oxide minerals. Fine needles of actinolite are found in patches of chlorite and pumpellyite, and also line veins and fill open spaces. Epidote is a common vein mineral and often occurs in association with prehnite or scattered throughout the groundmass as a patchy secondary phase. K-feldspar and oxychlorite are both rare secondary phases. K-feldspar usually occurs as an alteration product of plagioclase, whereas oxychlorite occurs as small grains associated with chlorite.

Stage 1: Metamorphic Minerals – Greenschist	
Vein and open space filling	*Groundmass and phenocryst alteration*
Chlorite: $(Mg,Al,Fe)_3(Si,Al)_4O_{10}(OH)_2 \cdot (Mg,Al,Fe)_3(OH)_6$ Epidote: $Ca_2Fe^{3+}Al_2O(Si_2O_7)(SiO_4)OH$ Prehnite: $Ca_2Al(AlSi_3O_{10})(OH)_2$ Pumpellyite: $Ca_2MgAl_2(SiO_4)(Si_2O_7)(OH)_2 \cdot H_2O$	Actinolite: $Ca_2(Mg,Fe^{2+})_5Si_8O_{22}(OH)_2$ Albite: $NaAlSi_3O_8$ Chlorite: $(Mg,Al,Fe)_3(Si,Al)_4O_{10}(OH)_2 \cdot (Mg,Al,Fe)_3(OH)_6$ Epidote: $Ca_2Fe^{3+}Al_2O(Si_2O_7)(SiO_4)OH$ K-feldspar: $KAlSi_3O_8$ Prehnite: $Ca_2Al(AlSi_3O_{10})(OH)_2$ Pumpellyite: $Ca_2MgAl_2(SiO_4)(Si_2O_7)(OH)_2 \cdot H_2O$ Titanite: $CaTiOSiO_4$
Stage 2: Alteration minerals	
Vein and open space filling	*Groundmass and phenocryst alteration*
Analcime: $Na_{16}(Al_{16}Si_{32}O_{96}) \cdot 16H_2O$ Apophyllite: $KCa_4Si_8O_{20}(F,OH) \cdot 8H_2O$ Chabazite: $Ca_2(Al_4Si_8O_{24}) \cdot 12H_2O$ Natrolite: $Na_{16}(Al_{16}Si_{24}O_{80}) \cdot 16H_2O$ Thomsonite: $Na_4Ca_8(Al_{20}Si_{20}O_{80}) \cdot 24H_2O$	Analcime: $Na_{16}(Al_{16}Si_{32}O_{96}) \cdot 16H_2O$ Calcite: $CaCO_3$ Chlorite: $(Mg,Al,Fe)_3(Si,Al)_4O_{10}(OH)_2 \cdot (Mg,Al,Fe)_3(OH)_6$
Stage 3: Metamorphic Minerals – Blueschist	
Vein and open space filling	*Groundmass and phenocryst alteration*
Actinolite: $Ca_2(Mg,Fe^{2+})_5Si_8O_{22}(OH)_2$ Albite: $NaAlSi_3O_8$ Calcite: $CaCO_3$ Chlorite: $(Mg,Al,Fe)_3(Si,Al)_4O_{10}(OH)_2 \cdot (Mg,Al,Fe)_3(OH)_6$ Epidote: $Ca_2Fe^{3+}Al_2O(Si_2O_7)(SiO_4)OH$ Lawsonite: $CaAl_2Si_2O_7(OH)_2 \cdot H_2O$ Phengite: $K_2(Mg,Fe,Al)_3AlSi_3O_{10}(OH)_2$ Pumpellyite: $Ca_2MgAl_2(SiO_4)(Si_2O_7)(OH)_2 \cdot H_2O$ Quartz: SiO_2 Reibeckite: $Na_2Fe^{2+}{}_3Fe^{3+}{}_2Si_8O_{22}(OH)_2$ Titanite: $CaTiOSiO_4$ Stipnomelane: $K_{0.6}(Fe,Mg)_6(Si_8Al)(O,OH)_{27} \cdot 2\text{-}4H_2O$	Actinolite: $Ca_2(Mg,Fe^{2+})_5Si_8O_{22}(OH)_2$ Albite: $NaAlSi_3O_8$ Chlorite: $(Mg,Al,Fe)_3(Si,Al)_4O_{10}(OH)_2 \cdot (Mg,Al,Fe)_3(OH)_6$ Lawsonite: $CaAl_2Si_2O_7(OH)_2 \cdot H_2O$ Na-pyroxene: $NaAlSi_2O_6$ Pumpellyite: $Ca_2MgAl_2(SiO_4)(Si_2O_7)(OH)_2 \cdot H_2O$ Reibeckite: $Na_2Fe^{2+}{}_3Fe^{3+}{}_2Si_8O_{22}(OH)_2$ Titanite: $CaTiOSiO_4$ Stipnomelane: $K_{0.6}(Fe,Mg)_6(Si_8Al)(O,OH)_{27} \cdot 2\text{-}4H_2O$
Stage 4: Alteration/Weathering Minerals	
Vein and open space filling	*Groundmass and phenocryst alteration*
Smectite and/or smectite-chlorite	Smectite and/or smectite-chlorite

Table 3.3.1: Outline of the four stages of alteration and metamorphism found in the Poya terrane, complete with the observed mineral assemblages, for both vein/open space filling and groundmass/phenocryst alteration, and the chemical formula for each mineral.

The secondary minerals in this phase of metamorphism reflect the introduction of Ca and Fe into veins and open spaces. Experimental work suggests this is the result of interaction between hot host rocks and seawater, which may result in a loss of these elements from the seawater (Guy *et al.*, 1992) and may reflect low R/W ratios and hence low permeability. The apparent low porosity is supported by the lack of secondary minerals, such as epidote, albite, titanite, actinolite and K-feldspar, in the veins and open spaces. The apparent enrichment of Fe may simply indicate a

change in seawater chemistry as a result of fluid/rock interactions, whereby, the secondary mineral assemblage may reflect a change in oxidation state, from Fe^{+2} to Fe^{+3}, and the precipitation of oxidised phases such as epidote and oxychlorite. The presence of a wide variety of secondary minerals in the groundmass indicates no bulk change in the groundmass chemistry as supported by whole rock geochemistry.

Metamorphism was been closely followed by and overlapped with a lower temperature event, resulting in the precipitation of zeolites, primarily in late stage veins and open spaces. Zeolite minerals include analcime, apophyllite, thomsonite, natrolite and chabasite. Zeolite precipitation is also associated with the formation of chlorite and calcite throughout open spaces, veins and the groundmass but no zeolites occur within the groundmass. Plagioclase phenocrysts alter to analcime, and both plagioclase and clinopyroxene are partially altered to chlorite. Chlorite alteration is likely, in part, to be related to the earlier higher temperature stage of metamorphism. Again it can be argued using selective whole rock analyses that the bulk chemistry of the groundmass is little changed, where as the veins and open spaces are enriched in Na. The precipitation of primarily sodic zeolites reflects cooling of the system, from around 300°C to less than 250°C (Bischoff and Dickson, 1975; Seyfried and Mottl, 1982; Gillis and Robinson, 1988). There is no evidence to suggest a change in the R/W ratios.

The blueschist facies rocks contain a varied mineralogy and several generations of veins suggesting a complex metamorphic history (for more detail see Black and Brothers, 1977). Relict primary minerals are common and in many cases primary textures are preserved. Metamorphic minerals are commonly zoned and overgrown. Relict primary pyroxenes are rimmed by more sodic pyroxene, amphibole or pumpellyite, whereas primary amphiboles are rimmed by riebeckite or actinolite. Feldspars have been replaced by albite-pumpellyite mattes. Opaque minerals are replaced by titanite and to a lesser extent by pyrite and/or hematite. In all cases the groundmass has been replaced by chlorite – pumpellyite – albite ± lawsonite ± stipnomelane. Using oxygen isotope data for quartz-phengite pairs and mineral chemistry, Black and Brothers (1977) suggest metamorphic temperatures of approximately 350°C and pressures of 7kb. Several generations of veins are present within these rocks. Vein minerals include pumpellyite, calcite, stipnomelane, albite, actinolite, riebeckite, epidote, titanite, phengite, chlorite and quartz. Veins containing epidote and riebeckite are younger than the pumpellyite bearing veins. In this case, it appears that the oxidation state of Fe is reflected in the changing vein mineral assemblage. In general, the veining is thought to post date the highest temperature and pressure phase of blueschist metamorphism. In this manner the vein mineralogy and paragenetic sequence may reflect thermal relaxation as the temperatures and pressures of the system decreased following the blueschist phase of metamorphism.

The last stage of alteration in the Poya basalts was essentially the product of weathering and occurs after the blueschist metamorphic event. Smectite and chlorite-smectite clays are found throughout the many samples, replacing phenocryst and groundmass minerals, which had already undergone some amount of alteration. In places most of the pre-existing clay minerals have been altered to smectite.

New Zealand

There have been two distinct phases of alteration in the Tangihua massifs (Table 3.3.2). Most of the massifs contain low-temperature hydrothermal/diagenetic minerals such as zeolites, but some of the massifs also exhibit mineral assemblages characteristic of higher temperature alteration. The massifs containing the higher temperature assemblages are associated with the products of either cogenetic intrusive processes or much younger intrusive rocks, which have been responsible for the higher grade of alteration. The secondary phases, produced by high-temperature hydrothermal alteration, in the Tangihua Complex, are described in detail by: Leitch (1966), Mason (1973) and Farnell (1973). For a more detailed description of the low temperature alteration mineral assemblages, than is given below, see Nicholson and Black (1998).

Early high-temperature alteration minerals	
Vein and open space filling	*Groundmass and phenocryst alteration*
Analcime: $Na_{16}(Al_{16}Si_{32}O_{96}) \cdot 16H_2O$ Mesolite: $Na_{16}Ca_{16}(Al_{48}Si_{72}O_{240}) \cdot 64H_2O$ Natrolite: $Na_{16}(Al_{16}Si_{24}O_{80}) \cdot 16H_2O$ Stilbite: $NaCa_4(Al_9Si_{27}O_{72})$ Thomsonite: $Na_4Ca_8(Al_{20}Si_{20}O_{80}) \cdot 24H_2O$	Actinolite: $Ca_2(Mg,Fe^{2+})_5Si_8O_{22}(OH)_2$ Chlorite: $(Mg,Al,Fe)_3(Si,Al)_4O_{10}(OH)_2 \cdot (Mg,Al,Fe)_3(OH)_6$ Epidote: $Ca_2Fe^{3+}Al_2O(Si_2O_7)(SiO_4)OH$ Pumpellyite: $Ca_2MgAl_2(SiO_4)(Si_2O_7)(OH)_2 \cdot H_2O$
Transitional phase alteration minerals	
Vein and open space filling	*Groundmass and phenocryst alteration*
Chabazite: $Ca_2(Al_4Si_8O_{24}) \cdot 12H_2O$ Clinoptilolite: $(Na,K)_6(Al_6Si_{30}O_{72}) \cdot 20H_2O$ Heulandite: $(Na,K)Ca_4(Al_9Si_{27}O_{72}) \cdot 24H_2O$ Laumontite: $Ca_4(Al_8Si_{16}O_{48}) \cdot 16H_2O$	Calcite: $CaCO_3$ Chlorite-smectite and/or smectite Prehnite: $Ca_2Al(AlSi_3O_{10})(OH)_2$
Late phase alteration minerals	
Vein and open space filling	*Groundmass and phenocryst alteration*
Apophyllite: $KCa_4Si_8O_{20}(F,OH) \cdot 8H_2O$ Calcite: $CaCO_3$	Smectite and/or smectite-chlorite Calcite: $CaCO_3$

Table 3.3.2: Outline of the three stages of alteration and metamorphism found in the tangihua Complex, complete with the observed mineral assemblages, for both vein/open space filling and groundmass/phenocryst alteration, and the chemical formula for each mineral.

Low-temperature hydrothermal alteration of the Tangihua Complex is characterised by the zeolites in veins, filling open spaces, in the groundmass and in phenocrysts. The alteration assemblages can be divided into three main phases based primarily on their formation temperatures but they have also been influenced by the water/rock ratios. The early higher-temperature phase of

alteration was accompanied by the formation of chlorite, pumpellyite, actinolite, epidote and quartz, which occur both in the groundmass and replace phenocrysts whereas in the later alteration phases only chlorite-smectite, smectite and rare actinolite are present in the groundmass. Most of the secondary minerals form only veins and fill open spaces reflecting both the chemistry of the fluids and the lack of fracture permeability which restricts the pervasive nature of the alteration.

Initially the alteration is characterised by Na^+ enrichment from the fluids with the precipitation of sodic zeolites, such as analcime, stilbite and thomsonite, in veins and open spaces. The enrichment of Na^+ in the fluids is thought to be the result of a combination of a decrease water/rock ratios and the hotter fluids (Bischoff and Dickson, 1975; Seyfried and Mottl, 1982; Gillis and Robinson, 1988). Secondary minerals in the groundmass and phenocrysts suggest a temperature of hydrothermal alteration of approximately 250°-300°C given that discrete chlorite appears at temperatures of ~230 to >275°C (Kristmannsdottir, 1975; Schifman and Fridleifsson, 1991), actinolite at >250°C (Kristmannsdottir, 1975) and epidote at >230°C (Bird *et al.*, 1984). Precipitation of the cogenetic zeolite assemblage in veins and open spaces possibly occurred within this temperature range. Thomsonite has a moderately well constrained temperature of formation of between 150° and 275°C whereas stilbite generally precipitates at temperatures between 70° and 200°C.

The transitional phase of alteration results from cooling within the system. During this phase, the water/rock ratio remained low. At low water/rock ratios the pH of the fluids is buffered and hence reduced to near-neutral with the fluids becoming enriched in Mg^{2+}, whereas Ca^{2+} and to a lesser extend K^+ are removed (Guy *et al.*, 1992). The secondary phases in the groundmass are minor and include calcite, mixed layer chlorite-smectite (>150°-180°C; Kristmannsdottir, 1975; Schifman and Fridleifsson, 1991) and lesser amounts of prehnite whereas the precipitating zeolites range from Ca-rich to K-rich end members.

The last phase of alteration in these rocks was a low-temperature (<50°C) phase characterised by the precipitation of Ca- and minor K-rich minerals in the veins and open spaces, such as calcite and apophyllite. Plagioclase phenocrysts are almost totally replaced by smectite and calcite, which may overprint earlier alteration of plagioclase to K-feldspar. Most other primary phenocrysts and groundmass assemblages have altered to smectite and lesser amounts of both calcite and interlayered chlorite - smectite.

The enrichment of K^+ in the rock and Na^+ and Ca^{2+} in the fluids, suggests high water/rock ratios (Gillis and Robinson, 1988; Guy *et al.*, 1992). This phase of alteration corresponds to the cold seawater alteration zone of Bednarz and Schmincke (1989). At some stage the fluids become oversaturated with respect to Ca^{2+} resulting in the precipitation of calcite as the final mineral phase in the paragenetic sequence. Calcite precipitation may have overprinted earlier K-rich assemblages

which are typically characteristic of this type of alteration (Gillis and Robinson, 1988; Guy *et al.*, 1992), however, there is no evidence that this phase was ever present.

DISCUSSION

There are several of ophiolites on the south-west Pacific rim with an early Tertiary emplacement age, such as the Papuan Ultramafic Belt, the Tangihua Complex of New Zealand and the Massif du Sud ultramafics and the Poya terrane basalts of New Caledonia (Davies, 1968; Prinzhofer *et al.*, 1980; Cluzel *et al.*, 1997). The ophiolites in Papua New Guinea and the Massif de Sud, in New Caledonia, include major belts of ultramafic and plutonic rocks, which represent deep levels of oceanic lithosphere whereas the Tangihua Complex and the Poya terrane are dominated by rocks derived from the uppermost levels of the oceanic crust.

The overall structure of the Southwest Pacific region can be summarised as resulting from successive openings of marginal basins that isolated ridges of either continental, oceanic or intermediate nature since the late Cretaceous. Current tectonic models for the Cenozoic evolution of New Caledonia involve incipient collision between a south-west facing arc and thinned continental margin crust, the attempted subduction of which choked the system (Aitchison *et al.*, 1995). Progressive development of this collision zone can be found from Papua New Guinea through to New Zealand. In New Zealand, ophiolite formation was the result of the westward obduction of an arc/back-arc oceanic crustal sequence across the continental margin (Nicholson *et al.*, (b) in review). As such, ophiolitic basalts from these areas have been subjected to many different forms of alteration and/or metamorphism. By studying the alteration in these contrasting systems we are able to make deductions about the different tectonic regimes active in the Southwest Pacific during the Cretaceous. As discussed in detail below, the ophiolites of the Tangihua Complex provide an excellent opportunity to study the effects of low-temperature hydrothermal alteration of basalts, whereas the metamorphism of the Poya terrane basalts give further insights into the tectonic evolution of New Caledonia during ophiolite emplacement.

New Caledonia

There have been four distinct stages of alteration, and/or metamorphism, in the basalts of the Poya terrane. Initially there was probably a "typical" low temperature, low pressure ocean floor alteration sequence within the Poya terrane basalts, which proceeded, or was associated with, higher temperature seafloor hydrothermal alteration. In this instance any lower temperature event would have been overprinted by a greenschist to prehnite-pumpellyite metamorphic event. This later event occurred at temperatures <300°C, low pressures, and was the result of mixing of hydrothermal

fluids and circulating seawater. Continued cooling of the system eventually allowed the precipitation of zeolites, however during this early period of alteration, mineral precipitation was inhibited by low porosity within the basalts.

During the early zeolite alteration stage, calcite and chlorite filled veins, both cross cutting and parallel to earlier veins. There is little offset between the vein sets which suggests no large scale tectonism was involved with either phases of veining. Veins associated with large scale tectonic events appears to be later and are infilled with late calcite, chlorite and minor opaques. Despite the obviously high degree of shearing throughout the region, it appears that the deformation was late stage and occurred at low temperatures given its associated mineral assemblage.

The later high pressure event, which probably occurred during the Late Eocene, was associated with ductile deformation and resulted in blueschist facies metamorphism which partially to totally overprinted the earlier alteration. The grade and pervasive nature of the blueschist metamorphism increases to the north-west along the east coast of New Caledonia. The polarity of the high pressure event, combined with kinematic analyses of low angle shears and normal faults, suggests a south or south-south-west convergence of the Poya Nappe (Cluzel *et al.*, 1997). Cluzel *et al.* (1995) proposed that the high pressure alteration is in fact the result of a period of subduction. In this model the ocean floor basalts of the Poya terrane were initially, partially, subducted beneath an eastward verging system. During this process the Poya terrane basalts recrystallised under blueschist facies conditions, whereas the northern Pouébo terrane (Figure 3.3.1b; considered to be an extension of the Poya terrane basalts; Cluzel *et al.*, 1999; Picard *et al.*, 1999.) has undergone further metamorphism to the eclogite facies. The entire subduction system later becomes choked, resulting in the overthrusting, deformation and delamination of the upper sequences of the oceanic crust, hence emplacing the Poya terrane ophiolites and the overlying Massif de Sud (ultramafics). This model explains the variations within the blueschist phase, the slightly younger obduction related vein sets and accounts for the limited extent of this phase on the western side of the island.

The final stage of alteration within the Poya terrane is one of simple weathering. This phase produced smectite and interlayered chlorite-smectite of both primary and secondary minerals

New Zealand

There have been many studies made of the high-temperature hydrothermal alteration of basalts; these include the Ocean Drilling Project (e.g. Jeffery *et al.*, 1986) and oceanic ridge hot springs (e.g. Edmonds *et al.*, 1979 a,b; Campbell *et al.*, 1988; Bowers *et al.*, 1988; Massoth *et al.*, 1989). In contrast most of the data about the fluid and solid phases involved in low-temperature alteration processes derives from experimental studies (e.g. Seyfried and Bischoff, 1979). The ophiolites of the Tangihua Complex, however, provide an excellent opportunity to make a field

based study of the effects of low-temperature hydrothermal alteration on basalts. Hence, in combination with other investigations of low-temperature alteration of basalts, such as those mentioned above, the alteration history of the Tangihua Complex can be determined.

The alteration in the Tangihua Complex has been be divided into three main phases which are similar to those observed in both field studies and experimental work on ocean floor basalts (Gillis and Robinson, 1988; Bednarz and Schmincke, 1989; Guy *et al.*, 1992). The development of this type of alteration sequence reflects a relatively simple and/or stable tectonic history. The initial stage of alteration was characterised by the precipitation of zeolites into veins and other open spaces. The zeolites appear to have been the most responsive to changes in the water/rock ratios, fluid chemistries and temperature. The lack of characteristic groundmass alteration minerals may be due to the low permeability in the rocks. The zeolite stage of alteration occurred before ophiolite obduction, as evidenced by the cross cutting relationships between the zeolite bearing veins and the younger, obduction generated, vein sets and shears. However, it is possible that the initial stages of obduction (and hence, both extension and compression of the system) were responsible for changes in the permeability of the system effecting the last stages of alteration. Changes in permeability, and hence the water/rock ratios, would have influenced the precipitating mineral phases, however, the influence of such a change is hard to quantify, and possibly inconsequential, given that the last alteration phase occurs at low temperatures, <50°C, which was most likely the dominant factor.

CONCLUSIONS

The two systems studied are thought to be related due to the presence of similar lithological units and paleontological ages (Avias, 1953; Lillie and Brothers, 1969; Fleming, 1970; 1979; Paris and Bradshaw, 1977; Stevens, 1977), and the similarities between the formation and obduction of the basalts within the ophiolitic complexes of the Poya terrane and the Tangihua Complex. Consequently, information regarding the conditions of alteration and metamorphism within both systems can yield valuable information about the tectonic environment in the Southwest Pacific.

In New Zealand, the ocean floor alteration of the Tangihua Basalts suggests that little or no major tectonic activity occurred between their formation, approximately 80Ma, and their L. Eocene obduction, approximately 40Ma. This enabled a "typical" low temperature, seafloor alteration sequence to develop in a manner comparable to other systems. The alteration mineral assemblages also indicate that the obduction event itself was cold and at low pressures as there was no overprinting by either high temperature or high pressure phases.

In New Caledonia, the patterns of alteration and metamorphism suggest a more varied tectonic history, characterised by greenschist metamorphism followed by a period of lower

temperature and pressure, zeolite precipitation. The presence of zeolite filled, cross cutting vein sets suggest that there was some tectonic stress within the Poya terrane basalts during this time, however, the lack of major offset within the veins indicates that this tectonic event was not major. Zeolite precipitation was followed, in turn, by a higher temperature and pressure blueschist event. The blueschist stage of metamorphism is thought to be the result of either partial subduction of the oceanic crust or, less probably, the consequent obduction of the upper parts of the ocean crustal sequence.

The final stage of alteration in both systems is a simple weathering. This suggests that tectonism has not greatly affected either system between the obduction event and the present day.

ACKNOWLEDGEMENTS

This research has been supported by the University of Auckland, New Zealand, the French Embassy, Wellington, NZ, and by the Université Joseph Fourier, France. Special thanks to Dr. P.R.L. Browne for reading the draft and making many useful comments.

SECTION 3.4

Summary

The patterns of alteration and metamorphism seen in the Tangihua Complex, New Zealand and the Poya terrane, New Caledonia, are different. Hence the post-formational history of the two units is also different.

The Tangihua Complex exhibits a "typical" low temperature, seafloor alteration sequence developed in a manner comparable to other systems. The development of this type of alteration sequence reflects a relatively simple and/or stable tectonic history. The initial stage of alteration was characterised by the precipitation of zeolites into veins and other open spaces at temperatures ranging up to 350°C. This was followed by a transitional, cooling phase of alteration and finally by a low temperature (<50°C) phase of alteration that was dominated by the precipitation of calcite. The zeolite stage of alteration occurred before ophiolite obduction, as evidenced by the cross cutting relationships between the zeolite bearing veins and the younger, obduction generated, vein sets and shears, which are dominated by calcite. Hence, in New Zealand, the ocean floor alteration of the Tangihua Basalts suggests that little or no major tectonic activity occurred between their formation, approximately 80Ma, and their L. Eocene obduction, approximately 40Ma.

Alteration in the Poya terrane can be characterised by four distinct stages of alteration, and/or metamorphism. The first phase of metamorphism was a greenschist to prehnite-pumpellyite event that occurred at temperatures <300°C. Cooling of the system eventually allowed the precipitation of zeolites, however during this early period of alteration, mineral precipitation was inhibited by low porosity within the basalts. During the early zeolite alteration stage, calcite and chlorite filled veins, both cross cutting and parallel to earlier veins. There is little offset between the vein sets which suggests no large scale tectonism was involved with either phases of veining. However, low temperature alteration was followed by a higher pressure event, associated with ductile deformation, which resulted in blueschist facies metamorphism. The grade and pervasive nature of the blueschist metamorphism increases to the north-west along the east coast of New Caledonia. The final stage of alteration within the Poya terrane is one of simple weathering. This phase produced smectite and interlayered chlorite-smectite of both primary and secondary minerals. The patterns of alteration and metamorphism suggest a more varied tectonic history for the Poya terrane than in the Tangihua Complex.

CHAPTER FOUR: WHOLE ROCK GEOCHEMISTRY

SECTION 4.1

Geochemistry of the Tangihua Complex: an overview

This Chapter begins, in section 4.1, by presenting some background information, including an introduction, sample selection and preparation procedures, and some information regarding element mobility during hydrothermal alteration and metamorphism. Section 4.1 will finish with a brief summary of the principle observations and diagrams. Sections 4.2 and 4.3 are both designed for publication and consequently some background information is repeated in each. The first manuscript was submitted for publication to *Tectonophysics* in January, 1999, and the second was submitted to the *Tectonophysics* in October, 1999. The paper in section 4.2 deals specifically with the chemistry of the Tangihua Complex basalts, whereas the second paper, section 4.3, presents the combined chemistry and tectonic implications, for both the Tangihua Complex and the Poya terrane. Section 4.4 contains new radiogenic isotope data for the Tangihua Complex. Finally, section 4.5 deals with the chemistry of the glass samples found within the Tangihua Complex and has not yet been submitted for publication.

INTRODUCTION

This study has investigated the geochemistry of the basaltic rocks in the Tangihua Complex and the Poya terrane and in particular concentrates on the Tangihua Complex basalts (TCB).

Basalts represent a major portion of the igneous rocks generated on Earth. Their major, trace, rare earth element and isotopic compositions can provide us with much information about the nature and history of their sources provided we can decipher the physical and chemical processes involved during magmatic evolution (i.e. partial melting, fractionation, mixing, contamination). Analyses of intrusive and cumulate compositions, from the Tangihua Complex, have been included for discussion and for comparative purposes.

Initial interpretation of the Tangihua Complex, as an ophiolite, was that of one generated in a mid-ocean ridge type spreading system (Malpas *et al.*, 1992). However, ophiolites are now more commonly interpreted as fragments of island arc or back-arc basin crust. Subduction is an important process during the formation of these ophiolitic complexes, that are better known today as "suprasubduction zone (SSZ) ophiolites" (Pearce *et al.*, 1984; Taylor and Nesbitt, 1988; Shervais, 1990; Jones *et al.*, 1991; Hawkins and Florendo, 1992). Studies of trace and rare earth element variations in tandem with other lines of geologic evidence have permitted more confident identification of SSZ ophiolites as forming in either a back-arc or island arc environment.

However, detailed understanding of magma genesis in a variety of extensional tectonic settings within present day SSZ is hampered by a paucity of data.

Recently, geochemical studies on several ophiolites have revealed the presence of volcanic and hypabyssal rock suites exhibiting both mid-ocean ridge basalt and island arc tholeiite affinities within the sample complex (e.g. Alabaster *et al.*, 1982; Coleman, 1984; Shervias and Kimbrough, 1985; Ishiwatari *et al.*, 1990, Pedersen and Furnes, 1991). The varying geochemistry of these rock suites are attributed to evolving mantle sources, different degrees of partial melting, crystallisation or other processes operative during magma generation, ascent and extrusion (Arculus, 1987; Furnes *et al.*, 1992, Taylor *et al.*, 1992).

Perhaps one of the most outstanding examples of re-interpretation of the environment of formation of an ophiolite is that of the Troodos Ophiolite. The Troodos Ophiolite was originally considered to be a fragment of typical oceanic crust produced at a mid-ocean ridge spreading centre (Moores and Vine, 1971; Gass and Smewing, 1973), but has since been convincingly re-interpreted as a SSZ ophiolite (McCulloch and Cameron, 1983; Rautenschlein *et al.*, 1985). Many other ophiolites are being interpreted for the first time or being re-interpreted as SSZ ophiolites. Such is the case with the Tangihua Complex. The data presented in this Chapter show that the Tangihua Complex was undoubtedly formed in a SSZ environment. The remaining debate is to the nature of this environment.

As with the Tangihua Complex, there has been much controversy over the years as to the generation and emplacement of the Poya terrane in New Caledonia. However, recent re-evaluation of the field relations, geochemistry and age of the PTB have resulted in new theories for its genesis and emplacement (Cluzel *et al.*, 1994; 1997; Eissen *et al.*, 1998; this study: Section 4.3, Figure 4.3.7). Although some controversy still exists, for the most part, the results of this study support the recent interpretations, which suggest the Poya terrane was generated during the opening of a marginal basin to the north-east of New Caledonia. In this sense the Poya terrane ophiolite is more of a classic example of a MOR-type ophiolite. However, as the geochemistry shows, there are signs of a subduction zone influence in the generation of the Poya terrane.

SAMPLE SELECTION AND ANALYTICAL PROCEDURE

A collection of over 120 basalt samples from the Tangihua Complex and 35 basalt samples from the Poya terrane have been analysed for major oxides and trace elements. From these, 34 TCB and 17 PTB samples with total volatile content < 4wt% were chosen for REE analyses. See Figures 4.1.1(a) and (b) for sample locations.

In general the samples were selected on the basis of location and freshness. From New Zealand, the samples selected for analysis range from the Flat Top Quarry, just north of the city of Auckland to the very northern most point of New Zealand, at North Cape. From New Caledonia, samples were taken from the Poya terrane along the east and west coasts, to provide as large a coverage as possible. Both field relations and petrographic analyses were used to select the freshest samples. All samples with LOI > 4wt% were discarded from discussion within this thesis and in published papers. However, the entire set of data is given in Appendix 8 and 9.

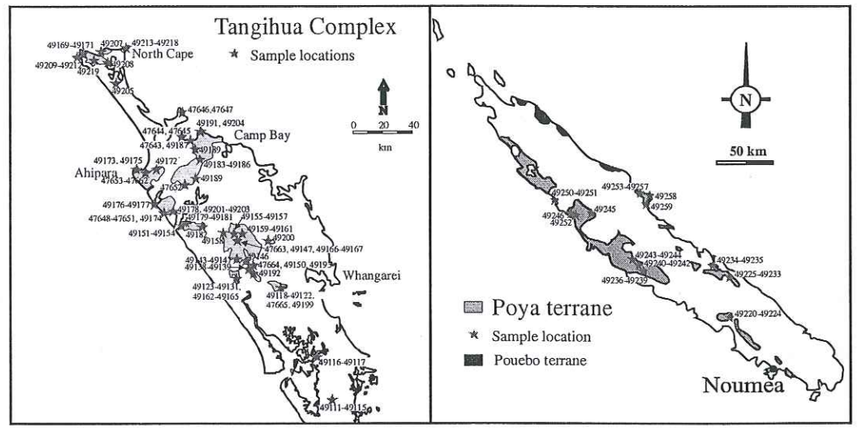

Figure 4.1.1: Sample location maps for the Tangihua Complex, Northland, New Zealand and the Poya terrane, New Caledonia. For more detail see Figure 1.4.1.

External surfaces of fresh rocks were removed by splitting and the remaining samples split into chips, which were then ground to a powder in a tungsten carbide ring grinder. H_2O+, H_2O- and CO_2 were determined by gravimetry, the remaining major oxides and trace elements were determined by XRF (after Norrish and Chappell, 1977) at the University of Auckland, New Zealand. Major oxide compositions were determined on glass fusion discs, whereas trace element content was determined using powder pellets bound with boric acid. Analytical precision was controlled by use of standard samples and duplicate measurements. The precision (2θ) of the major oxide determinations is generally less than 2%, and less than 5% for the trace elements (at ten times the detection limit of 1-2 ppm). All analyses were undertaken using uniform calibration conditions and are reported in diagrams on a 100%, volatile free basis.

Rare earth element (REE) abundances, Rb, Sr, Ba, Y, Zr, Nb, Cs, Ta, Th, U, Hf, Nb, La and Ce, were determined by Inductively Coupled Plasma Mass Spectroscopy (ICP-MS) at the Laboratoire de Geodynamique des Chaînes Alpines (LGCA – ESA5025), Université Joseph Fourier, Grenoble, France, following the procedure of Barrat *et al.*, 1996. The precision (2θ) for

ICP-MS analyses is generally better than 5% for all REE and trace elements. In some cases the precision may range up to10% for the elements analysed, specifically for Zr and Hf, due to chemical complexing in solution, however, Zr values were confirmed with XRF analyses and appear to be more precise.

Sr and Nd isotopic ratios were determined using chemical separation methods and then Inductively Coupled Plasma Mass Spectroscopy (ICP-MS) at the Toulouse Université, France. Approximately 0.1g of powdered sample was firstly leached in acid to remove alteration products and then attacked using HCl and HF to isolate the trace and rare earth elements. Secondly the samples were put through separation columns to isolate Sr and Nd. Sr separation required the addition of 4N, 1.5N and 6N HCl, H_2O and ammonium citrate, which isolates both Sr and Rb, a second column (μSr) used 1.5N HCl to eliminate Rb. A separate column was used to separate Nd, which used 0.3N HCl. The resulting solutes were then analysed for Sr and Nd isotopic ratios, respectively.

Oxygen isotopic analyses were performed at the Institute of Geological and Nuclear Sciences, Wellington, New Zealand. Prior to extraction of oxygen, samples and standards were placed in an oven for 48 hours at 150°C to remove absorbed and loosely bound water. Samples, still hot, were quickly placed in the sample chamber and evacuated to minimise re-absorption of moisture. Oxygen was extracted from the glass using a CO_2 laser and BrF_5, similar to the method described by Sharp (1990). Samples were left over night in a BrF_5 atmosphere (5 kpa) and then pre-treated repeatedly with BrF_5, prior to extraction, until CO_2 blank values were <0.1 micromoles. All samples were normalised to the quartz standard NBS 28 (assuming a value of +9.6‰) with one standard analysed for every four samples. All values are reported relative to VSMOW and reproducibility is generally better than 0.2‰.

CHEMICAL MOBILITY

A geochemical study of major, trace and rare earth elements is only of use when combined with an understanding of the ways in which geochemical processes control their behaviour. Element mobility is a major concern when trying to interpret geochemical data. In rocks that are known or suspected to have undergone some amount of weathering or hydrothermal alteration, such as those from the Tangihua Complex and the Poya terrane, it becomes necessary to evaluate the effects these processes have on different elements.

Trace element mobility is controlled by the mineralogical changes which take place in a rock during alteration and the nature of the altering fluid phase. In general the incompatible HFS elements, including the REEs (Sc, Y, Th, Zr, Hf, Ti, Nb, Ta and P) and some transitional metals

(Co, Ni, V and Cr) tend to be immobile (Winchester and Floyd, 1977; Wood *et al.*, 1981; Shervais, 1982). The LFS elements (Cs, Sr, Rb, K and Ba) and the transitional metals (Mn, Zn and Cu) are mobile, particularly at high temperatures (Seewald and Seyfried, 1990). Many exceptions to this generalisation exist (Hellman and Henderson, 1977; Hellman *et al.*, 1979); for example the traditionally immobile REEs appear to be more easily released from a glassy basalt than from a crystalline rock of the same composition (Humphries, 1984).

The main controls on trace element mobility, however are mineralogy and fluid chemistry. The REEs tend to be more easily mobilised by halogen-rich or carbonate-rich mineralising fluids in a rock in which they would normally be stable with respect to the movement of an aqueous fluid (Humphries, 1984). Yet another example of unusual trace element mobility, specifically REE, Y, B and P, occurs during the low temperature cryptic alteration of apatite (Banfield and Eggleton, 1989). Many authors have noted the presence of elevated P_2O_5 values in seemingly unaltered volcanic rocks (Green, 1978; Roden *et al.*, 1984; Foder *et al.*, 1989; Price *et al.*, 1991; Kuschel and Smith, 1992). In these cases the high P_2O_5 levels are accompanied by elevated REE, Y and Ba, and occur in rock suites which otherwise show 'normal' element behaviour patterns and display no petrologic evidence for possible REE enrichment. Banfield and Eggleton (1989) found that a six fold increase in the abundance of REEs accompanied the replacement of apatite by secondary phosphate minerals, such as rhabdophane ($(La,Ce,Y)PO_4{\cdot}H_2O$) and florencite ($CeAl_3(PO_4)_2(OH)_6$), during the weathering of granites.

Bignall (1994) has shown that the mobility of Rb and Ba can be related to potassic alteration. At the Orakeikorako-Te Kopia geothermal fields the replacement of feldspar by adularia was accompanied by almost proportional increases in K and Rb. At the same time an increase in Ba concentration was noted, although Ba levels are also effected by illite formation. Other effects of potassic alteration include lowering the concentration of the major elements Ca and Na, as K replacement occurs in the feldspars.

Many of the basaltic rocks in this study are known to have been subjected to hydrothermal alteration and low temperature metamorphism. Processes such as those above may account for some of the unusual trace element contents found in some of the samples. In general, however, the basaltic samples chosen for geochemical analyses show no signs of alteration or metamorphism.

See Chapter 3 for a detailed description of the effects of alteration and low temperature metamorphism in the Tangihua Complex and the Poya terrane.

GEOCHEMICAL SUMMARY OF THE TANGIHUA COMPLEX BASALTS

Major and trace element analyses of 120 lavas are tabulated in Appendix 8 and 9. Sr and Nd isotopic analyses are tabulated in Appendix 10, whereas O isotopic analyses are tabulated in Appendix 9. Representative major and trace element analyses are listed in Table 4.2.1 and Sr and Nd isotopes are listed in Table 4.4.1. The results of the O isotopes are given and discussed in Section 5.3.

A variety of schemes have been used to classify igneous rocks. This thesis utilises the IUGS classification scheme, which is based on total alkalis versus SiO_2 (Figure 4.1.2; Le Bas *et al.*, 1986; Le Maire *et al.*, 1989). To further classify the Tangihua lavas the plot of K_2O versus SiO_2 is used to assign a K-series (Figure 4.1.2; after Peccerillo and Taylor, 1976; Ewart, 1982; Tatsumi and Eggins, 1995), FeO^{total}/MgO versus SiO_2 (Figure 4.1.3) and the ternary AFM (Figure 4.1.4; total alkalies-FeO^{total}-MgO) diagram. These diagrams allow discrimination between the calc-alkaline and tholeiitic series (Kuno, 1968; Irvine and Baragar, 1971; Miyashiro, 1974). MORB and chondrite normalised trace element diagrams are shown in Figure 4.1.6 and 4.1.7, which illustrate the MORB and arc components in the Tangihua Complex. Figures 4.1.8 and 4.1.5 show the variations of Sr versus Nd isotopes and SiO_2 versus Mg# (=100*Mg/(Mg+Fe)) and are also used to estimate how close the lavas might have been to equilibrium with mantle peridotite (Tatsumi and Eggins, 1995).

Most studies of ophiolite complexes feature multiple analyses, which illustrate the MORB-like, the arc-like or the back-arc-like nature of the system. It is very rare in the literature to find ophiolites which have lavas with geochemical signatures indicating both arc and back-arc affinities (e.g. Taylor *et al.*, 1992; Gaggero *et al.*, 1997; Cortesogno *et al.*, 1998). It is more common to find literature which describes currently active arc/back-arc systems (e.g. Volpe *et al.*, 1987; Woodhead *et al.*, 1993; Gamble *et al.*, 1995). The Tangihua Complex shows a continuum between the back-arc and the arc lavas and, as such, provides a rare opportunity to study the processes that have generated both the arc and the back-arc in an ancient ophiolitic system.

Figures 4.1.2 – 4.1.9 provide a wealth of information regarding the basaltic Tangihua lavas. For convenience, the diagrams are grouped together on consecutive pages. The following is a listing of the principle observations:

(1) The lavas span a restricted compositional array with a dominant basaltic – basaltic andesite component and a very minor andesitic component (Figure 4.1.2). The average SiO_2 content is 52.6 wt.% with a standard deviation of 1.79 wt.%, maximum at 59.6 and a minimum at 49.5 wt.%.

(2) The lavas are subalkaline (Figure 4.1.2). The samples all contain normative hypersthene, plagioclase and diopside, with some containing normative quartz and others with normative olivine.

(3) The basalts can be categorised as a low-K series (Figure 4.1.3) with <0.4 wt.% K_2O.

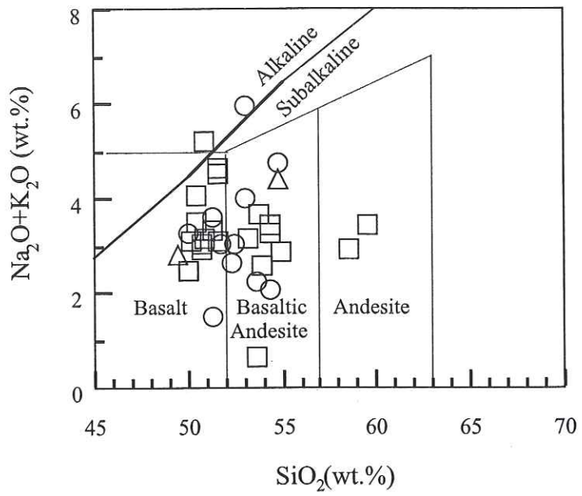

Figure 4.1.2: Geochemical classification of Tangihua lavas. Subalkaline basaltic - basaltic andesite predominate. The same symbols are used throughout the thesis. Circles : arc-type lavas. Squares : back-arc type lavas. Triangles: younger 'alkaline' intrusions. Field bounaries after Le Maitre *et al.* (1989), alkaline-subalkaline boundary after Rickwood (1989).

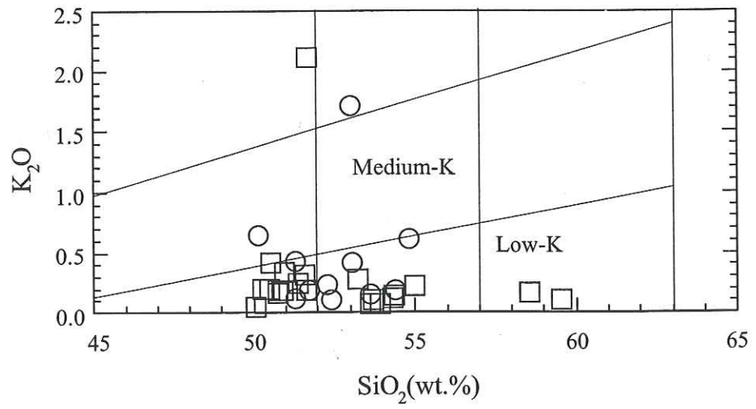

Figure 4.1.3: Geochemical classification of Tangihua lavas into a K-series Low-K series lavas predominate. Series boundaries after Ewart (1982).

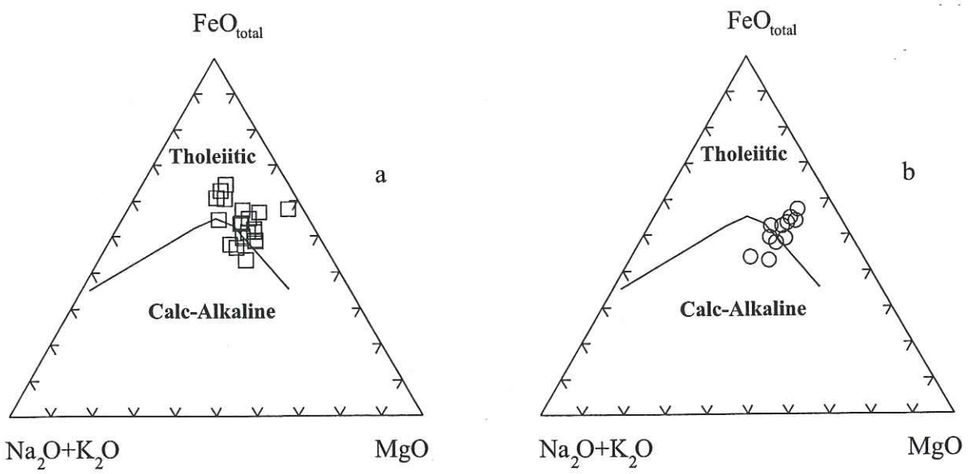

Figure 4.1.4: Tholeiitic versus calc-alkaline classification of the Tangihua lavas (AFM: after Irvine and Baragar, 1971). (a) Back-arc lavas define a predominantely tholeiitic trend. (b) Arc lavas define a more calc-alkaline trend. Symbols as in Figure 4.1.2.

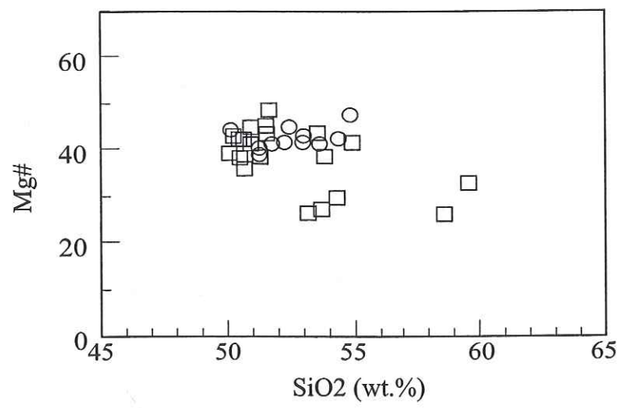

Figure 4.1.5: Variation diagram of Mg# versus SiO_2 for the Tangihua lavas. All lavas have Mg# < 50 and are far from equilibrium with mantle peridotite (Tatsumi and Eggins, 1995). Symbols as in Figure 4.1.2.

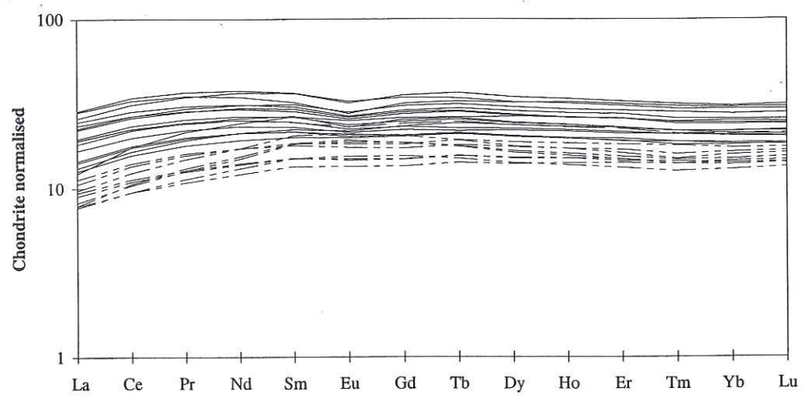

Figure 4.1.6: Chondrite normalised REE diagram for the Tangihua lavas. Normalising factors after Evensen *et al.* (1978). REE abundances increase with differentiation. Solid line: back-arc lavas. Dashed line: arc lavas.

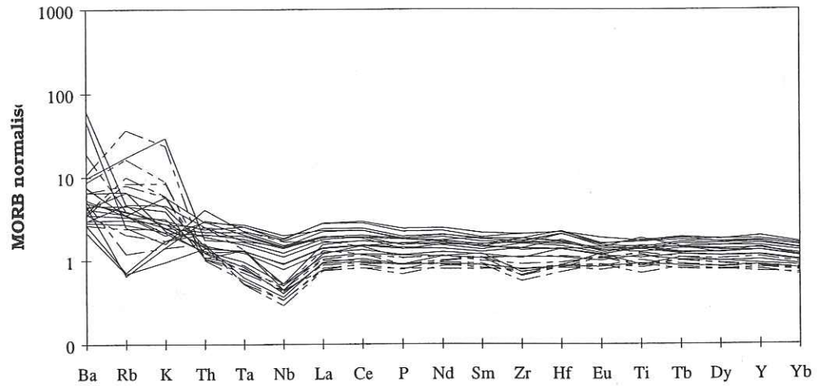

Figure 4.1.7: MORB normalised incompatible element diagram for the Tangihua lavas. Normalisation factors after Sun and McDonough, (1989). The Tangihua lavas have flat HFSE ratios and are enriched in LILE. Solid line: back-arc lavas. Dashed line: arc lavas.

(4) The lavas form a dominantly tholeiitic trend. However, when the back-arc lavas are separated from the arc lavas it becomes apparent that the arc lavas have a more calc-alkaline trend whereas the back-arc lavas are tholeiitic (Figure 4.1.4).

(5) Most of the lavas have Mg#<45 (Figure 4.1.5). The arc lavas have an average Mg#=42, whereas the back-arc lavas have an average Mg#=38.5. However, it should be noted that the back-arc lavas have the widest range in Mg# and the highest overall value of 48.2. Lavas which correspond to a primary liquid in equilibrium with mantle peridotite prior to eruption have Mg#>70 (Tatsumi and Eggins, 1995) and, therefore, the composition of the Tangihua basaltic lavas suggest that magmas were severely modified by some process(es) between melting and eruption.

(6) The lavas show a range in REE-contents (Figure 4.1.6). The arc lavas are the most depleted with between 8 and 20 times the chondrite value and the back-arc are less depleted with REE contents between 10 and 40 times the chondrite value. Both the arc and the back-arc chondrite normalised REE patterns are light REE depleted with many of the more evolved samples showing an Eu anomaly.

(7) The lavas show a large degree of scatter, but an overall enrichment, in LILE elements relative to MORB (Figure 4.1.7). The HFSE contents level out and are very close to MORB for the arc lavas but slightly enriched for the back-arc lavas. All lavas show a negative Nb anomaly which is strongly developed in the arc samples. Both the LILE and the HFSE concentrations increase with progressively with SiO_2 content.

(8) The $^{87}Sr/^{86}Sr$ and $^{143}Nd/^{144}Nd$ ratios are higher and lower, respectively, than MORB but overlap the OIB (Ocean Island Basalt) and SW Pacific arc/back-arc fields (Figure 4.1.8).

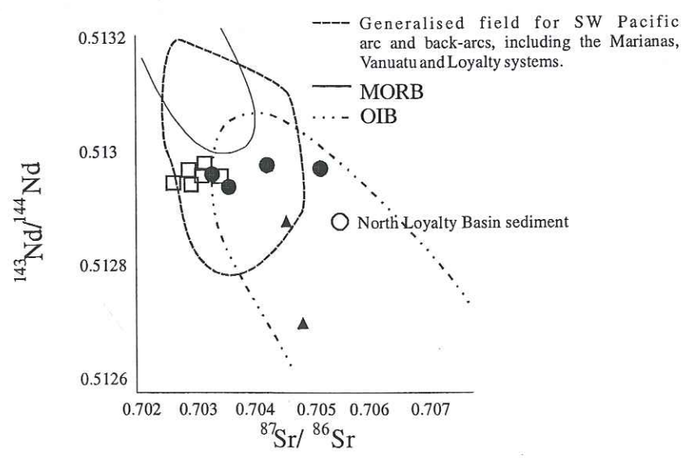

Figure 4.1.8: $^{87}Sr/^{86}Sr$ versus $^{143}Nd/^{144}Nd$ for the Tangihua Complex basaltic lavas. Circles: AIB, squares: BAB and triangles: younger instrusions.

(9) The lavas form trends on variation diagrams, which appear to be controlled by crystal fractionation (Figure 4.1.9). However, caution should be used when interpreting potential fractionation trends as the spatial relationships between massifs is unknown. MgO is used as the X-axes as the range in SiO_2 content is small and therefore, SiO_2 is not a good fractionation index.

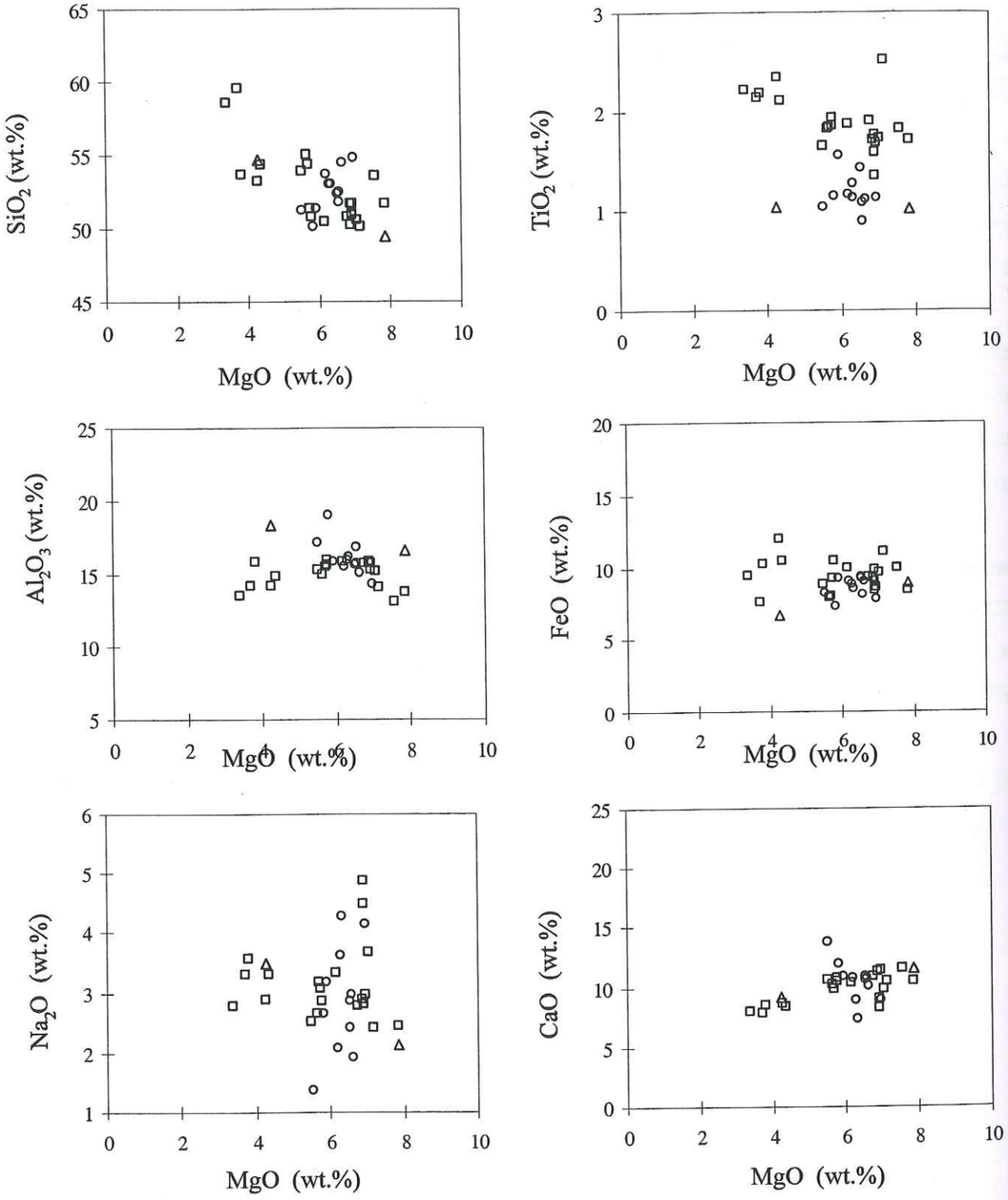

Figure 4.1.9: Variation diagrams for the Tangihua Complex basalts plotted with respect to MgO. Only samples analysed for REE are shown.

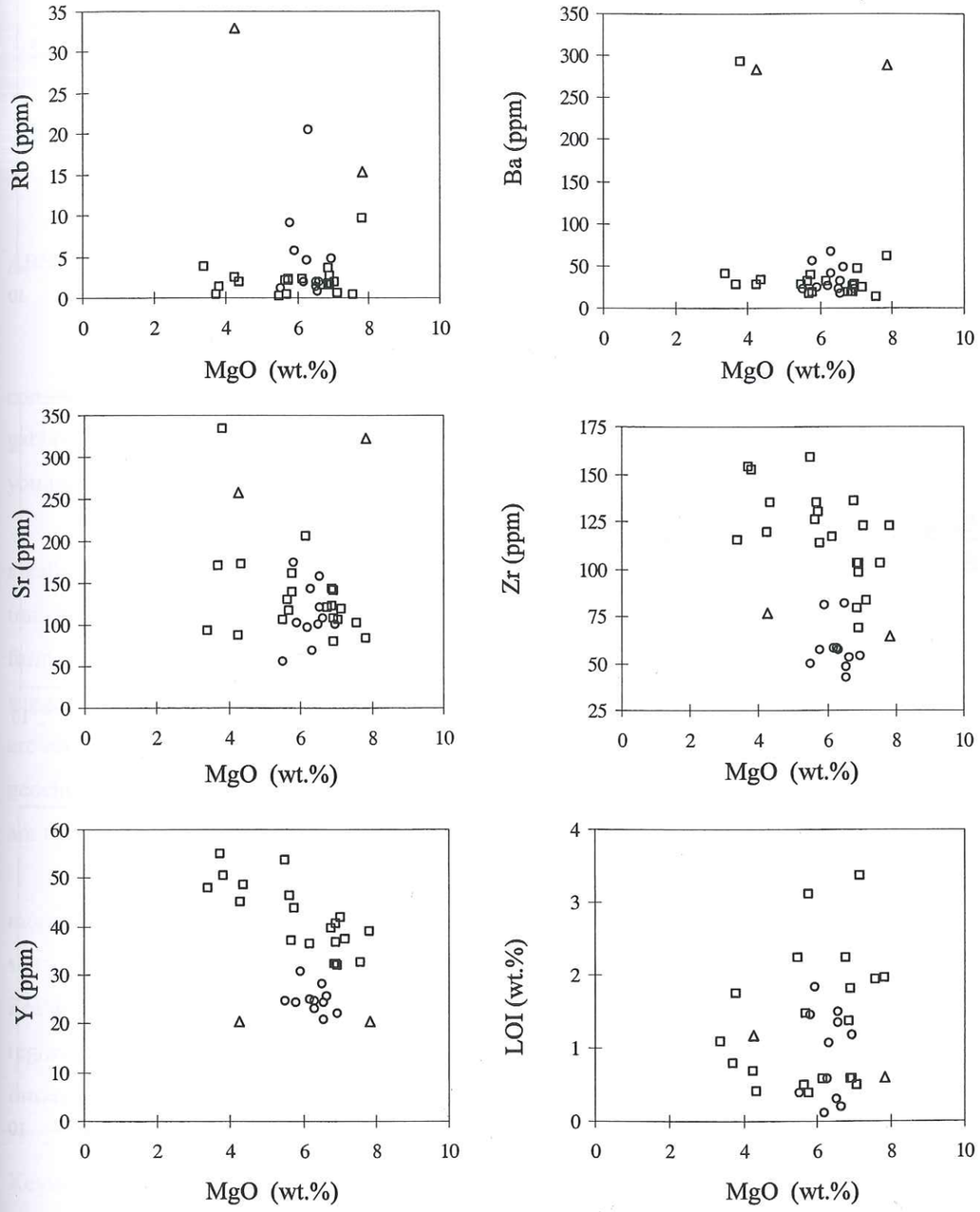

Figue 4.1.9: continued. Variation diagrams for the Tangihua Complex basalts plotted with respect to MgO.

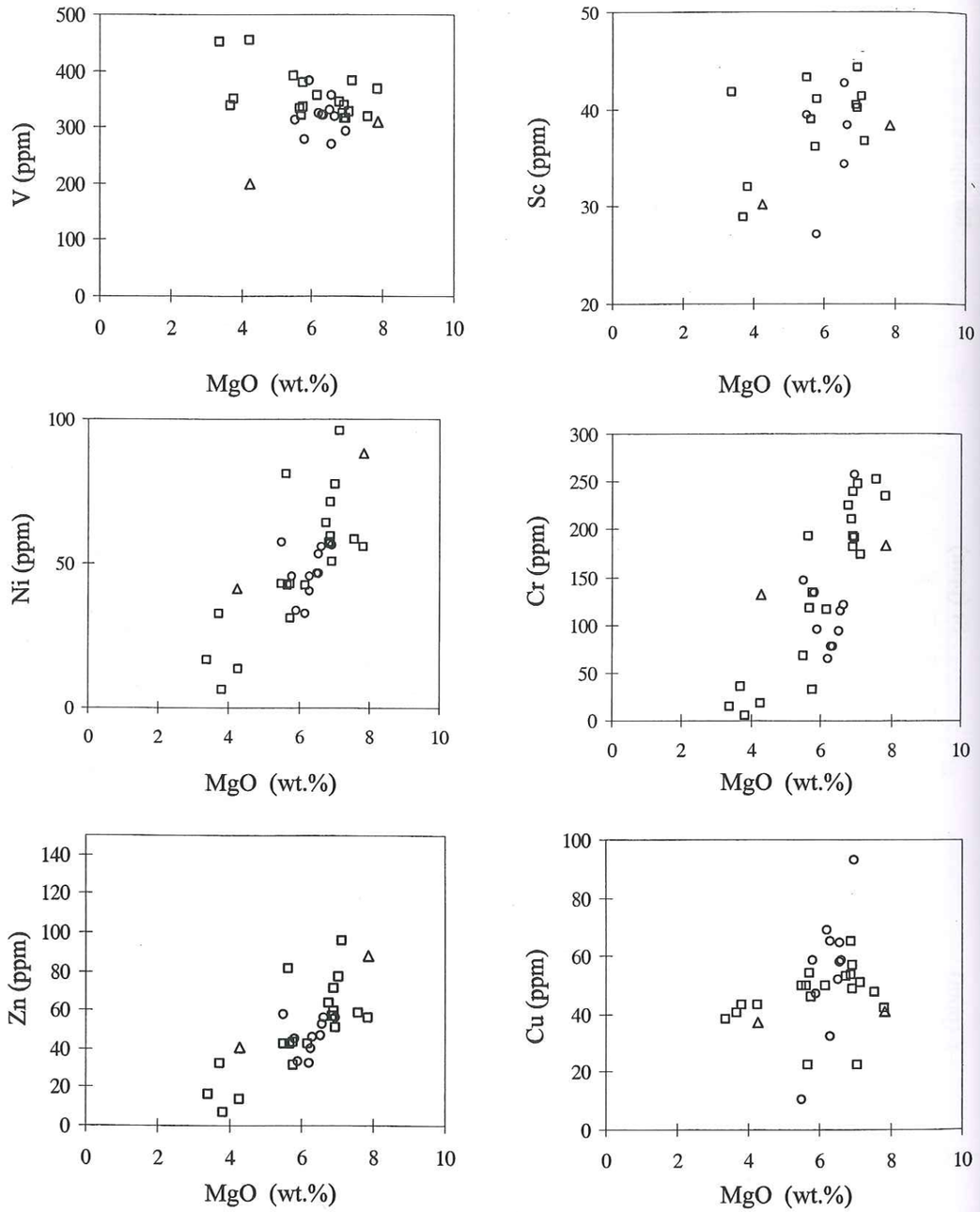

Figue 4.1.9: continued. Variation diagrams for the Tangihua Complex basalts plotted with respect to MgO.

SECTION 4.2

Geochemistry and tectonic significance of the Tangihua Ophiolite Complex, New Zealand

Nicholson, K.N., Black, P.M. and C. Picard, C., Accepted November 1999, by *Tectonophysics.*

ABSTRACT

The ophiolitic igneous complexes of the Tangihua Complex of Northland, New Zealand consist of massive and pillowed basaltic lava sequences with intercalated sediments and lesser gabbro, microgabbro and basaltic intrusions. The complex also includes minor felsic derivatives, younger alkalic intrusions (which exhibit within-plate characteristics) and rare ultramafic rocks.

The lavas are relatively homogeneous and are dominantly tholeiitic basalts with minor calc-alkaline and alkaline affinities. The complex nature of the chemistry, in particular those lavas with transitional arc signatures, and the presence of non-arc lavas, is clear evidence that these volcanics formed in a suprasubduction zone environment. The combined geochemical and tectonic constraints suggest that the Tangihua Complex formed in either a transitional zone between an arc and a back-arc setting, or in a zone of migration from arc to back-arc volcanism. As such, the field, age and geochemical data supports the model in which these rocks formed suprasubduction zone crust and are fragments recording some or all stages of arc initiation, arc rifting and back-arc basin formation.

The orientation of the arc-type rocks in the north relative to the back-arc volcanics in the more southern massifs may suggest subduction towards the west. Recent work in the SW Pacific shows Late Cretaceous ophiolites are present in Papua New Guinea, New Caledonia and New Zealand. The formation of these ophiolitic systems supports the presence of a large scale tectonic regime of convergence and consequent westward subduction stretching from Paupa New Guinea, through New Caledonia, to New Zealand during the Late Cretaceous.

Keywords are: SW Pacific, New Zealand, Ophiolite, Late Cretaceous - Oligocene, Geochemistry, Tectonic significance.

INTRODUCTION

The ophiolitic igneous complexes in the northern regions of the North Island of New Zealand are collectively called the Tangihua Complex and informally known as the Northland Ophiolite (Figure 4.2.1). The Tangihua Complex is one of a number of ophiolites on the SW Pacific rim emplaced during the Late Tertiary onto a variably thinned continental crust of Palaeozoic - Palaeocene age. The others include the Papuan Ultramafic Belt (Davies, 1968) and the Massif de Sud (Prinzhofer *et al.*, 1980) and the Poya terrane ophiolites of New Caledonia (Cluzel *et al.*, 1994; 1997).

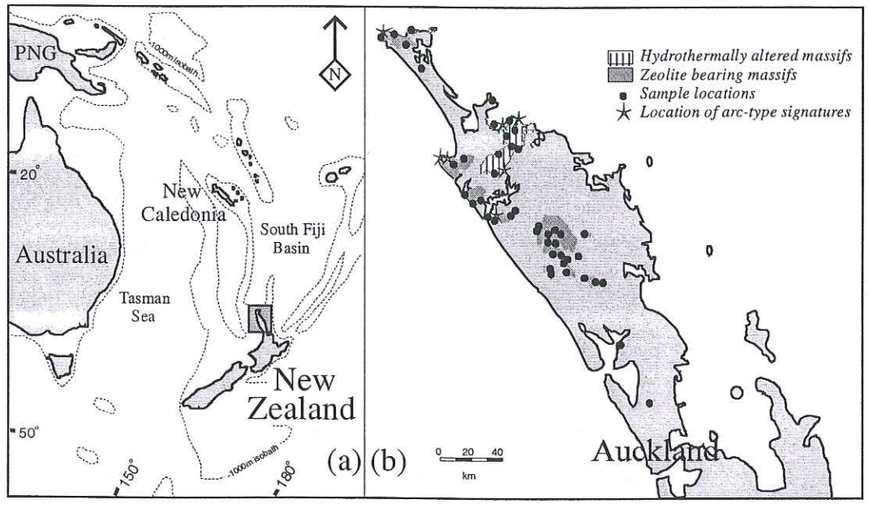

Figure 4.2.1: (a) Map showing the location of New Zealand in the SW Pacific region and (b) showing the ophiolitic massifs in the Tangihua Complex and sample locations.

Ophiolites are generally believed to represent fragments of oceanic crust formed at constructive plate margins. However, there is now widespread recognition that many ophiolites were formed at destructive plate margins. These ophiolites have been affected by suprasubduction zone processes and are thought to have formed during rifting and/or spreading in the early stages of island arc evolution. It is generally accepted that back-arc basins are extensional features produced by seafloor spreading similar to processes occurring at mid-ocean ridges (Saunders and Tarney, 1979, 1984; Crawford *et al.*, 1981; Taylor and Karner, 1983).

The resolution of the palaeotectonic environment of ophiolite formation can be extremely difficult. The development of regional tectonic and obduction models depends on the nature of the ophiolite; whether the ophiolite represents marginal basin crust or a fragment of a crust from a major oceanic spreading centre. This, the most recent study of the Tangihua Ophiolite in Northland New Zealand, is a comprehensive agglomeration of new analyses and previous work. In the past,

studies have concentrated on structural aspects (Spörli and Aita, 1994), palaeontological features (Hayward *et al.*, 1989) and/or cumulate and intrusive petrology (Hopper and Smith, 1996; Thompson *et al.*, 1997). In recent years the idea that the Northland ophiolites were influenced by suprasubduction processes has come to the fore (Malpas *et al.*, 1992; Hopper and Smith, 1996; Thompson *et al.*, 1997). Each individual piece of research has suggested magma generation at or near a back-arc environment, however, individually the evidence was often not conclusive. The development of such models for the formation of the Tangihua Complex has been hindered by the wide variety of rock types, the presence of low-grade but pervasive alteration and relatively limited exposures. Here we combine previous results with new geochemical analyses to demonstrate that the Tangihua ophiolite was formed in an arc - back-arc setting.

GEOLOGICAL SETTING

The ophiolites of the Tangihua Complex occur as structurally discrete bodies, which range in area from a few square meters to high-standing massifs of up to 900 km^2. Geophysical investigation shows that they generally form tabular, rootless bodies with an average thickness of 0.5 - 1.0 km (Quennell and Hay, 1964; Cassidy and Locke, 1987; Sharpe *et al.*, 1989). In general, the complex consists of massive and pillowed basaltic lava sequences with intercalated siliceous mudstone and micritic limestone. Gabbro, microgabbro and basaltic intrusions form a subordinate component (Brothers, 1974; Brothers and Delaloye, 1982; Hayward *et al.*, 1989; Malpas *et al.*, 1992). The complex also includes minor felsic derivatives, younger alkalic intrusions and ultramafic rocks in the North Cape area (Bennett, 1976).

The age of the Tangihua Ophiolite Complex is not well established but palaeontological evidence suggests formation during the Early Palaeocene or Late Cretaceous. The ophiolite complex is part of the Northland Allochthon, a series of thrust sheets containing both volcanic and sedimentary rocks, emplaced over a very short time period in the late Oligocene (Ballance and Spörli, 1979; Brook *et al.*, 1988; Malpas *et al.*, 1992; Hopper and Smith, 1996). The timing of emplacement of the ophiolite is not well established and has been estimated as occurring during the Late Oligocene on the basis of palaeontological evidence and stratigraphic relations. Structural and stratigraphic evidence suggests emplacement from the northeast (Brothers and Delaloye, 1982; Brothers, 1983; Spörli, 1989; Malpas *et al.*, 1992).

The allochthon overlies an autochthonous sequence of Late Tertiary sediments which lie in tectonic contact on Permian - Jurassic basement metagreywackes of the Waipapa terrane. Geophysical data indicates a maximum depth to the metagreywacke basement of 4 km to 5 km

(Woodward, 1970; Stern *et al.*, 1987). K-Ar dates of the igneous rocks of the ophiolite range from Mesozoic to Pliocene (Brothers and Delaloye, 1982), whereas palaeontological evidence suggests Late Cretaceous to Palaeocene. The Tangihua Ophiolite has therefore been interpreted as a dismembered slice of Late Cretaceous and Palaeocene oceanic crust thrust onto the quasi-continental crust of northern New Zealand at the end of the Oligocene.

STRUCTURE

Deformational characteristics are broadly similar throughout the Tangihua Complex. Locally the rocks are intensely sheared but on an outcrop scale such rocks are often associated with relatively undeformed pillows or rocks exhibiting small scale structures.

Individual massifs contain structurally coherent sequences of mainly volcanic rocks up to several kilometres thick. The lithology within these sequences are typically shallow dipping, structurally upright units which are bounded by steeply dipping faults and/or shear zones. In some of the massifs the plutonic rocks are juxtaposed against the sedimentary units and the pillow basalts. All of these features suggest that the Tangihua Complex is not a single sheet of oceanic crust dismembered into individual massifs but rather that each massif is a structural melange in which different components of an oceanic lithosphere section have been assembled (Spörli, 1989; Spöril and Aita, 1994; Malpas *et al.*, 1994).

Shear sense indicators within younger, brittle, low-angle fault zones in the ophiolite indicate emplacement from the northeast (Hanson, 1991) with the position of the generating spreading ridge, if still preserved, lying to the northeast and trending north to northwest (Malpas *et al.*, 1994). The consistent north to northwest trends of the dykes, including those in the sheeted dike complexes at North Cape and Ahipara, indicate that the massifs have not rotated relative to each other. However, using palaeomagnetism, Cassidy (1993) has shown that rotation of between 50° and 120° has occurred in at least two of the Tangihua Massifs. Ophiolite rotation has occurred relative to the Northland Peninsula and is probably the result of the obduction event. Cassidy (1993) has suggested rotation about a vertical axis and, tentatively, latitudinal translation.

ROCK TYPES

Structural dismemberment in the Late Cretaceous Tangihua Complex is such that an intact ophiolite stratigraphy can not be seen although lithologies representing most parts of a complete ophiolite suite are present. Rock types within the complex are dominated by basaltic pillow lavas,

flows, breccias and hyaloclastites with lesser sheeted dykes. The basalts are dominantly tholeiitic (although calc-alkaline basalts are common) and relatively homogeneous, containing augite and plagioclase, with lesser amounts of orthopyroxene, olivine, rare quartz, iron oxides and ubiquitous minor phases.

Only limited outcrops occur of the lower parts of the ophiolite sequence such as cumulate gabbros and layered ultramafic rocks. However, the Tangihua Complex is also thought to include the werhlite and serpentines described in the Maramanui-Wahue area (Fortune, 1968), serpentines near Te Kau and a layered ultramafic complex near North Cape (Bennett, 1976). The North Cape ultramafics comprise a faulted sequence of serpentines and cumulate peridotites which occur together with layered gabbro and sheeted doleritic intrusions (Bennett, 1976). Most of the massifs contain massive flows and doleritic intrusions, however, along the east coast of the Northland Peninsula, intrusives dominate while pillow lavas and breccias dominate along the west coast. Layered plutonics are exposed at North Cape and in this area pillow lavas form only a minor constituent (Leitch, 1966). In the Doubtless Bay area doleritic intrusions and microgabbros dominate (Le Couteur, 1967).

A minor, yet important, component of the Tangihua Complex is the volcanic and plutonic rocks of alkaline character. The alkaline rock, described as lamprophyres (Brothers, 1983), are generally amphibole-bearing basalts. They commonly occur as pillow lavas and minor sheet flows which in places appear to overlie the tholeiitic sequences (Briggs, 1969), however their stratigraphic relationship is sometimes unclear. More rarely the alkaline rocks occur as small plutonic stocks ranging in composition from mafic to felsic (Thompson *et al.*, 1997).

PETROGRAPHY / MINERAL CHEMISTRY

Petrographically the Tangihua Basalts are generally microcrystalline basalts containing phenocrysts of plagioclase and clinopyroxene, although the basalts are often equigranular and range from glass though cryptocrystalline to fine grained with a groundmass composed primarily of plagioclase and pyroxene. Phenocryst content is sometimes as high as 20%. Primary phenocrysts are plagioclase > clinopyroxene > orthopyroxene >> magnetite, titanite. Rare olivine-rich and hornblende-bearing basalts also occur within the complex.

Secondary phases are clay minerals (smectite > chlorite > illite), biotite, zeolites, analcime, actinolite, prehnite, calcite and pyrite. Possible olivine phenocrysts have altered to clay minerals. Both pyroxene and plagioclase have partially altered to zeolites and/or clay minerals. The Tangihua rocks have all undergone low-temperature hydrothermal alteration and variable degrees of

metamorphism, ranging from zeolite facies up to greenschist facies. Greenschist metamorphism is associated with intrusive activity. Although unusual, comparable two-phase alteration sequences have been described elsewhere in ocean crustal material (e.g. Mevel, 1988). For more detailed studies of the secondary mineral assemblages see Black (1989) and Nicholson and Black (1998).

Plagioclase occurs as euhedral to subhedral grains, generally tabular in form ranging from microcrystalline to 2mm in length. Both simple and multiple twins are common. Plagioclase compositions occupy a limited range of An_{79-93} (Figure 4.2.2a), with an average of An_{84}. Rim compositions reflect limited, though significant, effects of alteration. Plagioclase rim compositions range from An_{47-81} with an average of An_{72}. In a ternary plot of CaO, K_2O and Na_2O, despite the scatter, there appears to be a trend in the rim analyses towards a more potassium-rich feldspar. It is unclear as to whether this trend reflects changing chemistry during fractionation or is simply the effect of alteration on the phenocrysts.

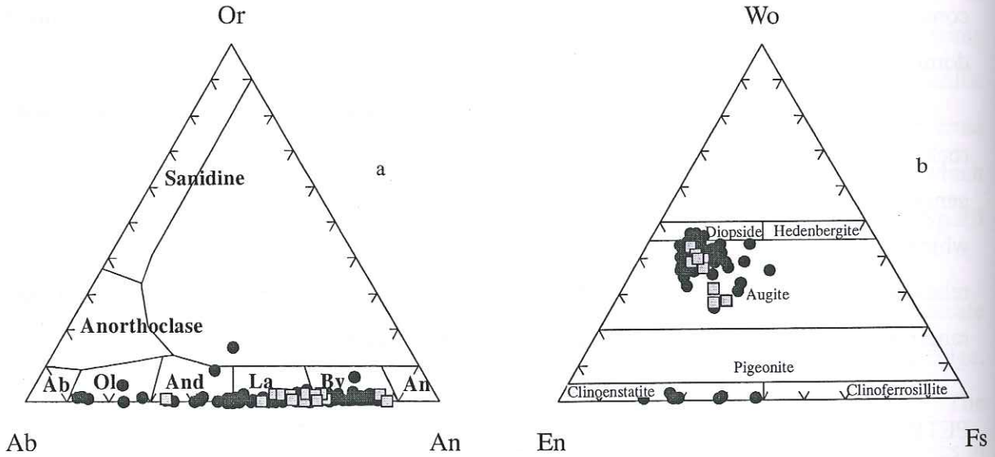

Figure 4.2.2. (a) Feldspar compositions from the Tangihua Complex basalts. Plagioclase composition calculated on the basis of 20 oxygens. (b) Composition of pyroxenes from the Tangihua Complex basalts. Pyroxene compositions calculated on the basis of 6 oxygens. The same symbols are used throughout the diagrams. Circles: arc basalts, Squares: back-arc basalts.

The pyroxene in the Tangihua Basalts is almost entirely clinopyroxene. It occurs as pale green, subhedral to euhedral, crystal, generally smaller than 0.5mm on their longest axes. Clinopyroxene phenocrysts are calcic augite (Figure 4.2.2b) and commonly contain inclusions of plagioclase and opaque minerals (possibly magnetite). They are often embayed and may contain exsolution lamellae of orthopyroxene. Where present, orthopyroxene is colourless to pale greenish brown. It occurs as tabular or subhedral crystals which are generally embayed and/or altering to clay minerals. Mg#s for orthopyroxene and clinopyroxene are basically the same. Core

compositions have an average Mg# of 68 while rim compositions have an average of Mg# 56. The wider distribution of rim compositions is non-systematic and probably reflects alteration.

GEOCHEMISTRY

A collection of 120 samples of predominately tholeiitic volcanic and minor plutonic rocks from the Tangihua Complex have been analysed for major oxides and trace elements. From these analyses, 40 samples with total volatile content < 4wt% were chosen for REE analyses. Representative analyses are given in Table 4.2.1 and illustrated in Figures 4.2.3 through 4.2.8.

External surfaces of fresh rocks were removed and the samples split into chips which were then ground to a powder in a tungsten carbide ring grinder. H_2O+, H_2O- and CO_2 were determined by gravimetry, the remaining major oxides and trace elements were determined by XRF (after Norrish and Chappell, 1977) at the University of Auckland, New Zealand. The precision (2σ) is generally less than 2% of the major oxide determinations and less than 5% for trace elements (at ten times the detection limit of 1-2 ppm). Rare earth element abundances were determined by inductively coupled plasma mass spectroscopy (ICP-MS) at the Laboratoiré de Geodynamique des Chains Alpines, Université Joseph Fourier, Grenoble, France. The precision (2σ) for ICP-MS analyses varies from 2-10% for the elements analysed.

In a few samples the presence of alteration is reflected in the abundances of the more mobile elements and LOI. However, an alkali-silica plot (Figure 4.2.3) shows relatively minor amounts of scatter in the total alkali content of the samples, indicating that the effects of alteration are minimal.

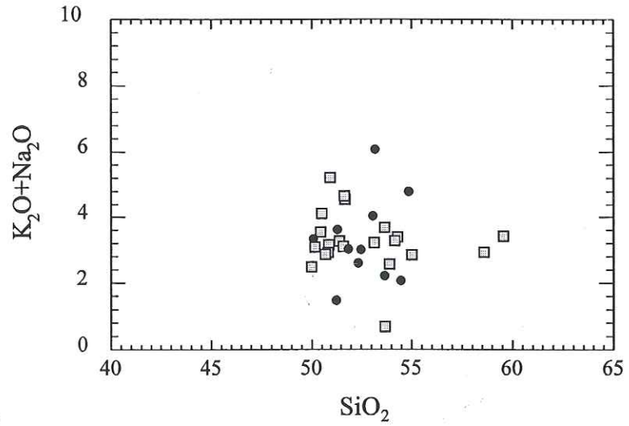

Figure 4.2.3. Total alkalis versus SiO_2 diagram showing the pervasive but weak nature of alteration in the Tangihua Ophiolite Complex basalts. Circles: arc basalts, Squares: back-arc basalts.

Sample	49211	47654	47656	49189	49130	49207	49123	49183	49186	47648	47662
Rock Type	Basalt	dol	matrix	basalt	basalt	bas clast	basalt	basalt	basalt	basalt	dol dyke
Major element data in wt.%. Recalculated to 100% with Fe2O3/FeO = 0.15											
SiO2	51.7	53.0	54.8	51.3	49.5	54.7	58.6	51.6	50.5	55.0	50.5
TiO2	1.1	1.3	1.1	1.6	1.0	1.0	2.2	1.4	1.9	1.8	1.7
Al2O3	15.7	16.0	14.3	15.9	16.6	18.4	13.5	15.7	15.8	14.9	15.2
Fe2O3	1.4	1.3	1.2	1.4	1.3	1.0	1.4	1.3	1.5	1.2	1.5
FeO	9.3	8.8	7.8	9.2	8.9	6.7	9.5	8.4	10.0	7.9	9.7
MnO	0.2	0.2	0.2	0.2	0.2	0.2	0.2	0.2	0.2	0.2	0.2
MgO	6.6	6.3	7.0	5.9	7.8	4.3	3.4	6.9	6.2	5.7	7.1
CaO	10.9	9.0	8.9	10.8	11.6	9.2	8.0	11.3	10.3	10.3	9.9
Na2O	2.9	3.6	4.1	3.2	2.1	3.5	2.8	2.8	3.3	2.7	3.7
K2O	0.2	0.4	0.6	0.4	0.7	0.9	0.2	0.3	0.2	0.2	0.4
P2O5	0.1	0.1	0.1	0.1	0.2	0.2	0.2	0.1	0.2	0.2	0.2
Total	100.0	100.0	100.0	100.0	100.0	100.0	100.0	100.0	100.0	100.0	100.0
LOI	1.5	0.6	1.2	0.1.83	0.6	1.2	1.1	0.6	0.6	0.5	0.5
Trace elements in ppm											
Ba	16.6	40.9	21.9	23.2	289.1	283.6	40.7	26.5	30.7	30.7	46.6
Rb	1.3	4.5	4.7	5.6	15.3	32.9	3.7	3.6	2.2	2.1	2.0
Sr	157.5	141.8	100.3	101.7	321.5	257.8	92.2	143.2	206.2	130.4	105.5
Ta	0.1	0.1	0.1	0.1	0.3	0.4	0.2	0.2	0.2	0.3	0.4
Th	0.2	0.1	0.1	0.2	2.6	3.2	0.2	0.2	0.2	0.3	0.3
Zr	48.0	57.9	54.1	80.6	64.5	76.3	115.4	78.9	116.6	126.0	122.9
Nb	0.8	1.0	1.0	1.2	4.6	4.9	1.2	1.8	2.6	4.0	4.6
Y	24.2	24.6	21.9	30.5	20.5	20.5	47.9	32.2	36.5	46.3	41.8
Hf	1.7	1.8	1.7	2.3	2.0	2.4	4.2	2.8	3.0	4.3	4.2
V	356.9	321.2	293.0	380.8	308.5	200.8	450.1	314.6	354.5	333.6	325.4
Cr	113.7	77.2	256.3	93.9	183.6	131.5	15.0	181.2	115.9	192.0	247.4
Ni	46.3	40.2	56.3	33.3	88.1	41.0	16.3	59.2	42.1	81.1	77.3
Co	47.8	34.0	82.8	37.0	50.6	41.7	49.8	42.8	36.4	52.7	44.4
U	0.1	0.1	0.2	0.1	0.7	1.2	0.6	0.1	0.1	0.4	0.2
Sc	42.6				38.4	30.2	41.7	40.5		39.0	41.3
Cu	64.5	32.4	93.1	47.2	41.2	37.2	38.1	65.2	49.6	49.5	22.3
Zn	80.6	69.0	58.6	71.2	72.4	77.1	110.1	80.8	79.9	88.6	85.9
Pb	0.7	1.3	0.7	0.5	4.7	10.0	0.9	0.6	0.8	0.6	0.3
Ga	18.0				18.0	19.7	20.4	17.6		18.3	17.2
Cs	0.0	0.1	0.0	0.1	0.2	3.4	0.2	0.1	0.1	0.1	0.0
La	2.0	2.2	2.5	2.6	10.3	9.7	3.6	3.1	4.1	6.0	5.8
Ce	6.6	7.0	7.5	8.7	23.6	23.1	12.4	10.0	12.8	18.2	17.1
Pr	1.2	1.2	1.2	1.5	3.1	3.0	2.3	1.7	2.1	3.0	2.8
Nd	7.1	6.5	6.4	8.1	13.6	12.0	12.8	9.1	11.0	14.8	13.9
Sm	2.8	2.3	2.1	2.8	3.5	2.8	4.7	3.1	3.6	4.7	4.4
Eu	1.1	0.9	0.9	1.1	1.1	0.9	1.7	1.2	1.2	1.6	1.5
Gd	3.8	3.0	2.8	3.7	3.6	3.0	6.2	4.2	4.5	5.9	5.6
Tb	0.7	0.6	0.5	0.7	0.6	0.5	1.2	0.8	0.8	1.1	1.1
Dy	4.2	3.8	3.5	4.8	3.4	3.3	7.9	5.1	5.6	7.3	6.9
Ho	0.9	0.9	0.8	1.1	0.7	0.7	1.7	1.1	1.2	1.6	1.5
Er	2.6	2.4	2.2	3.0	2.0	2.0	5.1	3.2	3.5	4.6	4.3
Tm	0.4				0.3	0.3	2.3	0.5		0.7	0.6
Yb	2.5	2.4	2.1	2.9	1.9	2.0	4.8	3.0	3.4	4.3	4.0
Lu	0.4	0.4	0.3	0.5	0.3	0.3	0.8	0.5	0.5	0.7	0.6

Table 4.2.1: Representative major oxide and trace elements data from the Tangihua Complex basalts.

This study has focused mainly on the basalts within the Tangihua Complex with the aim of characterising the magma sources. The samples in the study have SiO_2 contents ranging between 49 and 60wt% (Figure 4.2.3), although most of the samples fall between 49 and 55wt% SiO_2. This corresponds to the basaltic through to basaltic-andesite fields of the IUGS classification scheme. Mg#s range from 26 to 50 in these samples. The samples are predominantly tholeiitic, however, there is a distinct calc-alkaline trend as seen in Figure 4.2.4b, and two of the samples reflect a more alkaline composition.

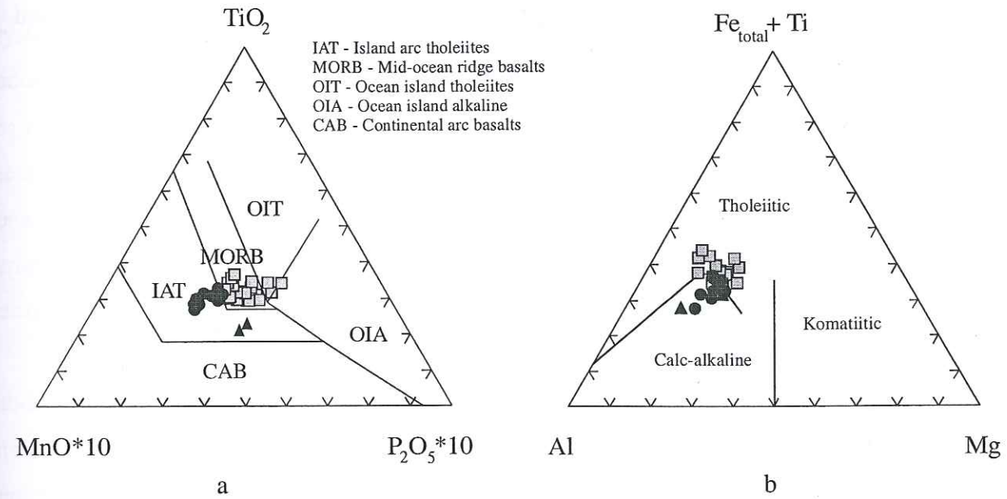

Figure 4.2.4: (a) Ternary plot of TiO_2-MnO*10-P_2O_5*10 showing the island arc and MORB signatures of the basalts from the Tangihua Complex. (b) The ternary plot of Fe_{total} + Ti- Al-Mg (Jensen diagram) shows two different trends for the basalts of the Tangihua Complex which are calc-alkaline and tholeiitic. Circles: arc basalts, Squares: back-arc basalts, Triangles: alkaline basalts.

The ternary element plot of TiO_2-MnO*10-P_2O_5*10 (Figure 4.2.4) uses primarily immobile elements to classify rock types. This diagram after Jenner *et al* (1991) is able classify the samples allowing, in this case, the distinction between three different suites of basaltic lavas. The basalts from the Tangihua Ophiolite clearly fall into the island arc tholeiite (IAT) suite and the MORB suite. The two OIB samples also plot within the AIT field although, again, they are distinct from the rest of the sample set. Other diagrams, such as Nb/Th versus Y after Jenner *et al.* (1991; Figure 4.2.7b) illustrate the typically arc-like signature for some of the samples but more MORB-like signatures for the remainder.

The overlap between the MORB-like samples and the arc-like samples is most apparent in the trace and rare earth element spidergrams. Figure 4.2.5a shows the chrondrite normalised trace and rare earth elements, after Evensen *et al.* (1978) while Figure 4.2.5b shows N-MORB normalised trace and rare earth elements, after Sun and McDonough (1989). One of the most obvious features of both Figures 4.2.5a and 4.2.5b is the continuum between the samples. With the exception of the two alkaline samples, all the samples show only variations of is essentially the same pattern. At first glance the patterns shown in Figure 4.2.5a reflect very MORB-like signatures, however, the depletion of elements, such as Nb, Ta and Zr, in Figure 4.2.5b reflects distinct arc (for the arc samples) and BAB signatures for the MORB-like samples. Similar shaped chrondrite normalised patterns have been documented in other arcs such as in the South Sandwich Island arc (Hawkesworth *et al.*, 1977).

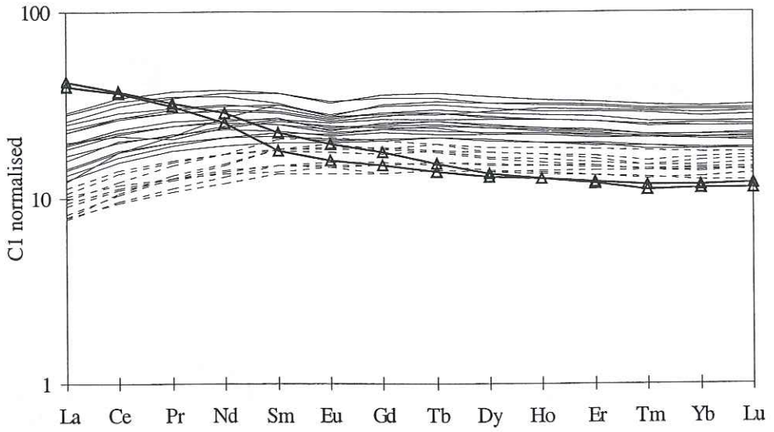

Figure 4.2.5a. Chrondrite normalised REE diagram for the Tangihua lavas. Normalising factors after Evensen *et al.* (1978). REE abundances increase with differentiation. Solid line: back-arc lavas. Dashed line: arc lavas. Solid lines with triangles: alkaline basalts.

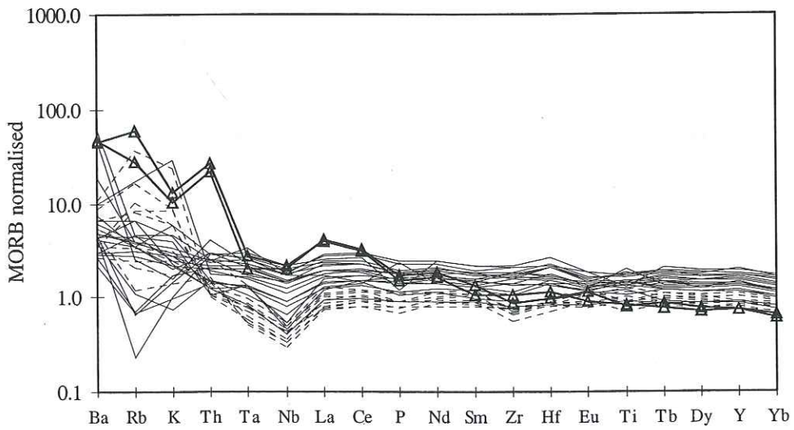

Figure 4.2.5b. MORB-normalised incompatible diagram for the Tangihua lavas. Normalisation factors after Sun and McDonough, (1989). The Tangihua lavas have flat HFSE ratios and are enriched in LILE. Solid line: back-arc lavas. Dashed line: arc lavas. Solid lines with triangles: alkaline basalts.

A feature of the trace element abundance patterns illustrated in Figures 4.2.5a and 4.2.5b is the relative depletion of Nb, Ta and Zr. Distinguishing between back-arc and MORB signatures is very difficult, especially if the samples have undergone some degree of metamorphism, however, negative anomalies in the HFS elements are a widely accepted indicator of a subduction zone setting. Geochemical studies on differentiation products of modern MORB (Perfit *et al.*, 1983) show that Nb behaves as incompatibly as LREE. Nb depletion is not affected by fractional crystallisation as samples display variable Nd anomalies when compared to their REE concentrations. Similarly, Briqueu *et al.* (1984) observed that the negative Nb anomalies in modern arc volcanics were independent of degree of fractional crystallisation. As Nb is not transported in the slab (REFERENCE), the depletion of Nb is thought to reflect formation in a suprasubduction zone setting. In this case the presence of clearly arc-type basalts in combination with definite depletion of both Nb and Zr (Figure 4.2.5b) suggests the complete suite of samples represents a transition from volcanism at the arc to the back-arc region.

Pearce (1980) classified trace element profiles from oceanic basalts into oceanic non-subduction zone basalts, N, T and E-type MORB which show flat to humped enrichment patterns, and oceanic basalts with a subduction zone component which show selective enrichment of LIL and depletion of HFS elements. The enrichment of LFS elements relative to HFS elements has been attributed to the enrichment of the mantle wedge by LIL-enriched fluids derived from the subducted oceanic crust (Gill, 1981). Saunders and Tarney (1984) found a correlation between the degree of LIL enrichment in back-arc basalts and the maturity of the back-arc basin. The degree of LIL enrichment within the mantle wedge and subduction zone melts is proportional to the age of the subduction zone, older systems having undergone more metasomatism. The only slight enrichment of LIL elements relative to HFS elements suggests that the Tangihua ophiolite represents a relatively immature system.

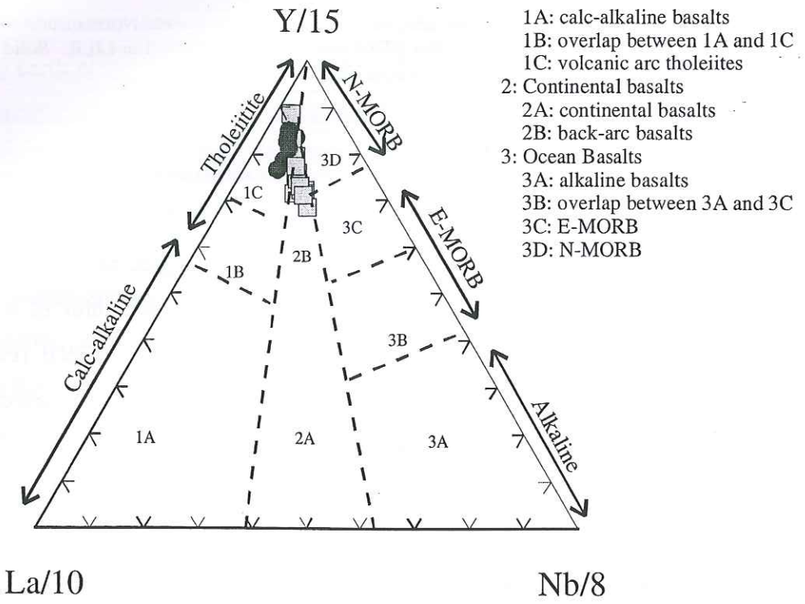

1A: calc-alkaline basalts
1B: overlap between 1A and 1C
1C: volcanic arc tholeiites
2: Continental basalts
2A: continental basalts
2B: back-arc basalts
3: Ocean Basalts
3A: alkaline basalts
3B: overlap between 3A and 3C
3C: E-MORB
3D: N-MORB

Figure 4.2.6: Ternary plot of La-Y-Nb (after Cabanis and Lecolle, 1989) is used to further discriminate between volcanic arc basalts, oceanic basalts and continental basalts. Circles: arc basalts, Squares: back-arc basalts.

In Figure 4.2.5a and 4.2.5b we have used the Th, HFSE and REE abundances and patterns to divide the volcanics into the three aforementioned geochemical groups. These groups are: arc basalts characterised by a strong negative Nb anomaly with respect to Th and La, back-arc basalts characterised by a lesser negative Nb anomaly, and alkaline basalts characterised by La/Sm >2. Note that there appears to be a continuum between groups one and two, i.e. arc basalts and back-arc basalts. To illustrate this continuum we have used several diagrams. The variation of Nb/Th ratios plotted against Y (Figure 4.2.7b; after Jenner *et al.*, 1991). Nb/Th ratios record the development of the negative Nb anomaly as illustrated in primitive mantle normalised plots, starting at values in excess of that found in primitive mantle (Nb/Th ratio of approximately 7.4) to values substantially lower than those of primitive mantle (i.e. Th enriched relative to Nb). The transition zone, spanning the Nb/Th reference line, was defined by samples that have a clearly defined negative Nb anomaly but generally plot in the N-MORB fields of the ternary classification diagrams such as Figure 4.2.4. Y was chosen to illustrate the behaviour of the HREE. The ternary plot of Y/15-La/10-Nd/8 (Figure 4.2.6; after Cabanis and Lecolle, 1989) also illustrated the differences between arc-type and back-arc lavas. This diagram clearly shows that there are two trends of magma evolution; one for the arc lavas and one for the back-arc lavas: reflecting the various influences of the subduction system.

Figure 4.2.7 shows the variation of Ta and Th with respect to Yb. As both Th/Yb and Ta/Yb ratios remain unchanged during partial melting their values reflect differences and/or similarities in source composition. It is necessary, however, to consider the effects of fractional crystallisation, crustal contamination and/or subduction. In this diagram the composition of the Tangihua Complex basalts appears to reflect slightly different petrogenetic histories including differing amounts of

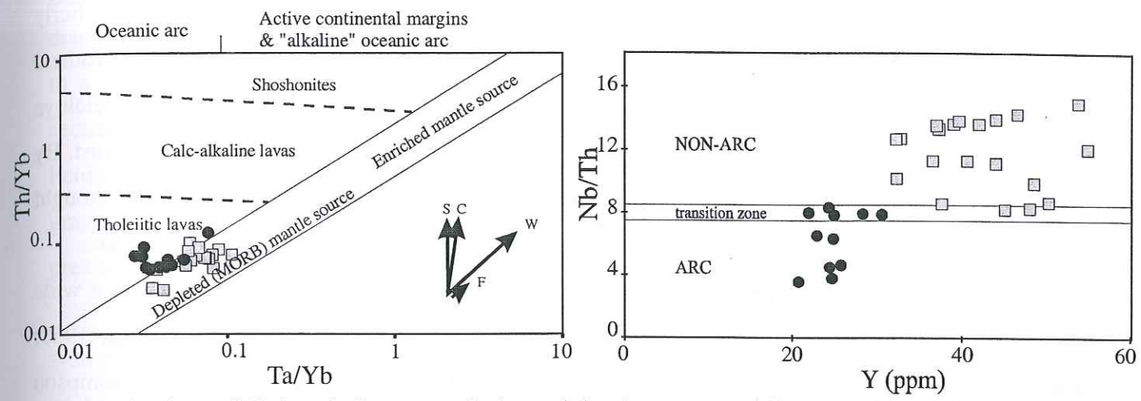

a b

contamination, differing influences of the subduction zone and/or possibly differing source compositions.

Figure 4.2.7: (a) Ta/Yb versus Th/Yb diagram (Pearce, 1984) for the Tangihua Complex basalts. The vectors indicate chemical variations resulting from crystal fractionation (F), source effects (W), crustal contamination (C) and subduction (S). (b) Nd/Th versus Y (ppm) illustrate the typically arc-like signature of some of the basalts from the Tangihua Complex. Nb/Th ratios record the development of the negative Nd anomaly as seen in primitive mantle (PM) normalised plots, starting at values in excess of that found in the primitive mantle (PM has a Nb/Th ration of approximately 7.4, Jenner *et al.*, 1991) to values substantially lower than those of PM (i.e. Th enriched relative to Nd) as a result of subduction zone processes. Circles: arc basalts, Squares: back-arc basalts.

In conclusion, the complex nature of the chemistry, in particular those lavas with transitional arc signatures, and the presence of non-arc lavas, is clear evidence that these volcanics formed in a suprasubduction zone environment. Modern back-arc-basin volcanic rocks, within the suprasubduction zone environment, demonstrate geochemical characteristics ranging from arc to non-arc. Moreover the spatial and temporal association of rocks with different geochemical signatures can be quite complex (e.g. Marsh *et al.*, 1980; Wood *et al.*, 1981; Jenner *et al.*, 1987; Johnson *et al.*, 1987; Perfit *et al.*, 1987; Valleir *et al.*, 1991; Jenner *et al.*, 1991). Given the geochemical and the tectonic constraints (the lack of a well developed arc and back-arc systems) we suggest that the Tangihua Complex formed either in a transitional zone between an arc setting and a back-arc setting, or in a zone of migration from arc to back-arc volcanism. As such, the field, age, geochemical data supports a model in which these rocks formed suprasubduction zone crust and are fragments recording some or all stages of arc initiation, arc rifting and back-arc basin formation.

DISCUSSION

Early interpretations of the formation of the Tangihua Complex were formulated before the acceptance of plate tectonic theory (Quennell and Hay, 1964; Hughes, 1966). Briggs (1969) was possibly the first to suggest that the Tangihua Complex may be allochthonous, with a northerly emplacement direction, but this hypothesis was rejected due to the lack of evidence. Brothers (1974) was the first to describe the Tangihua Complex as ophiolite and Brothers and Delaloye (1982) placed the rocks of the Tangihua Complex into a stylised section through the ocean crust. By the mid 1980's the allochthonous model was generally accepted and the entire complex was thought to be analogous with a spreading ridge system (e.g. Larsen, 1987; Arden, 1988; Martin, 1988).

Geochemical and petrological studies have shown that the Tangihua Complex has a wide variety of magmatic affinities ranging though tholeiitic, calc-alkaline to alkaline (Briggs, 1969; Larsen, 1987; Arden, 1988; Martin, 1988; Malpas *et al.*, 1992; Hopper and Smith, 1996; Thompson *et al.*, 1997). The diverse geochemistry suggests that the Tangihua lavas are not the product of a simple spreading system but rather the result of a complex magmatic history which Thompson *et al.* (1997) attribute to modification by suprasubduction processes. The results of this study allow further refinement of the tectonic environment and model of formation of the Tangihua Complex. The geochemistry shows that the Tangihua basalts originated in an arc setting which later evolved into a back-arc setting, allowing for the transition from arc to back-arc and N-MORB-like signatures.

The current emplacement models for the Tangihua Complex have tried to account for the diverse chemistry of the rock types, the plate-tectonic constraints, the preservation of mainly the upper levels of the ophiolite sequence and the close association with the allochthonous sedimentary rocks. However, the observed predominately MORB geochemistry of previously analysed samples suggested generation at either a major spreading centre or in a back-arc basin, with little possibility for refinement (Malpas *et al.*, 1992).

Most models can not account for the necessary tectonic setting for the obduction of the Tangihua ophiolites. Typically the models involve westward obduction of oceanic crust across a continental margin and either delamination or ramping of the upper sections of the ocean crust sequence. Thus far there have been no models for the obduction of the Northland Allochthon which are without problems, and none account for the significant presence of arc lavas within the ophiolite complex.

Our model invokes a north-south trending subduction zone, with westward dipping subduction, in the initial phases of normal arc volcanism beginning in the Late Cretaceous (Figure 4.2.8a). A period of extension, or arc roll-back occurs before the arc is well developed. The new back-arc region is located in very close proximity to, possibly directly on top of, the fledgling arc, thus accounting for the presence of both arc and back-arc lavas, where the diaphiric rise of MORB-type lavas interferes with arc magmatism. Eventually arc magmatism stops and partial melts of the diaphir feed the embryonic marginal basin (Figure 4.2.8b). A change in the tectonic regime results in a compressional phase in Figure 4.2.8c. During this phase an accretionary prism, containing sedimentary material, arc lavas and back-arc lavas is created and then overthrust onto the Northland Peninsula. Downward dragging of the eastern edge of the continental crust allowed subsequent gravity sliding of the allochthon (Ballance and Spörli, 1979). Rebound of the crust has caused the present day uplifted basement ranges along the eastern margin of the Northland Peninsula.

As this new model argues that the Tangihua Ophiolites were not formed at a major spreading system, but rather in an arc, back-arc system, there is no need for delamination of the upper sections of the ophiolitic sequence, as proposed by Malpas *et al.* (1992) and Thompson *et al.* (1997).

The presence of minor amounts of alkaline volcanics rocks within suprasubduction zone modified ophiolite suites have been recognised in Oman, Cyprus and Newfoundland (Baker, 1979; Lippard *et al.*, 1986). The relationship between the alkaline and the tholeiitic Tangihua volcanic rocks is problematic, although the alkaline volcanics appear to generally be younger (Briggs, 1969). It has been suggested that the alkaline volcanics within the Tangihua Ophiolite represent small amounts of melting of enriched mantle material (see Hamilton, 1995) which has been dragged down into the mantle by the subducting slab (Thompson *et al.*, 1997). This material was then erupted close to or within the developing back-arc basin region and, in this instance, contains distinct subduction zone signatures. As such the presence of the alkaline volcanic rocks is in character with the proposed arc - back-arc evolution model for the generation of the Tangihua Ophiolite.

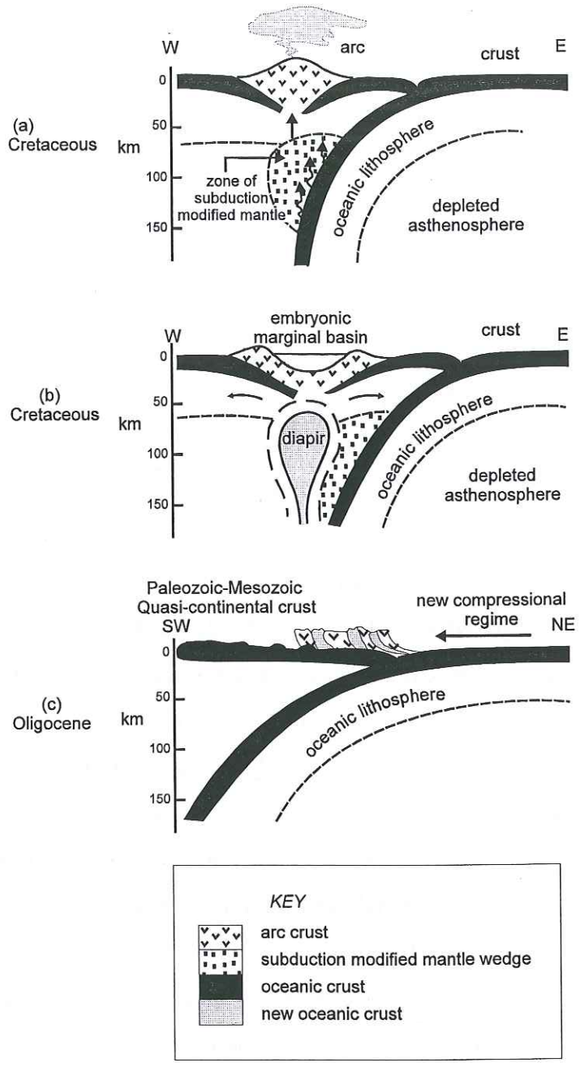

Figure 4.2.8: Model for the development of a back-arc basin (modified after Crawford *et al.* 1981) and the subsequent emplacement of the Tangihua Complex onto the Northland Peninsula. (a) Normal island arc magmatism probably begin during the Late Cretaceous. (b) Evolution into a back-arc system. (c) A changing tectonic regime results in a compressional phase, thrusting the arc, back-arc and sedimentary rocks onto the Northland Peninsula.

It is interesting to note that the arc-type rocks mainly occur in only the northern massifs (Figure 4.2.1b). The southern massifs are more back-arc in character. This suggests that the position of the arc lay to the north. However, if the massifs have rotated, for example Cassidy (1993) reports between 50° and 120° clockwise rotation, the position of the arc-type lavas suggests that the arc position was to the west of Northland Peninsula, and that subduction was towards the east. More data is needed to accurately determine the direction of subduction. According to Taylor *et al.* (1992) it is possible to deduce the relative distance from the arc trench using certain trace and

rare earth element ratios. Using their methods it is possible to show that the Tangihua Complex generally formed close to the volcanic arc with minor back-arc migration.

The general structure of the Southwest Pacific region has resulted from successive opening and closing of marginal basins since the Late Cretaceous. Recent work in New Caledonia by Cluzel *et al.* (1994; 1997) and Eissen *et al.* (1998) suggests that there was a similar subduction system active in New Caledonia during the Late Cretaceous. They invoke an eastward dipping subduction system, which is responsible for the generation of the Massif de Sud Ophiolite to the NE of New Caledonia. Other SW Pacific ophiolites of a similar age include the Papuan Ultramafic Belt (Davies, 1968) and the Poya terrane ophiolites of New Caledonia (Cluzel *et al.*, 1994; 1997).

Previous work in New Zealand and New Caledonia has confirmed a close resemblance of both litholigical and paleontological units in the Late Palaeozoic and Mesozoic of the two countries. Current tectonic models for the Cenozoic evolution of New Caledonia involve a collision between a southwest facing arc and thinned continental margin crust, the attempted subduction of which choked the system, resulting in ophiolite obduction (Cluzel *et al.*,1994; 1997; Eissen *et al.*, 1998). Progressive development of the Cenozoic collision zone can be traced from Papua New Guinea through to New Zealand.

The presence of these systems, the Tangihua Complex, the Poya terrane, the Massif du Sud and the Papua Ultramafic belt, suggests a large scale tectonic regime of convergence and consequent eastward subduction within the SW Pacific during the Late Cretaceous and Early Palaeocene.

ACKNOWLEDGEMENTS

This research has been supported by the University of Auckland, New Zealand, the French Embassy, Wellington, NZ, and by the Université Joseph Fourier, France.

SECTION 4.3

Geochemistry and tectonic significance of late Cretaceous ophiolitic basalts from New Zealand and New Caledonia.

Nicholson, K.N., Picard, C. and Black, P.M. Submitted in October, 1999, to *Tectonophysics.*

ABSTRACT

Our understanding of the tectonic evolution of the SW Pacific between the Cretaceous and the Miocene is incomplete. During the Cretaceous through to the Miocene there were a number of ophiolitic complexes formed and emplaced, including the Tangihua Complex of New Zealand and the Poya terrane ophiolites of New Caledonia. Both ophiolitic complexes contain rocks from only the uppermost levels of the oceanic crust, they have a similar age of formation, and they were both emplaced during the Eocene. Consequently, it is thought that the two systems are somehow related. However, the Poya terrane and the Tangihua Complex have significantly different geochemistries. The Poya terrane basalts are predominantly P- and N-MORB tholeiites, which appear to have been generated during the opening of a small marginal basin northeast of New Caledonia, whereas the Tangihua basalts range from back arc tholeiites to calc-alkaline arc basalts suggesting formation in an arc – back arc setting. The similarities in age, emplacement and stratigraphy, between the two systems must be a result of their relative proximity within the Southwest Pacific as the new geochemical information clearly shows that the Poya terrane and the Tangihua Complex are not directly related.

INTRODUCTION

Since the late Cretaceous, the tectonics of the SW Pacific is characterised by successive openings of marginal basins that isolated ridges of a continental, oceanic or intermediate nature (Figure 4.3.1). The Poya terrane of New Caledonia and the Tangihua Complex of New Zealand are two of a number of the ophiolitic complexes along the SW Pacific rim (Figure 4.3.2). These ophiolites formed during the late Cretaceous on the SW Pacific rim and emplaced during the lower Tertiary onto a variably thinned continental crust of Palaeocene - Palaeozoic age.

Both the Tangihua Complex and the Poya terrane are dominated by rocks from the uppermost levels of the oceanic crust, are characterised by suprasubduction zone processes and are generally thought to have formed during rifting and/or spreading in the early stages of island arc

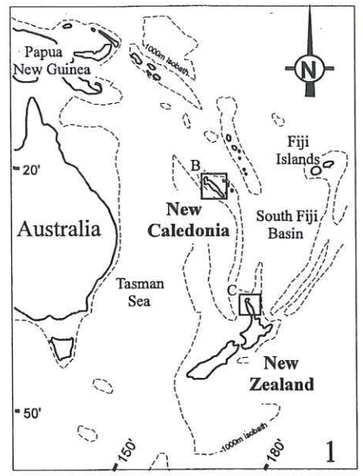

Figure 4.3.1: Location map of the Southwest Pacific region showing the position of New Zealand and New Caledonia.

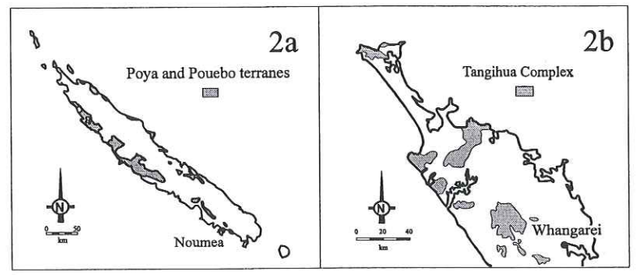

Figure 4.3.2: (a) Location map showing the relative positions of the Poya and Pouebo terranes in New Caledonia. (b) Location map showing the relative positions of the Tangihua Massifs in New Zealand.

evolution. Current tectonic models for the Cenozoic evolution of New Caledonia involve incipient collision between a south-west facing arc and thinned continental margin crust, the attempted subduction of which choked the system (Aitchison *et al.*, 1995a). Progressive development of this collision zone can be traced from Papua New Guinea through to New Zealand. In New Zealand, ophiolite formation was the result of the westward obduction of oceanic crust across a continental margin.

Due to the possible relationship between the Tangihua Complex and the Poya terrane ophiolites, the current study is part of a program which aims to compare the formation and emplacement of the two systems and to clarify the tectonic history of the south west Pacific during the lower Tertiary.

GEOLOGICAL SETTING

New Caledonia

The Poya terrane (Figure 4.3.2a) is a major geological unit in New Caledonia, approximately 200 km long, and is exposed along both the west and east coasts and overlies all pre-Neogene rocks except the ultramafic allochthon. It is a tectonically complex set of submarine mafic volcanic rocks, dolerites, gabbros and associated abyssal sediments. Geophysical evidence indicates that the Poya terrane extends up to 300 km north-westward in the basement of the northern lagoon of New Caledonia. Paleontological evidence suggests a Late Cretaceous, or slightly younger, age of formation for the Poya terrane (Aitchison *et al.*, 1995a; Meffre, 1995).

The Poya terrane was emplaced from the northeast as a relatively thin thrust sheet underlying the main ultramafic allochthon between 38 and 46 Ma (Cluzel *et al.*, 1994, 1995; Aitchison *et al.*, 1995a; Meffre, 1995). It is has been proposed that the Poya basalts (PTB) formed as part of an oceanic plateau. The tectonically disrupted plateau was then emplaced a single ophiolitic nappe and the different geochemical affinities can be explained in terms of the subsequent evolution of this plateau (Parat, 1996; Cluzel *et al.*, 1997).

New Zealand

The ophiolite massifs of the Tangihua Ophiolite Complex (informally the Northland ophiolite) occur as structurally discrete, rootless bodies ranging in area from a few square meters to high standing massifs of up to 900 km^2 (Figure 4.3.2b). In general, the complex consists of massive and pillowed basaltic lava sequences with intercalated sediments and minor gabbro, microgabbro and basaltic intrusions. Chemically the lavas are dominantly tholeiitic basalts with arc and back-arc affinities. The complex also includes minor felsic derivatives, younger alkalic intrusions (which exhibit within plate characteristics) and rare ultramafic rocks.

The age of the Tangihua Ophiolite Complex is not well established but paleontological evidence suggests formation during the early Palaeocene or late Cretaceous. The ophiolite complex is part of the Northland Allochthon which is thought to have been emplaced over a very short time period in the late Oligocene (Brook *et al.*, 1988; Ballance and Spörli, 1989; Malpas *et al.*, 1992; Hopper and Smith, 1996) as constrained through paleontological evidence and stratigraphic relations. Structural and stratigraphic evidence suggests emplacement from the northeast (Brothers and Delaloye, 1982; Brothers, 1983; Spörli, 1989).

ROCK TYPES

New Zealand

Structural dismemberment in the Late Cretaceous Tangihua Ophiolite Complex is such that an intact ophiolite stratigraphy can not be seen although lithologies representing most parts of a complete ophiolite suite are present. Rock types within the complex are notably dominated by basaltic pillow lavas, flows, breccias and hyaloclastites with lesser sheeted dykes. The Tangihua Complex basalts (TCB) are dominantly tholeiitic, although calc-alkaline basalts are common, and they are relatively homogeneous, containing augite and plagioclase, with lesser amounts of orthopyroxene, magnetite, rare quartz or olivine, and ubiquitous minor phases (Nicholson *et al.*, (b) in review).

Only limited outcrops occur of the lower parts of the ophiolite sequence, such as cumulate gabbros and layered ultramafic rocks. However, the Tangihua Ophiolite Complex is also thought to include rare werhlite and serpentinites. A minor, yet important, component of the TCB is the volcanic and intrusive rocks of clear alkaline character. The alkaline rocks are generally amphibole-bearing basalts which commonly occur as pillow lavas and minor sheet flows overlying the tholeiitic sequences, however their stratigraphic relationship is sometimes unclear.

New Caledonia

The Poya terrane is similar to the Tangihua Ophiolite Complex in that the lower sections of a typical ophiolite sequence are absent with no outcrops of ultramafic and only rare gabroic rocks. Outcrop is dominated by basaltic pillow lavas and flows with lesser hyaloclastites, fine grained tuffaceous sediments, calcareous sediments and radiolarian cherts (Espirat, 1966, 1971; Guillon and Gonord, 1972; Avias and Coudray, 1975; Rodgers, 1975; Gonord, 1977). Less common are gabbros, dolerites, rare sheeted dykes and serpentinites. Pillow basalts and dolerites (Formation des Basaltes; Routhier, 1953; Poya terrane; Cluzel *et al.*, 1994) overlain by shales are characteristic of lowland areas, particularly along the west coast. Radiolarian age dating indicates that these rocks are Late Cretaceous (Campanian) to lower Eocene in age (Aitchison *et al.*, 1995b; Meffre, 1995). Geochemical and isotopic data indicate that these predominantly tholeiitic Poya terrane basalts (PTB) may have been developed in a back arc basin or marginal sea environment (Cameron, 1989; Aitchison *et al.*, 1995b; Meffre *et al.*, 1996; Cluzel *et al.*, 1997; Eissen, 1998; Picard *et al.*, 1999).

PETROGRAPHY / MINERAL CHEMISTRY

New Zealand

Petrographically the Tangihua Complex basalts (TCB) are generally microcrystalline basalts containing phenocrysts of plagioclase and clinopyroxene. However, basalts, which are equigranular range from glass, though cryptocrystalline and fine grained, with a groundmass composed primarily

of plagioclase and pyroxene, are also found. Phenocryst content is sometimes as high as 25%. Primary phenocryst are plagioclase > clinopyroxene > orthopyroxene >> magnetite, sphene. Rare olivine rich and hornblende bearing basalts also occur within the complex. Secondary phases are clay minerals (smectite > chlorite > illite), biotite, zeolites, analcime, actinolite, prehnite, calcite, pyrite.

Plagioclase occurs as euhedral to subhedral grains, generally tabular in form, within the basalts. In size the grain of plagioclase range from microcrystalline to 2mm in length, it is very rarely larger. Both simple and multiple twins are common. The composition of plagioclase in the basalts occupies a limited compositional range with an average of An84 (Figure 4.3.3a).

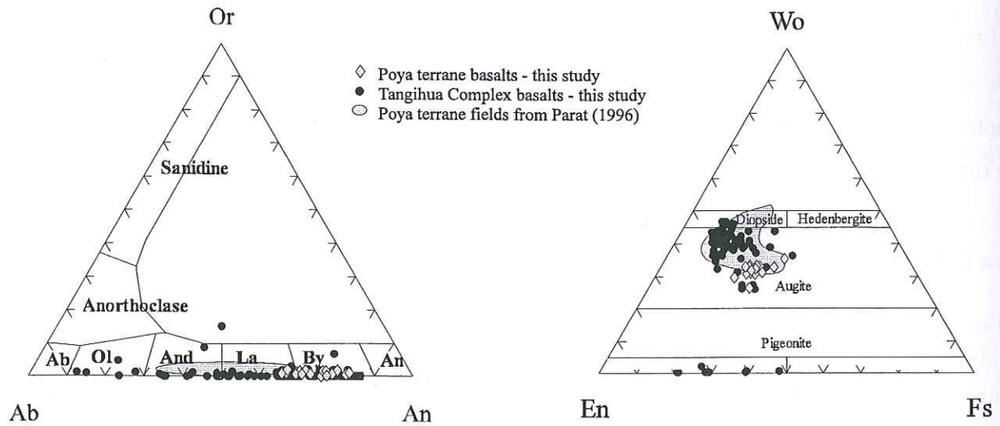

Figure 4.3.3: (a) Representative plagioclase analyses and (b) representative clinopyroxene analyses from basaltic lavas in the Tangihua Complex and the Poya terrane. Poya terrane data from this study and from Parat (1996). Plagioclase composition calculated on the basis of 20 oxygens. Pyroxene compositions calculated on the basis of 6 oxygens.

The pyroxene present in the TCB is almost entirely clinopyroxene. The clinopyroxene occurs as pale green, subhedral to euhedral crystals, which are generally smaller than 0.5mm on the longest axes. Clinopyroxene phenocrysts are calcic augite (Figure 4.3.3b) and commonly contain inclusions of plagioclase and opaque minerals (possibly magnetite). They are often embayed and may contain exsolution lamellae of orthopyroxene. Rare orthopyroxene is colourless to pale greenish brown. It occurs as tabular or subhedral crystals which are generally embayed and/or altering to clay minerals

Possible olivine phenocrysts have altered to clay minerals. Both pyroxene and plagioclase have partially altered to zeolites and/or clay minerals. The Tangihua rocks have all undergone low-temperature hydrothermal alteration and, where associated with intrusive activity, variable degrees of metamorphism ranging up to greenschist facies. Unusual, comparable two phase alteration sequences have been described elsewhere in ocean crustal material (e.g. Mevel, 1988). For more

detailed studies of the secondary mineral assemblages see Black (1989), Nicholson and Black (1998) and Nicholson *et al.* ((a) in review).

New Caledonia

The PTB range from almost aphyric massive flows, microgabbro plugs and dykes, through to intergranular and intersertial textured basalts with 2-10 modal % plagioclase and clinopyroxene phenocrysts. Less commonly the terrane contains olivine + plagioclase phyric or plagioclase + clinopyroxene phyric pillow basalts with largely devitrified glassy rims. Phenocryst content is sometimes as high as 20%. Primary phenocryst are plagioclase > clinopyroxene >> orthopyroxene, magnetite and sphene.

Where fresh, olivine has a composition of Fo_{83-85} (Eissen *et al.*, 1998) but is more commonly altered to chlorite and/or calcite. Plagioclase occurs as euhedral to subhedral grains, generally tabular in form, and ranging in size from microcrystalline to 4mm in length, although larger crystals are seen. Both simple and multiple twins are common. The composition ranges from An_{30} to An_{85} with an average of An_{55} (Figure 4.3.3a).

The clinopyroxene present in the PTB basalts occurs as pale green, subhedral to euhedral, crystals up to 2mm in length. Clinopyroxene phenocrysts are generally calcic augite (Figure 4.3.3b), however, in the alkaline basalts the pyroxene is dominantly diopside (Parat, 1996; this study). Clinopyroxene crystals are often embayed and may contain exsolution lamellae of orthopyroxene. Rare orthopyroxene is colourless to pale greenish brown grains, which are generally being altered to clay minerals

Low grade metamorphism is uniform throughout the PTB with virtually all samples containing mineral assemblages reflecting both the prehnite-pumpellyite and the greenschist metamorphic facies (Nicholson *et al.*, (a) in review). Secondary minerals include; prehnite, pumpellyite, epidote, chlorite, albite and titanite (200-400°C), which generally correspond with the prehnite-pumpellyite metamorphic facies. In most areas minor actinolite and K-feldspar also occur as secondary mineral phases, suggesting that the temperatures associated with metamorphism were upwards of 300°C which corresponds with greenschist facies.

GEOCHEMISTRY

A collection of over 120 samples from the TCB (Nicholson *et al.*, (b) in review) and 35 samples from the PTB have been analysed for major oxides and trace elements. From these analyses, 34 TCB and 17 PTB samples with total volatile content < 4wt% were chosen for REE analyses. This study has focused primarily on the basalts from both the TCB and the PTB.

Representative analyses are given in Table 4.3.1 and illustrated in Figures 4.3.4 through 4.3.8. Data used for the alkaline basalts of New Caledonia are from Eissen *et al.* (1998).

Sample#	49211	47654	49189	49123	49186	47659	49220	49225	49233	49239	49245	49251	49259
rock type	basalt	dol	basalt	basalt	basalt	basalt	basalt	basalt	basalt	basalt	basalt	basalt	basalt
	NZ	NZ	NZ	NZ	NZ	NZ	NC	NC	NC	NC	NC	NC	NC
Recalculated to 100% using $Fe_2O_3/FeO = 0.15$													
SiO_2	51.73	53.04	51.28	58.57	50.49	51.65	50.95	49.04	50.66	50.04	50.08	50.66	50.59
TiO_2	1.08	1.27	1.56	2.22	1.86	1.59	1.41	1.35	1.31	1.39	1.35	1.41	1.69
Al_2O_3	15.71	15.98	15.87	13.54	15.80	15.30	14.44	15.83	13.74	14.42	14.39	17.31	14.89
Fe_2O_3	1.40	1.32	1.38	1.42	1.49	1.36	1.48	1.34	1.42	1.54	1.56	1.19	1.49
FeO	9.31	8.83	9.24	9.48	9.95	9.06	9.88	8.96	9.47	10.26	10.38	7.95	9.92
MnO	0.18	0.18	0.19	0.22	0.21	0.20	0.22	0.26	0.18	0.24	0.2	0.17	0.16
MgO	6.56	6.30	5.92	3.39	6.17	6.93	8.09	7.74	6.58	8.19	7.85	6.05	8.24
CaO	10.91	8.96	10.82	8.03	10.32	9.09	9.71	11.04	15.59	11.13	10.08	11.73	6.48
Na_2O	2.86	3.61	3.17	2.78	3.32	4.48	2.89	3.34	0.92	2.56	3.12	3.24	3.01
K_2O	0.18	0.42	0.43	0.16	0.20	0.18	0.81	0.95	0.01	0.12	0.89	0.17	3.37
P_2O_5	0.09	0.10	0.13	0.18	0.19	0.18	0.12	0.14	0.12	0.1	0.1	0.14	0.15
Total	100	100	100	100	100	100	100	100	100	100	100	100	100
LOI	1.48	0.58	1.83	1.08	0.58	0.58	0.39	0.20	0.19	0.29	0.29	1.16	0.10
Traces elements (ppm)													
Ba	16.59	40.86	23.24	40.73	30.70	18.55	1983.0	63.50	13.38	143.52	55.21	6.17	392.63
Rb	1.34	4.46	5.61	3.72	2.18	2.59	12.61	13.20	0.11	24.10	0.63	3.30	86.34
Sr	157.49	141.75	101.67	92.23	206.22	79.04	201.00	85.38	39.93	427.35	113.69	260.73	40.09
Ta	0.07	0.10	0.10	0.17	0.20	0.29	0.38	0.18	0.31	0.37	0.35	0.18	0.37
Th	0.18	0.13	0.15	0.15	0.23	0.26	0.40	0.07	0.30	0.39	0.35	0.13	0.39
Zr	48.04	57.90	80.61	115.39	116.56	103.23	67.65	31.57	74.45	74.67	59.56	91.59	85.50
Nb	0.78	0.99	1.16	1.23	2.57	3.54	5.32	1.95	3.84	5.56	4.67	2.35	5.30
Y	24.23	24.61	30.53	47.87	36.53	36.85	23.21	24.44	24.93	31.30	21.99	30.51	26.37
Hf	1.69	1.78	2.28	4.19	3.04	3.60	1.88	1.32	2.01	2.07	1.66	2.40	2.46
V	356.91	321.22	380.84	450.10	354.47	315.45	376.09	267.85	296.45	341.77	350.18	286.71	330.38
Cr	113.66	77.23	93.87	15.03	115.93	239.74	176.60	377.68	282.02	182.06	175.55	211.49	256.14
Ni	46.33	40.20	33.26	16.33	42.13	56.56	78.89	99.70	74.72	94.18	94.98	73.09	91.41
Co	47.81	33.97	36.97	49.81	36.35	43.71	46.48	49.95	55.76	59.07	45.82	48.57	48.05
U	0.07	0.08	0.12	0.58	0.09	0.11	0.11	0.07	0.08	0.10	0.10	0.06	0.13
Sc	42.58			41.71		40.05	48.98	47.10	48.83	46.19	49.39	40.29	39.05
Cu	64.48	32.36	47.24	38.08	49.60	48.37	138.36	29.81	120.99	162.17	150.23	62.71	145.33
Zn	80.55	69.01	71.19	110.07	79.90	80.20	75.35	68.43	73.90	94.92	76.86	72.51	86.28
Pb	0.72	1.30	0.48	0.91	0.80	0.32	0.59	0.51	1.01	0.66	1.18	0.56	0.66
Ga	18.03			20.44		16.35	19.56	14.6	20.33	17.45	17.3	18.14	16.34
Cs	0.02	0.05	0.08	0.15	0.14	0.18	0.39	0.5	0.28	1.98	0.03	0.1	3.56
La	2.01	2.19	2.58	14.73	4.10	4.72	4.59	2.78	4.08	4.71	3.93	2.98	5.21
Ce	6.64	7.00	8.66	19.49	12.76	14.30	11.7	8.6	11.04	12.53	10.12	9.66	15.12
Pr	1.22	1.21	1.51	23.79	2.14	2.33	1.71	1.45	1.73	1.94	1.5	1.66	2.35
Nd	7.07	6.54	8.11	27.10	11.03	11.94	8.25	7.61	8.69	9.52	7.25	8.74	11.68
Sm	2.81	2.31	2.84	30.44	3.55	3.79	2.54	2.59	2.75	3.05	2.25	2.96	3.49
Eu	1.09	0.86	1.06	28.55	1.24	1.34	0.94	1.03	1.04	1.2	0.88	1.15	1.36
Gd	3.81	3.04	3.72	30.37	4.54	4.95	5.18	3.4	3.43	4.06	2.94	3.95	4.52
Tb	0.67	0.58	0.73	31.76	0.82	0.93	0.58	0.62	0.63	0.74	0.53	0.74	0.73
Dy	4.23	3.84	4.77	30.88	5.62	6.04	3.81	4.01	4.01	4.84	3.52	4.87	4.65
Ho	0.92	0.86	1.05	30.71	1.24	1.30	0.83	0.88	0.86	1.06	0.77	1.07	0.95
Er	2.57	2.43	3.04	30.52	3.52	3.75	2.37	2.45	2.45	3.05	2.2	3.03	2.63
Yb	2.48	2.36	2.88	29.07	3.39	3.49	2.26	2.26	2.29	2.87	2.07	2.84	2.3
Lu	0.39	0.36	0.45	29.42	0.52	0.54	0.35	0.34	0.34	0.43	0.32	0.43	0.33

Table 4.3.1: Representative whole rock geochemical data, including major oxides and trace elements, from the Tangihua Complex and the Poya terrane. NZ: New Zealand, NC: New Caledonia.

External surfaces of fresh rocks were removed by splitting and the samples split into chips, which were then ground to a powder in a tungsten carbide ring grinder. H_2O+, H_2O- and CO_2 were determined by gravimetry, the remaining major oxides and trace elements were determined by XRF (after Norrish and Chappell, 1977) at the University of Auckland, New Zealand. The precision (2σ) of the major oxide determinations is generally less than 2%, and less than 5% for the trace elements (at ten times the detection limit of 1-2 ppm). Rare earth element abundance's were determined by inductively coupled plasma mass spectroscopy (ICP-MS) at the Laboratoire de Geodynamique des Chaînes Alpines, Université Joseph Fourier, Grenoble, France using the method of Barrat, 1996. The precision (2σ) for ICP-MS analyses varies from 2-10% for the elements analysed.

The samples in the study have SiO_2 contents ranging between 49 and 60wt% although most of the PTB samples fall between 48 and 53 wt% SiO_2 where as most of the TCB samples fall between 49 and 55wt% SiO_2. This corresponds to the basaltic through to basaltic-andesite fields of the IUGS classification scheme. Both the PTB and the TCB samples are predominantly tholeiitic, however, there are alkaline affinities present within both ophiolites (Figure 4.3.4a).

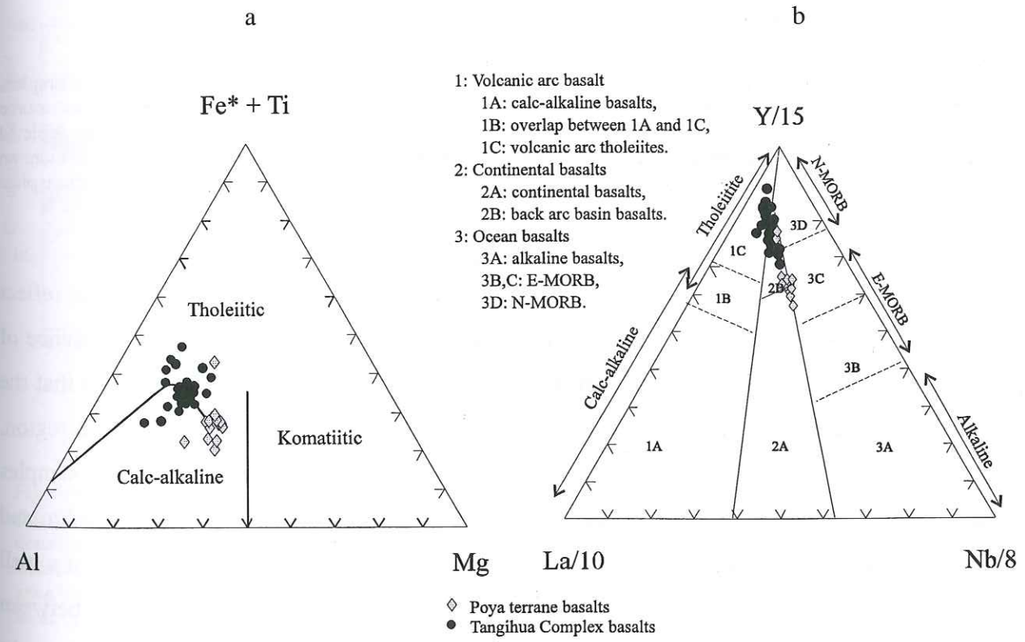

Figure 4.3.4: (a) The ternary plot of Fe *+ Ti- Al-Mg (Jensen diagram) shows two different trends for the basalts of the Tangihua Complex and the Poya terrane. (b) The Ternary plot of Y/15-La/10-Nb/8 showing the combined volcanic arc tholeiite and back-arc basin signatures of the Tangihua Complex basalts, and the back-arc basin/MORB signatures of the Poya terrane basalts

The ternary element plot of Y/15-La/10-Nb/8 (Figure 4.3.4b) uses primarily immobile HFS elements to classify rock types. The basalts from the TCB clearly fall into the volcanic arc tholeiite

suite and the back arc basin (BAB) suite where as the PTB fall within the MORB and BAB suites. Other diagrams, such as Nd/Th versus Y (ppm) after Jenner *et al.* (1991; Figure 4.3.5a) illustrate the typically arc-like signature for some of the TCB samples but a slightly enriched MORB-like signatures for the PTB samples and the remainder of the TCB samples.

a b

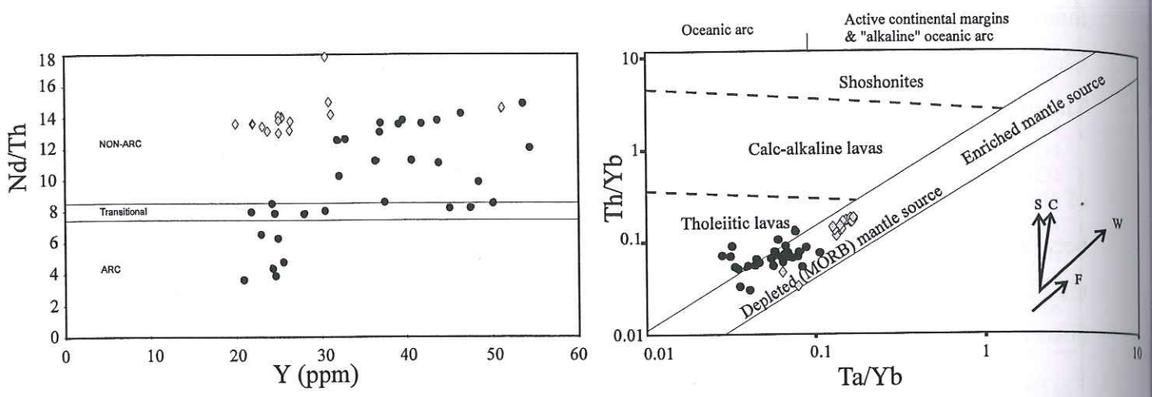

Figure 4.3.5: (a) Y versus Nb/Th plot showing the arc, MORB and transitional signature of the Tangihua Complex, whereas the Poya terrane are entirely MORB-like. (b) Ta/Yb versus Th/Yb plot showing the generally depleted source for both the Tangihua Complex and the Poya terrane. Note that the source for the Tangihua Complex is more depleted than that for the Poya terrane. This diagram also shows the effects of fractionation and subduction zone enrichment on the lavas from the Tangihua Complex. S=subduction zone enrichment, C=crustal contamination, W=within plate enrichment and F=fractionation.

The depletion of Nb, Ta and Zr in the TCB, as seen in Figure 4.3.6b, is thought to reflect formation from a subduction modified mantle (suprasubduction zone). In this case the presence of clearly arc-type basalts in combination with definite depletion of both Nb and Zr suggests that the complete suite of samples represents a transition from volcanism at the arc to the back-arc region. Where as the only slight enrichment of LIL elements relative to HFS elements in the TCB samples is believed to suggest ocean crust which has undergone only a small amount of metasomatism and is therefore fairly immature. Given the geochemistry and the tectonic constraints (the lack of a well developed arc and back-arc systems) we suggest that the TCB formed in a transitional zone between an arc setting and a back-arc setting, or in a zone of migration from arc to back-arc volcanism. As such, the field, age and geochemical data supports the model in which these rocks formed suprasubduction zone crust and are fragments recording some or all stages of arc initiation, arc rifting and back-arc basin formation.

As with the TCB, some of the Poya basalts have a slight but significant negative Nb anomaly relative to La as observed in back arc basins (BAB). They are depleted in LREE but

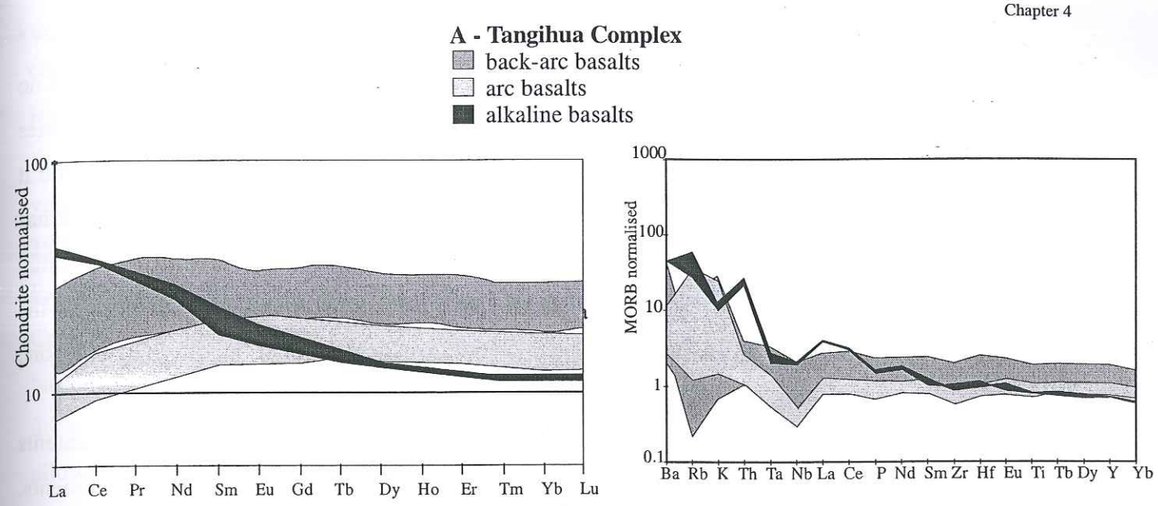

Figure 4.3.6: Chondrite and MORB normalised trace element plots for the Tangihua Complex (a) and the Poya terrane (b). The geochemical affinities of the basaltic lavas from the two systems are remarkably different. The Poya terrane is dominated by N- and P-MORB lavas whereas the Tangihua Complex is dominantly subduction modified N-MORB, which are separated into arc and back-arc type lavas. However, both systems show signs of modification by subduction zone processes, as seen by the Nb anomalies in the arc and back-arc lavas of the Tangihua Complex and the N-MORB lavas of the Poya terrane. In addition, both systems contain basaltic lavas with alkaline affinities.

generally display flat REE patterns. It is possible that much of the apparent BAB signature in the PTB is due to changing fO_2, and hence increased Mn content and Fe^{+3} as opposed to Fe^{+2}, during alteration and metamorphism (for more information see Nicholson *et al.*, (b) in review). However, unlike the TCB, the majority of the PTB samples have Ti/Zr and La/Nb ratios similar to MORB. Samples analysed as part of this study have a limited range of Mg#, between 40 and 50, which combined with low Cr and Ni contents are further characteristics of MORB affinities. PTB samples

052 137431 5
BIBLIOTHÈQUE SCIENCES GRENOBLE UNIVERSITAIRE

with P-MORB affinities display a light enrichment of LREE, a marked enrichment in LILE and no depletion of HREE. Other studies, however, have shown a predominance of P-MORB affinities based, in part, on isotopic work (Parat, 1996; Cluzel *et al.*, 1997; Picard *et al.*, 1999). In general it is likely that the formation of all of the Poya basalts is the result of extensional magmatism. It has been argued that the PTB were produced during the break-up stage of the development of a small ocean basin (Eissen *et al.*, 1998) in which case the BAB signatures might be explained by the assimilation of pre-existing arc material rather than being indicative of a suprasubduction zone setting.

Alkaline basalts are present within both ophiolite complexes. They have Nb contents approximately twice those of the MORB-like suite and show enrichment of incompatible elements. They are generally depleted in HREE, enriched in both the LREE and LILE. In New Caledonia they are thought to have formed as seamounts essentially in situ on the MORB-like PTB (Cluzel *et al.*, 1997), or they may have been scraped off their original oceanic substraight during subduction and emplaced along with the PTB (Eissen *et al.*, 1998). Where as in the Tangihua Complex, the alkaline volcanics possibly represent small amounts of melting of enriched mantle material which has been dragged down into the mantle by the subducting slab (Thompson *et al.*, 1997). This material was then erupted close to or within the developing back-arc basin region and, in this instance, contains distinct subduction zone signatures. In these systems the presence of alkaline basalts is in character with the proposed mechanisms of formation.

Figure 4.3.5b shows the variation of Ta and Th with respect to Yb. As both Th/Yb and Ta/Yb ratios remain relatively constant during partial melting their values reflect differences and/or similarities in source composition. This diagram is significant as it illustrates two important features. Firstly, this diagram shows that the composition of the TCB basalts reflects slightly different petrogenetic histories including differing influences of the subduction zone and possibly differing source compositions, between the arc basalts and the back arc basalts. Secondly, this diagram clearly show distinctly different sources for the ophiolitic basalts found in New Zealand and in New Caledonia.

GENERATION AND EMPLACEMENT MODELS

New Zealand

Early interpretations regarding the formation and emplacement of the Tangihua Complex were diverse (Quennell and Hay, 1964; Brothers, 1974; Brothers and Delaloye, 1982). Recent emplacement models for the Tangihua Complex (Malpas *et al.*, 1992; Hopper and Smith, 1996; Thompson *et al.*, 1997; Nicholson *et al.*, (b) in review), have tried to account for the diverse

chemistry of the rock types, the plate-tectonic constraints, the preservation of mainly the upper levels of the ophiolite sequence and the close association with the allochthonous sedimentary rocks.

Geochemical and petrological studies have shown that the TCB is composed of a wide variety of magmatic affinities ranging though tholeiitic, calc-alkaline to alkaline (Malpas *et al.*, 1992; Hopper and Smith, 1996; Thompson *et al.*, 1997; Nicholson *et al.*, (b) in review). Paleontological evidence suggests that the TCB were probably generated during the Late Cretaceous (approximately 80-100 Ma). The diverse geochemistry suggests that the Tangihua basalts are the result of a complex magmatic history, originating in an arc setting and evolving into a back-arc setting. This arc migration was a result of either extension or arc-roll back, which allowed for the transition from arc to back-arc and N-MORB-like signatures all within one apparent system (Figure 4.3.6, Nicholson *et al.*, (b) in review).

Throughout most of its geological history New Zealand has been associated with convergent plate margins. The early to mid Cretaceous saw the culmination of a long period of plate convergence and terrane amalgamation on the New Zealand sector of the Gondwana margin. As such, from the Permian to the Early Cretaceous rocks were predominately formed as a result of convergent margin tectonics and comprise incomplete remnants of magmatic arcs, forearc basins, trench slope basins and accretionary complexes. The only time when this was not the case occurred when a sudden change in the tectonic regime during the mid-Cretaceous, marked a shift from subduction to extension-dominated magmatism (105±5Ma; Bradshaw, 1989).

During this time (110 – 90 Ma; Ballance, 1993) the eastern margin of New Zealand was a subduction margin where as the western and southern margins were rifting (100 - 95Ma). In response to these contrasting situations, both the western and southern regions were hot and high standing where as the east was cold and accumulating trench and slope sediments (Ballance, 1993). Subduction beneath the New Zealand sector of Gondwana ceased in the early Late Cretaceous with the approach and incipient collision of the spreading ridge between the Phoenix and Pacific plates (Bradshaw, 1989; Spörli and Ballance, 1989; Mazengarb *et al.*, 1991). Ridge collision was immediately succeeded by crustal extension, leading eventually to fragmentation away from Gondwana (Weissel and Hayes, 1977; Laird, 1993). After oblique ridge-trench collision along the New Zealand margin, the Phoenix-Pacific Ridge propagated to the south-west to link with zones of incipient spreading in the Tasman Sea and south of Australia. Subsequently, the eastern part of the ridge continued to migrate south with increasing offset along the Udinsev Fracture Zone.

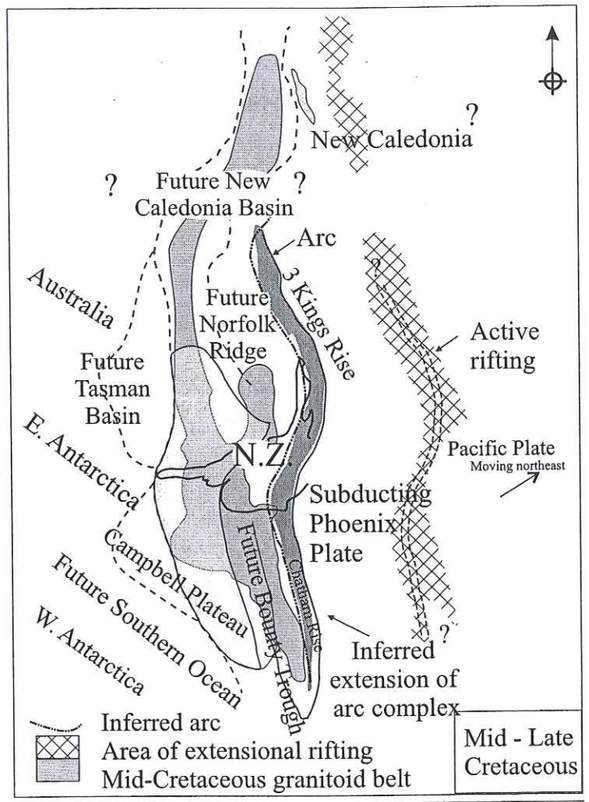

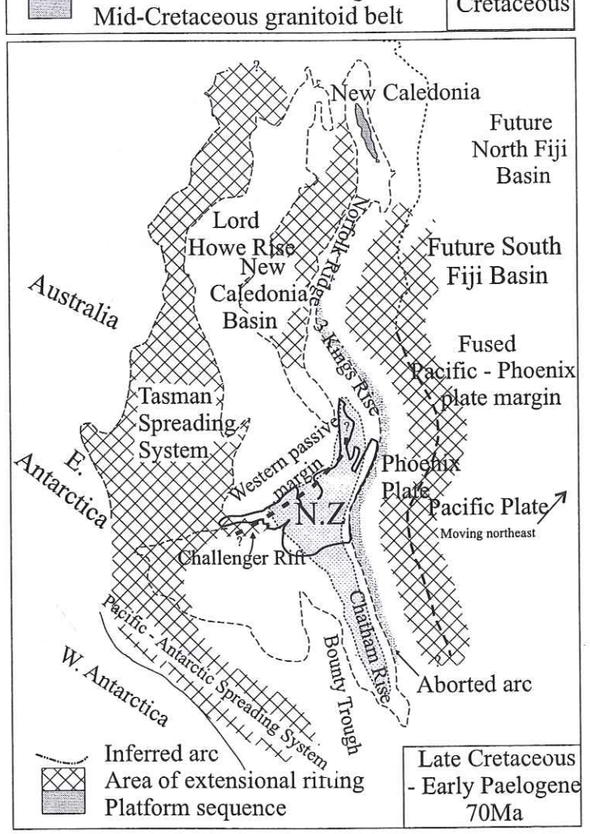

Figure 4.3.7: Generalised tectonic reconstrustion of the SW Pacific region from the mid-Cretaceous to recent showing (a) the collision between the Australasian Plate and the Phoenix-Pacific Plate and the proposed position of the associated arc volcanism near New Caledonia and New Zealand, (b) the capture of the Phoenix Plate by the Pacific Plate and the ensuing rifting.

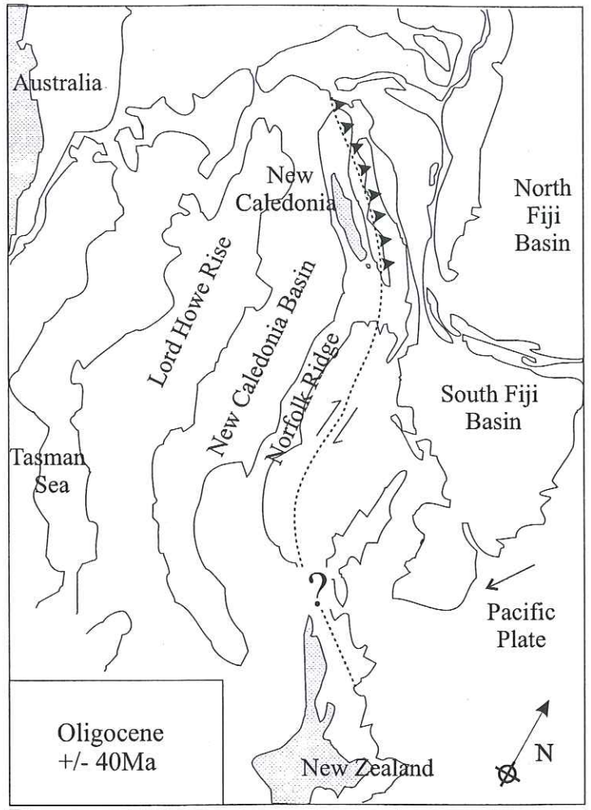

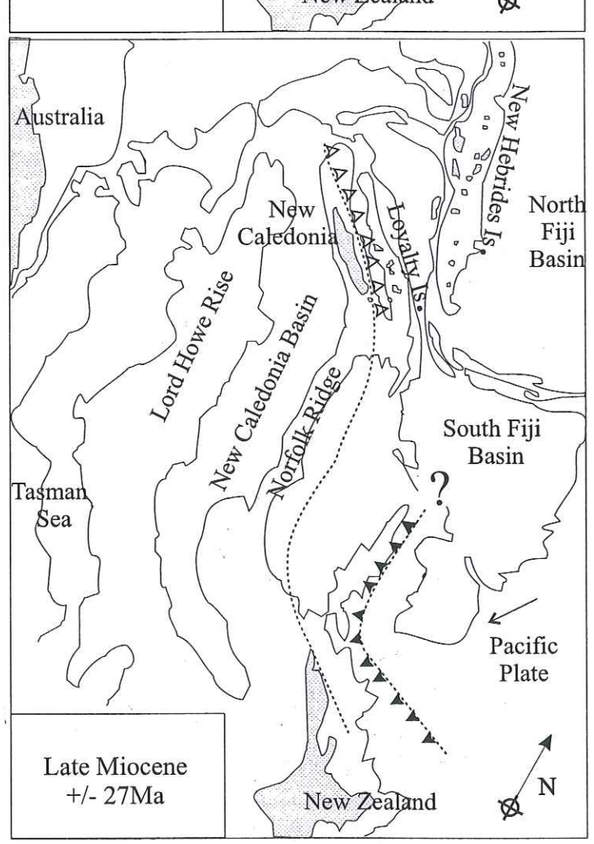

Figure 4.3.7: continued. (c) the intiation of a compression regeim and the initiation of subduction to the east of both the New Caledonian and the New Zealand landmass, (d) the obduction of the Tangihua Complex and possibly the Poya terrane due to continued subduction and (e) the current tectonic setting in the SW Pacific.

The opening of the Tasman and South Pacific spreading centres which began at about 100Ma eventually led to the production of new oceanic crust (Weissel and Hayes, 1977; Bradshaw; 1989). At this time the Phoenix plate was very small and rather than continued subduction, the Phoenix plate was captured by the Pacific plate. Resistance to subduction may have caused the break-up of brittle portions of the slab, allowing the entrainment of crustal material which was then circulated back beneath the ridge crest. Plate capture led to the stalling of the Phoenix-Pacific subduction and the initiation of rifting between the newly formed Phoenix-Pacific plate and West Antarctica (Luyenduk, 1995). It is proposed here, that the stalling of the Phoenix-Pacific ridge and associated subduction system, in combination with the initiation of rifting in the Tasman Sea, resulted in the generation of the Tangihua Ophiolite Complex. Subduction was initiated such that the downgoing slab was partially melted and arc-related volcanism commenced (≈85Ma). However, subduction was quickly aborted with the change to an extensional environment. The proceeding rift volcanism was then in contact with, and interacted with the remnant arc magmas and fragmented crustal material, hence, explaining the arc signatures in the otherwise N-MORB basalt chemistry. The presence of active subduction in New Zealand at this time is supported by the relationships recognised between several mid-Late Cretaceous stratigraphic domains in the North Island (Ballance, 1993; Mazengarb and Harris, 1994).

There was a Late Cretaceous erosional hiatus (≈80Ma) within New Zealand, suggesting isostatic rebound of the accretionary prism (Ballance, 1993). Subsidence and rapid onlap commenced in the east as a result of post-rift transgression, which affected the entire New Zealand landmass. Consequently, New Zealand became surrounded by subsiding passive margins on all sides. Locally, within the TCB, the ocean floor alteration of the basalts suggests that there was little or no major tectonic activity occurring between their formation, approximately 80Ma, and their obduction, approximately 40Ma. Thus enabling a 'typical' low temperature seafloor alteration sequence to develop (Nicholson *et al.*, (a) in review).

The reorganisation of plate motion in the Pacific region, around 42Ma, resulted in subduction between the Indian and Pacific plates, approximately 35Ma (Figure 4.3.7; Hayward, 1993). The very Late Oligocene to Early Miocene saw the southward propagation of the Indian-Pacific plate boundary through northern New Zealand. The following 8 – 10 Ma of regionally variable compressional tectonism (Hayward, 1993) resulted in the obduction of the allochthon (including the Tangihua Ophiolite Complex; Ballance and Spörli, 1979) from the northeast over Northland and the south-eastern part of the Reinga Ridge (Herzer *et al.*, 1997) and the initiation of arc volcanism.

During this phase an accretionary prism, containing sedimentary material, arc lavas and back-arc lavas was created and then overthrust onto the Northland Peninsula. Downward dragging

of the eastern edge of the continental crust allowed subsequent gravity sliding of the allochthon (Ballance and Spörli, 1979). Rebound of the crust has caused the present day uplifted basement ranges along the eastern margin of the Northland Peninsula.

New Caledonia

As with the Tangihua Ophiolite Complex, there has been much controversy over the years as to the generation and emplacement of the Poya terrane in New Caledonia. Recent re-evaluation of the field relations, geochemistry and age of the PTB has resulted in new theories for its genesis and emplacement (Cluzel *et al.*, 1994; 1997; Eissen *et al.*, 1998; this study: Figure 4.3.7), although some controversy still exists. The PTB is dominated by P-and N-MORB tholeiites with minor BAB affinities and alkaline basaltic rocks, suggesting formation during the opening of a marginal basin to the northeast of New Caledonia, approximately 70 – 80 Ma (such as the East New Caledonia Basin of Eissen *et al.*, 1998).

During the Late Cretaceous the eastern margin of the Australian sector of Gondwana was fragmented by progressive, subparallel rifting episodes. This phase of rifting in the South Pacific region produced the Tasman Sea, the New Caledonian Basin, the Norfolk-New Caledonia Ridge, the Lord Howe Rise and at least one small oceanic basin northeast of New Caledonia (Bradshaw, 1989). The Poya terrane ophiolite is thought to have formed within this small basin which was later closed by east directed subduction (Cluzel *et al.*, 1994; 1997; Eissen *et al.*, 1998).

The incipient collision of the western passive margin of the basin with the forearc of the Loyalty oceanic arc emplaced the main New Caledonian ophiolite sheets (both the Poya terrane and the Massif du Sud) from the north-northeast back onto the passive margin (Eissen *et al.*, 1998; Cluzel *et al.*, 1999). With the cessation of rifting in the Tasman Sea and the New Caledonia Basin, at approximately 56 Ma, the continued extension at the eastern margin of the Australian plate was taken up by the opening of the North Loyalty Basin, which later evolved into the South Fiji Basin. The oldest magnetic anomalies, in the North Loyalty Basin, are approximately 56Ma. The basin opening combined with the general northward displacement of the Australian plate, presumably generated regional NE-SW compression, which initiated subduction along the spreading ridge in the East New Caledonia Basin spreading centre (Eissen *et al.*, 1998; Cluzel *et al.*, 1999). Continued subduction, albeit relatively short lived, produced the primitive arc volcanoes of the Loyalty-d'Entrecasteaux arc.

A major change in the nature of the tectonics occurred during the middle Eocene in response to the approach and arrival of the eastern New Caledonian basin terranes. This led to the closure of the East New Caledonia Basin and eventually drew the PTB bearing rifted eastern margin of the Norfolk-New Caledonia Ridge towards the trench (Figure 4.3.7). Eventually a series of structurally

telescoped thrust slices developed as a result of continued collision. As the nappe pile developed, progressively deeper crustal levels of the collision zone were sampled, such as the PTB. Non sequential thrusting resulted in the subsequent emplacement of nappes of deeper material overthrusting shallower material.

The subduction systems began to fail around the same time as New Caledonia entered the trench itself (around 38Ma). Consequently fore-arc ophiolitic material was obducted over the New Caledonian basement and the PTB rocks. High pressure, low temperature metamorphism occurred within the collision zone and parts of the PTB were pushed to their deepest levels resulting in recrystallisation under blueschist to eclogite facies in the northeastern regions (Black and Brothers, 1977; Powell and Holland, 1988). Subsequent postcollisional culmination collapse resulted in tectonic denudation and unroofing of the high grade metamorphic rocks in the core complexes in the northeast of New Caledonia.

DISCUSSION

Previous work in New Zealand and New Caledonia has confirmed a close resemblance between both litholigical and paleontological units from the late Palaeozoic and Mesozoic of the two countries (Avias, 1953; Lillie and Brothers, 1969; Fleming, 1970; 1979; Paris and Bradshaw, 1977; Stevens, 1977;). This paper shows that there are also strong similarities between the formation and obduction of the basalts within the ophiolitic complexes of both New Caledonia and New Zealand. However, these similarities reflect the overall tectonic regime active in the Southwest Pacific, from the Late Cretaceous through to the Eocene, rather than a specific or direct relationship between the two ophiolites.

The Late Cretaceous break-up of eastern and southern Gondwana margin signalled the beginning of a period successive opening and closing of marginal basins that isolated ridges of continental, oceanic or intermediate nature throughout the Southwest Pacific. In New Caledonia one of the manifestations of this tectonic regime was the opening of a small oceanic basin to the northeast and the generation of the Poya terrane basalts. Where as, in New Zealand the tectonic regime was complicated by the interaction between the Phoenix and Pacific plates, opening of the Tasman Sea and the associated rifting, which formed a short lived subduction system from which the Tangihua Ophiolite Complex was generated.

The presence of active subduction to the north of New Zealand greatly influenced the chemistry of the TCB. As such, the Tangihua basalts are both tholeiitic and calc-alkaline and they reflect both back-arc and arc compositions. In New Caledonia there was little influence of prior subduction during the generation of the PTB. In this case the basalts are predominately P- and N-

MORB, basalts. Hence, although the formation of both the TCB and the PTB was the perpetuated by the same overall tectonic events, the chemistry of the rocks is significantly different.

The post formation history of the TCB and the PTB also show strong similarities but here again there are major differences. Between 80 and 35 Ma, New Zealand is characterised by a period of tectonic quiescence. All evidence suggests that the TCB experienced very little activity during this time. As major reorganisation of plates in the south-west Pacific, around 40Ma, caused subduction between the Indian and Pacific plates, resulted in the obduction of an allochthon sequence which included the Tangihua Ophiolite Complex. Obduction was from the northeast, over Northland and the south-eastern part of the Reinga Ridge, and appears to have happened relatively quickly. During the same period of time, 80 to 35 Ma, New Caledonia experienced a more active history. The cessation of rifting in the Tasman Sea and the New Caledonia Basin, at approximately 56 Ma resulted in the opening of the North Loyalty Basin and generated regional NE-SW compression. This was followed by the closure of the marginal basin in which the PTB formed and eventually the PTB was drawn into the trench. Subduction began to fail (around 38Ma) and the ophiolitic material was obducted over the New Caledonian basement. Subsequent postcollisional culmination collapse resulted in tectonic denudation and unroofing of the high grade metamorphic rocks in the core complexes in the northeast of New Caledonia. Thus, although their overall history is quite different, the obduction of both the TCB and the PTB was fuelled by the same Late Eocene reorganisational event in the Pacific.

The results of this work confirm that there are considerable similarities between the ophiolite formation, during the Late Cretaceous, and emplacement, during the Eocene, in both New Zealand and New Caledonia. However, the specific details of formation and emplacement are quite different which is reflected in the different chemistries. The presence of these two very similar systems, within the Southwest Pacific supports the presence of a large scale tectonic regime of rifting, convergence and consequent eastward subduction in the region during the Late Cretaceous and Early Palaeocene.

ACKNOWLEDGEMENTS

This research has been supported by the University of Auckland, New Zealand, the French Embassy, Wellington, NZ, and by the Université Joseph Fourier, France. Special thanks to Dr. D. Cluzel for reading the draft and making many useful comments.

SECTION 4.4

Sr and Nd Isotopes

Radiogenic isotope ratios in a magma are characteristic of the source region from which the magma was generated. Isotopic ratios are not effected by subsequent fractionational processes, as the mass difference between any give radiogenic isotope pair is very small, although there are some exceptions such as helium. This attribute has lead to the use of radiogenic isotopes for the characterisation of source regions and has allowed the identification of mixing processes between two different reservoirs.

There is a wide variety of chemical and physical properties in the different elements used in radiogenic isotope studies. Hence different isotopic pairs are sensitive to different petrological processes. $^{143}Nd/^{144}Nd$ and $^{87}Sr/^{86}Sr$ were chosen for use in this study. $^{143}Nd/^{144}Nd$ is particularly useful in the study of oceanfloor basalts as Nd isotopes are not significantly fractionated in the continental crust, by sedimentary processes nor by the processes of alteration and metamorphism. Hence, even during hydrothermal alteration $^{143}Nd/^{144}Nd$ ratios are immobile and reflect the true composition of the rock or magmas involved in a specific petrological process. The disadvantage of using Nd isotopes is their relative insensitively to the presence of small amounts of recycled crustal material mixed with larger proportions of mantle material.

$^{87}Sr/^{86}Sr$ is also considered to be relatively immobile during hydrothermal conditions and therefore reflects the original composition of the magmas. There is a high degree of fractionation between the mantle and the crust leading to the elevated strontium isotopic ratios in the continental crust relative to the mantle. Hence $^{87}Sr/^{86}Sr$ ratios are highly effected by the presence of small amounts of recycled crustal material mixed with larger amounts of mantle material and can therefore be used as an indicator for this process. One of the major disadvantages of using strontium isotopes is that it is also highly effected by contamination by seawater.

Table 4.4.1 gives the range of isotopic data for the Tangihua Complex basalts. The results have been separated into three different groups: arc basalts, back-arc basalts and younger intrusions (Figure 4.4.1). The remainder of the table shows examples of the isotopic composition of different systems for comparative purposes. It is apparent that firstly, the Tangihua arc basalts have higher radiogenic strontium than the back-arc basalts, however, their neodymium ratios are similar. This is thought to reflect the sensitivity of strontium isotopes to the presence of larger amounts of slab input in the arc relative to the back-arc. In general the $^{143}Nd/^{144}Nd$ values of both the arc and the back-arc samples are lower than N-MORB, and the $^{87}Sr/^{86}Sr$ values are consistently higher than N-

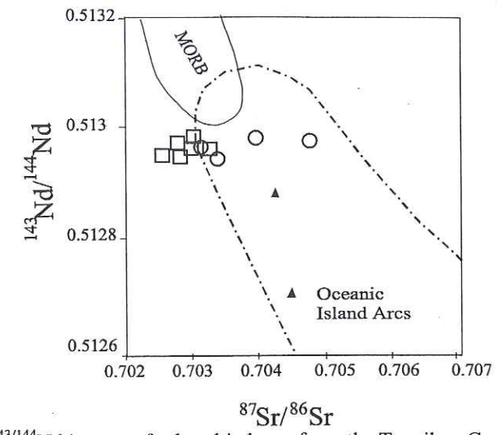

Figure 4.4.1: $^{87/86}Sr$ versus $^{143/144}Nd$ isotopes for basaltic lavas from the Tangihua Complex. Also shown are generalised fields for island arcs, oceanic island basalts (OIB) and MORB after Wilson (1989).

Location	Rock type	$^{87}Sr/^{86}Sr$	$^{143}Nd/^{144}Nd$	Reference
49211	Arc basalt	0.70359	0.51295	This study
47654	Arc basalt	0.70422	0.51299	This study
47656	Arc basalt	0.70512	0.51298	This study
49189	Arc basalt	0.70314	0.51299	This study
49164	Back-arc basalt	0.70292	0.51295	This study
49183	Back-arc basalt	0.70313	0.51297	This study
49186	Back-arc basalt	0.70346	0.51297	This study
47648	Back-arc basalt	0.70291	0.51298	This study
47662	Back-arc basalt	0.70263	0.51295	This study
49123	Back-arc basalt	0.70301	0.51297	This study
49130	Younger intrusions	0.70454	0.51289	This study
49207	Younger intrusions	0.70479	0.51272	This study
Pacific	N-MORB	0.70240-0.70256	0.5130-0.5133	1
Indian	N-MORB	0.70274-0.70311	0.5130-0.05131	1
Marianas	Young arc related basalt	0.70332-0.70378	0.512966-0.513032	2,3
Lr Antillies	Young arc related basalt	0.70359-0.70897	0.51212-0.512978	3
Samoan Islands	Ocean island basalt	0.70441-0.70651	0.512669-0.512935	4
Hawaii	Ocean island basalt	0.70317-0.70412	0.512698-0.51306	5

Table 4.4.1: $^{87}Sr/^{86}Sr$ and $^{143}Nd/^{144}Nd$ results for the Tangihua Complex and generalised fields from other systems. [1] Saunders *et al.*, 1988; [2] McDermott and Hawkesworth, 1991; [3] White and Patchett, 1984; [4] Stille *et al.*, 1983; [5] White and Hoffman, 1982.

MORB (Saunders *et al.*, 1988). Again, this reflects the presence of a slab-related component in both the arc and the back-arc lavas. Both the arc and the back-arc basalts of the Tangihua Complex compare well with other SW Pacific arcs, such as the Marianas (McDermott and Hawkesworth, 1991; White and Patchett, 1984). The younger intrusions have higher $^{87}Sr/^{86}Sr$ and much lower $^{143}Nd/^{144}Nd$. These basalts compare favourably with ocean island basalts such as Hawaii and the Samoan Islands (White and Hoffman, 1982; Stille *et al.*, 1983).

In conclusion the basaltic lavas from the Tangihua Complex can be divided into three distinctive groups based on different $^{87}Sr/^{86}Sr$ and $^{143}Nd/^{144}Nd$ systematics. Firstly, the Tangihua Complex contains arc-like lavas with $^{87}Sr/^{86}Sr$ = 0.70314-0.70512 and $^{143}Nd/^{144}Nd$ = 0.512947-

0.512987, which have isotopic ratios similar to other SW Pacific arc systems. Secondly, back-arc lavas are present. They have generally lower Sr isotopic ratio, $^{87}Sr/^{86}Sr$ = 0.702634-0.70346, than the arc basalts and similar Nd systematics, $^{143}Nd/^{144}Nd$ = 0.512952-0.512975. Finally the complex contains intrusive basaltic lavas with OIB isotopic systematics, $^{87}Sr/^{86}Sr$ = 0.704543-0.70479 and $^{143}Nd/^{144}Nd$ = 0.512712-0.51289. Further comparisons with SW Pacific arc and back-arc systems can be found in Chapter 7.

SECTION 4.5

Glass Chemistry

INTRODUCTION

It is now recognised that many, perhaps most, ophiolites have physical, petrological and geochemical characteristics, which differ from those observed in modern oceanic crust generated at spreading ridges. Some examples of the differences include the thinner relative thickness of the crustal section in ophiolites, the common occurrence of more highly differentiated rock types, and differences between the isotopic composition of the ophiolites and normal oceanic crust. Back-arc, or marginal basin basalts are an alternative site for the generation of oceanic crust, as are rifting/spreading events which take place in the early stages of island arc evolution, above subduction zones at destructive plate boundaries, hence, forming oceanic crust in a tensional environment. It has been suggested earlier in Chapter 4 that this is the environment in which the Tangihua Complex was formed.

Considerable complexity, however, exists in the geochemistry of basaltic lavas erupted along back-arc basin spreading centres, especially in young, poorly-developed systems. Although distinctive differences, in major, trace and isotope compositions exist between arc (IAB), back-arc basin (BAB) and mid-ocean ridge basalts (MORB), the considerable complexity and variations within these systems complicate geochemical interpretation. In the SW Pacific region, several back-arc basins containing basalts which geochemically resemble N-MORB, have been described (e.g. Lau, North Fiji and Woodlark in Aggrey *et al.*, 1988; Muenow *et al.*, 1990). However, there are also several back-arc basins containing basalts enriched relative to N-MORB in various combinations of H_2O, LILE and LREE, some HFSE and radiogenic isotopes (e.g. Volpe *et al.*, 1987; Price *et al.*, 1990; Vallier *et al.*, 1991; Falloon, *et al.*, 1992). In some instances, lavas of both geochemical affinities have been erupted within the same basin. In the case of the Tangihua Complex, basalts of both N-MORB and enriched, relative to MORB, chemistries have been found.

The problem of discrimination between different tectonic settings is further complicated in ancient volcanic rocks where many of the isotopic ratios and trace elements that are used to distinguish between different tectonic settings are sensitive to the alteration processes typically active on the seafloor. Although secondary alteration processes have not had a considerable effect on mobile element concentrations in the samples chosen for analyses, the effects of alteration can be found throughout the Tangihua Complex (see Chapter 3). In this instance the presence of abundant volcanic glass within the Tangihua Complex is fortuitous. Fresh volcanic glass reflects the

chemistry of the original magmas, and thus provides and opportunity to determine the true nature of the source for the Tangihua Complex. Although the chemistry of the Tangihua Complex has been dealt with in some detail in Sections 4.2 and 4.3 there has always been the possibility that alteration had an influence on the observed geochemical trends. By analysing glass samples and showing that they are fresh it is hoped that any debate over the previous conclusions will be laid to rest.

There are two different models for the generation of BAB basalts popular in the literature today (i.e. Sinton *et al.*, 1987; Volpe *et al.*, 1987; Price *et al.*, 1990; Falloon *et al.*, 1992; Danyushevsky *et al.*, 1993). The first model involves mixing of a typical N-MORB mantle source with a subduction-related component (either an arc-like melt or an H_2O-rich fluid) whereas the second model mixes a similar N-MORB mantle source with an H_2O bearing, enriched alkaline magma derived from an enriched lithospheric or shallow asthenospheric source. Both Falloon *et al.* (1992) and Danyushevsky *et al.* (1993) support the first model on evidence of H_2O, K_2O, Ta, Th and Hf systematics. Using whole rock major oxide, trace element and rare earth element data on glass samples from the Tangihua Complex, we support the findings of both Falloon *et al.* (1992), Danyushevsky *et al.* (1993) and previous workers (Sinton *et al.*, 1987; Volpe *et al.*, 1987). Hence the following sections illustrate that the basaltic lavas from the Tangihua Complex were generated by partial melting of the mantle wedge, resulting in N-MORB magmas which then variably interacted with a slab-derived fluid to form both the arc and the back-arc lava compositions found within the complex.

Twelve glass samples have been selected, on the basis of their freshness and their geographical distribution, for analyses using XRF and ICP-MS, ten of which where also analysed using oxygen isotopic techniques. This remainder of this Section presents major and trace element concentrations and oxygen isotopic data. Comparison of these results with the Tangihua basalt chemistry and with published data from both constructive and destructive plate margins allows the further constraint on the origin of the Tangihua Complex.

ALTERATION AND SAMPLE FRESHNESS

Before interpreting geochemical analyses of any rocks it is important to establish that the observed element abundances and isotopic compositions are free from the effects of secondary alteration processes. This is especially true for the mobile alkali elements, alkaline earth metals, Sr and O isotopes. Sea water alteration of basalts results in the deviation of O and Sr isotopes from their primary MORB values isotopic abundance of 5.7±0.3‰ and 0.7028±0.0004 (Muehlenbachs and Clayton, 1972; Morris and Hart, 1984, respectively). During low temperature alteration the

concentration of alkali elements, volatiles and the O isotope values generally increase, although at higher temperature both the Ca concentration and the O isotope value will begin to decrease.

Figure 4.5.1 shows the variation of δO^{18} with respect to K, Rb, Sr and LOI. All the data plotted show a relatively restricted compositional range. No one sample regularly has the highest K, Rb, Sr or LOI values, supporting that the glass samples analysed are free from the affects of hydrothermal alteration with the possible exception of 49121, which has the highest LOI (4.35%). The oxygen isotopic composition of the Tangihua glass samples ranges from 5.7 to 6.5‰ with a mean δO^{18} of 6.14‰ ± 0.2 (1σ, n=10), which is in the acceptable range for fresh mantle derived volcanic rocks (Rautenschlein *et al.*, 1985). This value slightly exceeds that normally found in

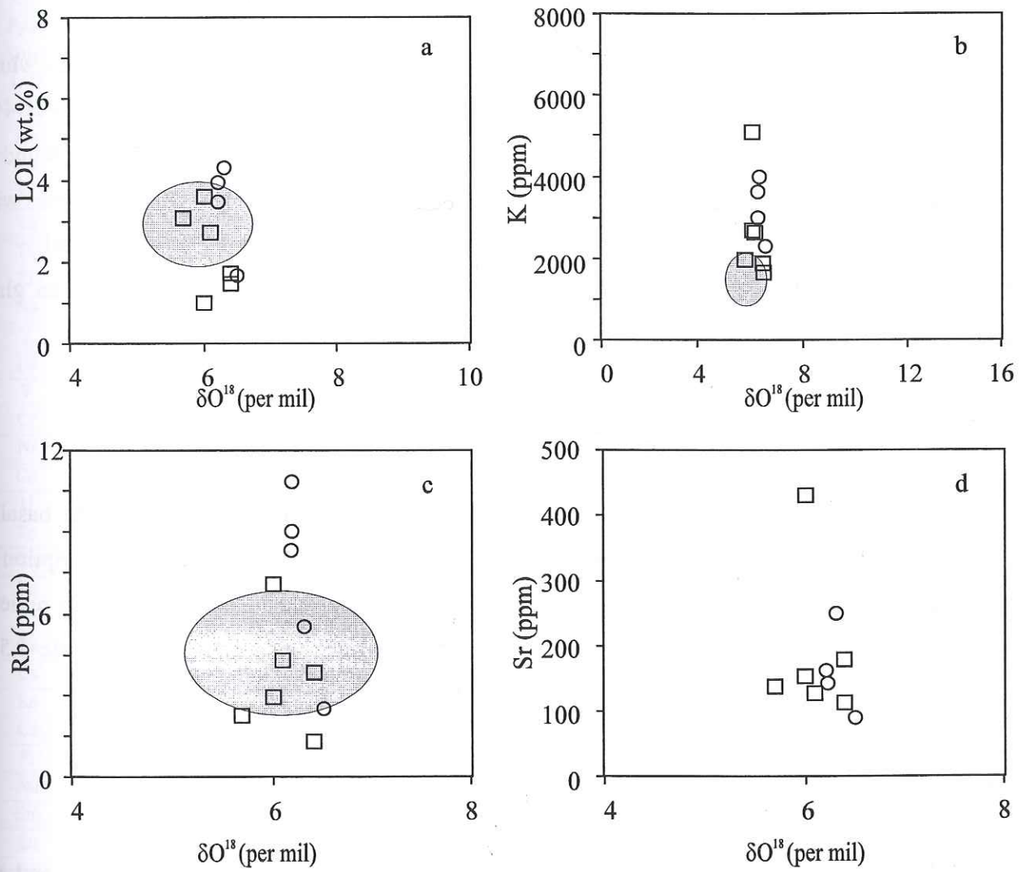

Figure 4.5.1: Discrimination diagrams showing δO^{18} with respect to LOI, K, Rb and Sr. Shaded areas are fields from the Troodos Ophiolite (Rautenschlein *et al.*, 1985). Despite pervasive alteration in the basaltic lavas of the Tangihua Complex, the glass samples are fresh with MORB-like values for δO^{18}.

fresh MOR tholeiites (5.7‰±0.3), which is not a concern as fractionation can increase the δO^{18} by up to 3% (Muehlenbachs and Byerly, 1982). With SiO_2 contents ranging up to 57wt% it is likely

that fractionation has had a minor effect on the δO^{18} content. Figure 4.5.1a shows LOI versus δO^{18} for both the Tangihua glass samples and samples from the Troodos Ophiolite (Rautenschlein *et al.*, 1985). The samples from the Tangihua Complex compare favourably with the Troodos samples, hence supporting the non altered LOI and δO^{18} values.

Sample#	49112	49117	49121	49135	49162	49164	49172	49193	49201	49219
V-SMOW δO^{18}	6.4	6.4	6.4	6	6.2	6.5	6.1	6	5.7	6.4
duplicates	6.2		6.3	6						

Table 4.5.2: Oxygen isotopic results for glass samples from the Tangihua Complex. δO^{18} values in per mil (‰). For analytical procedure see Appendix 6.

Volatile contents of the Tangihua Complex glasses range from 0.01 to 4.34, values which partially correspond to those reported for fresh arc and back-arc glasses and glass inclusions (1-4%; Woodhead *et al.*, 1993). For some samples the substantially lower values resemble those found in MORB glasses (ca. 0.3%; Woodhead *et al.*, 1993). Preliminary results seem to reflect samples with either arc or back-arc/MORB like signatures. This conclusion will be explored in more detail.

In summary the variation of elemental and isotopic compositions for the Tangihua glass samples appear to reflect primary values with one possible exception (49121).

CHEMISTRY OF THE TANGIHUA GLASSES

The chemistry of the Tangihua Complex glasses is very much the same as for the basaltic rocks and the glasses shows the same trends and characteristics as the basalts. A full description of the behaviour of the major oxides and trace elements is given in Nicholson *et al.* ((b) in review; Section 4.2). As such the major oxide and trace element data is presented here in Table 4.5.1, without further explanation and the reader is referred to Section 4.2.

DISCUSSION

The petrogenesis of arc magmas and the relative roles of the subducting slab and the overlying mantle wedge is the subject of current debate in the literature (Woodhead *et al.*, 1993). This debate has focused on the behaviour of LILE and the radiogenic isotopes of Sr, Nd and Pb which appear to be sensitive to the presence of subducting oceanic crust and sediments. There is still a large degree of uncertainty regarding the mechanisms of mass transfer agents, which enable slab-derived elements to be transported into the mantle wedge. There is also uncertainty as to the

Sample#	49112	49162	49206	49172		49164	49201	49135	49219	49193	49193b
rock type	glass	glass	glass	glass		glass	glass	glass	glass	glass	glass
location	Flat Top	Tongariro	Te Paki	Ahipara		Tongariro	Mitimiti	Houto	Te Paki	nr Houto	nr Houto
Recalculated to 100% using $Fe_2O_3/FeO = 0.15$											
SiO_2	56.09	56.87	41.89	55.28		53.21	51.37	51.04	51.85	51.06	52.25
TiO_2	1.15	1.49	0.51	1.73		2.35	1.86	2.01	1.99	2.15	2.18
Al_2O_3	16.23	14.61	3.06	15.02		14.22	15.95	15.13	14.64	15.81	16.08
Fe_2O_3	1.42	1.58	2.34	1.51		1.79	1.38	1.45	1.56	1.46	1.47
FeO	9.51	10.56	15.62	10.05		11.97	9.23	9.64	10.38	9.73	9.84
MnO	0.20	0.19	0.27	0.22		0.22	0.19	0.20	0.17	0.20	0.23
MgO	4.39	4.28	31.35	3.91		4.26	5.75	6.93	6.30	5.53	5.33
CaO	8.15	7.39	4.34	8.08		8.61	10.73	11.09	10.10	10.54	9.82
Na_2O	2.26	2.44	0.46	3.21		2.89	3.07	1.66	2.60	2.95	2.18
K_2O	0.48	0.45	0.11	0.84		0.28	0.24	0.62	0.20	0.33	0.37
P_2O_5	0.11	0.13	0.05	0.18		0.19	0.22	0.22	0.22	0.25	0.25
Total	100	100	100	100		100	100	100	100	100	100
LOI	0.02	0.22	0.01	1.34		0.68	3.10	3.61	0.03	2.31	2.31
Traces elements (ppm)											
Ba	77.35	61.72	45.15	88.56		27.91	37.79	101.55	26.24	49.40	104.92
Rb	10.80	8.30	0.83	14.36		2.51	2.21	7.06	3.82	2.89	4.13
Sr	160.92	142.84	166.36	128.69		86.40	138.40	429.96	112.11	154.91	197.44
Ta	0.10	0.15	0.07	0.26		0.17	0.44	0.32	0.31	0.42	0.35
Th	0.32	0.41	0.23	0.33		0.13	0.30	0.26	0.29	0.30	0.29
Zr	68.45	96.77	45.05	114.75		119.64	130.07	152.22	161.39	176.44	172.45
Nb	0.81	1.52	0.65	2.38		1.04	4.09	3.86	3.99	4.28	4.20
Y	25.39	32.87	18.23	38.71		44.90	43.67	43.18	45.42	48.65	47.15
Hf	1.96	2.75	1.35	3.28		3.22	4.26	4.04	4.08	4.58	4.39
V	300.95	357.22	118.94	373.03		452.49	333.87	320.38	360.47	350.19	348.69
Cr	42.64	26.94	1328.2	16.02		16.88	133.18	210.20	192.61	54.36	54.95
Ni	23.85	16.55	919.95	9.46		13.47	42.95	73.57	56.53	36.97	37.09
Co	0.00			0.00		50.57	52.44	0.00		0.00	0.00
U	0.13	0.33	0.08	0.13		0.06	0.13	0.14	0.26	0.14	0.13
Sc	36.04	34.31	26.86	35.79			36.17	39.26	43.64	36.61	38.57
Cu	74.52	49.82	8.69	41.86		43.44	53.84	54.57	59.40	49.88	49.04
Zn	84.49	101.37	103.97	97.04		100.94	89.77	93.88	97.10	99.29	97.81
Pb	1.72	2.19	0.31	1.00		0.79	0.73	0.70	0.76	0.82	0.81
Ga	14.76	18.01	4.82	18.70			19.33	16.79	18.87	19.32	17.35
Cs	0.61	0.38	0.08	0.32		0.11	0.04	0.06	0.11	0.04	0.06
La	2.59	3.14	1.83	4.32		2.99	5.44	5.23	5.66	5.96	5.72
Ce	7.78	10.02	5.28	13.12		11.15	16.68	16.47	17.24	18.60	17.89
Pr	1.31	1.69	0.88	2.18		2.08	2.74	2.72	2.84	3.09	2.96
Nd	6.86	8.99	4.47	11.40		11.52	14.12	14.04	14.28	15.80	15.19
Sm	2.36	3.06	1.62	3.76		4.09	4.53	4.48	4.70	5.13	4.91
Eu	0.89	1.14	0.66	1.40		1.46	1.53	1.56	1.59	1.68	1.65
Gd	3.24	4.13	2.26	5.09		5.35	5.78	6.00	6.13	6.76	6.45
Tb	0.59	0.77	0.41	0.93		0.99	1.08	1.08	1.11	1.19	1.16
Dy	3.87	5.22	2.78	6.03		6.76	6.96	7.09	7.18	7.74	7.43
Ho	0.88	1.16	0.62	1.36		1.50	1.49	1.55	1.56	1.69	1.64
Er	2.50	3.32	1.84	3.87		4.31	4.32	4.38	4.55	4.87	4.69
Yb	2.42	3.31	1.84	3.81		4.19	4.05	4.19	4.42	4.68	4.53
Lu	0.38	0.51	0.29	0.59		0.63	0.62	0.64	0.68	0.73	0.70

Table 4.5.1: Representative major oxide and trace element data for glass samples from the Tangihua Complex.

composition of both the mantle wedge and the subducting slab. Hence, although it seems probable that the subducting slab plays an important role in the petrogenesis of arc magmas (Sinton *et al.*, 1987; Muenow *et al.*, 1990; Falloon *et al.*, 1992), it has been argued that this contribution is minimal in favour of the involvement of an enriched mantle source (Hochstaedter *et al.*, 1990; Poreda *et al.*, 1985).

Certain element concentrations in the mantle wedge are not significantly changed by the addition of a slab component. These elements are generally the HFSE which have a high charge to ionic radius ratio such that they are relatively insoluble in the fluids derived from the subducting slab (Price *et al.*, 1990; Muenow *et al.*, 1991; Vallier *et al.*, 1991; Falloon *et al.*, 1992). In this instance the behaviour of the elements is assumed to be determined solely by the character of the mantle wedge and the process of melt generation therein. In addition, Danyushevsky *et al.* (1993) have demonstrated, on the bases of H_2O contents, that compositional spectrum seen in BABB throughout the world can be explained by the mixing of a typical D- to E-MORB source with an H_2O bearing, slab-related component. They have proposed a K_2O/H_2O ratio of 0.25 for this slab-related component, which corresponds to the lower limit of K_2O/H_2O in depleted MORB basalts (Falloon, *et al.*, 1992; Danyushevsky *et al.*, 1993).

Hence, when the abundance and ratio of various elements in the arc and back-arc samples have been compared, any differences in the source chemistry or the slab input would be reflected by systematic compositional differences. As such it can be shown that both the arc and back-arc have sampled a similar, or the same, section of the convecting upper mantle and incurred similar melt generation parameters. This is not to say, however, that these magmas are alike for both the arc and the back-arc have been variably influenced by the subducting slab as evidenced by their LILE contents.

One of the major difficulties of this section is that the H_2O content of samples from the Tangihua Complex were determined by simple gravimetric measures (LOI) whereas the data of other workers was collected using infrared spectroscopy, ion microprobe and/or high-temperature gas chromatography. By using LOI as representative of H_2O content we have introduced addition error to the data set (from here on LOI is referred to as H_2O). Another possible problem is that the glasses in this study are >80Ma whereas the glasses to which they are being compared are recent and thus have a limited amount of structurally unbound (i.e. alteration related) water. The differences in analytical technique and alteration introduce a degree of error in the data set and emphasis the questionable usefulness of H_2O content as a tool for constraining source parameters in oceanfloor basalts. Despite the problems, the results of this study show conclusive similarities between studies especially when combined with other indicator less mobile elements.

The analyses on which this study is based are shown in Table 4.5.2. The H_2O content of the glasses analysed ranged from 0.01 to 5.50 wt.%. Only samples with H_2O contents less than 4 wt.% are shown in figures and tables. The samples with exceptionally low H_2O contents (<0.25wt%) are thought to be the result of degassing, which this is supported by the vesicular nature of some of the glasses.

The glasses analysed in this and previous studies show a wide range of H_2O abundances. As H_2O, K_2O and TiO_2 behave as nearly incompatible elements during olivine ± plagioclase ± clinopyroxene crystallisation, their variation can not be solely explained by fractional crystallisation (Danyushevsky *et al.*, 1993). Furthermore, and assuming a reasonable melting model, differences in K_2O/H_2O values of an order of magnitude (as demonstrated by Danyushevsky *et al.*, 1993, and shown in Figure 4.5.2a) suggest that melts from different BABs can not be produced by various degrees of partial melting of the same mantle source. However, this is not the case for the Tangihua glass samples. Figure 4.5.2a shows that the consistent K_2O/H_2O ratios can be produced by differing degrees of partial melting. This data supports previous findings in Nicholson *et al.* (in prep, Chapter 5) which show that the Tangihua magmas were most likely generated by partial melting of a similar, or the same, mantle wedge source.

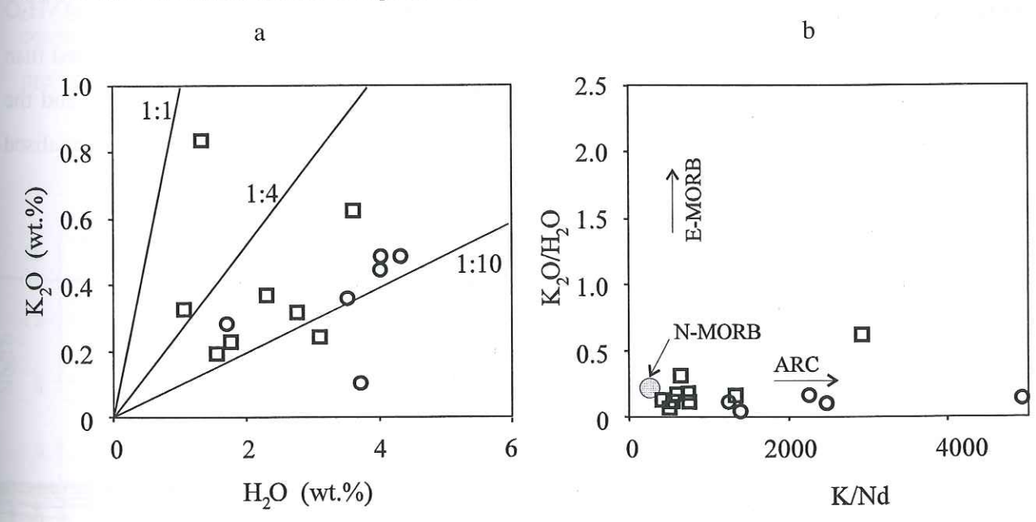

Figure 4.5.2: (a) H2O versus K_2O for the Tangihua glass samples. In general both the arc and the back-arc samples have a K_2O/H_2O ratio between 1:4 and 1:10. (b) K/Nd versus K_2O/H_2O showing the very arc-like K/Nd ratios of the Tangihua glass samples. Note also that many of the back-arc glass samples have high K/Nd ratios. Fields for N-MORB, E-MORB and ARC compositions from Danyushevsky *et al.* (1993).

The glasses from the Tangihua Complex are characterised by relatively high H_2O and H_2O/TiO_2 contents and a K_2O/H_2O ratio of approximately 0.25 (Figure 4.5.2a), which is similar to glass samples from the Lau and Woodlark basins (Danyushevsky *et al.*, 1993). Like the Tangihua Complex, both the Lau and Woodlark basins have been shown to be back-arc basins substantially

influenced by subduction zone processes (Volpe *et al.*, 1987). The Tangihua Complex differs from the Lau and Woodlark basins, in the presence of characteristically arc lavas. However, these types of glasses are, without exception, associated with unstable or complex tectonic settings within their respective basins (i.e. small overlapping spreading centres, incipient ridges located close to the arc volcanic front) or located in relatively narrow immature back-arc basins

Glass samples with the highest H_2O and high H_2O/TiO_2 ratios are the most arc-like samples. These samples also have relatively low TiO_2 contents but the K_2O/H_2O ratios remain close to 1:10 rather than 0.25. There are four samples in the Tangihua glasses, which fall into this category. The remainder are characteristically BAB basalts although some have a more distinctive N-MORB-like signature. The more N-MORB-like Tangihua samples are characterised by low H_2O, K_2O, H_2O/TiO_2 and K_2O/TiO_2 values. Again these differences reflect an unstable tectonic environment of formation. The proposed origin of these lavas (Danyushevsky *et al.*, 1993) is mixing of a typical N-MORB mantle source with a subduction related component. The presence of samples, which fall between a K_2O/H_2O ratio of 0.1 - 1 suggests differing degrees of mixing of a mantle source, of either D- or N-MORB composition, with a subduction-related component, characterised by a K_2O/H_2O value of 0.25 (Falloon, *et al.*, 1992; Danyushevsky *et al.*, 1993). The very low K_2O/H_2O values of some BAB glasses (<0.1) could reflect very depleted mantle sources, more depleted than those found in established MORB settings. Such a depleted source for the basaltic lavas and the glasses of the Tangihua Complex would explain their depleted MORB- and chondrite-normalised Figure 4.5.3).

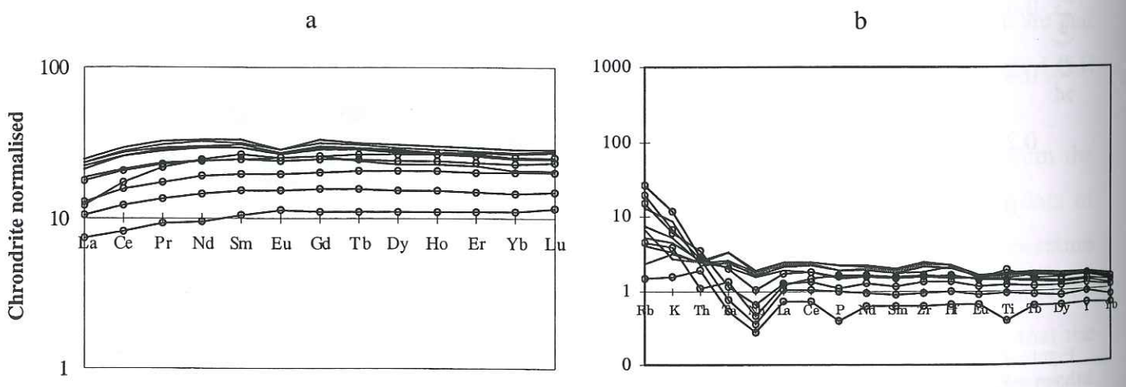

Figure 4.5.3: (a) Chondrite normalized trace element plots for glass samples from the Tangihua Complex. (b) MORB normalized trace element plots for glass samples from the Tangihua Complex. Black lines: back-arc glass samples, lines with circles:arc glass samples.

In Figure 4.5.2b the K_2O/H_2O ratio is plotted against the K/Nb values. This diagram supports the fact that there is a variable subduction component in the Tangihua glasses. MORB glasses typically have K/Nb ratios of <240 (Sun and McDonough, 1989) and variable K_2O/H_2O

ratios whereas arc-related volcanics are characterised by K/Nb ratios of > 1500 at a relatively constant K_2O/H_2O ratio of 0.25. The Tangihua glasses range from very MORB-like to very arc-like K/Nb ratios, overlapping with MORB and arc lavas at either end of the spectrum. This result suggests that in the case of the Tangihua Complex, basalt genesis is the result of varying amounts of slab-related fluid interacting with a depleted mantle wedge source.

In support of previous work on basalts from the Tangihua Complex (Nicholson *et al.*, (b) in review), the glass samples show a distinct Nd anomaly (Figure 4.5.3). Jenner *et al.* (1991) plot Nb/Th ratios against Y to demonstrate the development of the negative Nb anomaly in arc samples. In this diagram the glass samples exhibit the entire spectrum from arc-like to MORB-like Nb contents. The Tangihua Complex glass samples also have Ba/Nb and Th/Nb ratios, which range from being equal to, to significantly higher than MORB (Figure 4.5.4a and Figure 4.5.4b). The high Th/Nb ratios reflect the negative niobium anomaly, which is well developed in arc lavas but less so in the back-arc, independent of any alkali or alkaline earth enrichments. However, as with the Tangihua lavas, the values of the Ta/Nb ratios are significantly higher than the Ta/Nb = 0.06 chrondritic value, which has been found to be constant for a wide range of mantle derived magmas (Jochum *et al.*, 1986; 1989; Elliot *et al.*, 1997). All these ratios point to a significant slab component in the Tangihua glasses. To emphasis this, and to further support the conclusions of previous work (Nicholson *et al.*, (b) in review), the variation of Ta and Th is plotted with respect to

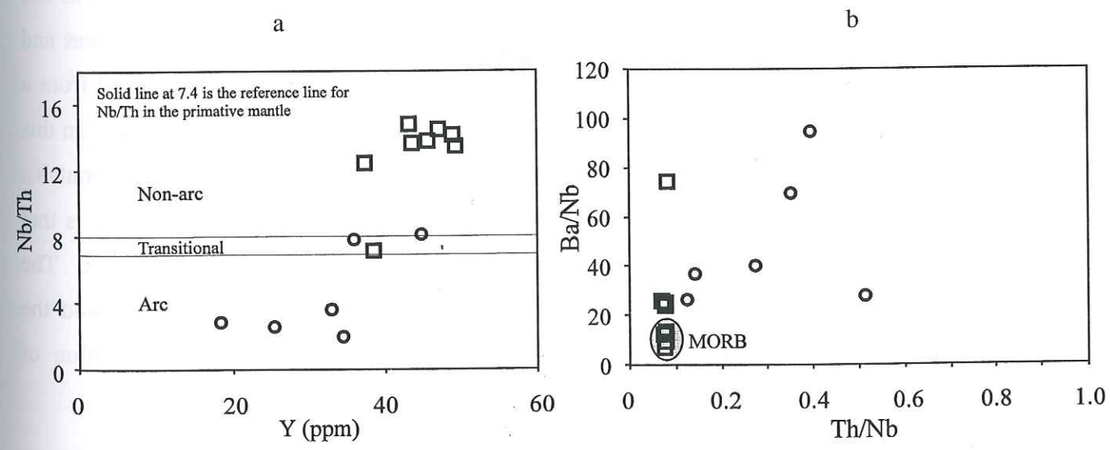

Figure 4.5.4: (a) Nb/Th ratios plotted against Y, showing the definite arc signatures in some of the Tangihua glass samples, the transitional character of a few of the samples and the MORB-like signatures of the remaining (back-arc) samples. After Jenner *et al.* (1991). (b) Th/Nb versus Ba/Nb ratios showing the effects of a slab component on the Tangihua glass samples. The slab input is more noticeable on the arc-like samples, where there is a noticeable increase in both the Ba/Nb and the Th/Nb ratios, indicating the involvement of both a slab-derived fluid and possibly a slab-derived melt. Enrichment is less noticeable in the back-arc samples which plot closer to the region of N-MORB, however, the elevated Ba/Nb values suggest the involvement of a slab-derived fluid. After Elliot *et al.* (1997).

Yb in Figure 4.5.5. In this diagram the composition of the Tangihua Complex glasses appear to reflect different petrogenetic histories such that the arc glasses have been affected by the addition of a greater slab component than the back-arc glasses. In turn, the back-arc glasses appear to reflect a greater degree of fractionation. This diagram also suggests a more depleted source for the arc lavas which, again, supports work in Section 5.2.

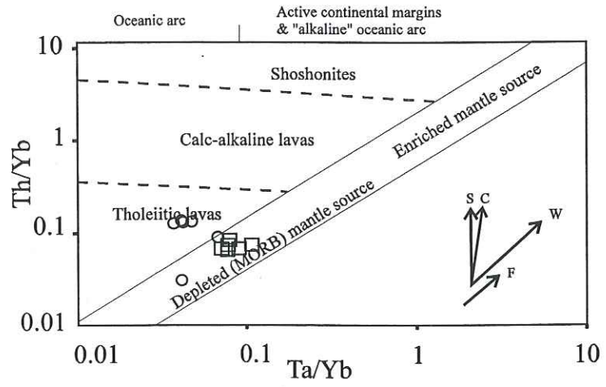

Figure 4.5.5: Ta/Yb versus Th/Yb plot showing the generally depleted source for both the arc and the back-arc glasses from the Tangihua Complex. S=subduction zone enrichment. C=crustal contamination, W=within plate enrichment and F=fractionation.

The chemistry of the Tangihua basaltic lavas and the Tangihua glass samples is remarkably consistent (See Sections 4.1, 4.2, 4.3 and 5.2). An effort has been made in this section, to use different element ratios to help support previous findings. Both the Tangihua Complex lavas and glasses exhibit a continuum from arc to back-arc chemistries, which have been generated from a slightly depleted N-MORB source and influenced by varying amounts of a slab component. In this respect the Tangihua Complex is a unique example of an ancient ophiolitic system which contains the entire spectrum of arc, back-arc and transitional magmas. What is even more unusual is that this suite of rocks, containing fresh volcanic glass, is found in a >90Ma ophiolite complex. The very presence of fresh glass in an ancient ophiolitic system has, in this instance, allowed the conformation of previously discussed geochemical results without the added complication of alteration and element mobility.

CHAPTER FIVE: PETROGENESIS

SECTION 5.1

Introduction

The Tangihua Complex provides a rare example of the transition from arc volcanism to back-arc volcanism, which has been preserved as an ophiolitic sequence. Understanding the evolution of volcanic arc/back-arc systems and their associated with subduction zones is a complicated problem. The processes active in subduction systems promote the transfer of material from the downgoing slab into the overlying mantle wedge. However, characterising the specifics of material transfer can be difficult, especially when trying to distinguish between the effects of the slab on the arc and the back-arc magmas.

Initially this Chapter deals with the specifics of generating the Tangihua arc and back-arc lavas. Section 5.2 covers partial melting, fractional crystallization and magma mixing followed by the introduction and characterisation of a slab component in the magmas. An attempt is also made to differentiate between a slab-derived fluid component and a slab-derived melt component in the arc and back-arc magmas. Section 5.2 is the fifth manuscript that has been submitted for publication in this thesis. It was submitted in December, 1999, to *Earth and Planetary Science Letters*.

SECTION 5.2

Petrogenesis of a Late Cretaceous volcanic arc/marginal basin transition zone, Tangihua Complex, New Zealand

Nicholson, K.N., Picard, C. and Black, P.M., Submitted December, 1999, to *Earth and Planetary Science Letters.*

ABSTRACT

The Tangihua Complex, Northland, New Zealand, provides a unique opportunity to study the transition between basaltic lavas with arc and back-arc signatures in an ophiolite complex. Some of the basaltic lavas present have distinctive enriched LILE and LREE contents, characteristic of arc lavas whereas the back-arc lavas have more subdued arc-like signatures, however the Tangihua lavas exhibit a complete continuum between the arc and the back-arc chemistries. The general depletion of Nb and the HFSE suggests derivation from a depleted mantle source, which is consistent with mantle wedge depletion by an earlier rifting episode. The arc lavas are marginally more depleted than the back-arc lavas. Geochemical modelling shows the back-arc lavas have undergone approximately 35% fractional crystallisation (FC) and the arc lavas have undergone approximately 30% FC. Chemistries intermediate between the arc and back-arc can be modelled by 30-50% simple mixing of the arc lavas with the back-arc lavas. High LILE/HFSE and LILE/LREE ratios suggest LILE enrichment by a slab-related aqueous fluid, particularly in the back-arc magmas. In the arc suite the presence of a slab-related aqueous fluid is also indicated as the primary mode of enrichment, however, the presence of small amounts of a slab-derived silicic melt is difficult to dismiss. Enrichment of the arc suite by a slab-related fluid, as opposed to a silicic melt, is supported by radiogenic isotope. $^{86}Sr/^{87}Sr$ ratios show a distinct trend towards higher values, as expected by sediment input, however $^{144}Nd/^{143}Nd$ is only slightly depleted in both the arc and the back-arc samples. Hence it is likely that the increase in radiogenic Sr is the result of transportation in the slab-generated fluid phase.

INTRODUCTION

The geodynamic history and magmatic evolution of volcanic arc/back-arc systems associated with subduction zones is complex. Magmatic arcs, developed above subduction zones, usually evolve in tensional tectonic settings because the trenches tend to retreat oceanwards as the subducting lithosphere sinks into the mantle (Molnar and Atwater, 1978; Hamilton, 1979; Seno and

Maruyama, 1984). In this instance the formation of a back-arc basin may occur if extension ultimately results in the arc splitting. Due to a complicated tectonic setting, the Tangihua Ophiolitic Complex, Northland, New Zealand, is an unusual example of arc/back-arc formation and magma generation (Figure 5.2.1). In the case of the Late Cretaceous Tangihua Complex, arc volcanism was never fully established and back-arc volcanism appears to have been short lived.

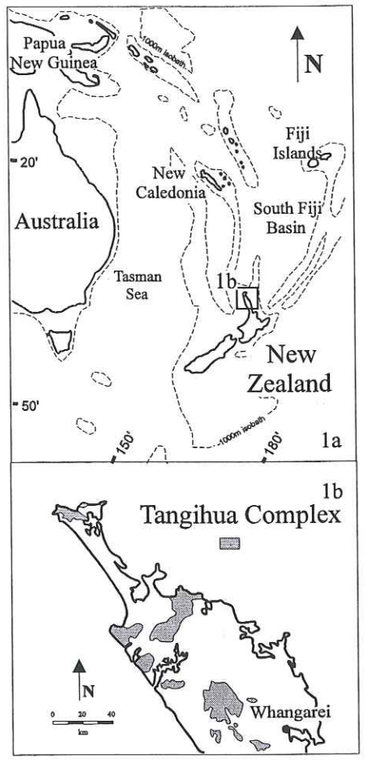

Figure 5.2.1: (a) Location map of the Southwest Pacific region showing the position of New Zealand. (b) Location map showing the position of the Tangihua Massifs in Northland, New Zealand.

The processes active in subduction systems promote the transfer of material from the downgoing slab into the overlying mantle wedge. Fluid flux from the downgoing slab is necessary to enable mantle melting and results in arc volcanism. Hence magmas generated in an arc setting (island arc basalts: IAB) have distinctive geochemical signatures, which are also present to a lesser extent in the back-arc (back-arc basin basalts: BABB). Volcanic arc magmas are generally characterised by enrichment in LILE and depletion of HFSE relative to MORB (e.g. Pearce, 1983). In contrast BAB basalts have HFSE abundances similar to MORB and show moderate LILE concentrations. The degree and nature of the both slab input and the source composition are a matter of some debate in the literature. Woodhead *et al.* (1993) interpreted the HFSE systematics of IAB and BABB to indicate that the BABB are derived from sources similar to MORB whereas IAB

are derived from more depleted sources. Whereas McCulloch and Gamble (1991) suggest that the depletion in the IAB sources might be due to the withdrawal of the BAB lavas from the source region.

The affinity of some Tangihua Basaltic lavas with arc or back-arc compositions suggests that they may have a similar origin (Nicholson *et al.*, (b) in review). It is now generally accepted that many IAB have trace element and isotopic signatures influenced by melts or fluids derived from marine sediments and altered oceanic crust associated with the subducting slab. To evaluate quantitatively the feasibility of fractionation and modification by subduction related fluids, we have investigated a simple FC and mixing model. In this model, slab derived fluids are mixed convectively with sub-ridge mantle to form localised heterogeneities; during upwelling these heterogeneity's melt and these contaminated melts mix with typical MORB melt produced from depleted mantle in the same melting regime.

This paper gives only a brief over view of the background geology and other information. More detail regarding the geology, petrography, major and trace element geochemistry is given in Nicholson *et al.*, (b) in review and Nicholson *et al.*, (c) in review.

GENERAL GEOLOGY

The ophiolites of the Tangihua Complex, which occur throughout the Northland Peninsula, New Zealand, consist predominantly of massive and pillowed basaltic lava sequences with minor intercalated siliceous mudstone and micritic limestone. Gabbro, microgabbro and basaltic intrusions form a subordinate component (Brothers, 1974; Brothers and Delaloye, 1982; Hayward *et al.*, 1989; Malpas *et al.*, 1992) as do minor felsic derivatives, younger alkalic intrusions and ultramafic rocks (Bennett, 1976). The age of the Tangihua Ophiolite Complex is not well established, however, paleontological evidence suggests formation during the early Palaeocene or late Cretaceous and emplacement during the late Oligocene (Ballance and Spörli, 1979; Brook *et al.*, 1988; Malpas *et al.*, 1992; Hopper and Smith, 1996).

Petrographically the Tangihua Basalts are generally microcrystalline basalts predominately containing phenocrysts of euhedral to subhedral grains of plagioclase (An_{55-80}) and calcic augite (average Mg# = 68), although the basalts are often equigranular and range from glass, though cryptocrystalline to fine grained with a groundmass composed primarily of plagioclase and pyroxene. Phenocryst content is sometimes as high as 40%. Primary phenocrysts are plagioclase > clinopyroxene > orthopyroxene >> magnetite, titanite. Rare olivine-rich and hornblende-bearing basalts also occur within the complex. When interpreting the geochemical data it is important to remember that the Tangihua Complex has been subjected to pervasive low-temperature

hydrothermal alteration and variable degrees of metamorphism, ranging up to greenschist facies (Black, 1989; Nicholson and Black, 1998; Nicholson *et al.*, (a) in review).

MAJOR OXIDE CHEMISTRY

In this study the data set includes samples from 16 different massifs. This may result in scatter in some element concentrations, i.e. Zr, which may be the result of minor source heterogeneities. It is possible that the different massifs have different parental magmas and that the scatter is due to slightly different fractionation paths. However, given that the scatter is small and in most instances there are only two or three samples from each massif (Appendix 1), the data is considered to have originated from the same source. This conclusion is supported by the high degree of sheering, over thrusting and erosion, which precludes the consideration of each massif as an independent system.

The samples in the study plot in the basaltic through to the basaltic-andesite fields of the IUGS classification scheme, and have SiO_2 contents ranging between 49 and 60wt%. Mg# range from 26 to 50 in these samples. The samples are predominantly tholeiitic, however, there is a distinct calc-alkaline trend as seen in Figure 5.2.2, while two of the samples reflect a more alkaline composition. The basalts from the Tangihua Ophiolite clearly fall into the island arc tholeiite suite and the back-arc basin suite (Nicholson *et al.*, (b) in review).

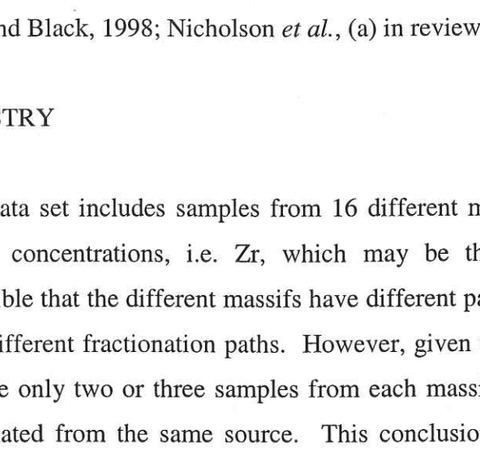

Figure 5.2.2: Al-Mg-Fe+Ti ternary diagram showing the calc-alkaline trend in the arc lavas and the tholeiitic trend in the back-arc lavas. Circles: IAB. Squares: BABB.

It is important to emphasis that the BAB basalts are uniformly tholeiitic in nature and in general are clearly distinguishable from the samples of the arc suite (Nicholson *et al.*, (b) in review). This distinction is based purely on geochemical analyses as there appears to be no field

evidence and little petrographic evidence to support these differences. Both arc and back-arc lavas are found in many of the massifs. The arc basalts display both minor tholeiitic trends and calc-alkaline affinities. The calc-alkaline nature of these rocks appears to dominate, suggesting that the tholeiitic trend may be a reflection of magma mixing.

The distinction between BAB and arc-type lavas is reinforced by major element variations. Figure 5.2.3 shows MgO variation with other major oxides for the Tangihua samples. The BAB show a wide range of concentrations for all elements when compared with the arc lavas with MgO concentrations of 3.39-7.84% and 5.52-6.96% respectively. Each suite has a distinct trend for TiO_2,

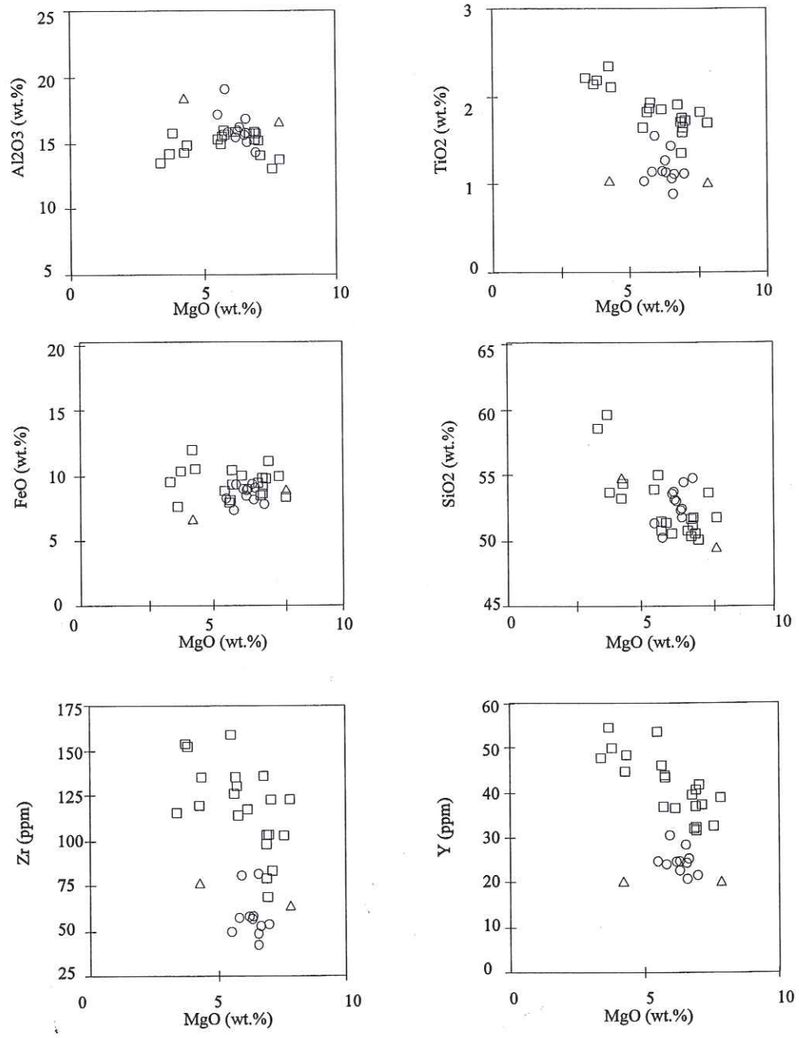

Figure 5.2.3: Variation diagrams for the Tangihua Complex lavas. See text for explanation. Circles: IAB, squares: BABB and triangles: alkaline basalts.

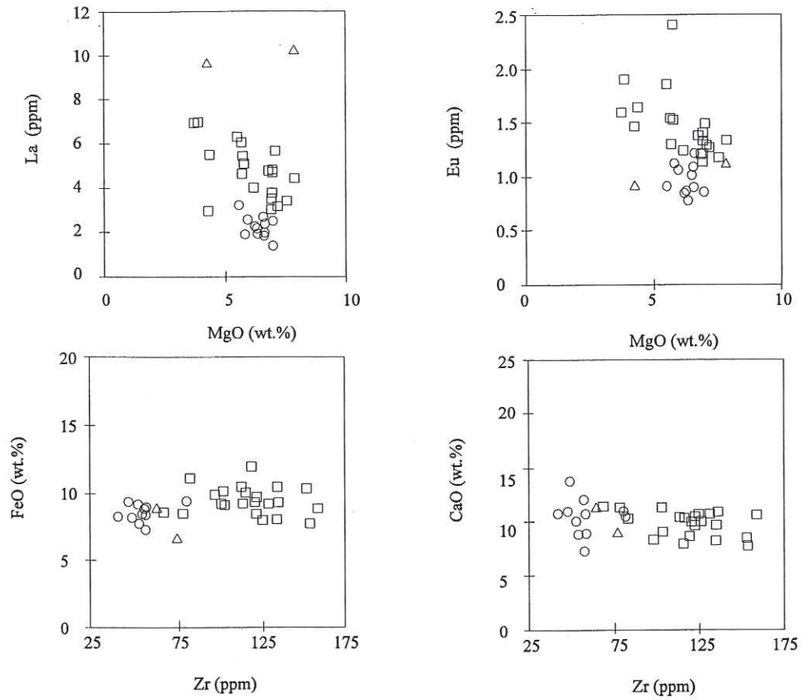

Figure 5.2.3: continued. Variation diagrams for the Tangihua Complex lavas.

FeO and SiO_2. The BAB basalts have constant to increasing FeO and increasing TiO_2 and hence resemble a tholeiitic magma evolution. The arc basalts show constant to decreasing FeO, with relative FeO depletion at similar MgO contents, and are consequently analogous to a more calc-alkaline trend. Experimental studies indicate that dissolved H_2O can decease the thermal stability of olivine, pyroxene and plagioclase in basaltic magmas (Grove and Baker, 1984; Sisson and Grove, 1993a) whereas the effect on Fe-Ti oxide stability is minimal (Sisson and Grove, 1993a). As such the influence of H_2O activity on the early or late crystallisation of Ti-magnetite, controls the style of differentiation (Miller *et al.*, 1994). Therefore sub-alkaline basaltic magmas with high water contents, such as IAB, should follow a calc-alkaline differentiation trend whereas those with low water contents, such as BABB, follow a tholeiitic differentiation trend (Sisson and Grove, 1993a).

Major oxide variations are broadly consistent with magma evolution via fractional crystallisation involving removal of the observed phenocryst phases. Initially fractionation is dominated by plagioclase, although pyroxene fractionation is also important. Later decreasing MgO with increasing Zr suggests that pyroxene becomes the dominant phenocryst phase to fractionate. Removal of clinopyroxene and/or plagioclase is suggested by trends of CaO vs. Zr, whereas trends shown by FeO vs. Zr reflect the removal of magnetite (Figure 5.2.3). From some of

the binary plots (i.e. SiO_2 vs. MgO) it is possible to discern parallel fractionation trends which may simply be scatter in the data, but it might also indicate different primitive liquids.

It is clear from these variations that the genesis of BABB and IAB suites of the Tangihua Complex are difficult to reconcile solely by simple fractional crystallisation of the same parental source. Assuming that these suites have originated contemporaneously from the same eruptive system then either two differing parental magmas were supplying the system or a more complex process of fractionation, assimilation and/or contamination was involved in their petrogenesis.

TRACE ELEMENT GEOCHEMISTRY

MORB and chondrite normalised multi-element and incompatible trace element concentrations for representative samples are shown in Figure 5.2.4a (Sun and McDonough, 1989) and 5.2.4b (Evensen *et al.*, 1978). The basalts display a continuum which ranges between trends typical of rocks formed in island arc and those seen in marginal basins, such as enrichment in LILE relative to N-MORB and negative HFSE anomalies relative to LILE, P and REE. All of the samples show only variations of what appears to be essentially the same pattern. At first glance the patterns shown in Figure 5.2.4a seem to reflect very MORB like signatures, however, the depletion of elements, such as Nb, Ta and Zr reflects distinct arc and BAB signatures.

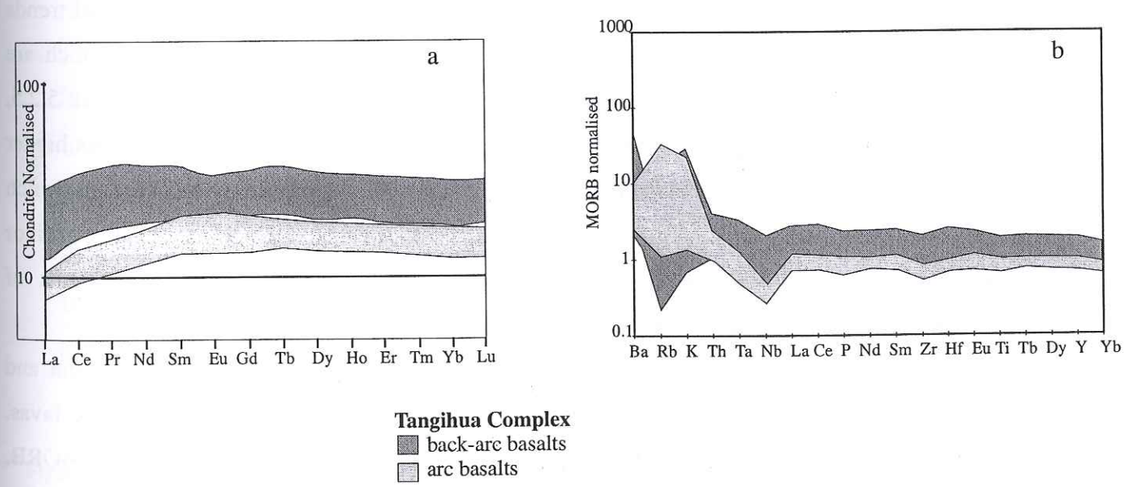

Figure 5.2.4: (a) Chondrite and (b) MORB normalised trace element plots for the Tangihua lavas. Note the enrichment of LILE relative to N-MORB and depletion of HFSE relative to LILE.

Both rock suites have sub-parallel profiles and display varying degrees of the typical characteristics of island arc magmas. Most notably the LFSE are enriched relative to the REE and

HFSE. In turn, REE/HFSE ratios (e.g. La/Nb, Sm/Zr and Nd/P) are high in the IAB relative to MORB, which is typical of more primitive island arc tholeiites, however these ratios are somewhat closer to MORB for the BABB samples. REE patterns for both samples are similar with the BAB samples slightly more LREE enriched than the arc lavas with $(La/Y)_n$ generally slightly lower in the arc samples. These characteristics strongly suggest the presence of a slab-derived component in the upper mantle source region of both the arc and the back-arc basalts.

On the basis of trace and major element variations, the tholeiitic and calc-alkaline suites of the Tangihua Complex have taken different shallow level fractionation paths. However, the general trace element interrelationships of the two suites are remarkably similar. This suggests that the suites could be related by a similar mantle source or indeed a single parental magma (Taylor and Nesbitt, 1995).

SIGNIFICANCE OF MAJOR AND TRACE ELEMENT DATA

Due to the degree of crystal fractionation in the Tangihua lavas, highly incompatible element ratios are used to characterise the possible source. The highly incompatible element ratios also tend not to be fractionated during mantle melting. Trace element ratios used to distinguish MORB and ocean island basalts from arc lavas and continental basins clearly show that many of the Tangihua lavas are unlike MORB and OIB samples. The Tangihua basalts form subparallel trends extending well outside the MORB/OIB fields towards low Nb/U, Ce/Pb, and Th/Nb, which are more commonly associated with arc volcanism or continental crust. For example see Figure 5.2.5, which show Nb/U, Ce/Pb and Th/Nb ratios below the values of MORB and Ba/Nb values higher than MORB. In the incompatible element ratios some variation is seen throughout the data, which is not easily explained by crystal fractionation alone. This scatter could be the result of minor differences in the primitive sources, different degrees of alteration or different amounts of differentiation between the magmas (Meijer and Reagan, 1983; Elliott *et al.*, 1997).

Trace element abundance patterns, normalised to the composition of N-MORB (Sun and McDonough, 1989; Figure 5.2.4b), show that the most depleted samples are similar to arc lavas. The arc samples have abundances of the most incompatible trace elements similar to N-MORB, such as enrichment in Pb (relative Ce and Sr) and depletion in Nb and Ta (relative to U and K), but in spite of the relative depletion of Nb and Ta, the absolute abundance of these elements are equal to or greater than those of N-MORB. However, the Tangihua lavas have lower concentrations of the most highly incompatible elements and lower light/heavy REE ratios than are seen in typical SW Pacific arc systems (McCulloch and Gamble, 1991; Elliott *et al.*, 1997), hence these lavas are thought to be relatively depleted.

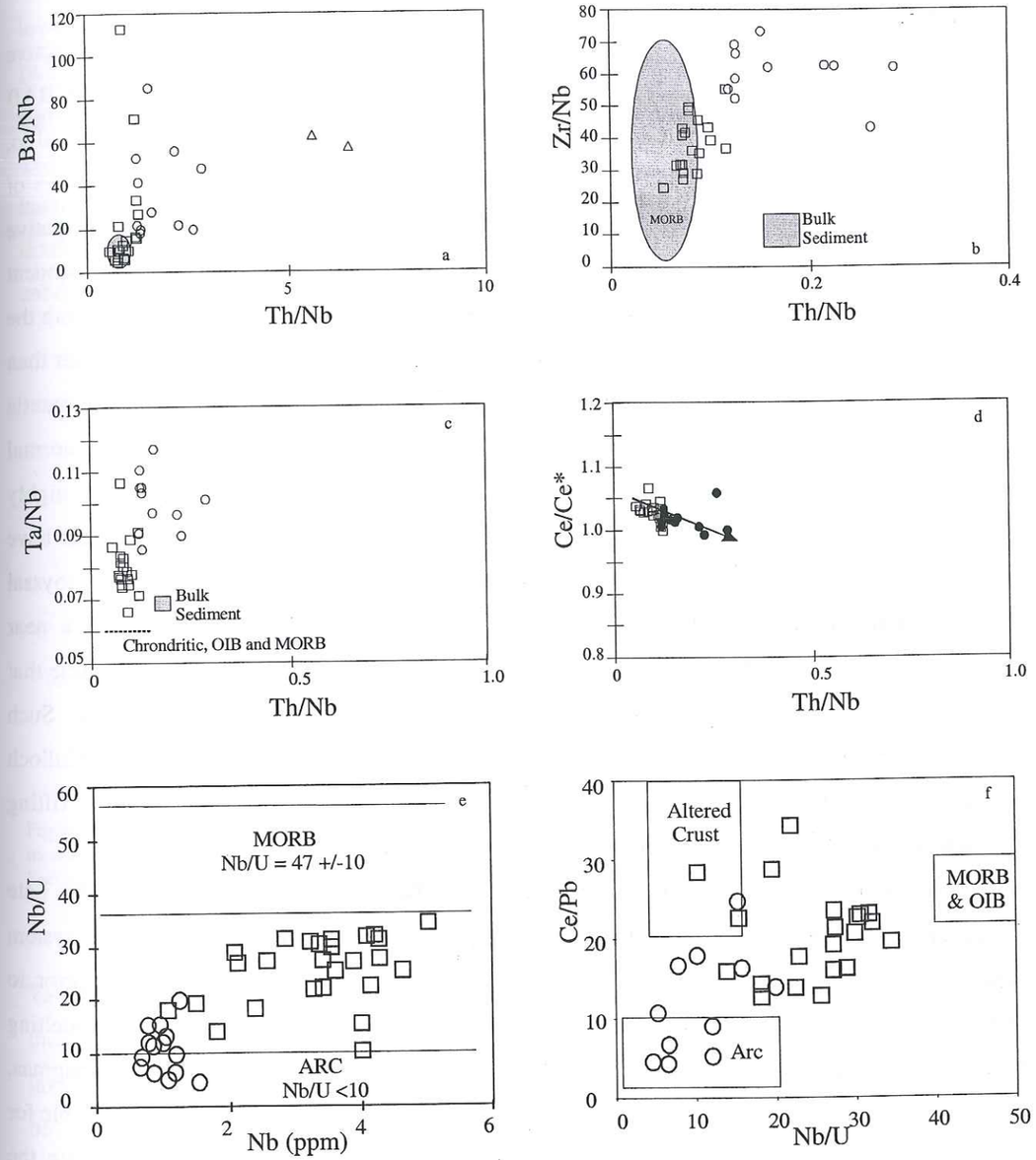

Figure 5.2.5: Element ratio diagrams showing the relative effects of a slab-derived aqueous fluid and possibly a slab-derived melt on the lavas from the Tangihua Complex. MORB and ARC fields after Plank and Langmuir (1998), Elliot *et al.* (1997) and Klein *et al.* (1995). Symbols as in Figure 5.2.2 except for (d) in which solid circles are used for the arc lavas to emphasis the trend towards a Ce anomaly. Different scales are used for Th/Nb in Figures 5.2.5a-d in order to emphasis the effects of the slab contribution.

SOURCE COMPOSITION

Negative niobium anomalies and relative alkali earth enrichments are highly distinctive characteristics of arc lavas (Gill, 1981; Hawkesworth *et al.*, 1991). Both the IAB and the BAB lavas from the Tangihua Complex have Ba/Nb and Th/Nb ratios, which range from being equal to, to significantly higher than MORB (Figure 5.2.5). According to Elliott *et al.* (1997) elevation of these ratios can not be caused by the same processes. The high Th/Nb ratios reflect the negative niobium anomaly, which is well developed in the arc lavas but less so in the back-arc, independent of any alkali or alkaline earth enrichments. However, it is the values of the Ta/Nb ratios in both the arc and back-arc rocks which proves the most interesting. These ratios are significantly higher than the Ta/Nb = 0.06 chrondritic value, which has been found to be constant for a wide range of mantle derived magmas (Jochum *et al.*, 1986; 1989). Relative to Nb, Ta is more compatible in normal mantle assemblages (Green *et al.*, 1989; Forsythe *et al.*, 1994). Although both elements are highly incompatible, even highly incompatible elements can be fractionated in mantle residues that have experienced fractional melt extraction. Studies of basalts (Langmuir *et al.*, 1992) as well as abyssal peridotites (Johnson *et al.*, 1990) have shown that melt production beneath ridges is a near fractional process. Hence, the observed HFSE ratios implicate the presence of a subarc mantle that was previously depleted by a fractional melting event, as occurs beneath mid-ocean ridges. Such melt depletion of the mantle wedge seems likely to occur during back-arc spreading (McCulloch and Gamble, 1991; Woodhead *et al.*, 1993). In the case of the Tangihua Complex, a prior rifting event before 100Ma may have depleted the mantle wedge.

In light of the tectonic setting and the evolution of the arc/back-arc system during the Late Cretaceous, it is thought to be most likely that the cessation of a short lived subduction system stranded an arc-type magma chamber at shallow depths. Due to rifting in the region prior to subduction, the mantle wedge is thought to have been depleted when slab-related mantle melting and arc volcanism began. The ensuing rifting saw the generation of depleted MORB-type magmas, which mixed with the remnants of arc-type magma and hence generated the magmas responsible for the chemical systematics seen in the Tangihua Complex. It is difficult, however, to explain the more depleted nature of the arc magmas relative to the apparently cogenetic back-arc magmas. This may, as such, be geochemical evidence for the migration or shift from the volcanic arc front to the back-arc region or simply back-arc volcanism. Hence as the subduction zone steepens or 'rolls back' away from the immature arc front we see a decreasing influence of the slab in the magmas produced and possibly the melting of a less depleted section of the mantle wedge. It is important to remember that these levels of source depletion might also suggest minor source heterogeneities.

Radiogenic isotopic variations within the Tangihua samples are minor compared to the range in incompatible trace elements and ratios. The $^{87}Sr/^{86}Sr$ and $^{143}Nd/^{144}Nd$ ratios are higher and lower, respectively, than MORB (Figure 5.2.6). These compositions overlap the OIB, BAB and IAB fields. Local sediment has $^{143}Nd/^{144}Nd$ values (Ben Othman *et al.*, 1989), which are significantly lower than MORB and could account for the lowering of the ratios seen in the Tangihua samples. The fact that the arc samples have slightly higher $^{143}Nd/^{144}Nd$ ratios than the back-arc samples might be reflecting small source heterogeneities. The arc samples also show dramatically different $^{87}Sr/^{86}Sr$ ratios. This is thought to reflect the addition of fluids from the subducting slab.

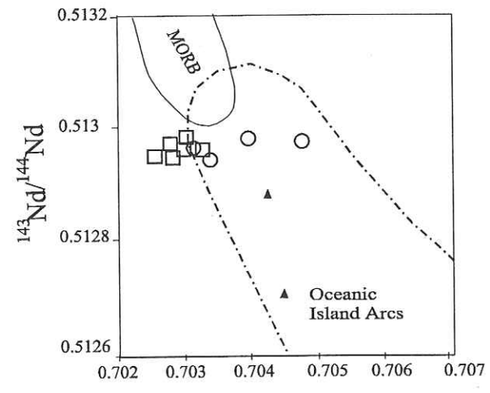

Figure 5.2.6: Sr and Nd isotopic composition of the Tangihua lavas. Notice the relatively constant $^{143/144}Nd$ with increasing $^{87/86}Sr$, thought to be the result of increasing sediment input. Symbols as in Figure 5.2.2. For more detail see Section 4.4.

Based on evidence from major and trace element variations, the basaltic lavas from the Tangihua BAB and the arc suites have taken different shallow level fractionation paths. However, their general trace element and isotopic characteristics are remarkably similar except that the arc lavas are relatively more depleted than the back-arc lavas. This suggests that the two suites could be related by a similar mantle source or a similar parental magma before contamination via subduction zone processes occurred. Hence, the arc lavas are though to be derived from a melt or melts extracted from a source region that has undergone addition of a LREE enriched component, which is assumed to be subduction related. In turn, the back-arc lavas appear to be derived from a similar source, influenced by little interaction with subduction related enriched component.

MODELLING OF MELTING, FRACTIONATION AND MIXING

One of the most important uses of trace and rare earth elements in modern igneous petrology is in the modelling of geochemical processes. Trace element modelling depends upon the mathematical expressions which describe the equilibrium partitioning of trace elements between minerals and melt during igneous processes and a precise knowledge of trace element partition coefficients. It is possible to model many different processes in igneous petrology, including fractional crystallisation and partial melting.

The modelling of partial melting processes assumes some knowledge of the source composition of the magma. For the Tangihua Complex, it has been shown that the source composition was very similar to N-MORB or a slightly depleted N-MORB. Hence, in attempting to model the partial melting process the average N-MORB of Sun and McDonough (1989) has been used for the starting composition. Batch melting, or equilibrium partial melting, occurs when a partial melt is generated and is continuously reacting with the solid residue at the sight of melting until conditions are such that the melt is able to escape as a separate 'batch' of magma (Hanson, 1978). Batch melting was modelled using the equation:

$$C_L/C_0 = 1/[D_{RS} + F\,(1\text{-}D_{RS})]$$

where C_L is the concentration of a trace element in the melt, C_0 is the concentration of a trace element in the unmelted source, D_{RS} is the bulk partition coefficient and F is the weight fraction of melt produced. An example of the results is given in Table 5.2.1.

Element	Primitive Mantle[1]	47656	%P M[2]	49212	%P M[2]	47651	%P M[2]	49183	%P M[2]
		Arc		Arc		Back-arc		Back-arc	
Mg#		**47.3**		**44.7**		**48.2**		**45.0**	
Nd	1.354	6.44	21.0	6.19	21.9	12.32	11.0	9.13	14.8
Sm	0.444	2.14	20.7	2.32	19.2	4.12	10.8	3.08	14.4
Zr	11.2	54.06	20.7	41.85	26.8	122.17	9.2	78.88	14.2
Hf	0.309	1.65	18.7	1.47	21.0	3.33	9.3	2.80	11.0
Ti	1300	6748.2	19.3	5331.8	24.4	10266.8	12.7	8134.3	16.0
Tb	0.108	0.53	20.4	0.56	19.2	0.98	11.1	0.79	13.8
Y	4.55	21.89	20.8	20.68	22.0	39.00	11.7	32.17	14.1
Yb	0.493	2.07	23.8	2.15	23.0	3.51	14.0	3.00	16.5
Average			**20.7**		**22.2**		**11.2**		**14.3**

Table 5.2.1 Partial melting calculations for the Tangihua Complex arc and back-arc samples. In general the arc samples appear to have incurred a greater degree of partial melting than the back-arc samples. See text for further explanations. [1] Sun and McDonough (1989) [2] %PM = percent partial melting.

Using this model, and considering $D_{RS} \approx 0$, the weight fraction of melt produced from melting an N-MORB source is >21% for the most primitive arc lavas present and >11% for the most primitive back-arc lavas (Table 5.2.1). As expected, similar calculations for samples with a slightly lower Mg#, or less primitive, yield higher degrees of partial melting; >22% for the arc lavas

and >14% for the back-arc lavas. Analyses of other arc systems from the SW Pacific yield similar results (Figure 5.2.7). For comparative purposes the data in Figure 5.2.7 is regressed to a composition of MgO = 9 wt. %. Most of the Tangihua Complex basaltic lavas have MgO < 7 wt.% and Mg# < 45, hence none are characteristic of a primitive magma. Regressing the data to MgO = 9 wt.% attempts to reduce the effects of fractional crystallisation. This methods involves fitting a regression line to a specific element with respect to MgO and then extrapolating the value of the element at MgO = 9 wt.%. This method does not represent primary magma compositions, however, it does provide a common reference point for the comparison of different suites of lavas (Klein and Langmuir, 1989; Pearce and Parkinson, 1993; Turner and Hawkesworth, 1995).

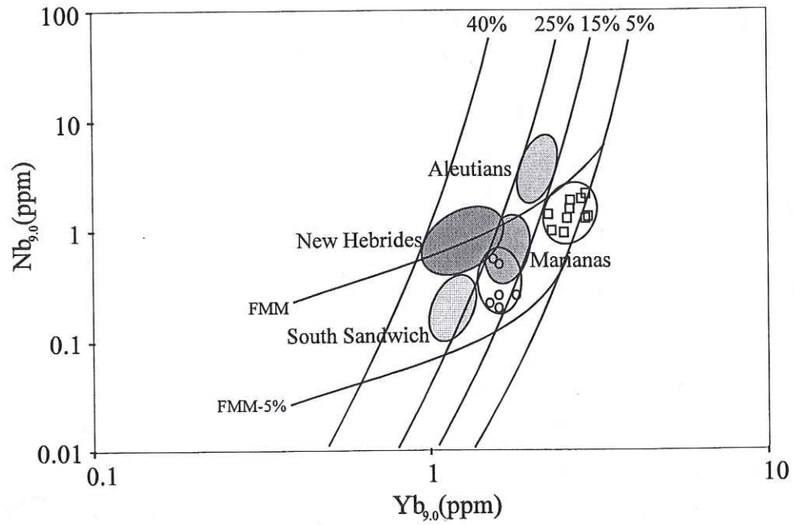

Figure 5.2.7: $Yb_{9.0}$ versus $Nb_{9.0}$ plot of the Tangihua basalts, regressed to 9.0 wt.% MgO, showing the degree of partial melting and source depletion in the Tangihua lavas and other SW Pacific arc systems. FMM = fertile MORB mantle. After Pearce and Parkinson (1995). Symbols as in Figure 5.2.2.

On Figure 5.2.7 the arc basalts from the Tangihua Complex require 15 – 25% partial melting of a fertile MORB mantle source (FMM) depleted by <5%, whereas the back-arc lavas require 5 – 15% partial melting of a less depleted FMM source (<3%). These values are in good agreement with the previously determined partial melting model (Table 5.2.1). Figure 5.2.7 also contains fields for other well studied arc systems. The same data is not yet available in the literature for the equivalent back-arc systems. The Mariana lavas require approximately 15-25% partial melting of a marginally depleted source, whereas the South Sandwich lavas require a greater degree of melting of a more depleted source while the New Hebrides lavas require more melting of a non-depleted source (Pearce and Parkinson, 1993; see also Pearce *et al.*, 1995; Peate *et al.*, 1997).

FRACTIONAL CRYSTALLISATION

In regarding the trends seen in the major oxide and trace elements bivariate plots (Figures 5.2.2 and 5.2.3) it is apparent that much of the scatter seen in both the back-arc and arc suites is due to fractional crystallisation of the observed phenocryst assemblage (e.g. Graham and Hackett, 1987; Singer *et al.*, 1992). This is confirmed by the patterns seen in Figures 5.2.4a and 5.2.4b. Modelling of the fractionation can account for most of the observed chemistries, however, it is important to remember that none of the 'end member' compositions used are primary. The most primitive basalt has an Mg# of 48.2, indicating that a significant degree of fractionation has already occurred. The following equation which describes fractional crystallisation or Rayleigh fractionation:

$$C_L/C_0 = F^{(D-1)}$$

where C_L is the concentration of a trace element in the liquid, C_0 is the initial concentration of a trace element in the primary magma, D is the bulk partition coefficient and *F* is the fraction of melt remaining. During fractional crystallisation the crystals are removed from the site of formation. Hence, this is not an equilibrium process, at best only surface equilibrium in achieved. Examples of the results for both the arc and the back-arc lavas are given in Table 5.2.2 and Table 5.2.3 respectively. In all cases, the observed phenocryst is used for the purposes of modelling.

By taking one of the more primitive arc samples (49212: MgO = 6.57 wt%, Mg# = 44.7) it is possible to create the observed arc chemistries using up to 30% FC of 2.5% magnetite, 15% orthopyroxene, 25% clinopyroxene and 57.5% plagioclase (Figure 5.2.8a). One other sample had higher Mg# but was not used as the same samples also had higher SiO_2, this sample could be an

Element	Parent 47651	Calculated Average F = 70	Observed 49137	Calculated Average F = 66	Observed 49177
K	1751.2	833.7	830.2	958.4	949.8
Ti	10266.8	13059.2	12818.5	13059.2	13069.1
Th	0.211	0.356	0.360	0.333	0.486
Zr	122.172	153.468	153.828	154.920	152.421
La	4.477	6.873	6.905	6.970	7.003
Ce	14.087	20.841	21.019	21.738	21.852
Nd	12.317	16.344	16.445	17.849	17.883
Sm	4.116	4.988	4.975	5.636	5.632
Eu	1.335	1.601	1.605	1.894	1.895
Gd	5.225	6.520	6.490	6.967	7.029
Tb	0.977	1.228	1.227	1.284	1.281
Dy	6.260	8.131	8.185	8.222	8.231
Er	3.780	5.243	5.272	5.121	5.128
Yb	3.510	4.984	5.024	4.867	4.889
Lu	0.531	0.771	0.777	0.752	0.753

Table 5.2.2: Calculated and observed values of specific elements from fractional crystallisation of a more primitive back-arc magma to a more evolved back-arc magma. Partition coefficients for each element in a given mineral phase are from Rollinson (1993) or references therein and are the same for both models. Values given for *F* are the averages from a total of 25 elements.

Element	Parent 49212	Calculated Average F =85	Observed 49181	Calculated Average F = 72	Observed 49189
K	845.8	*	5313.3	*	3569.9
Ti	5331.8	6848.1	6834.3	9276.0	9352.2
Th	0.192	0.172	0.124	0.153	0.147
Zr	41.850	57.309	57.009	80.550	80.605
La	1.871	1.903	1.921	2.587	2.582
Ce	6.066	6.787	6.753	8.621	8.656
Nd	6.193	7.271	7.296	8.121	8.110
Sm	2.317	2.837	2.847	2.837	2.839
Eu	0.896	1.114	1.119	1.057	1.064
Gd	3.183	3.773	3.782	3.700	3.719
Tb	0.563	0.664	0.663	0.724	0.725
Dy	3.588	4.122	4.137	4.765	4.773
Er	2.200	2.478	2.479	3.016	3.037
Yb	2.146	2.345	2.350	2.876	2.878
Lu	0.342	0.365	0.365	0.447	0.447

Table 5.2.3: Calculated and observed values of specific elements from fractional crystallisation of a more primitive arc magma to a more evolved arc magma. In this instance it is not possible to realistically model the fractionation of K. The low K content of 49212 may be due to K mobility during alteration. It is possible, however, to model the evolution of K with fractional crystallisation using other, slightly less primitive samples. Partition coefficients for each element in a given mineral phase are from Rollinson (1993) or references therein and are the same for both models. Values given for *F* are the averages from a total of 25 elements.

outlier or it may reflect source heterogeneities. Applying the same logic to the back-arc samples yields similar results. The most primitive back-arc basalt is sample 47651 which has an MgO content of 7.84 wt%, an Mg# of 48.2 and a similar mineral assemblage. Fractionating sample 47651 by up to 35% (2.5% magnetite, 15% orthopyroxene, 25% clinopyroxene and 57.5% plagioclase) can account for most of the back-arc samples present (Figure 5.2.8b), however there is a gap between the modelled arc samples and the most primitive back-arc samples (Figure 5.2.8c). The chemistry of the samples, which occur in this gap are difficult to model using FC processes.

Interestingly, simple mixing between the back-arc magmas and the arc magmas can account for the intermediate chemistries (Table 5.2.4). Mixing of between 30% and 70% back-arc/arc magma is needed to approximate the chemistry of the samples, which fall into the gap seen in Figure 5.2.8c. Table 5.2.4 shows the entire range from 100% arc to 100% back-arc sample, however most of the samples in the 'mixing gap' fall into the 30% to 70% back-arc/arc mix. Minor variations from these modelled chemistries can be accounted for by variations in the degree of fractionation within individual samples. However, as both the arc and back-arc magmas appear to be derived from a similar source, modified by differing degrees of subduction zone processes, fractionation and partial melting, it is difficult to determine if this model is correct.

It is more likely that the samples found in the 'mixing zone' are not a product of simple mixing (as above), but rather they may represent magmas which have been modified by differing

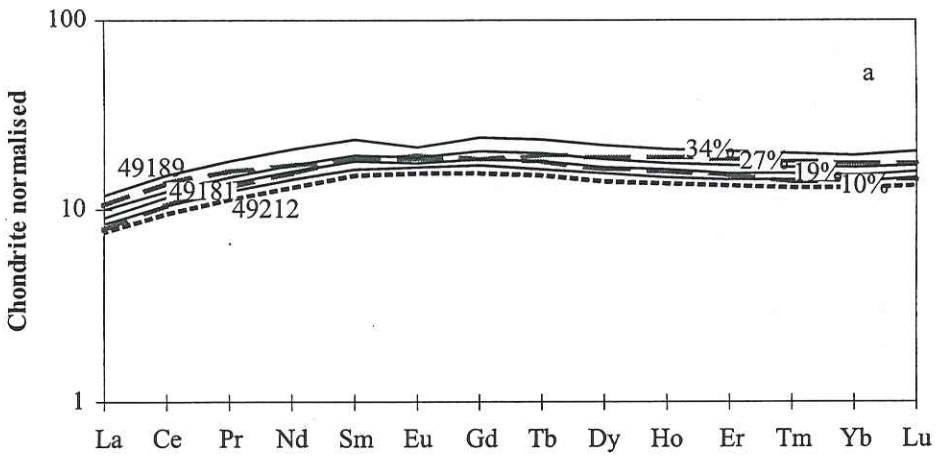

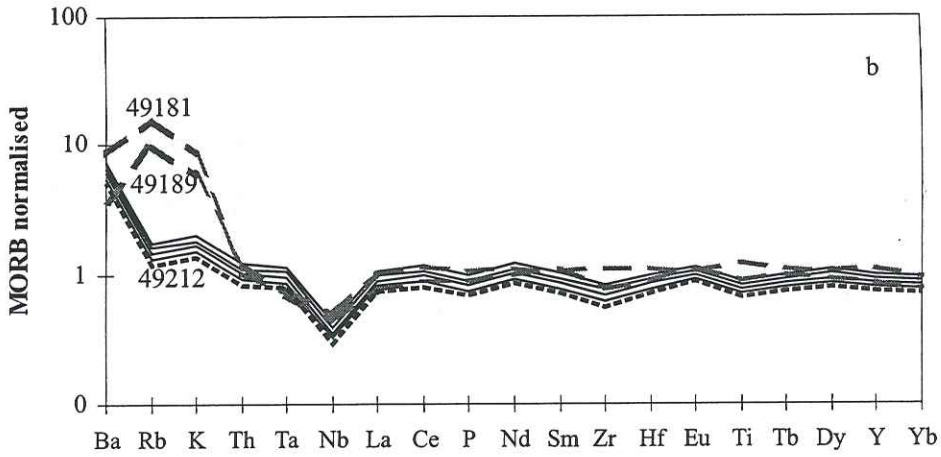

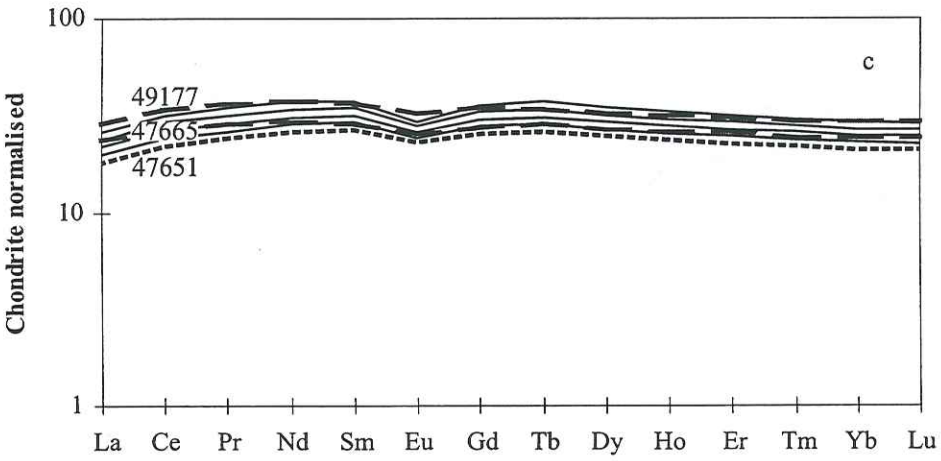

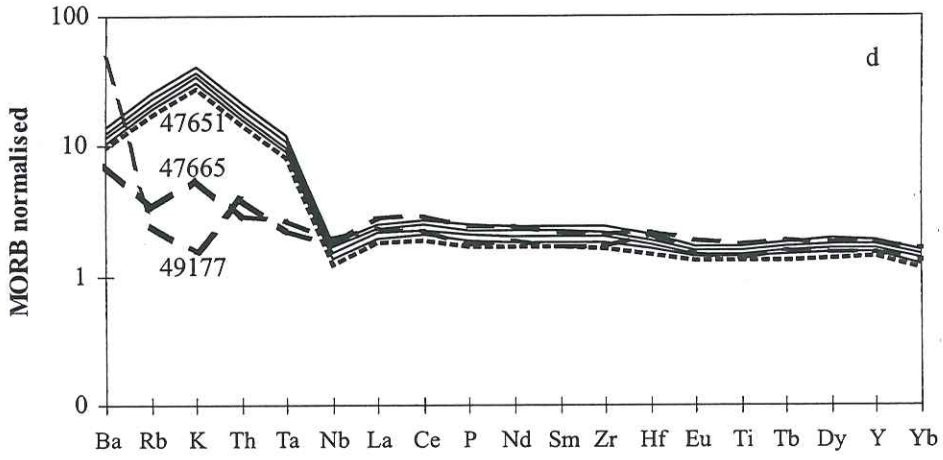

Figuire 5.2.8: Chondrite and MORB normalised diagrams showing fractional crystalisation modeling for (a&b) arc lavas and (c&d) back-arc lavas. Black lines represent 10%, 19%, 27% and 34% incriments of fractional crystallisation as shown in (a). Normalising factors after Sun and MacDonough (1989) and Evensen et al. (1978).

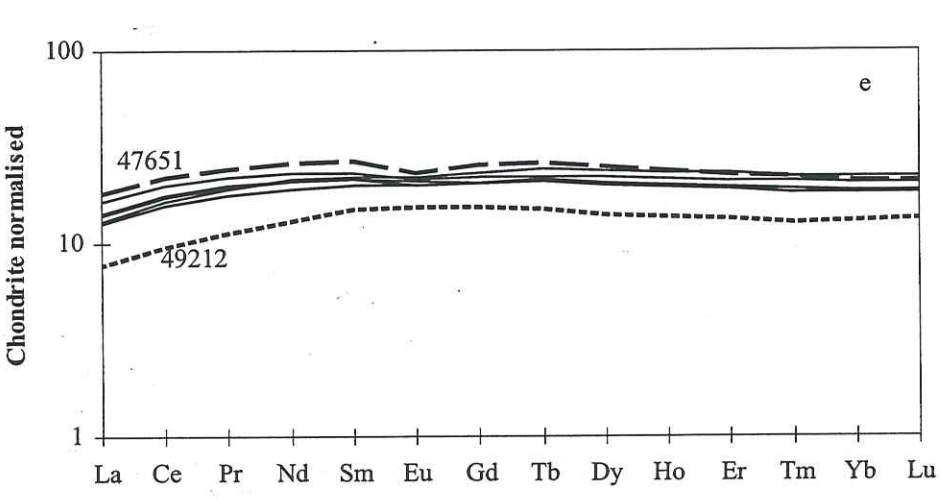

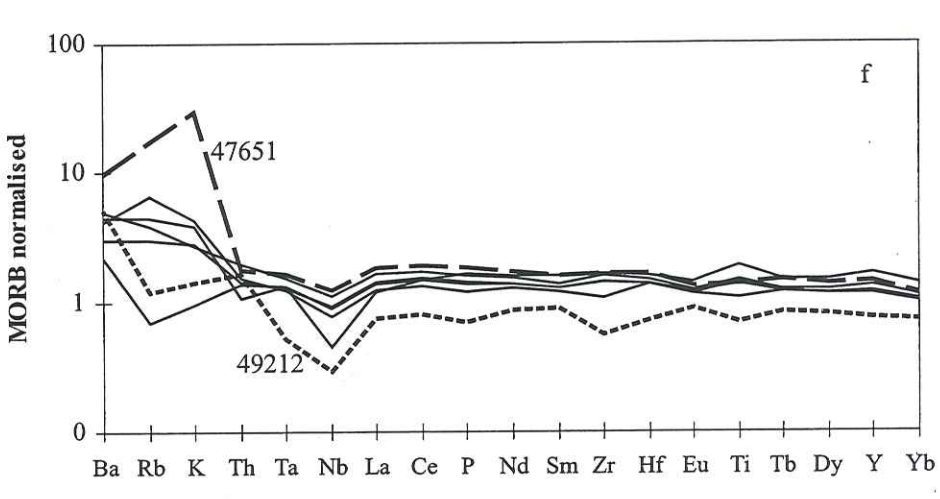

Figuire 5.2.8: continued. (e&f) Chondrite and MORB normalised diagrams showing the proposed mixing zone (or transtitional zone) between the arc lavas and the back-arc lavas. Normalising factors after Sun and MacDonough (1989) and Evensen et al. (1978).

degrees of subduction related fluids (i.e. less than the 'typical' arc magmas but more than the 'typical' back-arc magmas). Both mixing and varying degrees of fluid interaction would produce similar geochemical affinities and hence similar trace and rare earth element patterns as seen in Figure 5.2.4a and 5.2.4b. Mixing and variable slab input are plausible explanations for these intermediate chemistries given the complex nature of the systems.

	49212					47651
	100%ARC	90%ARC	70%ARC	50%ARC	30%ARC	100%BAB
Ba	31.986	34.904	40.740	46.576	52.412	61.166
Rb	0.666	1.561	3.352	5.143	6.933	9.619
K	0.102	0.303	0.704	1.106	1.507	2.109
Th	0.192	0.194	0.198	0.202	0.206	0.211
Ta	0.068	0.083	0.113	0.143	0.174	0.219
Nb	0.674	0.893	1.329	1.766	2.202	2.857
La	1.871	2.132	2.653	3.174	3.695	4.477
Ce	6.066	6.868	8.472	10.077	11.681	14.087
P	0.079	0.092	0.118	0.144	0.170	0.209
Pr	1.094	1.220	1.471	1.722	1.973	2.350
Nd	6.193	6.806	8.030	9.255	10.480	12.317
Sm	2.317	2.497	2.857	3.216	3.576	4.116
Zr	41.850	49.882	65.946	82.011	98.075	122.172
Hf	1.474	1.659	2.030	2.401	2.772	3.328
Eu	0.896	0.940	1.028	1.115	1.203	1.335
Ti	0.889	0.972	1.136	1.301	1.466	1.713
Gd	3.183	3.387	3.796	4.204	4.613	5.225
Tb	0.563	0.605	0.687	0.770	0.853	0.977
Dy	3.588	3.855	4.390	4.924	5.459	6.260
Ho	0.780	0.838	0.953	1.069	1.185	1.359
Y	20.681	22.513	26.176	29.839	33.502	38.997
Yb	2.146	2.283	2.555	2.828	3.101	3.510
Er	2.200	2.358	2.674	2.990	3.306	3.780
Lu	0.342	0.361	0.399	0.436	0.474	0.531

Table 5.2.4: Examples of the mixing calculations between arc and back-arc lavas from the Tangihua Complex. Simple mixing can account for the chemistry of the samples which fall between the most evolved arc samples and the most primitive back-arc samples.

NATURE OF THE SLAB COMPONENT

In most, possibly all, volcanic arcs the mafic lavas are thought to be generated by melting of the subarc mantle (e.g. Ringwood, 1974), which have been modified by subduction related processes (Gill, 1981; McCulloch and Gamble, 1991; Hawkesworth *et al.*, 1993a). The characteristic arc signatures can be seen primarily in incompatible element ratios (e.g. Elliot *et al.*, 1997). The covariation of specific incompatible element ratios are used to provide insight into the processes responsible for the arc signatures. However there is considerable uncertainty as to the composition of both the mantle wedge and the slab component. There is also much debate in the literature as to the mass transfer agents by which slab-derived elements are transported into the

mantle wedge. Possible independent mechanisms for slab input have been proposed, and include variably enrichment by OIB (Gill, 1984; Stern *et al.*, 1991), slab-derived aqueous fluids or slab-derived silicic melts (e.g. Woodhead *et al.*, 1993; Elliott *et al.*, 1997, and references therein).

From the incompatible element ratios used on the Tangihua basalts it is apparent that one or possibly two different processes were responsible for the slab input. High Ba/Nb and Ba/La ratios, particularly in the arc rocks, have been widely used as indicators of an aqueous fluid contributed from the slab (Gill, 1981; Pearce, 1982; Lin *et al.*, 1990; McCulloch and Gamble, 1991; Hawkesworth *et al.*, 1993a). This interpretation has been supported by high-temperature and high-pressure aqueous fluid partitioning experiments (Brenan *et al.*, 1995; Keppler, 1996). The results of the experimental work suggest that slab dehydration should produce fluids with high LILE/HFSE and LILE/LREE ratios. The importance of slab-derived fluids in accounting for extreme LILE/HFSE enrichments in arcs is emphasised by their increased influence on the most depleted magmas. In a strongly incompatible element depleted mantle wedge, the addition of a LILE-enriched fluid will significantly effect the total LILE budget of the source and therefore produce large LILE/HFSE ratios. This effect is buffered in more enriched mantle melts, hence the arc rocks show larger LILE/HFSE ratios unlike the more subdued ratios seen in the back-arc lavas. However, it should be noted that several of the back-arc samples exhibit high LILE/HFSE ratios supporting aqueous fluid input in the back arc region.

Unlike the ratios of LILE/HFSE, the back arc lavas show relatively MORB like Th/Nb ratios whereas the arc rocks are again enriched in Th/Nb relative to MORB. The arc lavas also exhibit a distinct trend towards a negative Ce anomaly (Ce/Ce* <1: see Rollinson, 1993) and higher LREE contents, which are generally thought to be immobile in a fluid component. The development of the Ce anomaly is directly proportional to the enrichment on LREE and Th/Nb ratios (Figure 5.2.5d). Oxidising conditions are necessary to produce a Ce anomaly, which are common in seawater and ocean sediments but are generally only prominent in the SW Pacific (Ben Othman *et al.*, 1989; Lin *et al.*, 1992; Plank and Langmuir, 1998). Elliott *et al.* (1997) have argued that the Ce anomaly in combination with high Th/Nb and $(La/Sm)_n$ ratios and lower $^{143}Nd/^{144}Nd$ suggest that variable enrichment in the Mariana mantle wedge was caused by variable addition of a subducted sedimentary component rather than a slab-derived aqueous fluid. In the case of the Mariana arc, simple bulk mixing of a sedimentary component with the subarc mantle is ruled out due to the small Nb anomaly in the Mariana sediments. Hence both a slab component and a slab-derived aqueous fluids are necessary to explain the chemistry seen in the Mariana arc. This is most likely also the case for the Tangihua basalts.

It is necessary here to emphasis the role, or lack there of, of crustal contamination in the Tangihua Complex. Crustal contamination can create enrichment in arc lavas similar to those seen

in the Tangihua Complex, however, this is unlikely for several reasons. Firstly, arcs which demonstrably have a crustal contamination component, generally tend to contain more fractionated lavas (Davidson, 1987; Hildreth and Moorbath, 1988) whereas the Tangihua Complex is dominantly mafic in nature. In addition, crustal contamination would result in a linear relationship between magmatic differentiation and element enrichment, which is not the case in the Tangihua lavas where the full range of incompatible element ratios are present for the most and least evolved samples. Finally, crustal contamination would significantly influence the radiogenic isotope composition. Average upper crust generally has $^{87}Sr/^{86}Sr > 0.7033$ and $^{143}Nd/^{144}Nd < 0.51226$. Mixing of the Tangihua lavas with a crustal component would result in a greater depletion of radiogenic Nd than is observed.

To sum up our findings for the nature of the slab input, we have concluded that the enrichment of Ba/Nb with Th/Nb and Ba/La with La/Sm, which is present in both the arc and the back-arc magmas, is attributed to the addition of a slab-derived aqueous fluid to a variably depleted mantle melt. This explanation is supported by the isotopic data. Fluids, particularly those generated from oceanic sediments and/or seawater, are know for having a greater effect on the $^{87}Sr/^{86}Sr$ ratios than on $^{144}Nd/^{143}Nd$. Hence the minor depletion of $^{144}Nd/^{143}Nd$ combined with a significant increase in $^{87}Sr/^{86}Sr$ relative to MORB supports interaction with a slab-derived fluid (Figure 5.2.6). It is impossible, however, to rule out the presence of a slab component in the arc rocks. The enrichments in the arc rocks could be generated by the addition of a both subducted sedimentary component and an aqueous fluid.

DISCUSSION

The geochemical data are consistent with eruption of the Tangihua Complex basaltic lavas in both an arc and a back-arc setting. Local field relations show, however, that both the back-arc and the arc lavas are intermixed and petrographically indistinguishable. More importantly there is the lack of evidence for a well-developed Late Cretaceous arc or back-arc within the Northland region and consequently a lack of more silicic lava types. The field relationships pose an interesting problem for the genesis and the eruptive setting of these magmas. How is it possible to have arc and back-arc magmas erupting, cogenetically in the same system, a system which must have been small and short lived? Hence, the Tangihua Complex reflects a unique opportunity to study volcanism which occurred in the transition zone between a volcanic arc and the ensuing marginal, or back-arc, basin.

Trace element data for the arc basalts in this study are consistent with derivation from a mantle source that was enriched in LILE relative to N-MORB. Tatsumi *et al.* (1986) showed that LILE and LREE are more readily transported by slab-derived fluid phases than are HFSE. Hence,

although magmas erupted at destructive plate boundaries are commonly considered to be derived from sources initially more depleted than N-MORB, subsequently interaction with components derived from subducted crust result in selective enrichment of LILE and LREE. The assumption of initially depleted sources is supported by the presence of harzburgite lithologies at the inner trench walls of several island arcs (e.g. Bonatti and Michael, 1989) and the eruption of boninites, which unquestionably are derived from very depleted sources (e.g. Crawford *et al.*, 1989). Magnesian olivine and Cr-rich chromite in primitive IAB and the low abundances of HFSE, which are probably not replenished in the sub-arc mantle during subduction zone metasomatism, are additional evidence for initially depleted sources (Woodhead *et al.*, 1993).

Additional support comes from the HFSE systematics of the basalts. Figure 5.2.9 shows that Zr, TiO_2 and Y contents in the Tangihua basalts are higher than in the average IAB from the SW Pacific region. The BAB basalts of the Tangihua complex compare well with the generalised BABB fields for the SW Pacific, whereas the arc lavas have slightly higher Ti/Zr ratios for a given Zr content than the fields for IAB from the SW Pacific. This data implies that the both suites of basalt could be derived from similar sources as other IAB by smaller degrees of partial melting and slab-derived fluid interactions. The low Zr contents and the steep trends in the Ti/Zr v. Zr diagram shown by IAB from the SW Pacific are interpreted to be the signature of their derivation from MORB sources, previously depleted by extraction of 5-10% melt (Woodhead *et al.*, 1993).

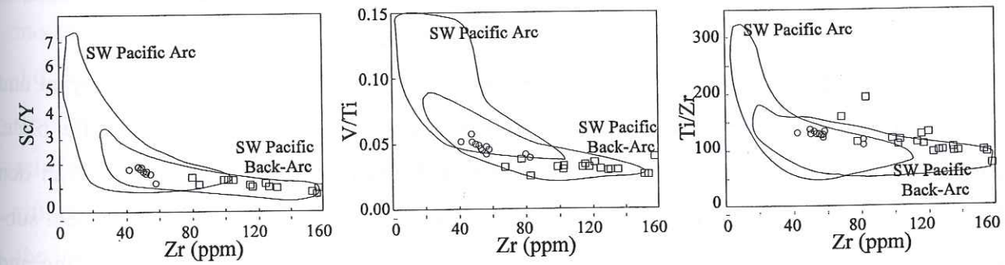

Figure 5.2.9: Zr versus Sc/Y, V/Ti and Ti/Zr ratios for the Tangihua Complex and average SW Pacific arc/back-arc systems. SW Pacific arc/back-arc fields after Woodhead *et al.*, 1993.

By comparison the similar Ti/Zr ratios as well as the similar Zr and Y abundances suggest that the Tangihua BAB basalts were derived from sources comparable to MORB and BAB sources. This suggests that although there may be minor localised source heterogeneity, in general, the source for both the BAB and the IAB in the Tangihua Complex are very similar. Sub-arc mantle is probably depleted by the extraction of a melt fraction(s) prior to their involvement in IAB genesis, this most likely occurred during an earlier rifting event by extraction of BABB (McCulloch and Gamble, 1991). In this instance variations in the HFSE in the arc lavas may reflect variable degrees

of previous depletion of the source mantle peridotite, whereas variations in the LILE and LREE contents of both BAB and arc rocks reflect differing input from the subducting slab. These findings are consistent with work done by Danyushevsky *et al.* (1993), who conclude that K_2O-H_2O data for basalts from Pacific back-arc basins, associated with complex tectonic settings (e.g. incipient spreading ridges, spreading ridges located close to the arc volcanic front), can be explained by addition of a subduction related component to a depleted MORB mantle source (N-MORB or D-MORB).

A simple tectono-magmatic model that can account for the origin of arc and back-arc magmas in the Tangihua Complex is illustrated in Figure 5.2.10 (See Section 4.2 for more detail). In the first stages of this model, approximately 110 – 90Ma (Ballance, 1993), the north-eastern margin of New Zealand was a subduction margin whereas the western and southern margins were rifting (100 - 95Ma). During this time the subarc mantle was depleted by volcanism in the back-arc region. Subduction beneath the New Zealand sector of Gondwana ceased in the early Late Cretaceous with the approach and incipient collision of the Phoenix and Pacific plates (Bradshaw, 1989; Spörli and Balance, 1989; Mazengarb *et al.*, 1991). Ridge collision was immediately succeeded by crustal extension, leading eventually to fragmentation away from Gondwana (Weissel and Hayes, 1977; Laird, 1993). After oblique ridge-trench collision along the New Zealand margin, the Phoenix-Pacific Ridge propagated to the south-west to link with zones of incipient spreading in the Tasman Sea and south of Australia. Subsequently, the eastern part of the ridge continued to migrate south with increasing offset along the Udinsev Fracture Zone.

In the second stage of the model, the small size of the Phoenix plate makes it buoyant and rather than continuing to be subducted, the Phoenix plate was captured by the Pacific plate. Resistance to subduction may have caused break-up of the brittle portions of the slab (van den Beukel, 1990). Thus fragments of the slab may either flounder or be sheared into the adjacent sub-oceanic mantle, to be carried by shallow asthenospheric flow and entrained in the upwelling and melting regime beneath the adjacent ridge. Plate capture led to the stalling of the Phoenix-Pacific subduction and the initiation of rifting between the newly formed Phoenix-Pacific plate and West Antarctica (Luyenduk, 1995).

In stage three of our model, we have proposed, that the stalling of the Phoenix-Pacific ridge and associated subduction system, in combination with the initiation of rifting in the Tasman Sea, resulted in the generation of the Tangihua Ophiolite Complex (Nicholson *et al.*, (b) in review). Subduction was initiated such that the downgoing slab was partially melted (>100Ma). However, subduction was quickly aborted with the change to an extensional environment. The proceeding rift volcanism was then in contact with, and interacted with a slab-derived aqueous fluid and possibly a slab-derived melt, hence, explaining the arc signatures in the previously depleted, N-MORB, basalt

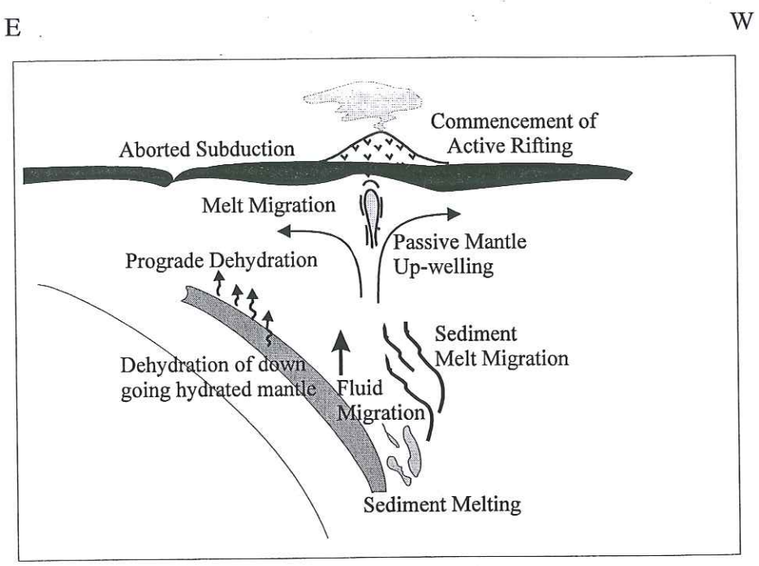

Figure 5.2.10: Cartoon of the development of a back-arc basin (modified after Elliott *et al.*, 1997) overlying an aborted subducted slab and the subsequent generation of the Tangihua Complex.

chemistry. The presence of active subduction in New Zealand at this time is supported by the relationships recognised between several mid-Late Cretaceous stratigraphic domains in the North Island (Ballance, 1993; Mazengarb and Harris, 1994).

It is also possible to explain the chemistry of the arc and back-arc lavas in stage three of our model using a non-depleted mantle wedge. This alternative scenario assumes that the earlier rifting did not in fact result in a depleted mantle wedge or that a different, non-depleted, section of the wedge was samples in the genesis of the Tangihua magmas. In this case, depletion of the arc lavas relative to the back-arc requires that the back-arc lavas were generated before the arc lavas. If rifting began before the aborted subducting slab began to dehydrate then N-MORB lavas, such as the back-arc lavas, would be generated and deplete the mantle wedge. Over time the stranded slab dehydrated, producing the slab-derived aqueous fluid, which rose and interacted with the now depleted mantle wedge, hence producing the arc lavas after the back-arc. Although this model is plausible it is more complicated and does not adequately explain the depleted nature of the arc lavas, therefore this model is not favoured.

Another alternative scenario for stage three of our model invokes lateral changes in chemistry along the arc/back-arc region to explain the geochemical variations. In this scenario the Tangihua Complex is located at the transition zone between the arc and the back-arc (e.g. Miller *et al.*, 1994). The precise location of the Tangihua Complex, in this transition zone, would account for the interfingering of the arc and back-arc magmas, although, the arc/back-arc system must still be young and short lived. The most significant problem with this model is the lack of a well developed

arc front and back-arc which, coupled with the presence of magmas which appear to be the result of mixing between the arc and the back-arc magmas, render this model unlikely. It is also difficult, in this model, to explain the continuum between the arc and back-arc chemical trends using systems which evolved separately. As a consequence, we conclude that the simple tectono-magmatic model, invoking the partial subduction of the Phoenix plate, is the most likely to account for the generation of the Tangihua Complex and the chemistries found therein.

ACKNOWLEDGEMENTS

This research has been supported by the University of Auckland, New Zealand, the French Embassy, Wellington, NZ, and by the Université Joseph Fourier, France. This manuscript has benefited from reading and comments by T. J. Worthington.

SECTION 5.3

Summary

The geochemical data of both the basaltic lavas and the glass samples from the Tangihua Complex are consistent with eruption in both an arc and a back-arc setting. Local field relations show, however, that both the back-arc and the arc lavas are intermixed. Petrographically the arc and back-arc lavas are also indistinguishable. More importantly there is the lack of evidence for a well-developed Late Cretaceous arc or back-arc within the region and consequently a lack of more silicic lava types.

The low Zr contents and the steep trends in the Ti/Zr v. Zr diagram shown by IAB suggest derivation from a previously depleted MORB source. Ti/Zr ratios, Zr and Y abundances in the BABB suggest that they were also derived from a slightly depleted MORB source. This suggests that although there may be minor localised source heterogeneity, in general, the source for both the BAB and the IAB in the Tangihua Complex are very similar. The sub-arc mantle was probably depleted by the extraction of a melt fraction(s) prior to their involvement in IAB genesis, this most likely occurred during an earlier rifting event.

In support of these conclusions, geochemical modelling shows that the Tangihua lavas were derived from between 10 – 20 % partial melting of a slightly depleted MORB-mantle source. The arc lavas appear to represent approximately 20% partial melting of a source depleted by up to 5%, whereas the back-arc lavas have undergone only 10% partial melting of a less depleted (<3%) source. Modelling of crystallisation shows the back-arc lavas have undergone approximately 35% fractional crystallisation (FC) and the arc lavas have undergone approximately 30% FC. The chemistries intermediate between the arc and back-arc can be modelled by 30-70% simple mixing of the arc lavas with the back-arc lavas.

Trace element data for the arc basalts in this study are consistent with derivation from a mantle source that was enriched in LILE and LREE relative to N-MORB. LILE and LREE are more readily transported by slab-derived fluid phases than are HFSE, hence interaction with components derived from subducted crust result in selective enrichment of LILE and LREE. Additional support comes from the HFSE systematics of the basalts. Zr, TiO_2 and Y contents in the Tangihua basalts are higher than in the average IAB from the SW Pacific region. Both the arc and the back-arc magmas show LILE and LREE signatures that can be attributed to interaction with a slab-derived fluid, whereas the arc lavas also show enrichments related to interaction with a slab-derived melt.

A simple tectono-magmatic model that can account for the origin of arc and back-arc magmas in the Tangihua Complex has been developed. Initially the north-eastern margin of New Zealand was a subduction margin whereas the western and southern margins were rifting. During this time the subarc mantle was depleted by volcanism in the back-arc region. Subduction beneath the New Zealand sector of Gondwana ceased in the early Late Cretaceous with the approach and incipient collision of the Phoenix and Pacific plates (Bradshaw, 1989; Spörli and Ballance, 1989; Mazengarb *et al.*, 1991).

The small Phoenix plate was buoyant and was captured by the Pacific plate. Plate capture led to the stalling of the Phoenix-Pacific subduction and the initiation of rifting between the newly formed Phoenix-Pacific plate and West Antarctica (Luyenduk, 1995). The stalling of the Phoenix-Pacific ridge and associated subduction system, in combination with the initiation of rifting in the Tasman Sea, resulted in the generation of the Tangihua Ophiolite Complex (Nicholson *et al.*, (c) in review). Subduction was initiated and the downgoing slab was partially melted before the subduction system was aborted with the change to an extensional environment. The proceeding rift volcanism was then in contact with, and interacted with a slab-derived aqueous fluid and possibly a slab-derived melt, explaining the arc signatures in the previously depleted, N-MORB, basalt chemistry.

CHAPTER SIX: AGE OF THE TANGIHUA COMPLEX

CHAPTER 6

Ar/Ar Age Dating

INTRODUCTION

There is much uncertainty in the literature as to the age of the Tangihua Complex and the Northland Allochthon (Farnell, 1973; Brothers and Delaloye, 1982; Brook *et al.*, 1988; from Hayward *et al.*, 1989; Hollis and Hanson, 1991). Previous workers have reported fossil ages ranging from the Early Tertiary to the mid-Cretaceous (Farnell, 1973; Brook *et al.*, 1988; Hollis and Hanson, 1991) and early K-Ar dating has reported a similar range in ages (Brothers and Delaloye, 1982).

Intercalated sedimentary rocks make up less than 1% of the total volume of the Tangihua Complex (Isaac *et al.*, 1994). The sediments are dominated by siliceous, or less commonly calcareous, mudstones, which are rarely fossiliferous. Perhaps the most widely accepted age of the Tangihua Complex comes from Hayward *et al.* (1989). They reported *Inoceramus* and formaminifera in intercalated siliceous mudstone and micritic limestone units suggesting mostly late Cretaceous ages, although early Cretaceous bivalves are present at Houto. However, older ages (possibly Early Cretaceous; Isaac *et al.*, 1994) have been reported from the northern massifs, whereas late Palaeocene radiolarian have been reported from Camp Bay (Hollis and Hanson, 1991).

Radiometric K-Ar dating on whole rock and mineral separates from various massifs yield a bimodal age distribution of *ca.* 100 Ma and *ca.* 42 Ma (Brothers and Delaloye, 1982). Similarly, K-Ar ages within individual massifs range from about mid-Tertiary to mid-Cretaceous (Brothers and Delaloye, 1982). However, due to the pervasive nature of the alteration, the rocks may have undergone some amount of argon leakage or argon homogenisation rendering a degree of uncertainty to the radiometric ages (Brothers and Delaloye, 1982). Never the less, it has become commonly accepted that the older age of *ca.* 100 Ma represents the age of formation of the seafloor basalts. In places within specific massifs, major faults exhibiting only the lower temperature phase of alteration. The younger age, *ca.* 42 Ma, may reflect post-formation tectonic, hydrothermal or magmatic events which occurred during emplacement of the ophiolitic sequence (Malpas *et al.*, 1992).

NEW Ar/Ar AGE DATING

In this study, seven samples were dated using the Ar-Ar method at the University of Michigan, Department of Geology. Figure 6.1.1 shows the location of the samples and Table 6.1.1 gives a brief description of the results of each sample. The Ar-Ar spectra and a description of the method are in Appendix 11. The samples were chosen on the bases of freshness and their geochemical characteristics: three of the samples have arc signatures and four of the samples have back-arc signatures. Despite choosing samples with LOI< 2 wt.% (in most cases LOI<1 wt.%) all of the samples yielded alteration ages at approximately 30Ma. Sample #47648 gave an formation age of ≈100Ma which is supported by similar plateaus in two of the other samples (49181 and 49159). Two of the arc samples gave ages older than Cretaceous as did one of the back-arc samples. As the samples show obvious signs of alteration, the results of the Ar-Ar dating should be interpreted with caution. Any comments or conclusions should be tempered by geological constraints.

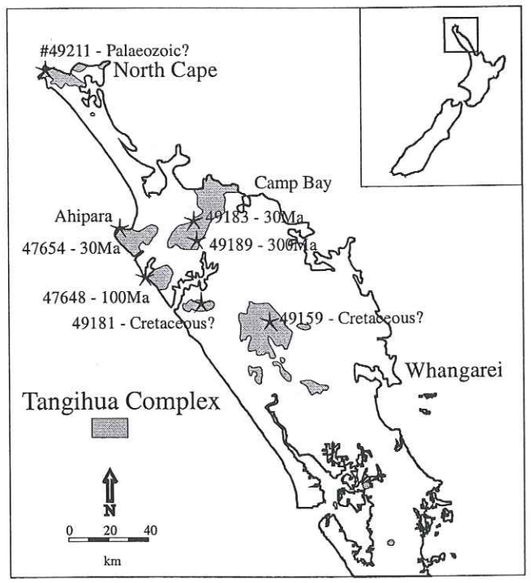

Figure 6.1.1: Location map of the seven samples dated from the Tangihua Complex. Stars denote the location of each sample. Where possible the age of formation is given, otherwise the 30Ma age reflects alteration.

The alteration age predates, only slightly, the age of initiation of volcanism in the Northland Volcanic Arc (Smith and Black, 1995). The Northland Volcanic Arc is a northwest oriented system of early Miocene (approximately 25 - 30Ma) arc volcanism (Smith and Black, 1995). As the alteration mineralogy in the Tangihua Complex supports a simple tectonic history with only one major event (Nicholson and Black, 1998; Nicholson *et al.*, (a) in review; Section 3.3), it is likely

that the 30Ma age reflects the obduction event. Hence, the initiation of the Northland Volcanic Arc may have caused the obduction of the Tangihua Complex (and the remainder of the allochthon). Although dating the alteration of the Tangihua Complex was not the intention of this study, the alteration age is important. This new age data helps to constrain the arrival and initiation of volcanism in the Northland Volcanic Arc.

Several of the samples had a minor Cretaceous plateau, and one of the samples had a definite age of ≈100Ma. This is the date that is believed to represent the age of formation. Previous work has also indicated age of approximately late Cretaceous (Brothers and Delaloye, 1982; Hayward *et al.*, 1989). This age fits well with the tectonic model presented in Section 4.2 and Section 4.3 (Nicholson *et al.*, (b) and (c) in review) with the arrival and attempted subduction of the Phoenix-Pacific plates. Bradshaw (1989) has documented a regional shift from subduction to

Sample	Affinity	Location	LOI	Age – alteration	Age – formation	Comments
49211	Arc	Cape Maria Von Dieman	1.48	≈30Ma	Palaeozoic ?	The plagioclase age spectrum is disturbed, but gives a clear indication of a much older component (Palaeozoic?). The whole rock is dominated by the 30 Ma alteration event.
49181	Arc	Opononi	1.44	≈30Ma	Cretaceous ?	This sample is less altered as the Ca/K is very high. The separate suggests a ca 30 Ma alteration age, whereas the whole rock suggests a Cretaceous or even older signature.
49189	Arc	Maungamuka	1.83	≈30Ma	300-305 Ma ?	Both separate and whole rock ages suggest ca 30 Ma (alteration). Note that the age spectra assume an initial 40Ar/36Ar ratio of 295.5 (=atmospheric Ar). From the isochron fits, it seems that some of the structure seen in the age spectra is due to a non-atmospheric initial component (maybe 40/36 about 300-305).
47654	Arc	Ahipara	0.58	≈30Ma		Whole rock (separate disappeared upon cleaning). Age of 30 Ma (alteration).
49159	Back-arc	Maungakahia	0.40	≈30Ma	Cretaceous ?	The plagioclase separate age spectrum is fairly disturbed. There is a hint of an older (Cretaceous ?) component. The whole rock run has pretty strong evidence for an event at about 30 Ma (alteration) The plagioclase component must be relatively small volumetrically as there are no really high ages.
49183	Back-arc	Peria	0.58	≈30Ma		The Ca/K for the separate is very low. The whole rock suggest a ca 30 Ma (alteration).
47648	Back-arc	Whangapei Harbour	0.50	≈30Ma	≈100Ma Cretaceous	Both the plagioclase and the whole rock isochrons suggest a slightly elevated initial 40/36 ratio. Plagioclase gives an isochron age of about 100 Ma, and the whole rock gives one about 30 Ma.
47662	Back-arc	Ahipara	0.49	≈30Ma	≈400Ma	This separate has the clearest old signature (ca 400 Ma). Whole rock again suggests a ca 30 Ma alteration.

Table 6.1.1: Summary table of Ar/Ar dating results for the Tangihua Complex. Notice that all samples have an alteration age of approximately 30Ma.

extension dominated magmatism at ≈105Ma. Between 110 – 90 Ma (Ballance, 1993) the eastern margin of New Zealand was a subduction margin where as the western and southern margins were

rifting (100 - 95Ma). During the early Late Cretaceous, subduction beneath the New Zealand sector of Gondwana ceased due to the approach and incipient collision of the spreading ridge between the Phoenix and Pacific plates (Bradshaw, 1989; Spörli and Ballance, 1989; Mazengarb *et al.*, 1991). Ridge collision was immediately succeeded by crustal extension, leading eventually to fragmentation away from Gondwana (Weissel and Hayes, 1977; Laird, 1993). As discussed in Section 4.3, the Phoenix plate was small and buoyant, making continued subduction difficult and resulting in the fusing of the Phoenix and Pacific plates. It has been proposed (Nicholson *et al.*, (c) in review; Section 4.3) that it was during the subduction of the Phoenix plate, ≈100Ma, that the Tangihua Complex magmas first formed. However, subduction was short lived, hence, the abortion of the subduction system, followed by rifting, that lead to the change to a more back-arc style of magmatism.

This new 100Ma age of formation is important, not only for constraining the age of formation of the Tangihua Complex but also for its ability to constrain the tectonic setting of New Zealand and the SW Pacific during the Cretaceous. Much work on the pre-Cenozoic evolution of the SW Pacific is poorly constrained due to limited age data. This new data helps to constrain the arrival of the Phoenix-Pacific Plate and the ensuing oblique collision with Gondwana.

Another important ramification of a 100Ma age of formation for the Tangihua Complex is its relationship with New Caledonia. Paleontological evidence suggests a Late Cretaceous (≈80Ma), or slightly younger, age of formation for the Poya terrane (Aitchison *et al.*, 1995a; Meffre, 1995; Eissen *et al.*, 1998). The age of formation of the Poya terrane is not well constrained, however, there is little evidence to suggest that it could be as old as the Tangihua Complex. Thus the new ages for the Tangihua Complex suggest that there is little or no relationship between the two systems despite possible geochemical affinities (see Section 4.3).

Finally there are the three ages which suggest an even older, Palaeozoic, age of formation for the Tangihua Complex. This age is interesting as it corresponds to the age of the oldest rocks in Northland (Hay, 1960; Maehl, 1970; Sporli and Grant-Mackie, 1976; Sporli and Gregory, 1981; Ramsay and Moore, 1985; Meshesha and Black, 1989). It is possible that these ages are the result of alteration in the samples. However, it is also possible that these rocks were underlying the Tangihua Complex when it was formed and were obducted at the same time. Parts of the underlying Waipapa terrane contain basaltic tuffs and lavas (Jennings, 1987; 1989). In this instance the lavas may have formed as part of the opening of the South Fiji Basin. This explanation is plausible, however, if this were the case then there should be differences in the chemistry of the lavas. There appears to be no difference between the lavas from these samples and the remainder of the Tangihua Complex, which suggests that these ages reflect alteration and not an entirely new system. A further study is in progress, which may help to elucidate these relationships.

CHAPTER SEVEN: COMPARISONS

SECTION 7.1

Introduction

The Tangihua Complex has, until now, been considered a 'typical' ophiolite complex. As an ophiolite formed as part of a spreading system, the Tangihua Complex has been compared to ophiolites such as Cyprus, Oman and Newfoundland (Thompson *et al.*, 1997). The generation and emplacement of such an ophiolite within the SW Pacific between the Late Cretaceous and the Miocene posed several problems (Malpas *et al.*, 1992). However, the new geochemical results of this study suggest that the basaltic lavas of the Tangihua Complex were generated in an arc/back-arc system.

During this time the SW Pacific region was characterised by multiple episodes of convergence and divergence, forming marginal basins and volcanic arcs which were generally short lived. However, at approximately 80-100 Ma the progressive development of a collision zone can be traced from Papua New Guinea through New Caledonia to New Zealand. Although there is much uncertainty regarding the specific plate movements during the Late Cretaceous, it is believed that in New Zealand the situation was complicated by the presence of the Phoenix micro-plate, which stalled subduction, preventing the development of a mature arc system and initiating spreading. Hence, the new interpretation of the Tangihua Complex as an arc/back-arc system is easier to explain in terms of both the chemistry (See Chapters 4 and 5) and regional tectonics (See Sections 4.2, 4.3 and 5), which invites comparison between the Tangihua Complex and other arc/back-arc systems in the SW Pacific.

Initially, the Tangihua Complex is compared to active arc/back-arc systems within the SW Pacific and from around the world (Figure 1.1.1). Despite the significant age difference, there are distinct similarities which show conclusively that the Tangihua Complex is an ancient arc/back-arc system preserved as part of the Northland Allochthon. The Tangihua Complex is then compared to the Poya terrane of New Caledonia. The ophiolites of New Caledonia are geographically the closest ophiolites of Cretaceous age to the Tangihua Complex and several aspects of the Poya terrane suggest similarities to the Tangihua Complex. Finally, this chapter will compare the Tangihua Complex basalts to other lava types within the Tangihua Complex and the Northland Allochthon. In addition to the basaltic rocks studied in this thesis, the Tangihua Complex contains several other lava types, such as minor gabbros and younger intrusions. Although they have not been discussed in detail they are an important component within the ophiolite.

SECTION 7.2

SW Pacific Arcs and Back-arcs

PETROGRAPHY

The majority of the basaltic lavas found in the Tangihua Complex are moderately porphyritic with up to 50% phenocrysts. The complex also contains less porphyritic lavas and fresh basaltic glass. The mineral assemblage is dominated by plagioclase with lesser amounts of clinopyroxene > orthopyroxene > magnetite ± olivine ± hornblende, reflecting a simple anhydrous phenocryst assemblage. This assemblage is fairly typical of island arc and back-arc basaltic lavas.

As such there are several comparable systems within the Pacific containing lavas with a similar phenocryst assemblage, although minor differences do occur. The samples from the Bonin-Izu and Marianas are possibly the most similar to the Tangihua lavas. They contain plagioclase ± pyroxene ± spinel ± olivine ± hornblende. The lavas are dominated by plagioclase with lesser clinopyroxene, minor orthopyroxene and spinel, while olivine and hornblende are rare (Pearce *et al.*, 1995 and references therein). The SW Pacific arc/back-arc lavas are generally porphyritic although aphyric and glassy lavas do exist. Lavas from the South Sandwich Islands and the Aleutians are also similar and contain both tholeiitic and calc-alkaline affinities. The tholeiitic lavas contain plagioclase with lesser clinopyroxene, olivine and spinel whereas the calc-alkaline lavas contains plagioclase with lesser clinopyroxene, orthopyroxene and minor hornblende (Kay and Kay, 1985; Miller *et al.*, 1992). Other arc/back-arc systems generally have minor differences, which separate them petrographically from the Tangihua Complex.

The lavas from the Tonga-Kermadec volcanoes (Ewart, 1982; Gamble *et al.*, 1990; Worthington, 1998) are grossly similar to the Tangihua lavas. They contain plagioclase ± pyroxene ± spinel ± olivine, however, hornblende is reported absent and minor alkali feldspar and quartz are reported from Fonualei dacites (Ewart *et al.*, 1973). Lavas from continental margin arcs, such as the Taupo Volcanic Zone, are generally dissimilar to the Tangihua lavas. The Taupo Volcanic Zone lavas are predominately more felsic and contain a greater proportion of pyroxene phenocrysts relative to plagioclase (Graham *et al.*, 1995).

GEOCHEMISTRY

The Tangihua lavas are dominantly basaltic-basaltic andesite and have both arc and back-arc affinities. They are members of the low-K series and have low Mg#s. The back-arc lavas have a tholeiitic trend, whereas the arc lavas have a more calc-alkaline trend. The REE, LILE and HFSE

concentrations generally increase with SiO_2 content and decease with MgO content, reflecting incompatible behaviour during crystal fractionation processes. The Tangihua lavas are characterised by LREE depleted, LILE enriched chondrite and MORB normalised patterns and have negative Nb anomalies relative to MORB. These characteristics are typical of subduction related lavas elsewhere. Hence, despite their formation in a complex, previously undocumented, tectonic environment there are many similarities between the Tangihua arc rocks and lavas found in other arc systems and there are many similarities between the Tangihua back-arc samples and other 'typical' back-arc lavas.

Arc	Back-arc	Rock Types	TiO_2	Ti/Zr	Sc/Y
Average SW Pacific Arc			**.69±.18**	**76-220**	**1.38-5.2**
Tangihua[1]		**50-55**	**1.2**	**124**	**1.53**
Tonga[2]				100-320	1.5-7.5
Kermadec[2&3]		51	.44	75-260	1.5-4.5
Vanuatu[2&4]		50	.4-1.5	75-210	1.1-5.2
Mariana[2&3]		52	.75-.97	50-150	1-5
Izu-Bonin[2]				75-225	1.8-4.9
South Sandwich[2&5]				80-140	
Average SW Pacific Back-arc			**1.19±.39**	**71-127**	**1.14-2.2**
	Tangihua[1]	**50-60**	**1.9**	**100**	**.9**
	Lau[2]	50-59		75-175	1-2.8
	Havre[2]			80-100	1-2
	North Fiji[2&5]	50-58	1.32-1.93	80-180	1-1.5
	Mariana[2&5]	54-57	.75-1.61	60-100	1-1.7
	Izu-Bonin[2]			70-130	1.7-3
	Scotia Sea[2&5]	54		60-75	

Table 7.2.1: Some average element contents and element ratios from the Tangihua Complex and other arc/back-arc systems. [1] This study, [2] Woodhead *et al.*, 1993, [3] McCulloch and Gamble, 1991, [4] Peate *et al.*, 1997, [5] Vallier *et al.*,1991. See Figure 1.1.1 for location of these arc/back-arc systems.

In the SW Pacific, arc lavas have been well studied (Vallier *et al.*, 1991; Woodhead *et al.*, 1993; Turner *et al.*, 1997). The average SW Pacific island arc is dominated by basaltic – basaltic andesite lavas which are low-K and have a wide range of Mg#s. Pacific arcs also tend to have negative Ce anomalies. In general the average SW Pacific arcs are similar to the Tangihua Complex (see Table 7.1.1). Average SW Pacific arc compositions include: Zr = 40 ± 19.6, Y = 16.5 ± 7.1 and TiO_2 = 0.69 ± 0.18 (Woodhead *et al.*, 1993), whereas the Tangihua Complex arc lavas have average: Zr = 58.05, Y = 24.7 and TiO_2 = 1.2. Element ratios such as Ti/Zr, Sc/Y, Ba/Nb are also comparable (Figure 7.1.1; Woodhead *et al.*, 1993; McCulloch and Gamble, 1991).

Back-arc systems within the SW Pacific are less well studied than their associated arcs (Vallier *et al.*, 1991; Woodhead *et al.*, 1993). However, from the data available it is apparent that the back-arc lavas from the Tangihua Complex are fairly typical of the SW Pacific back-arc systems. When looking at the same set of elements as used for comparison of the arc systems, the back-arc lavas of the Tangihua Complex are remarkably similar to those in the average SW Pacific back-arc. Both systems are characterised by basaltic-basaltic andesites with low-K and a range in Mg#. Average SW Pacific back-arc: Zr = 79.7 ± 36.4, Y = 26.4 ± 8.6 and TiO_2 = 1.19 ± 0.38 (Woodhead *et al.*, 1993) whereas the Tangihua Complex back-arc lavas have average: Zr = 117.8,

Y = 41.5 and TiO_2 = 1.9. Here again the element ratios of Ti/Zr, Sc/Y, Ba/Nb are comparable (Figure 7.1.1a,b,c; Woodhead *et al.*, 1993; McCulloch and Gamble, 1991).

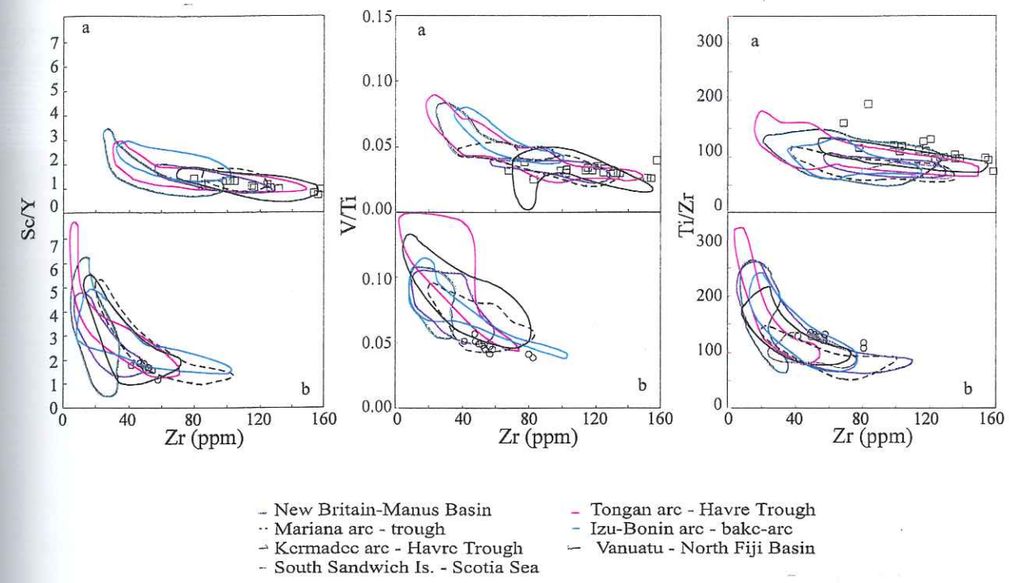

Figure 7.2.1: Variation diagrams showing the similarities between other arc/back-arc systems and the Tangihua Complex. Data fields after Woodhead *et al.* (1993). a: back-arc, b: arc.

One of the most important factors to note when comparing the Tangihua Complex to other arc and back-arc systems is the general geochemical trends. The SW Pacific arcs are characterised by lower HFSE and higher LILE than their associated back-arcs. This same pattern is seen in the Tangihua Complex. Element ratios such as Ba/La and Nb/Th amplify the enrichment and depletion processes caused by interaction with a subduction related component (See Chapter 5 for more detail). The same general trends can been seen in incompatible elements, such as Zr, Y and TiO_2, where the back-arc lavas are enriched relative to the arc lavas.

One of the fundamental differences between the Tangihua lavas and those found in other SW Pacific arc systems is their TiO_2 content. The Tangihua Complex has a higher average TiO_2 content than any other arc/back-arc system in the SW Pacific. The Marianas' system has a relatively high TiO_2 content with average values ranging between 0.75 – 0.97 for the arc lavas and 0.75 – 1.61 for the back-arc lavas. From the available literature it is apparent that the Marianas' also have similarly high Zr and Y contents, similar element ratios and similar Sr and Nd isotopic ratios (Woodhead *et al.*, 1993). The Valu Fa Ridge, which is part of the Lua Basin, has TiO_2 contents ranging from 1.4 to 1.9 wt.% and elsewhere within the Lau Basin there are back-arc basalts with TiO_2 contents ranging up to 2 wt.%. Hence, although on average the TiO_2 contents of various

SW Pacific arc/back-arc systems are lower, within each system there are regions with more comparable values to those found within the Tangihua Complex. This is most likely due to the input of a generally similar SW Pacific sedimentary component and similarly depleted N-MORB sources with minor hetrogenieties.

The same general patterns can be seen in $^{87}Sr/^{86}Sr$ versus $^{143}Nd/^{144}Nd$ plots for the Tangihua Complex and several other SW Pacific arc/back-arc systems (Figure 7.1.2). In all cases, as a result of the increased slab component in the arc lavas, the arc suite plots towards higher radiogenic Sr compositions relative to the back-arc suite. The Tangihua arc lavas initially overlap with the back-

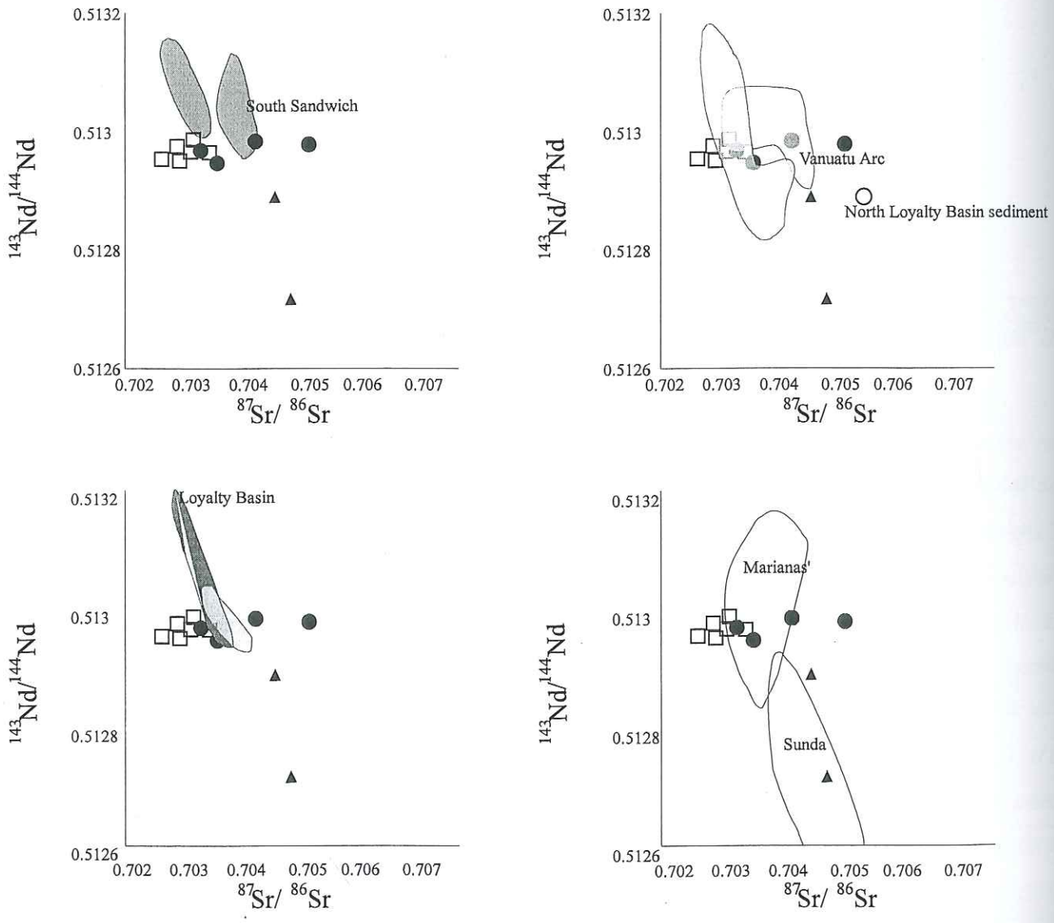

Figure 7.2.2: $^{87/86}$ Sr versus $^{143/144}$ Nd plots for the Tangihua Complex and several other SW Pacific arc/back-arc systems. As expected the overall trend towards higher $^{87/86}$ Sr and lower $^{143/144}$ Nd is repeated in each system.

arc samples but some have much higher radiogenic Sr, which is higher than the Marianas', Lau, South Sandwich, Vanuatu arc/back-arc systems, but still within the overall field for the SW Pacific. In conclusion the Tangihua arc and back-arc lavas are similar to other arc/back-arc systems from within the SW Pacific.

SECTION 7.3

The Poya Terrane, New Caledonia

The islands of New Caledonia are approximately 1500 km NE of New Zealand. As with the Tangihua Complex, the existing tectonic models for the Cenozoic history of New Caledonia (Brothers and Blake, 1972; Paris, 1981; Kroenke, 1984) were proposed in the early days of plate tectonics. Recently, however, Aitchison *et al.* (1995) proposed a model involving collision between a SW facing arc and thinned continental margin crust, the progressive development of this collision zone can be traced from Papua New Guinea through to New Zealand.

The Poya terrane is characterised by pillow basalts and dolerites overlain by shales and outcrops areas along both coasts. Radiolarian age dating suggests that these rocks are Late Cretaceous (Campanian) in age (Aitchison *et al.*, unpublished). Isotopic and REE data indicate that these predominantly tholeiitic basalts may have been developed in a back arc basin or marginal sea environment (Rodgers, 1975; Cameron, 1989; Cluzel *et al.*, 1999; Nicholson *et al.*, (c) in review).

BASALT PETROGRAPHY

The Poya terrane basalts are petrographically very similar to the Tangihua basalts. The PTB range from almost aphyric massive flows, microgabbro plugs and dykes, through to intergranular and interstitial textured basalts with 2-10 modal % plagioclase and clinopyroxene phenocrysts. Primary phenocryst are plagioclase + clinopyroxene >> orthopyroxene, magnetite and sphene with rare olivine. Plagioclase phenocryst compositions range from An_{53} to An_{73}, which is similar to the plagioclase in the Tangihua Complex (compositions in the range of An_{66-87} with an average of An_{74} and average of An_{62}). The composition of clinopyroxene phenocrysts is also similar between the two systems. The Poya terrane contains calcic augite with a compositional range of $En_{39-51}Fs_{10-24}Wo_{35-45}$. Both the plagioclase and the clinopyroxene compositions are comparable between the two systems, however, the PTB contain much less orthopyroxene than the TCB. The more limited compositional range of the PTB samples is probably due to the more limited sample set.

ALTERATION AND METAMORPHISM

The alteration and metamorphism in the Tangihua Complex and the Poya terrane is similar in some ways but there are also important differences. While both systems contain weak but pervasive low grade metamorphism reflecting a transition between zeolite, prehnite-pumpellyite

and greenschist facies metamorphism (See Section 3.3; Nicholson *et al.*, (a) in review), the Poya terrane contains a higher temperature mineral assemblage indicating a blueschist event. Another fundamental difference is the lack of the lower-temperature phases typical of seafloor alteration processes in the Poya terrane. The key factor in these differences is they suggest not only differing temperatures for the alteration process but also different tectonic histories. The secondary mineralogy of the Tangihua Complex suggests a relatively simple post-formational tectonic history that involves possibly only one event. In short, the only major tectonic event seen in the Tangihua Complex was it's obduction, which must have been cold and at low pressures in order that the seafloor alteration assemblages have been preserved. The Poya terrane has a more complex post-formational tectonic history. The typical seafloor alteration assembles seen in oceanfloor basalts has been over printed by a later higher temperature and pressure event. This later event is related to pre- or syn-obduction processes in which the entire allochthon was partial subducted (See Section 3.3; Nicholson *et al.*, (a) in review for more details).

GEOCHEMISTRY

As with the alteration and metamorphism, at first glance the geochemistry of the Tangihua Complex and the Poya terrane are very similar. Both systems are dominated by samples with SiO_2 contents ranging between 48 and 55wt%. Both the PTB and the TCB samples are predominantly tholeiitic, low-K basalts with Mg#s ranging between 40 and 50. However, the PTB fall within the MORB and BAB suites and TCB are relatively depleted in Nb, Ta and Zr relative to the PTB and the PTBs have Ti/Zr and La/Nb ratios similar to N-MORB (See Section 4.3).

Both complexes contain minor alkaline basalts and intrusions of tholeiitic affinity. Unlike the Tangihua Complex, the Poya terrane also contains samples with P-MORB affinities, which display LREE and LILE enrichment and no depletion of HREE. Figure 4.3.5b (Section 4.3) shows the variation of Ta and Th with respect to Yb. This diagram is significant as it shows that the composition of the TCB basalts reflects different petrogenetic histories including differing influences of the subduction zone and possibly differing source compositions, between the arc basalts and the back arc basalts. Secondly, this diagram clearly shows distinctly different sources for the ophiolitic basalts found in New Zealand and in New Caledonia.

In general it is likely that the formation of all of the Poya basalts is the result of extensional magmatism with a very minor subduction zone influence (Cluzel *et al.*, 1994;1995;1997). It has been argued that the PTB were produced during the break-up stage of the development of a small ocean basin (Eissen *et al.*, 1998) in which case the BAB signatures might be explained by the assimilation of pre-existing arc material rather than being indicative of active arc volcanism. In

contrast the Tangihua Complex was formed in a complex tectonic setting involving the evolution from a juvenile subduction system to a back-arc or marginal basin spreading centre.

The results of this work confirm that there are considerable similarities between the ophiolite formation, during the Late Cretaceous, and emplacement, during the Eocene, in both New Zealand and New Caledonia. However, the specific details of formation and emplacement are quite different and are reflected in the different chemistries. However, the presence of these two systems, within the Southwest Pacific supports the presence of a large scale tectonic regime of rifting, convergence and consequent eastward subduction in the region during the Late Cretaceous and Early Palaeocene.

SECTION 7.4

Other Cretaceous Igneous Rocks of Northland, New Zealand

SIMPLIFIED BACKGROUND STRATIGRAPHY – NORTHLAND, NEW ZEALAND

Throughout the Northland Peninsula the basement rocks consist of indurated Permian-Jurassic sediments and minor volcanics of the Murihiku and Waipapa terranes (Spörli and Ballance, 1985). The basement is overlain by the insitu Early Cretaceous (?) basalts, pyroclastic flows and sediments of the Houhora Complex, which, in turn, are unconformably overlain by a Late Cretaceous transgressive sequence (Whatuwhiwhi Formation, Waiari Formation; Hayward *et al.*, 1989). In western Northland early Late Cretaceous shallow marine sediments and overlying Palaeocene-early Eocene sandstones are also present.

During a southeast-directed marine transgression, mid-Eocene – Oligocene terrestrial and marine sediments (Te Kuiti Group) were deposited. These units are overlain in the north and east of the Northland Peninsula by sequences of limestone, conglomerate, sandstone and mudstone of the Akarana Supergroup which records rapid subsidence from shelf to bathyal depths during the earliest Miocene (Brook *et al.*, 1988). During the Oligocene the Northland Allochthon was emplaced from a generally northeast direction. The Northland Allochthon includes the predominately mafic volcanic rocks of the Tangihua Complex and the highly deformed early Cretaceous flysch (Tupou Complex) unconformably overlain by Late Cretaceous – early Eocene flysch, limestone and mudstone (Mangakahia Group) and middle Eocene – Oligocene mudstones, sandstones and limestones of the Motatau Complex (Hayward *et al.*, 1989).

IGNEOUS ROCKS WITHIN THE TANGIHUA COMPLEX

The Tangihua Complex, although dominantly composed of basaltic lavas, contains two additional volcanic lava types: calc-alkaline to alkaline basalts and intrusions ranging from plagiogranites through gabbros. The alkaline basalts occur throughout the Tangihua Complex as intrusions and are generally thought to be younger than the Tangihua Complex basalts, although, the exact nature of their relationship is unclear (Hughes, 1966; Briggs, 1969; Larsen, 1987; Thompson *et al.*, 1997). Although these lavas are referred to as 'alkaline' they plot in a variety of compositional fields which range from calc-alkaline to alkaline and from OIB to IAB (Thompson *et al.*, 1997; Chapter 4). It should be noted that the samples, which are more 'alkaline' and OIB, also have the highest LOI (up to 4.66 wt.%; Thompson *et al*, 1997). The samples analysed as part of

this study show no signs of alteration and are calc-alkaline arc basalts in nature, hence from here on the 'alkaline' intrusives will simply be referred to as 'younger' intrusions despite possible complications with their age. As it has been shown that K and Ca have been mobile within the Tangihua Complex it is possible that these samples are not truly alkaline in nature but rather slightly altered calc-alkaline lavas. Despite the possible alteration of some samples, the chondrite and MORB normalised trace element plots all show similar trends.

These younger intrusions are medium to course grained with large hornblende and titanaugite crystals and small (<1mm) interstitial plagioclase. They have Nb contents approximately twice those of the MORB-like suite and show enrichment of incompatible elements. They are generally enriched in both the LREE and LILE relative to the Tangihua basalts (Figure 7.1.4a). Previous workers have proposed that the alkaline volcanics represent small amounts of melting of enriched mantle material which has been dragged down into the mantle by the subducting slab (Thompson *et al.*, 1997). This material was then erupted close to or within the developing back-arc basin region and, in this instance, contains distinct subduction zone signatures. However, the necessity of an 'enriched' source for the younger intrusions should be questioned. The HFSE systematics on a MORB normalised plot shows that the source of the younger intrusions needs not be enriched (Figure 7.1.4) or only slightly enriched relative to the Tangihua arc/back-arc basalts. Given the chondrite and MORB normalised patterns for the younger intrusions it is possible that they have a similar source. The major difference between the two being the LILE and the LREE, which are indicative of a greater slab input in the younger intrusions. Isotopically the intrusions have consistently lower εNd values and higher $^{87}Sr/^{86}Sr$ than the Tangihua basalts, which further supports a greater slab component.

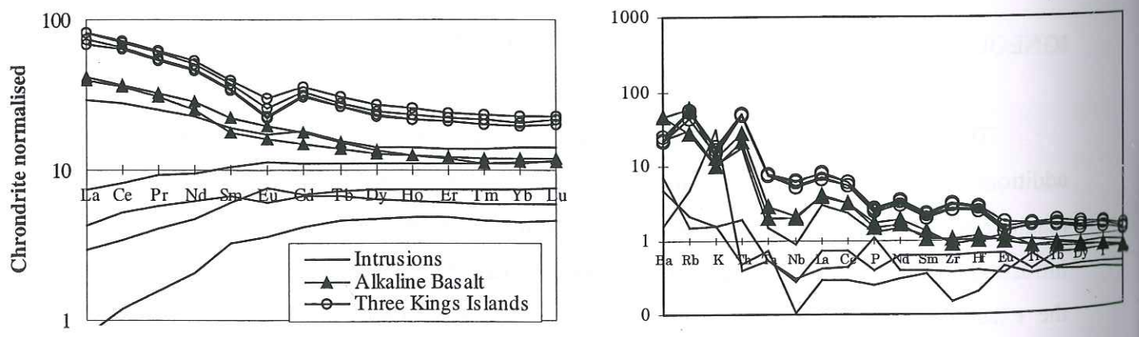

Figure 7.4.1: (a) Chondrite and MORB normalised trace element plots for the calc-alkaline basalts, intrusions and the Three Kings Islands basalts. (b) MORB normalised trace element plots for the calc-alkaline basalts, intrusions and the Three Kings Islands basalts.

Primary features in the plutonic units within the Tangihua Complex vary significantly. Grain size varies from fine (< 1mm) to very course (>15mm) with rare individual crystals reaching 30mm, however, the average grain size is fine (<1mm). Several units also exhibit well developed layering of both felsic and mafic minerals. As with the Tangihua basalts, clinopyroxene and plagioclase dominate the primary mineral assemblages with lesser amounts of iron oxides, orthopyroxene, hornblende and rare olivine. The Tangihua Complex also includes intrusive units, which again vary significantly. Both sills and dykes are aphyric to moderately porphyritic and range from quartz-diorite and microgabbro in composition. Plagioclase is the dominant phenocryst phase with lesser amounts of hornblende, clinopyroxene, iron oxides, olivine and rare quartz. The intrusions generally have a lack of orthopyroxene and a higher proportion of hornblende and olivine than the Tangihua basalts.

Geochemically the intrusions and the plutonics are very similar. They are dominantly tholeiitic in composition and fall into the low-K series. The more mafic end-members have high Mg#s (Figure 7.1.5), Ni, Cr and low REE contents. However, their chondrite and MORB normalised trace element plots are remarkably similar to those of the Tangihua basalts (Figure 7.1.4b). Given their overall chemistries and the shape of their normalised trace element plots it is apparent that the plutonic rocks are related to the Tangihua basalts. It is possible to model, using PFC from the more mafic plutonic lavas through to the Tangihua basaltic lavas using up to 60% fractionation of predominately plagioclase and pyroxene. Hence they appear to be more evolved members of the Tangihua Complex lavas series. Many of the other plutonic and intrusive chemistries can be explained by either fractional crystallisation or mineral cumulation. However, in some instances, such as plagiogranites, interpretation of the processes is hindered by the high degree of weathering.

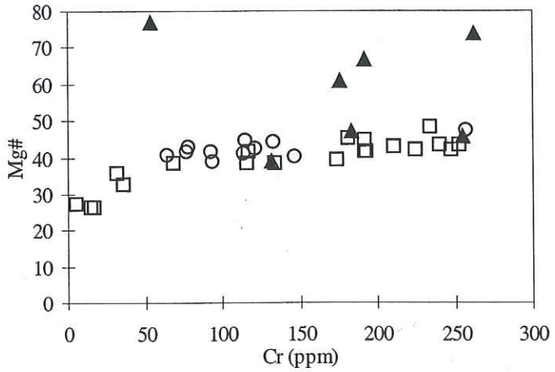

Figure 7.4.2: Mg# versus Cr for the Tangihua basalts, younger intrusions and plutonics.

THE HOUHORA COMPLEX

The Houhora Complex is small suite of pre-100Ma, probably Cretaceous, volcanic-hypabyssal igneous rocks and partially reworked submarine volcaniclastics (Isaac *et al.*, 1994; Mortimer *et al.*, 1998). This complex includes the volcanics rocks found at Mt Camel and the Three Kings Islands (Isaac, 1996). Volcanic rocks include a wide spectrum of compositions from weakly porphyritic basalt and andesite to dacite and rhyolite. As in the Tangihua Complex, pillow basalts are common. Throughout the complex rocks are sericitised and prehnite is common.

The lavas belong to the low-K series and generally have low Mg#s, <40. However, the Houhora Complex basalts are distinctly different from the Tangihua Complex basalts. They have higher Nb/Y and Ti/V ratios and appear to be characteristic of intraplate basalts. Isotopically the Houhora basalts have consistently lower εNd values and higher $^{87}Sr/^{86}Sr$ than the Tangihua basalts (Figure 7.4.3; Mortimer *et al.*, 1998).

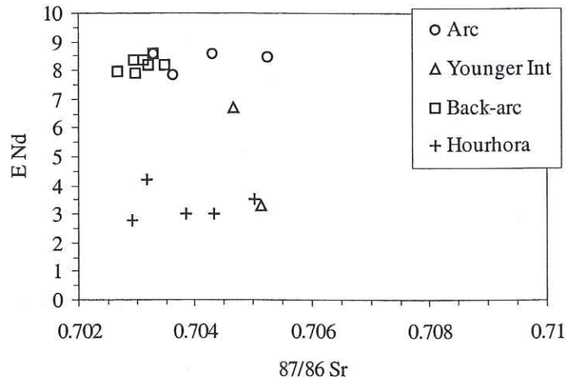

Figure 7.4.3: $^{87}Sr/^{86}Sr$ versus εNd for the Tangihua Complex basalts, the younger intrusions and the Houhora basalts. Values for the Houhora basalts are form Mortimer *et al.* (1998).

Chondrite and MORB normalised trace element plots for four samples from the Three Kings Islands, Houhora Complex, are given in Figure 7.4.1. The Three Kings Islands samples are remarkably similar to the contemporaneous younger intrusions of the Tangihua Complex (also seen in Figure 7.4.3) which previous workers have attributed to generation from a more enriched source. It is also interesting to note that both the younger intrusions and Houhora lavas have similar HFSE ratios which suggests generation from a similarly enriched source effected by differing amounts of partial melting and/or slab input. Generation from a similar source is likely given their relative proximity in the SW Pacific region. Further explanations for these similarities and possibly

discrepancies are beyond the scope of this thesis, however, future work should include age accurate age dating of both systems as they may be related.

SECTION 7.5

Summary

The basaltic lavas from the Tangihua Complex share many of the same geochemical and petrological characteristics as other arc/back-arc systems in the SW Pacific region. Although there is no one arc or back-arc system with which the Tangihua Complex is identical, the overall characteristics are similar. Minor geochemical differences are likely due to the age, thickness and nature of the subducting slab. The Tangihua basalts are also very similar to, and therefore probably related to, intrusive and plutonic rocks within the Tangihua Complex. These intrusions can be related by varying degrees of fractionation and/or mineral cumulation. Younger (calc-alkaline) intrusions within the Tangihua Complex bear a questionable relationship to the basaltic lavas. These intrusions have a higher slab component than the Tangihua basalts, however, both units may have been generated from a similar source. The younger intrusions are also very similar in nature to the lavas from the Three Kings Islands, which are part of the Houhora Complex. Although the age of the Houhora Complex is uncertain it appears as if there may be a relationship between these lavas and the younger intrusions, which in turn suggests a relationship with the Tangihua Complex.

Comparison of the petrography, alteration, metamorphism and geochemistry has shown that the lavas of the Tangihua Complex and the Poya terrane are very different. They formed in a different tectonic environment and have a different postformation history. Hence, although the regional tectonic regime was similar in both New Zealand and New Caledonia during the late Cretaceous the specific settings in which the two complexes were generated were different.

CHAPTER EIGHT: CONCLUSIONS

CHAPTER 8

Conclusions

This study of the Tangihua Complex has raised as many questions as have been answered. The geochemical analyses from this study have led to a new model to explain the generation of the ophiolite, which in turn has required a new interpretation of the tectonic setting of New Zealand during the Cretaceous, which better fits what we know of the tectonic history of New Zealand. The following is a summary of the findings of this thesis.

PETROGRAPHY

The basaltic rocks within the Tangihua Complex are generally porphyritic with a cryptocrystalline - microcrystalline groundmass. Glass is also present as are courser grained intrusive equivalents. The primary phenocryst assemblage is dominated by plagioclase with lesser amounts of clinopyroxene, orthopyroxene and magnetite while olivine, biotite and hornblende are rare. The groundmass mineral assemblage is dominated plagioclase and clinopyroxene with lesser amounts of orthopyroxene and magnetite. Groundmass phases are generally cryptocrystalline. The Tangihua Complex is unusual in terms of a 'typical' ophiolite in that it contains fresh glass. The presence of orthopyroxene should also be noted as unusual.

MINERAL CHEMISTRY

The majority of the plagioclase phenocrysts have compositions in the range of An_{66-87} with an average of An_{74}. Rim and groundmass compositions are slightly more sodic, averaging An_{60} and An_{63} respectively, possibly reflecting minor alteration. The composition of the clinopyroxene varies widely with a range of $En_{31-52}Fs_{10-33}Wo_{28-45}$. Phenocrysts cores have an average composition of $En_{47}Fs_{15}Wo_{38}$, rim compositions of $En_{42}Fs_{20}Wo_{38}$ and groundmass compositions of $En_{44}Fs_{16}Wo_{40}$. Mg#s fall between 34 and 73 with an average of 61, 56 and 52 for core, rim and groundmass compositions respectively. The average orthopyroxene composition is $En_{58}Fs_{38}Wo_4$ with Mg# = 46, and the average composition of olivine is Fo_{76}, with Mg#s ranging from 38 to 77 with an average of 65.

The TiO_2 of clinopyroxene phenocrysts are comparable to MORB whereas the lower values are characteristic of arc systems. The Ti:Al ratio in the clinopyroxene phenocrysts is approximately

1:5 indicating crystallisation at pressures of approximately 1atm. The geothermometer of Lindsley (1983) yielded an average temperature of approximately 1068°C ± 80°C.

ALTERATION AND METAMORPHISM

Characteristically, the majority of the Tangihua massifs contain low-temperature hydrothermal/diagenetic minerals although some of the massifs exhibit mineral assemblages characteristic of later, high temperature contact metamorphism. The low-temperature alteration assemblage can be divided into three main phases based primarily on temperature but also influenced by the water/rock ratios: an initial phase of Na-rich zeolite precipitation, followed by a transitional cooling phase, characterised by K-, Na- and Ca-rich zeolites, and finally, at <50°C. a period of K- and Ca-dominated mineralisation.

The alteration patterns in the Tangihua Complex suggests that little or no tectonic activity occurred between the formation and obduction of the ophiolite, enabling a classic, low temperature, seafloor alteration sequence to develop in a manner similar to that at other systems. The alteration mineral assemblages also indicate that the obduction event itself was cold as the vein mineral assemblage associated with obduction primarily contains Ca-bearing phases, suggesting temperatures of less than <50°C, and at low pressures as there are no overprinting by either high temperature or high pressure phases.

GEOCHEMISTRY

The basaltic lavas of the Tangihua Complex are relatively homogeneous and are dominantly tholeiitic basalts with lesser calc-alkaline and minor alkaline affinities. They are subalkaline, low-K series lavas which contain normative hypersthene, plagioclase and diopside.

Some of the lavas present have distinctive enriched LILE and LREE contents, characteristic of arc lavas whereas the back-arc lavas have more subdued arc-like signatures. The arc lavas appear to have a more calc-alkaline trend whereas the back-arc lavas are tholeiitic. Most of the lavas have Mg#<45. They exhibit a range in REE-contents. The arc lavas are the most depleted with between 8 and 20 times chondrite and the back-arc are less depleted with REE contents between 10 and 40 times chondrite. Both the arc and the back-arc chondrite normalised REE patterns are light REE depleted with many of the more evolved samples showing a Eu anomaly. The lavas show a large degree of scatter, but an overall enrichment, in LILE elements relative to MORB. The HFSE contents level out and are very close to MORB for the arc lavas but slightly

enriched for the back-arc lavas. All lavas show a negative Nb anomaly, which is strongly developed in the arc samples.

The trace element contents and $^{87}Sr/^{86}Sr$ and $^{143}Nd/^{144}Nd$ ratios are typical of other arc and back-arc systems found within the SW Pacific. Hence emphasising the point that the Tangihua Complex should be considered an ancient arc/back-arc system that has been obducted, and not simply as an ophiolite.

PETROGENESIS

The complex nature of the chemistry, in particular those lavas with transitional arc signatures, and the presence of non-arc lavas, is clear evidence that these volcanics formed in a suprasubduction zone environment. The combined geochemistry and tectonic constraints suggest that the Tangihua Complex formed either in a transitional zone between an arc and a back-arc setting, or in a zone of migration from arc to back-arc volcanism. The general depletion of Nb and the HFSE suggests derivation from a depleted mantle source, which is consistent with mantle wedge depletion by an earlier rifting episode. The arc lavas are marginally more depleted than the back-arc lavas. Geochemical modelling shows the back-arc lavas have undergone approximately 35% perfect fractional crystallisation (PFC) and the arc lavas have undergone approximately 30% PFC. Chemistries intermediate between the arc and back arc can be modelled by 30-50% simple mixing of the arc lavas with the back-arc lavas. High LILE/HFSE and LILE/LREE ratios suggest LILE enrichment by a slab-related aqueous fluid and possibly small amounts of a slab-derived silicic melt.

AGE

New Ar/Ar age dates from the Tangihua Complex help to confirm that the age of formation of the complex was ≈100Ma. More conclusively, the dates point to a major episode of alteration at ≈30Ma, which most likely corresponds to the age of emplacement of the Northland Allochthon. Finally, three of the samples showed evidence of older ages, possibly Palaeozoic. These older ages may be due to alteration, however the age corresponds to the age of the basement. It is possible that these samples were part of the basement assemblage that was obducted along with the allochthon. This later solution is unlikely due to the similarity of the chemistry of these 'older' samples to the remainder of the Tangihua Complex.

COMPARISONS

The lavas of the Tangihua Complex are similar in geochemical characteristics to most other SW Pacific arc and back-arc systems. The general enrichment of LILE and LREE relative to MORB and the depletion of specific elements, such as Nb, are indicative of magmas generated in or near a subduction zone. On a more specific level, the Tangihua lavas tend to have higher TiO_2 values which may be the result of small source heterogeneities.

The Poya terrane ophiolite of New Caledonia is geographically the closest ophiolite complex of a similar age to the Tangihua Complex. Despite many similarities between the two systems, close inspection of the alteration and geochemistry show that they are unrelated. However, it should be noted that the Tangihua Complex and the Poya terrane were most likely generated by the same regional tectonic regime.

The Tangihua Complex contains alkaline and intrusive magmas, which are also allochthonous. Of these lavas, many of the intrusives appear to be related geochemically to the Tangihua Complex. Ophiolites commonly contain intrusive and/or plutonic rocks. Some of the more alkaline lavas, however, have a less certain relationship with the Tangihua lavas. These lavas appear to be very similar to the Houhora Complex. It is possible that these lavas could be related, having experienced higher slab input and fractionation.

TECTONIC IMPLICATION

The Late Cretaceous break-up of the eastern and southern Gondwana margin signalled the beginning of a period of successive opening and closing of marginal basins that isolated continental, oceanic or intermediate ridges throughout the Southwest Pacific. During this time the eastern margin of New Zealand was a convergent margin. Subduction beneath the New Zealand sector of Gondwana ceased in the early Late Cretaceous with the approach and incipient collision of the spreading ridge between the Phoenix and Pacific plates. The Phoenix plate was quite small and rather than continuing to subduct, it was captured by the Pacific plate. Plate capture led to the initiation of rifting between the newly formed Phoenix-Pacific plate and West Antarctica (Luyenduk, 1995). It is proposed here, that the stalling of the Phoenix-Pacific ridge and associated subduction system, in combination with the initiation of rifting in the Tasman Sea, resulted in the partial subduction and dehydration of portions of the Phoenix Plate, which then reacted with the previously depleted mantle wedge. Remnants of the ensuing volcanism include the obducted Tangihua Complex of Northland. As subduction was short lived, due to a rapid change to an extensional environment, a mature arc system, such as Tonga-Kermadec, was never developed.

In conclusion, this thesis has shown that the Tangihua Complex of Northland New Zealand is a mixture of arc and back-arc lavas, which formed in a complex tectonic environment. The complex is unusual for many reasons. Firstly, it is not what could be described as a 'typical' ophiolite. Secondly, the complex contains abundant fresh glass, which is exceptional in a >80Ma system that has been obducted. Finally, the Tangihua Complex it is the first ophiolite documented to contain both arc and back-arc chemistries. Because the complex has been obducted, there is reasonable access to both the arc and back-arc lavas, which has allowed the first detailed study of such an unusual system.

RECOMMENDATIONS FOR FUTURE WORK

There are still many aspects of the Tangihua Complex which remain unknown. A programme of future work should include a synthesis of the previous structural studies, such as old MSc theses, on the complex and associated sedimentary material in hopes of gaining insight into the obduction processes. Further geophysical work would also help to determine the nature of obduction and the relationship between the complex and the basement material.

Although, this study has provided 7 new Ar/Ar ages, the complex is lacking in accurate dates, which may help solve questions as to the direction of the subduction system and the age of obduction. Accurate knowledge of the age of the complex would also allow further constraints on the tectonic history and a possible links to New Caledonia.

Finally no future work programme should be completed without further investigation into the younger intrusive material and the possible relationship with the Houhora Complex about which so little is known. One particular question that needs to be resolved is whether the lavas of the Houhora Complex are genetically related to the Tangihua Complex.

REFERENCES

REFERENCES

Aggrey, K.E., Muenow, M.R. and Sinton, J.M., 1988, Volatile abundances in submarine glasses from the North Fiji and Lau back-arc basins, *Geochimica et Cosmochimica Acta* 52: 555-566.

Aitchison, J. C., Clarke, G. L., Meffre, S. and Cluzel, D., 1995, Eocene arc-continent collision in New Caledonia and implications for regional southwest Pacific tectonic evolution, *Geology* 23: 161-164.

Aitchison, J. C., Cluzel, D. and Meffre, S., 1995b, Cretaceous/Tertiary Radiolarians from New Caledonia, *Geological Society of New Zealand Misc. Publications* 81A, 1-70.

Aitchison, J.C., Ireland, T.R., Clarke, G.L., Cluzel, D., Davis, A.M. and Meffre, S., 1999, Regional implications of U/Pb SHRIMP age constraints on the tectonic evolution of New Caledonia, *Tectonophysics* 299: 333-343.

Alabaster,T., Pearce, J.A. and Malpas, J., 1982, The volcanic stratigraphy and petrogenesis of the Oman ophiolite complex, *Contributions to Mineralogy and Petrology* 81: 168-183.

Alt, J. C., Teagle, D.A.H., Brewer, T., Shanks, W.C. and Halliday, A., 1998, Alteration and mineralisation of an oceanic forearc and the ophiolite-ocean crust analogy, *Journal of Geophysical Research* 103: 12,365-12,380.

Alt, J.C., 1994, A sulfur isotopic profile through the Troodos Ophiolite, Cyprus: Primary composition and the effects of seawater hydrothermal alteration, *Geochimica et Cosmochimica Acta* 58: 1825-1840.

Alt, J.C., 1995, Subseafloor processes in mid-ocean ridge hydrothermal systems, *In*: Humphris, S., et al. (eds.), Seafloor Hydrothermal Systems: Physical, Chemical, Biological and Geological Interactions, Geophysical Monograph Series 91: 85-114.

Alt, J.C., Teagle, D.A.H., Bach, W., Halliday, A.N. and Erzinger, J., 1996, Stable and strontium isotopic profiles through hydrothermally altered upper oceanic crust, ODP Hole 504B, *Proc. Ocean Drilling Program Scientific Results* 148: 47-70.

Arculus, R. J., 1987, The significance of source versus process in the tectonic controls of magma genesis, *Journal of Volcanology and Geothermal Research* 32: 1-12.

Arden, B.G., 1988, Petrology of the Maungapohatu Massif, Northland, New Zealand. Unpublished MSc Thesis, University of Auckland.

Avias, J. and Coudray, J., 1975, Sur la nature et l'origine des «épanchements volcano-sédimentaries paléogènes» de la Nouvelle-Calédonie, *C. R. Acad. Sci.* 280: 545-546.

Avias, J., 1953, Contribution à l'étude stratigraphique et paléontologique des formations antécrétacées de la Nouvelle-Calédonie centrale, *Sci. Terre* 1:1-276.

Baker, D.F., 1979, Geology and geochemistry of an alkali volcanic suite (Skinner Cove Formation) in the Humber Arm Allochthon, Newfoundland, Unpublished MSc. thesis, Memorial University

Ballance, P.F. and Spörli, K.B., 1979, Northland Allochthon, *Journal of the Royal Society of New Zealand* 9: 259-275.

Ballance, P.F., 1993, The paleo-Pacific, post-subduction, passive margin thermal relaxation sequence (Late Cretaceous – Paleogene) of the drifting New Zealand continent, *In*: Ballance, P.F. (ed.), Sedimentary Basins of the World, 2: South Pacific Sedimentary Basins, Elsvier, Netherlands, 93-107.

Banfield, J. F. and Eggleton, R. A., 1989, Apatite replacement and rare earth mobilisation, fractionation and fixation during weathering. *Clays and Clay Minerals* 37: 113-127.

Barrat, J.A., Keller, F., Amossé, J., Taylor, R.N., Nesbitt, R.W. and Hirata, J., Determination of rare earth elements in sixteen silicate samples by ICP-MS after Tm addition and Im exchange separation, *Geostand. Newsletter* 20: 133-139.

Bartels, K.S., Kinzler, R.J. and Grove, T.L., 1991, High pressure phase relations of primitive high-alumina basalts from Medicine Lake volcano, northern California, *Contributions to Mineralogy and Petrology*, 108: 253-270.

Barton, M., Miller, C.A. and Fleming, T.H., 1992, Pre-eruptive water contents of arc magmas and continental tholeiites: implications for the role of subduction in magma genesis, *Transactions of the American Geophysical Union*, 73: 352.

Bednarz, U. and Schmincke, H.-U. 1989. Mass transfer during sub-seafloor alteration of the upper Troodos crust (Cyprus). *Contributions to Mineralogy and Petrology* 102: 93-101.

Ben Othman, D., White, W.M. and Patchett, J., 1989, The geochemistry of marine sediments, island arc magma genesis, and crust-mantle recycling, *Earth and Planetary Science Letters* 94: 1-21.

Bennett, M. C., 1976, The ultra-mafic complex at North Cape, northernmost New Zealand. *Geological Magazine* 113: 61-76.

Bickle, M.J. and Teagle, D.A.H., 1992, Strontium alteration in the Troodos Ophiolite: Implications for fluid fluxes and geochemical transport in mid-ocean ridge hydrothermal systems, *Earth and Planetary Science Letters* 113: 219-237.

Bird, D.K., Schiffman, P., Elders, W.A., Williams, A.E. and McDowell, S.D., 1984, Calc-silicate mineralisation in active geothermal systems, *Economic Geology* 79: 186-226.

Bischoff, J.L. and Dickson, F.W. 1975. Seawater-basalt interaction at 200°C and 500 bars: implications for origin of sea-floor heavy metal deposits and regulation of seawater chemistry. *Earth and Planetary Science Letters* 25: 385-397.

Black, P. M. and Brothers, R.N., 1977, Blueschist ophiolites in the mélange zone, northern New Caledonia, *Contributions to Mineralogy and Petrology* 65: 69-78.

Black, P. M., 1989, Hydrothermal metamorphism in Tangihua Volcanics, Northland, New Zealand: a review and synthesis, *In*: Geology of Northland: accretion, allochthons and arcs at the edge of the New Zealand micro-continent, eds.: Spörli, K. B. and Kear, D., *Royal Society of New Zealand Bulletin* 26.

Blake, M. C., Brothers, R. N. and Lanphere, M. A., 1977, Radiometric ages of blueschists in New Caledonia, International Symposium Geodynamics South-west Pacific, Nouméa, 1976, Technip Editions, Paris, 279-281.

Bloomer, S.H., Ewart, A., Hergt, J.M. and Bryan, W.B., 1994, Geochemistry and origin of igneous rocks from the outer Tonga forearc (Site 841), *In*: Hawkins, J.W., Parson, L.M. and Allan, J.F. (eds.), *Proceedings of the Ocean Drilling Program, Scientific Results, 135: 625-646.*

Bonatti, E. and Michael, P.J., 1989, Mantle peridotites from continental rifts to ocean basins to subduction zones, *Earth and Planetary Science Letters,* 91: 297-311.

Bowers, T.S., Campbell, A.C., Measures, C.I., Spivack, A., Khadem, M. and Edmond, J.M. 1988. Chemical controls on the composition of vent fluids at 13°-11°N and 21°N, East Pacific Rise. *Journal of Geophysical Research* 93: 4522-4536.

Bradshaw, J.D., 1989, Cretaceous geotectonic patterns in the New Zealand region, *Teconics*, 8, 803-820.

Brenan, J.M., Shaw, H.F., Phinney, D.L. and Ryerson, F.J., 1995, Mineral-aqueous fluid partitioning of trace elements at 900°C and 2.0GPa: constraints on the trace element chemistry of mantle and deep crustal fluids, *Geochimica et Cosmochimica Acta* 59: 3331-3350.

Briggs, R.M., 1969, Igneous geology of the Opouteke-Pakotai area, Northland. Unpublished MSc Thesis, University of Auckland.

Briqueu, L., Bougault, H. and Joron, J.L., 1984, Qualifications of Nb, Ta, Ti and V anomalies in magma associated with subduction zones: petrogentic implications. *Earth and Planetary Science Letters,* 68: 297-308.

Brook, F. J., Isaac, M. J. and Hayward, B. W, 1988, Geology of autochthonous and allochthonous strata in the Omahura area, northern New Zealand, *New Zealand Geological Survey record* 32.

Brothers, R. N. and Blake, M. C., 1972, Tertiary plate tectonics and high-pressure metamorphic in New Caledonia, *Tectonophysics* 17: 359-391.

Brothers, R. N. and Delaloye, M., 1982, Obducted ophiolites of North Island, New Zealand: origin, age, emplacement and tectonic implications for Tertiary and Quaternary volcanism, *New Zealand Journal of Geology and Geophysics* 25: 257-274.

Brothers, R. N., 1974, Kaikoura Orogeny in Northland, New Zealand, *New Zealand Journal of Geology and Geophysics*, 17: 1-18.

Brothers, R. N., 1983; Tertiary accretion of ophiolite seamounts, North Island, New Zealand. *In:* Hashimoto, M. and Uyeda, S. (eds.), Accretion tectonics in the circum-Pacific region, Tokyo, Terrapub.: 307-318.

Brothers, R.N. and Lillie, A.R., 1985, Regional Geology of New Caledonia, *In*: Nairn, A.E.M., Stehli, F.G. and Uyeda, S. (eds.), The Ocean Basins and Margins, Volume 7b, Plenium Press, New York and London.

Byran, W.B., 1972, Morphology of quench crystals in submarine basalts, *Journal of Geophysical Research* 77: 5812-5818.

Cabanis, B. and Lecolle, M., 1989, Le diamramme La/10-Y/15-Nb/8: un outil pour la discrimination des séries volcanique et la mise en évidence des processus de mélange et/ou de contamination crustale, *C.R. Acad. Sci. Ser. II* 309: 2023-2029.

Cameron, W. E., 1989, Contrasting boninite-tholeiite associations from New Caledonia, *In*: Crawford, A. J. (ed.), Boninites, Unwin Hyman, London.

Campbell A.C., Bowers, T.S., Measures, C.I., Falkner, K., Khadem, M. and Edmond, J.M. 1988. A time series of various fluid composition from 21°N East Pacific Rise (1979, 1981, 1986) and the Guyamas basin, gulf of California (1982, 1985). *Journal of Geophysical Research* 93: 4537-4549.

Cassidy, J. and Locke, C. A., 1987, Thin ophiolites of North Island, New Zealand, *Tectonophysics,* 139: 315-319.

Cassidy, J., 1993, Tectonic implications of paleomagnetic data from the Northland ophiolite, New Zealand. *Tectonophysics*, 223: 199-211.

Cawood, P.A., 1991, Processes of ophiolite emplacement in Oman and Newfoundland, *In*: Peters, T. et al. (eds.), Ophiolite genesis and evolution of the oceanic lithosphere, Oman Ministry of Petroleum and Minerals, 501-516.

Cluzel, D., Aitchison, J., Clarke, G., Meffre, S. and Picard, C., 1995, Dénudation tectonique du complexe à nayau métamorphique de haute pression d'âge tertiaire (Nord de la Nouvelle-Calédonie, Pacifique, France), *C. R. Acad. Sci. Paris, Séries IIa,* 321: 57-64.

Cluzel, D., Aitchison, J., Clarke, G., Meffre, S. and Picard, C., 1994, Point de vue sur l'évolution tectonique et géodynamique de la Nouvelle-Calédonie, *C. R. Acad. Sci. Paris, Séries II,* 319: 683-690.

Cluzel, D., Aitchison, J.C., Black, P.M. and Picard, C., 1999, Origin and fate of Southwest Pacific marginal basins; an appraisal from New Caledonia,), *In*: Baldwin, L. and Lister, G.S. (eds.) Penrose Conference Abstract Volume, pp. 77-79.

Cluzel, D., Picard, C., Aitchison, J. C., Laporte, C., Meffre, S. and Parat, F., 1997, La nappe de Poya (ex-formation des Basalts) de Nouvelle-Calédonie (Pacific Sud-Ouest): un plateau océanique Campanien-Paléocène supérier obducté à l'Éocène supérieur, *C. R. Acad. Sci. Paris, Séries IIa,* 324: 443-451.

Coleman, R.G., 1984, The diversity of ophiolites, *Geol. Mijnbouw* 63: 141-150.

Collot, J. Y., Rigolot, P and Missègue, F., 1988, Geologic structure of the northern New Caledonia Ridge, as inferred from magnetic and gravity anomalies, *Tectonics* 7: 991-1013.

Conrad, WK. and Kay, R.W., 1984, Ultramafic and mafic inclusions from Adak Island: crystallisation history, and implications for the nature of primary magmas and crustal evolution in the Aleutian arc, *Journal of Petrology* 25: 88-125.

Crawford, A.J., Beccaluva, L. and Serri, G., 1981, Tectono-magmatic evolution of the west Philippine - Mariana region and the origin of boninites. *Earth and Planetary Science Letters*, 54: 346-356.

Crawford, A.J., Falloon, T.J. and Green, D.H., 1989, Classification, petrogenesis and tectonic setting of boninites, *In*: Crawford, A.J. (ed.), Boninites, Unwin Hyman, Boston, Mass.: 1-48.

Danyushevsky, L.V., Falloon, T.J., Sobolev, A.V., Crawford, A.J., Carroll, M. and Price, R.C., 1993, The H2O content of basalt glasses from Southwest Pacific back-arc basins, *Earth and Planetary Science Letters* 117: 347-362.

Davidson, J.P., 1987, Crustal contamination vs. subduction zone enrichment: Examples from the Lesser Antillies and implications for mantle source compositions of island arc volcanic rocks, *Geochimica et Cosmochimica Acta* 51: 2185-2198.

Davies, H. L., 1968, Papuan Ultramafic Belt, 23rd International Geological Congress, Section 1, p. 209-220.

Davis, B.T.C. and Boyd, F.R., 1966, The join $Mg_2Si_2O_6$ – $CaMgSi_2O_6$ at 30kilobars pressure and its application to pyroxenes from kimberlites, *Journal of Geophysical Reseach* 71:3567-3576.

Dupuy, C., Dostal, J. and Leblanc, M., 1981, Geochemistry of an ophiolitic complex from New Caledonia, *Contributions to Mineralogy and Petrology* 76: 77-83.

Edmonds J.M., Measures, C., McDuff, R.E., Chan, L., Collier, R., Grant, B., Gordon, L.I. and Corliss, J. 1979a. Ridge crest hydrothermal activity and the balances of the major and minor elements in the ocean: The Galapagos data, *Earth and Planetary Science Letters* 46:1-18.

Edmonds, J.M., Measures, C., Mangum, B., Grant, B., Sclater, F.R., Collier, R., Hudson, A., Gordon, L.I. and Corliss, J. 1979b. On the formation of metal-rich deposits at ridge crests. *Earth and Planetary Science Letters* 46:19-30.

Eissen, J.-P., Crawford, A.J., Cotton, J., Meffre, S., Bellon, H. and Delaune, M., 1998, Geochemistry and tectonic significance of basalts in the Poya terrane. New Caledonia, *Tectonophysics*, 284, 203-219.

Elliott, T., Plank, T., Zindler, A., White, W. and Bourdon, B., 1997, Element transport from slab to volcanic fromt at the Mariana arc, *Journal of geophysical Research* 102: 14991-15019.

Espirat, J.J., 1966, Carte géologique de la Nouvelle-Calédonie au 1/50 000 Feuille Bourail, Bureau de Recherches Géologiques et Minières, Orléans.

Evensen, N.M., Hamilton, P.J. and O'Nions, R.K., 1978, Rare earth element abundances in chrondrite meteorites. *Geochimica et Cosmochimica Acta* , 42: 1199-1212.

Ewart, A. and Bryan, W.B., 1973, The petrology and geochemistry of the Tangan islands, *In*: Coleman, P.J. (ed.), The Western Pacific: Island Arcs, Marginal Seas, Geochemistry, University of Western Australia Press, pp. 503-522.

Ewart, A., 1982, The mineralogy and petrology of Tertiary-Recent orogenic volcanic rocks: with special reference to the andesite-basaltic compositional range, *In*: Thorpe, R.S. (ed.) Andesites, Wiley, Chichester, pp. 25-95.

Falloon, T.J., Malahoff, A., Zonenshain, L.P., and Bogdanov, Y., 1992, Petrology and geochemistry of back-arc basin basalts from Lau Basin spreading ridges at 15, 18 and 19°S, *Mineral. Petrol.* 47: 1-35.

Farnell, E. J., 1973, Geology of the Cape Reinga area, Northland, Unpublished MSc Thesis, University of Auckland.

Fleming, C.A., 1970, The Mesozoic of New Zealand: Chapters in the history of the circum-Pacific mobile belt, *Q. J. Geological Society,* 125: 125-170.

Fleming, C.A., 1979, The Geological History of New Zealand and Its Life, Auckland University Press, Auckland.

Foder, R. V., Dobosi, G. and Bauer, G. R., 1992, Anomalously high rare-earth element abundances in Hawaiian lavas. *Analytical Chemistry* 64: 639-643.

Forsythe, L.M., Nielsen, R.L. and Fisk, M.R., 1994, High-field strength element partitioning between pyroxene and basaltic to dacitic magmas, *Chemical Geology* 117: 107-125.

Fortune, W. B., 1968, Igneous geology of the Mamaranui-Waihue area, Northland, Unpublished MSc Thesis, University of Auckland.

Furnes, H., Pedersen, R.B. and Albrektsen, B.A. 1992, Magma development of the Leka Ophiolite Complex, central Norwegian Caledonides, *Lithos* 27: 259-277.

Gaggero, L., Spadea, p., Cortesogno, L., Savelieva, G.N. and Pertsev, A.N., 1997, Geochemical investigations of the igneous rocks from the Nurali ophiolite mélange zone, Southern Urals, *Tectonophysics* 276: 139-161.

Gamble, J.A., Smith, I.E.M., Graham, I.J., Kokelaar, B.P., Cole, J.W., Houghton, B.F. and Wilson, C.J.N., 1990, The petrology, phase relations and tectonic setting of basalts from the Taupo Volcanic Zone, New Zealand and the Kermadec island arc – Havre trough, SW Pacific, *Journal of Volcanology and Geothermal Research* 54: 265-290.

Gamble, J.A., Wright, I.C., Woodhead, J.D. and McCulloch, M.T., 1995, Arc and back-arc geochemistry in the southern Kermadec arc-Ngatoro Basin and offshore Taupo Volcanic Zone, SW Pacific, *In*: Smellie, J.L (ed.), Volcanism Associated with Extension at Consuming Plate Margins, *Geological Society Special Publications No*. 81: 77-93.

Gass, I.G. and Smewing, J.D., 1973, Intrusions and metamorphism at constructive margins: evidence from the Troodos massif, *Nature* 242: 26-92.

Gill, J.B., 1981, Orogenic andesites and plate tectonics. Springer-Verlag, Berlin.

Gillis, K.M. and Robinson, P.T. 1988. Distribution of alteration zones in the upper oceanic crust. *Geology* 16: 262-266.

Gillis, K.M. and Robinson, P.T., 1990, Patterns and processes of alteration in the lavas and dikes of the Troodos Ophiolite, Cyprus, *Journal of Geophysical Research* 95: 21,523-21,548.

Gillis, K.M. and Thompson, G., 1993, Metabasalts from the Mid-Atlantic Ridge: New insights into hydrothermal systems in slow-spreading crust, *Contributions to Mineralogy and Petrology* 113: 502-523.

Gillis, K.M., 1995, Controls on hydrothermal alteraion in a section of fast spreading oceanic crust, *Earth and Planetary Science Letters* 134: 473-489.

Gonord, H., 1977, Recherches sur la géologie de la Nouvelle-Calédonie, sa place dans l'ensemble structural du Pacifique Sud-Ouest. Unpublished thesis, University of Toulouse.

Graham, C.M. and Harmon, R.S., 1983, Stable isotope evidence on the nature of crust-mantle interactions, *In*: Hawkesworth, C.J. and Norry, M.J, Shirva (eds.), Continental Basalts and Mantle Xenoliths, pp. 20-45.

Graham, I.J. and Hackett, W.R., 1987, Petrology of calc-alkaline lavas from Ruapehu Volcano and related vents, Taupo Volcanic Zone, New Zealand, *Journal of Petrology* 28: 531-567.

Graham, I.J., Cole, J.W., Briggs, R.M., Gamble, J.A. and Smith, I.E.M., 1995, Petrology and petrogenesis of volcanic rocks from the Taupo Volcanic Zone: a review, *Journal of Volcanology and Geothermal Research* 68: 59-87.

Green, T. H., 1978, Rare earth geochemistry of basalts from Norfolk Island, and implications for mantle heterogeneity in rare earth elements. *Geochemical Journal* 12: 165-172.

Green, T.H., Sie, S.H., Ryan, C.G. and Cousens, D.R., 1989, Proton microprobe-determined partitioning of Nb, Ta, Zr, sr and Y between garnet, clinopyroxene and basaltic magmas at high pressure and temperature, *Chemical Geology* 74: 201-216.

Grove, T.L. and Baker, M.B., 1984, Phase equilibrium controls on the tholeiitic versus calc-alkaline differentiation trends, *Journal of Geophysical Research*, 89: 3253-3274.

Guillon, J. H. and Gonord, H., 1972, Premières données radiométrique concordant les basalts de Nouvelle-Calédonie. Leurs relations avec les grands événements de l'histoire géologique de l'arc mélanésien interne au Cénozoïque, *C. R. Acad. Sci.* 275: 309-312.

Guy, C., Schott, J., Destrigneville, C. and Chiappini, R. 1992. Low-temperature alteration of basalt by interstitial seawater, Mururoa, French Polynesia. *Geochimica et Cosmochimica Acta* 56: 4169-4189.

Hamilton, W., 1979, Tectonics of the Indonesian Region, *USGS Professional Paper*, 1078.

Hamilton, W.B., 1995, Subduction systems and magmatism, *In*: Smellie, J.L (ed.), Volcanism Associated with Extension at Consuming Plate Margins, *Geological Society Special Publications No*. 81: 3-28.

Hannington, M.D., Jonasson, I.R., Herzig, P.M. and Petersen, S., 1995, Physical, chemical and microbial processes affecting sulfide deposition, *In*: Humphris, S., et al. (eds.), Seafloor Hydrothermal Systems: Physical, Chemical, Biological and Geological Interactions, Geophysical Monograph Series 91: 85-114.

Hanson, J. A., 1991, Mylonitic fabric in Tangihua Volcanics, Camp Bay, Northland, Unpublished MSc Thesis, University of Auckland.

Hawke, M.M., 1983, Mineralogy of some igneous rocks from the Kermadec Islands and Taupo Volcanic Zone, New Zealand, Unpublished PhD thesis, University of Auckland.

Hawkesworth, C.J., Gallagher, K., Hergt, J.M. and McDermott, F., 1993, mantle and slab contributions in arc magmas, *Annual Review, Earth and Planetary Science* 21: 175-204.

Hawkesworth, C.J., Hertg, J.M., Ellam, R.M. and McDermott, F., 1991, Element fluxes associated with subduction related magmatism, *Philosophical Transactions of the Royal Society of London* A335: 393-405.

Hawkesworth, C.J., O'Nions, R.K., Pankhurst, R.J., Hamilton, P.J. and Evensen, N.M., 1977, A geochemical study of island-arc and back-arc tholeiites from the Scotia Sea. *Earth and Planetary Science Letters*, 36: 253-262.

Hawkins, J.W. and Florendo, F., 1992, Supra-subduction zone magmatism: Implications for the origin of Philippine ophiolites, *Acta Geologica Taiwanica* 30: 163-171.

Hawkins, J.W., 1974, Geology of the Lau Basin, a marginal sea behind the Tonga Arc. *In*: Geology of Continental Margins,

Hay, R.F., 1960, The Geology of the Mangakahia Subdivision, *New Zealand Geological Survey Bulletin 61.*

Hayward, B. W., Brook, F. J. and Isaac, M. J., 1989, Cretaceous to middle Tertiary stratigraphy, paleogeography and tectonic history of Northland, New Zealand, *In*: .: Spörli, K. B. and Kear, D. (eds.), Geology of Northland: accretion, allochthons and arcs at the edge of the New Zealand micro-continent, *Royal Society of New Zealand Bulletin,* 26.

Hayward, B.W., 1993, The tempestuous 10 million year life of a double arc and intra-arc basin – New Zealand's Northland basin in the Early Miocene, *In*: Ballance, P.F. (ed.), Sedimentary Basins of the World, 2: South Pacific Sedimentary Basins, Elsvier, Netherlands: 113-139.

Herzer, R. H., Chaproniere, G.C.H., Edwards, A.R., Hollis, C.J., Pelletier, B., Raine, J.I., Scott, G.H., Stagpoole, V., Strong, C.P., Symonds, P., Wilson, G.J. and Zhu, H., 1997, Seismic stratigraphy and structural history of the Reinga Basin and its margins, southern Norfolk Ridge system, *New Zealand Journal of Geology and Geophysics*, 40: 425-451.

Hildreth, W. and Moorbath, S., 1988, Crustal contributions to arc magmatism in the Andes of central Chile, *Contributions to Mineralogy and Petrology* 98: 455-489.

Hochstaedter, A.G., Gill, J.B., Kusakabe, M., Newman, S., Pringle, M., Taylor, B. and Fryer, P., 1990, Volcanism in the Sumisu Rift, I. Major element, volatile, and stable isotope geochemistry, *Earth and Planetary Science Letters* 100: 179-194.

Hollis, C. J. and Hanson, J. A., 1991, Well preserved Late Paleocene radiolaria from Tangihua Complex, Camp Bay, eastern Northland, *Tane* 33: 65-76.

Hopper, D. J. and Smith, I. E. M., 1996, Petrography of the gabbro and sheeted basaltic intrusives at North Cape, New Zealand. *New Zealand Journal of Geology and Geophysics*, 39: 389-402.

Housh, T.B. and Luhr, J.F., 1991, Plagioclase melt equilibria in hydrous systems, *American Mineralogist*, 76: 455-489.

Hughes, W., S., 1966, Igneous rocks from the Northern Wairoa district, Unpublished MSc thesis, University of Auckland.

Humphries, S. E., 1984, The mobility of the rare earth elements in the crust. In: Henderson, P. (Editor), *Rare earth element geochemistry*. Elesvier, Amsterdam, pp. 315-341.

Isaac, M.J. (compiler), 1996, Geology of the Kaitaia Area, IGNS 1:250 000 geological map 1, Insitute of geological and Nuclear Sciences Limited, Lower Hutt, New Zealand.

Isaac, M.J., Herzer, R.H., Brook, F.J. and Hayward, B.W., 1994, Cretaceous and Cenozoic sedimentary basins of Northland, New Zealand, Institute of Geological and Nuclear Sciences Monograph 8.

Ishiwatari, A., Ikeda, Y and Koide, Y., 1990, The Yakuno ophiolite, Japan: Fragments of Permian island arc and marginal basin crust with a hotspot, *In*: Malpas, J.G., Moores, E.M., Panayiotou, A. and Xenophontos, C. (eds.), Ophiolites: Oceanic Crust Analogues, Proc. Symp. "Troodos 1987", Geol. Surv. Dep. Cyprus, pp. 497-506.

Jeffery, C.A., Honorez, J., Laverne, C. and Emmermann, R. 1986. Hydrothermal alteration of a 1 km section through the upper oceanic crust, deep sea drilling project hole 504b: Mineralogy, chemistry and evolution of seawater-basalt interactions. *Journal of Geophysical Research* 91:309-355.

Jenner, G.A., Cawood, P.A., Rautenschlein, M. and White, W.M., 1987, Composition of back-arc basin volcanics, Valu Fa Ridge, Lau Basin: evidence for a slab derived component in their mantle source. JVGR, 32: 209-222.

Jenner, G.A., Dunning, G.R., Malpas, J., Brown, M. and Brace, T., 1991, Bay of Islands and Little Port complexes, revisited: age, geochemical and isotopic evidence confirm suprasubduction-zone origin. *Canadian Journal of Earth* Sciences 28: 1635-1652.

Jennings, W., 1987, The stratigraphy, structure, geochemistry and metamorphism of the Waipapa basement in Omahuta and Puketi Forest district, Northland, New Zealand, Unpublished MSc Thesis, University of Auckland.

Jennings, W., 1989, Metamorphism in the Waipapa terrane, Omahuta and Puketi Forests, Northland, New Zealand, *Royal Society of New Zealand bulletin* 26: 23-28.

Jochum, K.P., McDonough, W.F., Palme, H. and Spettel, B., 1989, Compositional constraints on the contiental lithospheric mantle from trace elements in spinel peridotite xenoliths, *Nature* 340: 548-550.

Jochum, K.P., Seufert, H.M., Spettel, B. and Palme, H., 1986, The solar system abundances od nb, Ta and Y, and the relative abundances of refactory lithophile elements in differentiated planetary bodies, *Geochimica et Cosmochimica Acta* 50: 1173-1183.

Johnson, K.T.M., Dick, H.J.B and Shimizu, N., 1990, Melting in the oceanic mantle: and ion microprobe study of diopsides in abyssal peridotites, *Journal of Geophysical Research* 95: 2661-2678.

Johnson, R.W., Jaques, A.L., Langmuir, C.H., Perfit, M.R., Staudigel, H., Dunkley, P.N., Chappell, B. and Taylor, S.R., 1987, Ridge subduction and forearc volcanism: petrology and geochemistry of rocks dredged from the western Solomon Arc and Woodlark Basin. *In*: Taylor, S.R. and Exon, N.F. (eds.), Marine geology, geophysics and geochemistry of the Woodlark basin - Solomon Islands, Circum Pacific Council for Energy and Mineral Resources, Houston, TX, Earth Sci Series, 7: 155-226.

Jones, G., Roberston, A.H.F and Cann, J.R., 1991, Genesis and emplacement of the supra-subduction zone Pindos Ophiolite, Northwestern Greece, *In*: Peters, Tj., Nicolas, A. and Coleman, R.G. (eds.), Ophiolite Genesis and Evolution of the Oceanic Lithosphere, Kluwer, Dordrecht, pp. 771-799.

Kay, S.M. and Kay, R.W., 1985, Aleutain tholeiitic and calc-alkaline magma series. I: The mafic phenocrysts, *Contributions to Mineralogy and Petrology* 90: 276-290.

Keppler, H., 1996, Constraints from partitioning experiments on the composition of subduction-zone fluids, *Nature* 380: 237-240.

Klein et al., 1995

Keyser, T.K. and O'Neil, J.R., 1978, Oxygen isotope relations amoung oceanic tholeiites, alkali basalts and ultra mafic modules, USGS Open File Report 78-701: 237-240.

Knittel, U. and Oles, D., 1995, Basaltic volcanism associated with extensional tectonics in the Taiwan-Luzon island arc: evidence for non-depleted sources and subduction zone enrichment, *In*: Smellie, J.L (ed.), Volcanism Associated with Extension at Consuming Plate Margins, *Geological Society Special Publications No*. 81: 77-93.

Kristmannsdottir, H., 1975, Hydrothermal alteration of basaltic rocks, in: Iceland Geothermal Areas, 2nd United Nations Symposium on the Development and use of Geothermal Resources, May 20-29, San Francisco, USA, pp441-445.

Kroenke, L. W., 1984, Cenozoic development of the southwest Pacific, *UN ESCAP, CCOP/SOPAC Technical Bulletin* 6.

Kuschel, E. and Smith, I. E. M., 1992, Rare earth mobility in young arc-type volcanic rocks from Northern NZ. *Geochimica et Cosmochimica Acta* 56: 3951-3955.

Kushiro, I. and Yoder, H.S., 1966, Anorthite-forsterite and anorthite-enstatite reactions and their bearing the basalt-eclogite transition, *Journal of Petrology* 7: 337-362.

Laird, M.G., 1993, Cretaceous continental rifts: New Zealand region, *In*: Ballance, P.F. (ed.), Sedimentary Basins of the World, 2: South Pacific Sedimentary Basins, Elsvier, Netherlands: 37-47.

Langmiur, C.H., Klein, E. and Plank, T., 1992, Petrological systematics of mid-ocean ridge basalts: constraints on melt generation beneath ocean ridges, *In*: Phipps Morgan, J., Blackman, D.K. and Sinton, J.M. (eds.), Mantle flow and melt generation at mid-ocean ridges, AGU, Washington, DC, 183-280.

LaPierre, H., Dupuis, V., Lepinay de, B.M., Tardy, M., Maury, R.C., Hernandez, J.and Loubet, M., 1997, Is the lower Duarte igneous complex (Hispaniola) a remnant of the Caribbean plume-generated oceanic plateau? Journal of Geology 105: 111-120.

Larsen, J. M., 1987, Structure and petrography of the Tangihua massif at Ahipara, Northland, New Zealand: Unpublished MSc thesis, University of Auckland.

Le Bas, M.J., Le Maitre, R.W., Streckeisen, A. and Zanettin, B., 1986, A chemical classification of volcanic rocks based on the total alkali-silica diagram, *Journal of Petrology* 27: 745-750.

Le Couteur, P., 1967, The geology of a region NW of Whangaroa Harbour, Northland, Unpublished MSc thesis, University of Auckland.

Le Maitre, R. W. (ed.), 1989, A Classification of Igneous Rocks and Glossary of Terms. Blackwell, Oxford, 193 pp.

Leitch, E.C. 1966. The geology of the North Cape area, northern-most New Zealand. Unpublished MSc. thesis, University of Auckland.

Leterrier, J., Maury, R.C., Thonon, P., Girard, D. and Marchal, M., 1982, Clinopyroxene composition as a method of identification of the magmatic affinities of paleo-volcanic series, *Earth and Planetary Science Letters* 59: 139-154.

Lillie, A.R. and Brothers, 1969, R.N., The geology of New Caledonia, *New Zealand Journal of Geology and Geophysics,* 13: 145-183.

Lin, P.N., 1992, Trace element and isotopic characteristics of western Pacific pelagic sediments: Implications for the petrogenesis of Mariana Arc magmas, *Geochimica et Cosmochimica Acta* 56: 1641-1654.

Lin, P.N., Stern, R.J., Morris, J.D. and Bloomer, S.H., 1990, Nd- and Sr-isotopic compositions of lavas from the northern Mariana and southern Volcano arcs: Implications for the origin of island arc melts, *Contributions to Mineralogy and Petrology* 105: 381-392.

Lindsley, D.H., 1983, Pyroxene thermometry, *American Mineralogist*, 68: 477-493.

Lippard, S.J., Shelton, A.N. and Gass, I.G., 1986, The ophiolite of Northern Oman, *Geological Society of London*, memoir 11.

Luyenduk, B.P., 1995, Hypothesis for Cretaceous rifting of east Gondwana caused by subducted slab capture, *Geology*, 23: 373-376.

Maehl, H.W.E., 1970, Geology of the Whangaroa – Marble Bay – Te Ngaere district, Northland, Unpublished MSc Thesis, University of Auckland.

Malpas, J., Smith, I. E. M. And Williams, D., 1994, Comparative genesis and tectonic setting of ophiolitic rocks of the South and North Islands of New Zealand: Proceedings of the 29th International Geological Congress, Part D, 29-46.

Malpas, J., Spörli, K. B., Black, P. M. and Smith, I. E. M., 1992, Northland ophiolite, New Zealand, and implications for plate-tectonic evolution of the southwest Pacific: Geology, v. 20, p. 149-152.

Marsh, N.G., Saunders, A.D., Tarney, J., and Dick, H.J.B., 1980, Geochemistry of basalts from the Shikoku and Daito Basins, DSDP Leg 58, *In*: Stout, L.N. (ed.), Initial Reports Deep Sea Drilling Project 58, US Government Printing Office, Washington DC, 805-842.

Martin, H. R., 1988, Igneous geology of the Berghan Point area, Northland, Unpublished MSc thesis, University of Auckland.

Mason, A. P., 1953: The geology of the central portion of Hokianga County, North Auckland, Transactions of the Royal Society of New Zealand 81, 349-374.

Mason, D.O. 1973. Geology of the Parakao, Pakotai and Pupuke copper deposits, Northland. Unpublished MSc., University of Auckland.

Massoth, G.J., Butterfield, D.A., Lupton, J.E., McDuff, R.E., Lilley, M.D. and Jonasson, I.R. 1989. Submarine venting of phase-separated hydrothermal fluids at Axial Volcano, Juan de Fuca Ridge. *Nature* 340:702-705.

Mazengarb, C. and Harris, D.H.M., 1994, Cretaceous stratigraphic and structural relations of Raukumara Peninsula, New Zealand; stratigraphic patterns associated with the migration of a thrust system, *Annales Tectonicæ*, 8: 100-118.

Mazengarb, C., Francis, D.A. and Moore, P.R., 1991, Sheet Y16 Tauwhareparae, Geological Map of New Zealand 1:50,000, DSIR, Wellington.

McCulloch, M.T. and Cameron, W.E., 1983, Nb-Sr isotopic study of primitive lavas from the Troodos ophiolite, Cyprus: evidence for a subduction related setting, *Geology* 11: 727-731.

McCulloch, M.T. and Gamble J.A., 1991, Geochemical and geodynamic constraints on subduction zone magmatism, *Earth and Planetary Science Letters,* 102: 358-374.

McDermott, F. and Hawkesworth, C.J., 1991, Th, Pb and Sr isotope variations in young island arc volcanics and oceanic sediments, *Earth and Planetary Science Letters* 104: 1-15.

Meffre, S., 1995, The development of island arc-related ophiolites and sedimentary sequences in New Caledonia, Unpublished PhD Thesis, University of Sydney.

Meffre,S., Aitchison, J.C. and Crawford, A.J., 1996, Geochemical evolution and tectonic significance of boninites and tholeiites from the Koh ophiolite, New Caledonia, *Tectonics* 15: 67-83.

Meijer, A. and Reagan, M., 1983, Petrology and geochemistry of the island of Sarigan in the Mariana arc; calc-alkaline volcanism in an arc setting, *Contributions to Mineralogy and Petrology* 77:337-354.

Meschede, M., 1986, A method for discrimination between different types of mid-ocean ridge basalts and continental tholeiites with Nb-Zr-Y diagram. *Chemical Geology*, 56: 207-218.

Meshesha, M.Y. and Black, P.M., 1989, The geology of Purerua Peninsula, Bay of Islands, Northland, New Zealand, *In:* Spörli, K. B. and Kear, D. (eds.), Geology of Northland: accretion, allochthons and arcs at the edge of the New Zealand micro-continent, *Royal Society of New Zealand Bulletin 26.*

Mevel, C., 1988, Metamorphism in ocean layer 3, Gorringe Bank, Eastern Atlantic, *Contributions to Mineralogy and Petrology,* 100: 496-509.

Miller, C.A., Barton, M., Hanson, R.E. and Fleming, T.H., 1994, An Early Cretaceous volcanic arc/marginal basin transition zone, Peninsula Hardy, southernmost Chile, *Journal of Volcanology and Geothermal Research*, 63: 33-58.

Miller, D.M., Langmuir, C.H., Goldstein, S.L. and Franks, A.L., 1992, The importance of parental magma composition to calc-alkaline and tholeiitic evolution: evidence from Umnak Island in the Aleutians, *Journal of Geophysical Research* 97:321-355.

Monlar, P. and Atwater, T., 1978, Interarc spreading and cordilleran tectonics as alternatives related to the age of subducted oceanic lithosphere, *Earth and Planetary Science Letters,* 41: 330-340.

Moores, E.M. and Vine, F.J., 1971, The Troodos Massif, Cyprus and other ophiolites as oceanic crust: Evaluation and Implication, *Royal Society of London Philisophical Transactions Series A* 268:443-465.

Morimoto, N., Fabries, J., Ferguson, A.K., Ginzbrug, I.V., Ross, M., Seifert, F.A. and Zussman, J., 1988, Nomenclature of pyroxenes, *Mineralogical Magazine* 52: 535-550.

Morris, J.D. and Hart, S.R., 1984, isotopic and incompatible element constraints on the genesis of island arc volcanics from Cold Bay and Amak Island, Aleutians, *Geochimica et Cosmochimica Acta* 47: 2015-2030.

Mortimer, N., Herzer, R. H., Gans, P. B., Parkinson, D. L. and Seward, D., 1998, Geology of the area between the Three Kings and West Norfolk Ridges, SW Pacific Ocean, in preparation.

Mottl, M.J., 1983, Metabasalts axial hot springs and the structure of hydrothermal systems at mid-ocean ridges. *Geological Society of America Bulletin* 94: 161-180.

Mottl, M.J., Holland, H. and Corr, R.F. 1979. Chemical exchange during hydrothermal alteration of basalts by seawater - II: experimental results for Fe, Mn, and sulfur species. *Geochimica et Cosmochimica Acta* 43: 869-884.

Muehlenbachs, K. and Byerly, G., 1982, ^{18}O-enrichment of silicic magmas caused by crystal fractionation at the Galapagos spreading center, *Contributions to Mineralogy and Petrography* 79: 76-79.

Muenow, D.W., Garcia, M.O., Aggrey, K.E., Bednarz, U. and Schmincke, H.U., 1990, Volatiles in submarine glasses as a discriminant of tectonic origin: application to the Troodos ophiolite, *Nature* 343:159-161.

Muenow, D.W., Perfit, M.R. and Aggrey, K.E., 1991, Abundances of volatiles and genetic relationships among submarine basalts from the Woodlark Basin, southwest Pacific, *Geochimica et Cosmochimica Acta* 55: 2231-2239.

Nicholson, K. N. and Black, P. M., 1998, Low-temperature alteration of basalts from the Tangihua Complex, New Zealand, *Proceedings of the 9th International Water/Rock Interaction*, 675-678.

Nicholson, K. N., Black, P. M. and Picard, C., (a) in review, A comparative study of the alteration in ophiolitic basalts from the Poya terrane, New Caledonia, and the Tangihua Complex, New Zealand, Submitted to *Journal of Metamorphic Petrology.*

Nicholson, K. N., Black, P. M. and Picard, C., (b) in review, Basalt geochemistry from the Tangihua Ophiolite Complex, New Zealand: evidence for generation in an arc - back arc setting, Submitted to *Tectonophysics*.

Nicholson, K. N., Picard, C. and Black, P. M., (c) in review, Geochemistry and tectonic significance of late Cretaceous ophiolitic basalts from New Zealand and New Caledonia.

Nicholson, K.N., Picard, C. and Black, P.M., in preparation, Petrogenesis of a Late Cretaceous volcanic arc/marginal basin transition zone, Tangihua Complex, New Zealand, Submitted to *Earth and Planetary Science Letters.*

Norrish, K. and Chappell, B.W., 1977, X-ray flourescence spectography. *In*: Zussman, J. (ed.), Physical methods in determinative mineralogy. Academic Press, New York, 201-272.

Papike, J.J., Cameron, K.L. and Baldwin, K., 1974, Amphiboles and pyroxenes: characterisation of OTHER than quadrilateral components and estimates of ferric iron from microprobe data, *Geological Society of America, Abstracts with Programs* 6: 1053-1054.

Parat, F., 1996, Les laves de l'unite de Poya: Traceurs geochimiques et geodynamiques de l'evolution Cretace-Paleocene du SW Pacifique, Unpublished D.E.A. Mémoire, Université Joseph Fourier.

Paris, J. P., 1981, Géologie de la Nouvelle-Calédonie, *Mémoires B.R.G.M.* 113.

Paris, J.P. and Bradshaw, J.D., 1977, Triassic and Jurassic paleogeography and geotectonics of New Zealand and New Caledonia, International Symposium Geodynamics South-west Pacific 1976, Technip Editions, 195-208.

Parrot, J.F and Dugas, F., 1980, The disrupted ophiolite belt of the southwest Pacific: evidence of an Eocene subduction zone, *Tectonophysics* 66: 349-372.

Pearce, J. A., 1991, Ocean floor comes ashore *Nature* 354: 110-111.

Pearce, J.A. and Parkinson, I.J., 1993, Trace element models for mantle melting: applications to volcanic arc petrogenesis, *In*: Prichard, H.M., Alabaster, T., Harris, N.B.W. and Neary, C.R. (eds.), Magmatic Processes and Plate Tectonics, *Geological Society Special Publication No 76*, pp. 373-403.

Pearce, J.A., 1980, Geochemical evidence for the genesis and eruptive settings of lavas from Tethyan ophiolites, *In*: Panayiotou, A. (ed.), Ophiolites, Geological Survery Dept. Cyprus, 261-272.

Pearce, J.A., 1982, Trace element characteristics of lavas from destructive plate boundaries. *In*: Thorpe, R.S. (ed.), Andesites, John Wiley and Sons, 525-548.

Pearce, J.A., 1983, Role of sub-continental lithosphere in magma genesis at active continental margins, *In:* Hawkesworth, C.J. and Nurry, M.J. (eds.), Continental Basalts and Mantle Xenoliths, Shiva Publishing, pp.230-249.

Pearce, J.A., Ernewein, M., Bloomer, S.H., Parson, L.M., Murton, B.J. and Johnson, L.E., 1995, Geochemistry of Lau Basin volcanic rocks: influence of ridge segmentation and arc proximity, *In*: Smellie, J.L. (ed.), Volcanism Associated with Extension at Consuming Plate Margins, *Geological Society Special Publication No* 81, pp. 53-75.

Pearce, J.A., Lippard, S.J. and Roberts, S., 1984, Characteristics and tectonic significance of supra-subduction zone ophiolites. *In*: Kokelaar, B.P. and Howells, M.F. (eds.), Marginal Basin Geology, *Geol. Soc. Spec. Pub.*, 16: 77-94.

Peate, D.W., Pearce, J.A., Hawkesworth, C.J., Colley, H., Edwards, C.M. and Hirose, K., 1997, Geochemical variations in Vanuatu Arc lavas: the role of subducted material and a variable mantle wedge composition, *Journal of Petrology* 38: 1331-1358.

Peccerillo, A. and Taylor, S.R., 1976, Geochemistry of Eocene calc-alkaline volcanic rocks from the Kastamonu area, northern Turkey, *Contributions to Mineralogy and Petrology* 58: 63-81.

Pedersen, R.B. and Furnes, H., 1991, geology, magmatic affinity and geotectonic environment of some Caledonian ophiolites in Norway, *Journal of Geodynamics* 13: 183-203.

Perfit, M.R., Fornari, D.J., Malahoff, A. and Embley, R.W., 1983, Geochemical studies of abyssal lavas recovered by DSRV Alvi from Eastern Galapagos Rift, Inca Transform and Ecuador Rift, 3, Trace element abundances and petrogenesis. *Journal of Geophysical Research*, 88: 10551-10572.

Perfit, M.R., Langmuir, C.H., Baekisapa, M., Chappell, B., Johnson, R.W., Staudigel, H. and Taylor, S.R., 1987, Geochemistry and petrology of rocks from the Woodlark Basin: addressing the questions of ridge subduction. *In*: Taylor, S.R. and Exon, N.F. (eds.), Marine geology, geophysics and geochemistry of the Woodlark basin - Soloman Islands, Circum Pacific Council for Energy and Mineral Resources, Houston, TX, Earth Sci Series, 7: 113-154.

Pflumio, C., 1991, Evidences for polyphased oceanic alteration of the extrusive sequence of the Semail ophiolite from the Salahi block (northern Oman), In: Peters, T., Nicolas, A. and Coleman, R.G. (eds.), Ophiolite Genesis and Evolution of Oceanic Lithosphere, Klewer Acad., Mass., pp. 313-352.

Picard, C., Cluzel, D. and Boyet, M., 1999, Rare earth and isotopic geochemistry of the Post-Early Cretaceous volcanics in New Caledonia: geodynamic implications (abstract), *In*: Baldwin, L. and Lister, G.S. (eds.) Penrose Conference Abstract Volume, pp. 77-79.

Picard, M., 1995, Ouverture de bassins marginaux dans le pacifique sud-ouest: Paléovolcanisme et reconstitution des environement géodynamiques. Extrémité nord de la Nouvelle-Caledonie. Unpublished D.E.A. Mémoires, Université Ecole Nationale des Mines de Paris.

Plank, T. and Langmuir, C.H., 1998, The chemical composition of subducting sediment and its consequences for the crust and mantle, *Chemical Geology* 145: 325-394.

Poreda, R., 1985, Helium-3 and deuterium in back-arc basalts: Lau Basin and the Mariana Trough, *Earth and Planetary Science Letters* 73: 244-254.

Powell, R. and Holland, T. J. B., 1988, An internationally consistent data set with uncertainties and correlations: 3. Applications to geobarometry, worked examples and a computer program, *Journal of Metamorphic Geology* 6: 173-204.

Presnall, D.C., Dixon, J.R., O'Donnell, T.H. and Dixon, S.A., 1979, Generation of mid-ocean ridge tholeiites, *Journal of Petrology* 20: 3-35.

Price, R.C., Gray, C.M., Wilson, R.E., Frey, F.A. and Taylor, S.R., 1991, The effects of weathering on rare-earth element, Y and Ba abundances in Tertiary basalts from southeastern Australia, *Chemical Geology* 93: 245-265.

Price, R.C., Johnson, I.E. and Crawford, A.J., 1990, Basalts of the North Fiji Basin: the generation of back arc basin magmas by mixing of depleted and enriched mantle sources, *Contributions to Mineralogy and Petrography* 105-106-121.

Prinzhofer, A., 1981, Structure et pétrologie d'un cortège ophiolitique: Le massif du sud (Nouvelle-Calédonie): La transition manteaucroûte en milieu océanique. Unpublished PhD Thesis, École Nationale Supérieure des Mines, Paris.

Prinzhofer, A., Nicolas, A., Cassard, D., Moutte, J., Leblanc, M., Pars, P and Rabinovitch, M., Structures in the New Caledonia Peridotites-Gabbros: Implications for Oceanic Mantle and Crust, *Tectonophysics,* 69: 85-112.

Quennell, A. M. and Hay, R. F., 1964, Origin of the Tangihua Group of North Auckland, *New Zealand Journal of Geology and Geophysics* 7: 638-639.

Ramsay, W.E.H. and Moore, P.R., 1985, Mineralogy and chemistry of a pillow lava, Northland, New Zealand and its tectonic significance, *New Zealand Journal of Geology and Geophysics* 28: 471-485.

Rautenschlein, M., Jenner, G.A., Hertogen, J., Hofmann, A.W., Kerrich, R., Schmincke, H.-U. and White, W.M., 1985, Isotopic and trace element compositions of volcanic glasses from the Akaki Canyon, Cyprus: implications for the origin of the Troodos ophiolite, *Earth and Planetary Science Letters* 75: 369-383.

Rickwood, P.C., 1989, Boundary lines within petrologic diagrams which use major oxides and minor elements, *Lithos* 22: 247-263.

Ringwood, A.E., 1974, The petrologic evolution of island arc systems, *Journal of the Geological Society of London* 130: 183-204.

Roden, M. F., Frey, F. A. and Clague, D. A., 1984, Geochemistry of tholeiitic and alkalic lavas from the Koolau Range, Oahu, Hawaii: Implications for Hawaiian volcanism. *Earth and Planetary Science Letters* 69:141-158.

Rodgers, K. A., 1975, Lower Tertiary tholeiitic basalts from Southern New Caledonia, *Mineral Magazine* 40: 25-32.

Rollinson, H.R., 1993, Using geochemical data: evaluation, presentation, interpretation, LongmanGroup Limited, England.

Routhier, P., 1953, Étude géologique du versant occidental de la Nouvelle-Calédonie entre le col de Boghen et la pointe d'Arama, *Mém. Soc. géol. France, N. S.*, 32, n°67.

Saccocia, P.J. and Gillis, K.M. 1995. Hydrothermal upflow zones in the oceanic crust. *Earth and Planetary Science Letters* 136: 1-16.

Samson, S.D. and Alexander, E.C., 1987, Calibration of the interlaboratory ^{40}Ar-^{39}Ar dating standard, Mmhb-1. *Chemical Geology* 66: 27-34.

Saunders, A.D. and Tarney, J., 1979, The geochemistry of basalts from a back-arc spreading centre in the Scotia Sea. *GCA*, 43, 555-572.

Saunders, A.D. and Tarney, J., 1984, Geochemical characteristics of basaltic volcanism within back-arc basins. *In*: Kokelaar, B.P. and Howells, M.F. (eds.), Marginal Basin Geology, *Geol. Soc. Spec. Pub.*, 16: 59-76.

Saunders, A.D., Norry, M.J. and Tarney, J., 1988, Origin of MORB and chemically depleted-mantle reservoirs: Trace element constraints, *Journal of Petrology Special Lith. Issue*: 415-445.

Schiffman, P. and Fridleifsson, G.O., 1991, The smectite-chlorite transition in Drill Hole NJ-15, Nesjavellir geothermal field, Iceland: XRD, BSE and electron microprobe investigations, *Journal of Metamorphic Geology* 9: 679-696.

Seno, T. and Maruyama, S., 1984, Paleogeographic reconstruction and origin of the Philippine Sea, *Tectonophysics*, 102: 53-84.

Seyfried, W.E.Jr. and Bischoff, J.L. 1979. Low temperature basalt alteration by seawater: An experimental study at 70°C and 150°C. *Geochimica et Cosmochimica Acta* 43:1937-1947.

Seyfried, W.E.Jr. and Mottl, M.J. 1982. Hydrothermal alteration of basalt by seawater under seawater-dominated conditions. *Geochimica et Cosmochimica Acta* 46: 985-1002.

Sharpe, B. M., Locke, C. A. And Cassidy, J., 1989, Gravity investigations of the Maungataniwha and Ahipara ophiolite Massifs, Northland, New Zealand, *In*: Spörli, K. B. and Kear, D. (eds.), Geology of Northland: accretion, allochthons and arcs at the edge of the New Zealand micro-continent, *Royal Society of New Zealand Bulletin 26*.

Sharp, Z.D., 1990, Laser-based microanalytical method for the in situ determination of oxygen isotope ratios of silicates and oxides. *Geochimica et Cosmochimica Acta* 54: 1353-1357.

Shervias, J.W. and Kimbrough, D.L., 1985, Geochemical evidence for the tectonic setting of the Coast Range ophiolite: A composite island arc – oceanic crust terrane in western California, *Geology* 13: 35-38.

Shervias, J.W., 1990, Island arc and ocean crust ophiolites: Constraints in the petrology, geochemistry and tectonic style of ophiolite assemblages in the Californian Coast Ranges, *In*: Malpas, J.G., Moores, E.M., Panayiotou, A. and Xenophontos, C. (eds.), Ophiolites: Oceanic Crust Analogues, Proc. Symp. "Troodos 1987", Geol. Surv. Dep. Cyprus, pp. 507-520.

Shor,G.G., Kirk, H.K. and Menard, H.W., 1971, Crustal structure of the Melanesian area, *Journal of Geophysical Research* 76: 2562-2586.

Singer, B.S., Myers, J.D. and Frost, C.D., 1992, Mid-Pleistocene lavas from the Seguam volcanic center, central Aleutian arc: closed-system fractional crystallisation of a basalt to rhyodacite eruptive suite, *Contributions to Mineralogy and Petrology* 110: 87-112.

Sinton, J.M. and Fryer, P., 1987, Mariana Trough lavas from 18°N: implications for the origin of back-arc basin basalts, *Journal of Geophysical Research* 92: 12782-12802.

Sisson, T.W. and Grove, T.L., 1993a, Experimental investigations of the role of H_2O in calc-alkaline differentiation and subduction zone magmatism, *Contributions to Mineralogy and Petrology*, 113: 143-166.

Smith, I.E.M., Black, P.M. and Itaya, T., 1995, Inception and evolution of Cenozoic arc-type volcanism in northern New Zealand, *1995 PACRIM Proceedings*: 563-568.

Spencer, K.J. and Lindsley, D.H., 1981, A solution model for coexisting iron-titanium oxides, *American Mineralogist*, 66: 1189-1201.

Spöril, K.B., and Aita, Y., 1994, Tectonic significance of Late Cretaceous radiolaria frol the obducted Matakoa Volcanics, East Cape, North Island, New Zealand. *Geoscience Reports Shizuoka University*, 20: 115-134.

Spörli, K. B., 1989, Tectonic framework of Northland, New Zealand, *In*: , Spörli, K. B. and Kear, D. (eds), Geology of Northland: accretion, allochthons and arcs at the edge of the New Zealand micro-continent, *Royal Society of New Zealand Bulletin 26.*

Spörli, K.B. and Ballance, P.F., 1989, Mesozoic – Cenozoic ocean floor/continent interaction and terrane configuration, southwest Pacific area around New Zealand, *In*: Avraham, B. (ed.), The Evolution of the Pacific Margins, Oxford Monogr. Geol., Geophys., 8: 176-190.

Spörli, K.B. and Grant-Mackie, J.,A., 1976, Upper Jurassic fossils from the Waipapa Group of Tawharanui Peninsula, North Auckland, New Zealand, *New Zealand Journal of Geology and Geophysics* 19: 21-34.

Spörli, K.B. and Gregory, M.R., 1981, Significance of Tethyan fusulinid limestones of New Zealand, *In*: Cresswell, M.M. and Vella, P., (eds.) Gondwana Five, Balkema, Rotterdam: 223-229.

Spörli, K.B., 1989, Tectonic framework of Northland, New Zealand, *In*: Spörli, K.B. and Kear, D., (eds.), Geology of Northland: accretion, allochthons and arcs at the edge of the New Zealand micro-continent, *Royal Society of New Zealand Bulletin 26.*

Stern, R.J., Bloomer, S.H., Lin, P.-N. and Smoot, C., 1989, Submarine arc volcanism in the southern Mariana Arc as an ophiolite analogue, *Tectonophysics* 168: 151-170.

Stern, R.J., Morris, J.D., Bloomer, S.H. and Hawkins, J.W., 1991, The source of the subduction component in convergent margin magmas: trace element and radiogenic isotope evidence from Eocene boninites, Mariana forearc, *Geochimica et Cosmochimica Acta* 55: 1467-1481.

Stern, T., Smith, E. G. C., Davey, F. J. and Muirhead, K. J., 1987, Crustal and upper mantle structures in the northwestern North Island from seismic refraction data. *Royal Astronomical Society geophysical Journal* 91: 913-927.

Stevens, G.R., 1977, Mesozoic biogeography of the south-west Pacific and its relationship to plate tectonics, International Symposium Geodynamics South-west Pacific 1976, Technip Editions, 309-326.

Stewart, R.B., Price, R.C. and Smith, I.E.M., 1996, Evolution of high-K arc magmas, Egmont Volcano, Taranaki, New Zealand,: evidence from mineral chemistry, *Journal of Volcanology and Geothermal Research* 74: 275-295.

Strong, C. P., Hollis, C. J. and Wison, G. J., 1995, Foraminifera, radiolarian and dinoflagellate biostratigraphy of Late Cretaceous to Middle Eocene pelagic sediments (Muzzle Group), Mead Stream, Marlborough, New Zealand, *New Zealand Journal of Geology and Geophysics* 38: 171-212.

Sun, S.S. and MacDonough, W.F., 1989, Chemical and isotopic systematics of oceanic basalts: implications for mantle composition and processes. *In*: Saunders, A.D. and Norry, M.J. (eds.), Magmatism in Ocean Basins, *Geological Society of London, Special Publications*, 42: 313-345.

Tatsumi, Y. and Eggins, S., 1995, Subduction Zone Magmatism, Blackwell Science, Mass, 211pp.

Tatsumi, Y., Hamilton, D.L. and Nesbitt, R.W., 1986, Chemical characteristics of fluid phase released from the subducted lithosphere and origin of arc magmas: evidence from high-pressure experiments and natural rocks, *Journal of Volcanology and Geothermal Research*, 29: 293-309.

Taylor, B. and Karner, G.D., 1983, On the evolution of marginal basins. *Reviews of Geophysics and Space Physics*, 21(8): 1727-1741.

Taylor, R.N., Murton, B.J. and Nesbitt, R.W., 1992, Chemical transects across intra-oceanic arcs: implications for the tectonic setting of ophiolites. *In*: Parson, L.M., Murton, B.J. and Browning, P. (eds.), Ophiolites and their Modern Oceanic Analogues, *Geological Society Special Publications*, 60: 117-132.

Taylor, S.R. and Nesbitt, R.W., 1995, Arc volcanism in an extensional regime at the initiation of subduction: a geochemical study of Hahajima, Bonin Islands, Japan, *In*: Smellie, J.L. (ed.), Volcanism Associated with Extension at Consuming Plate Margins, *Geological Society Special Publication No.* 81, 115-134.

Thompson, G. M., Malpas, J. and Smith, I. E. M., 1997, The geochemistry of tholeiitic and alkalic plutonic suites within the Northland Ophiolite, northern New Zealand; magmatism in a back arc basin: *Chemical Geology* 142:113-123.

Turner, S.P., Hawkesworth, C. J., Rogers, N., Bartlett, Worthington, T.J., Hergt, J., Pearce, J.A. and Smith, I.E.M., 1997, ^{238}U-^{230Th} disequiliria, magma petrogenesis, and flux rates beneath the depleted Tonga-Kermadec island arc, *Geochimica et Consmochimica Acta* 61: 4855-4884.

Valleir, T.L., Jenner, G.A., Frey, F.A., Gill, J.B., Davis, A.S., Volpe, A.M., Hawkins, J.W., Morris, J.D., Cawood, P.A., Morton, J.L., Scholl, D.W., Rautenschlein, M., White, W.M. and Williams, M., 1991, Subalkaline andesites from Valu Fa Ridge, a back-arc spreading center in southern Lau Basin: Petrogenesis, comparitive chemistry and tectonic implications. *Chemical Geology*, 91: 227-256.

van den Beukel, J., 1990, Breakup of young oceanic lithosphere in the upper part of a subduction zone: implications for the emplacement of ophiolites, *Tectonics* 9: 825-844.

Volpe, A.M., MacDougall, J.D. and Hawkins, J.W., 1987, Mariana Trough basalts (MTB): trace element and Sr-Nd isotopic evidence for mixing between MORB-like and arc-like melts, *Earth and Planetary Science Letters* 82: 241-254.

Weissel, J.K. and Hayes, D.E., 1977, Evolution of the Tasman Sea reappraised, *Earth and Plentary Science Letters,* 36: 77-84.

Wells, P.R.A., 1977, Pyroxene thermometry in simple and complex systems, *Contributions to Mineralogy and Petrology* 62: 129-139.

White, W.M. and Hoffman, A.W., 1982, Sr and Nd isotope geochemistry of oceanic basalts and mantle evolution, *Nature* 296: 821-825.

White, W.M. and Patchett, J., 1984, Hf-Nd-Sr isotopes and incompatible element abundances in island arcs: Implications for magma origins and crust-mantle evolution, *Earth and Plentary Science Letters* 67: 167-185.

Wilson, M., 1989, Igneous Petrogenesis: a global tectonic approach, Unwin Hyman Inc., London.

Wood, B. and Banno, S., 1973, Garnet-orthopyroxene and orthopyroxene-clinopyroxene relationships in simple and complex systems, *Contributions to Mineralogy and Petrology* 42: 109-124.

Wood, D.A., Mattey, D.P., Joron, J.-L., Marsh, N.G., Tarney, J. and Treuil, M., 1981, A geochemical study of 17 selected samples from basement cores reocovered at sites 447, 448, 449, 450 and 451, DSDP Leg 59, *In*: Orlofsky, S. (ed.), Initial Reports Deep Sea Drilling Project 59, US Government Printing Office, Washington DC, 743-752.

Woodhead, J., Eggins, S. and Gamble, J., 1993, High field strength and transitional element systematics in island arc and back-arc basin basalts: evidence for multi-phase melt extraction and a depleted mantle wedge, *Earth and Planetary Science Letters,* 114: 491-504.

Woodward, D. J., 1970, Interpretation of gravity and magnetic anomalies at Hokianga, Northland, *New Zealand Journal of Geology and Geophysics,* 13: 364-369.

Worthington, T.J., 1998, Geology and petrology of Raoul Volcano: magmas genesis and fractionation processes beneath the Tonga-Kermadec arc, Unpublished PhD thesis, University of Auckland.

APPENDICES

Au #	Field #	Grid Reference NZMS 260	Location	Description
			New Zealand	
47643	NZT1	O04 583906	Doubtless Bay	Pillow basalt
47644	NZT2A	O04 513908	Te Kuiti	Dolerite
47645	NZT2B	O04 513908	Te Kuiti	Dolerite
47646	NZT3A	O04 513908	Te Kuiti	Andesite, pebble
47647	NZT3B	O04 513908	Te Kuiti	Andesite
47648	NZT4	N05 270580	Whangapei Harbour	Pillow basalt
47649	NZT5	N05 270580	Whangapei Harbour	Alkali-basalt
47650	NZT6	N05 270580	Whangapei Harbour	Pillow breccia
47651	NZT7	N05 270580	Whangapei Harbour	Dolerite dyke
47652	NZT8	N05 270580	Whangapei Harbour	Pillow basalt
47653	NZT9-1	N05 222693	Ahipara	Gabbro
47654	NZT9-2	N05 222693	Ahipara	Massive basalt
47655	NZT9-3A	N05 222693	Ahipara	Massive basalt – mixing zone marbles
47656	NZT9-3B	N05 222693	Ahipara	Massive basalt – mixing zone matirx
47657	NZT10	N05 217686	Ahipara	Gabbro
47658	NZT11	N05 218685	Ahipara	Plagiogranite
47659	NZT13	N05 193702	Ahipara	Pillow basalt
47660	NZT14	N04 185710	Ahipara	Dolerite dyke
47661	NZT15	N04 185710	Ahipara	Pillow basalt
47662	NZT16	N05 191702	Ahipara	Pillow basalt
47663	NZT17	P06 870210	Te Huia	Massive dolerite
47664	NZT18	P07 977060	Kirikopuni	Massive basalt
47665	NZT19	P08	Herekino Harbour	Massive basalt
47666	NZT20		Herekino Harbour	Basaltic glass
49111	KNN1	Q10 495112	Helensville	Basaltic glass
49112	KNN2	Q10 495112	Helensville	Basaltic glass
49113	KNN3	Q10 495112	Helensville	Fine grained massive basalt
49114	KNN4	Q10 495112	Helensville	Fine grained massive basalt
49115	KNN5	Q10 495112	Helensville	Course grained massive basalt

49116	KNN6		Port Albert	Fine grained massive basaltic breccia
49117	KNN7		Port Albert	Basaltic glass
49118	KNN8	Q07 114955	Dargerville	Granophyr
49119	KNN9	Q07 120947	Dargerville	Interpillow sediments
49120	KNN10	Q07 125945	Dargerville	Fine grained dolerite
49121	KNN11	Q07 125945	Dargerville	Basaltic glass
49122	KNN12	Q07 125945	Dargerville	Dolerite
49123	KNN13	P07 840979	Waihui Quarry	Massive basalt
49124	KNN14	P07 840979	Waihui Quarry	Interpillow material
49125	KNN15	P07 840979	Waihui Quarry	Light intrusive diorite
49126	KNN16	P07 840979	Waihui Quarry	Medium dark intrusive diorite
49127	KNN17	P07 840979	Waihui Quarry	Darker intrusive diorite
49128	KNN18	P07 844997	Waihui Quarry	Glassy breccia
49129	KNN19	P07 844997	Waihui Quarry	Massive basalt
49130	KNN20	P07 844997	Middleton Rdy	Porphyritic basalt
49131	KNN21	P07 927873	Wahui Quarry	Medium grained intrusive, diorite
49132	KNN22	P07 020947	Kirikopuni	Pillow basalt
49133	KNN23	P07 020947	Kirikopuni	Basaltic glass
49134	KNN24	P07 020947	Kirikopuni	Interpillow sediments
49135	KNN25	P07 002028	Houto	Basaltic glass
49136	KNN26	P07 002028	Houto	Basaltic glass
49137	KNN27	P07 002028	Houto	Altered basalt
49138	KNN29	P07 927027	Tangihua Valley Rd	Basaltic breccia
49139	KNN30	P07 927032	Tangihua Valley Rd	Weathered massive basalt
49140	KNN31	P07 927032	Tangihua Valley Rd	Weathered massive basalt
49141	KNN32	P07 887078	Mangakahia Forest	M,assive basalt
49142	KNN33	P07 887078	Mangakahia Forest	M,assive basalt
49143	KNN34	P06 842116	Forsyth Downs	Weathered basalt
49144	KNN35	P06 840115	Forsyth Downs	Limestone
49145	KNN36	P06 840115	Forsyth Downs	Gabbro
49146	KNN37	P06 892109		Altered pillow basalt
49147	KNN38	P06 838208	Waimatinui Rd	Gabbro
49148	KNN39	P06 856192		Sediments

49149	KNN40	P06 856192		Altered igneous rock
49150	KNN41	P07 974053	Mangatipa	Massive basalt
49151	KNN42	O06 496316	Waima Forest	Pillow basalt
49152	KNN43	O06 496316	Waima Forest	Interpillow sediments
49153	KNN44	O06 489333	Hautura	Pillow basalt
49154	KNN45	O06 486 333	Hautura Quarry	Massive basalt
49155	KNN46	P06 794308	Quarry	Massive basalt
49156	KNN47	P06 797318	Quarry	Massive basalt
49157	KNN48	P06 762257	Along road	Pillow basalts
49158	KNN49	P06 831257	Small quarry	Pillow basalts
49159	KNN50	P06 957236	Lovatt Rd	Massive weathered basalt
49160	KNN51	P06 975215	Lovatt Rd	Massive basalt
49161	KNN52		200m east of KNN51	Courser grained igneous rock
49162	KNN53	P07 844972	Tongariro	Basaltic glass
49163	KNN54	P07 844972	Tongariro	Pillow basalt
49164	KNN55	P07 844972	Tongariro	Celedonite
49165	KNN56	P07 844972	Tongariro	Basaltic glass
49166	KNN57	P07 844972	Tongariro	Massive basalt
49167	KNN58	P06 861211	Waimaternui	Quartz diorite
49168	KNN59	P06 798213	Waimaternui	Quartz diorite
49169	KNN60	M02&N02 830513	Cape Rienga	Pillow basalt
49170	KNN61	M02&N02 830513	Cape Rienga	Massive basalt
49171	KNN62	M02&N02 847517	Tapotupotu Bay	Pillow basalt
49172	KNN63		Ahipara Quarry	Pillow basalt and basaltic glass
49173	KNN64		Ahipara	Immiscibility zone, massive altered basalt
49174	KNN65		Whanpapei Harbour	Pillow basalt
49175	KNN66		Ahipara	Altered basalt
49176	KNN67		Pongaru quarry	Altered glass
49177	KNN68		Quarry	Massive basalt
49178	KNN69		Mitimiti	Pillow basalt
49179	KNN70		Opononi	Pillow basalt
49180	KNN71		Opononi	Interpillow sediments
49181	KNN73		Johnston Rd	Massive dolerite

49182	KNN74		Waima Forest	Massive basalt
49183	KNN75		Peria	Massive basalt
49184	KNN76		Fern flat	Massive basalt with veining
49185	KNN77		Fern flat	Very course basalt?
49186	KNN78		Fern flat	Massive basalt
49187	KNN79		Coopers beach	Dolerite
49188	KNN80		Coopers beach	Massive basalt
49189	KNN82		Mangamuka Gorge	Massive basalt
49190	KNN83		Mangamuka Gorge	Pillow basalt
49191	KNN84		Hihi beach	Massive basalt
49192	KNN85		Mangakahia	Weathered basalt
49193	KNN86		Houto -Pedersons quarry	Basaltic glass
49194	KNN87		Houto	Dolerite
49195	KNN88		Houto	Massive basalt
49196	KNN89	P07 000004	Houto	Pillow basalt
49197	KNN90	P07 000004	Houto	Gabbro, very weathered
49198	KNN91	Q07 153945		Sandstone
49199	KNN92	P06 057216	Pipiwai	Pillow basalt
49200	KNN93		Mitimiti	Massive basalt
49201	KNN94		Mitimiti	Dolerite
49202	KNN95		Mitimiti	Glass
49203	KNN96			
49204	KNN97		Bergan Point	Massive basalt
49205	KNN98		Te Kao	Course gabbro
49206	KNN99		Te Kao	Finer gabbro
49207	KNN100	M02&N02 981535	Hooper point	Basalt clast in polymictic conglomerate
49208	KNN101	M02&N02 989443	Spirits Bay Rd quarry	Gabbro cut by zeolite veins
49209	KNN102	M02&N02 989443	Spirits Bay Rd quarry	Zeolites
49210	KNN103	M02&N02 989443	Spirits Bay quarry	Zeolites
49211	KNN104	M02&N02 889459	Cape Maria Von Dieman	Massive basalt
49212	KNN105	M02&N02 889459	Cape Maria Von Dieman	Massive dolerite – weathered and veined
49213	KNN110	M02&N02 124558	North Cape	Serpentinite from quarry
49214	KNN111	M02&N02 124532	Waikuku beach	Dolrite dykes

49215	KNN112	M02&N02 123533	North Cape	Cummulate gabbro
49216	KNN113	M02&N02 102544	Mahurangi Pt	Gabbro
49217	KNN114	M02&N02 158538	Mahurangi Pt	Gabbro
49218	KNN115	M02&N02 155544	Mahurangi Pt	Gabbro
49219	KNN116		Te Paki quarry	Basaltic glass

Au #	Field #	Grid Reference Lat & Long	Location	Description
New Caledonia				
49220	NC1	21°48'02" 166°03'09"	Nassirah	Basalt clast from Eocene Flysh
49221	NC2	21°48'02" 166°03'09"	Nassirah	Weakly altered basalt
49222	NC3	21°48'02" 166°03'09"	Nassirah	Courser grained basalt
49223	NC4	21°48'02" 166°03'09"	Nassirah	Massive basalt
49224	NC5	21°48'02" 166°03'09"	Nassirah	Limestone
49225	NC6	21°34'07" 166°07'03"	NW of Thio	Massive basalt
49226	NC7	21°34'07" 166°07'03"	NW of Thio	Epidote veining
49227	NC8	21°34'08" 166°07'02"	NW of Thio	Dolerite
49228	NC9	21°34'06" 166°06'09"	NW of Thio	Foliated basalt
49229	NC10	21°34'05" 166°06'05"	NW of Thio	Basalt clast
49230	NC11	21°34'05" 166°06'05"	NW of Thio	Sediments
49231	NC12	21°34'04" 166°06'03"	NW of Thio	Massive basalt
49232	NC13	21°34'04" 166°06'03"	NW of Thio	Chert
49233	NC14	21°34'05" 166°06'00"	NW of Thio	Massive basalt with calcite and clays
49234	NC15	21°33'06" 165°58'08"	Cascade de Ciu	Altered basalt
49235	NC16	21°33'03" 165°58'05"	Cascade de Ciu	Altered basalt
49236	NC17	21°29'06" 165°25'06"	Near Nandai – quarry	Interpillow sediment
49237	NC18	21°29'06" 165°25'06"	Near Nandai – quarry	Fresh pillow basalt
49238	NC19	21°29'04" 165°24'08"	Near Nandai	Courser grained basalt
49239	NC20	21°29'04" 165°24'08"	Near Nandai	Basalt
49240	NC21	21°28'07" 165°23'06"	Near Nandai	Massive basalt
49241	NC22	21°28'07" 165°23'06"	Near Nandai	Massive basalt
49242	NC23	21°28'07" 165°23'06"	Near Nandai	Massive basalt
49243	NC24	21°28'01" 165°19'02"	Near C. de Bonhomme	Sediments
49244	NC25	21°28'01" 165°19'02"	Near C. de Bonhomme	Massive basalt?
49245	NC26	21°06'07" 164°58'06"	E of Pouembout	Altered basalt
49246	NC27	21°05'08" 164°47'07"	Presqu'ile de Foue	Pillow basalt
49247	NC28	21°04'06" 164°46'00"	Presqu'ile de Foue	Interpillow sediments

49248	NC29	21°04'06" 164°46'00"	Along beach	Pillow basalt
49249	NC30	21°04'06" 164°46'00"	Along beach	Sediments
49250	NC31	20°58'04" 164°38'06"	Voh	Altered basalt
49251	NC32	20°58'04" 164°38'06"		Fresher basalt
49252	NC33	21°05'04" 164°53'05"	Kone- Poindimie Rd	Basalt
49253	NC34	20°56'00" 165°20'07"	Poindimie beach	Massive basalt
49254	NC35	20°56'00" 165°20'07"	Poindimie beach	Sediments
49255	NC36	20°56'00" 165°20'07"	Poindimie beach	Altered basalt
49256	NC37	20°56'00" 165°20'07"	Poindimie beach	Vein material
49257	NC38	20°56'00" 165°20'07"	Poindimie beach	Vein material
49258	NC39	20°56'04" 165°23'06"	Along coast	Massive basalt
49259	NC40	20°57'05" 165°23'07"	Pambou	Massive basalt

Mineral	AU#		SiO2	TiO2	Al2O3	FeO	MnO	MgO	CaO	Na2O	K2O	Cl	P2O5	Cr2O3	Total	An
							New Zealand									
PLAG	49170		50,49	0,00	30,99	0,84	0,00	0,55	14,40	3,47	0,00	0,00	0,00	0,00	100,74	80,6
PLAG	49170		50,77	0,00	29,96	0,97	0,00	0,33	13,68	3,80	0,00	0,00	0,00	0,00	99,51	78,3
PLAG	49170		52,12	0,00	28,93	1,12	0,00	0,38	12,61	4,27	0,00	0,00	0,00	0,00	99,44	74,7
PLAG	49170		50,25	0,00	30,14	0,69	0,00	0,41	13,84	3,27	0,22	0,00	0,00	0,00	98,81	79,9
PLAG	49170		49,61	0,00	31,24	0,66	0,00	0,43	15,07	2,93	0,00	0,00	0,00	0,00	99,95	83,7
PLAG	49170		49,92	0,00	31,48	0,71	0,00	0,41	15,15	3,10	0,00	0,00	0,00	0,00	100,78	83,0
PLAG	49170		49,18	0,00	31,71	0,69	0,00	0,46	15,37	2,87	0,00	0,00	0,00	0,00	100,29	84,3
PLAG	49170		51,09	0,00	29,32	0,46	0,00	0,36	13,81	2,79	0,33	0,00	0,00	0,00	98,15	81,6
PLAG	49182		46,61	0,00	32,45	0,90	0,00	0,28	16,40	2,13	0,00	0,00	0,00	0,00	98,78	88,5
PLAG	49182		46,85	0,00	33,12	0,95	0,00	0,26	16,80	2,01	0,00	0,00	0,00	0,00	99,99	89,3
PLAG	49182		45,90	0,00	33,19	0,99	0,00	0,40	17,06	1,73	0,00	0,00	0,00	0,00	99,26	90,8
PLAG	49182		46,97	0,00	32,35	0,90	0,00	0,27	16,31	2,14	0,10	0,00	0,00	0,00	99,05	87,9
PLAG	49182		46,60	0,00	33,10	0,86	0,00	0,33	16,76	2,10	0,00	0,00	0,00	0,00	99,74	88,9
PLAG	49182		45,65	0,00	33,44	0,76	0,00	0,35	17,27	1,54	0,00	0,00	0,00	0,00	99,02	91,8
PLAG	49182		45,77	0,00	33,16	0,84	0,00	0,27	16,94	1,65	0,00	0,00	0,00	0,00	98,63	91,1
PLAG	49182		46,39	0,00	33,07	0,78	0,00	0,34	17,13	1,79	0,00	0,00	0,00	0,00	99,50	90,5
PLAG	49182		46,55	0,00	33,03	0,84	0,00	0,38	16,86	1,70	0,00	0,00	0,00	0,00	99,37	90,8
PLAG	49182		47,27	0,00	32,10	0,93	0,00	0,35	16,15	2,32	0,00	0,00	0,00	0,00	99,13	87,4
PLAG	49182		46,77	0,00	32,89	0,92	0,00	0,29	16,67	1,86	0,00	0,00	0,00	0,00	99,39	90,0
PLAG	49182		46,59	0,00	32,15	0,81	0,00	0,37	16,29	2,26	0,00	0,00	0,00	0,00	98,46	87,8
PLAG	49171		50,23	0,00	31,00	0,72	0,00	0,36	14,45	3,36	0,00	0,00	0,00	0,00	100,11	81,1
PLAG	49171		49,78	0,00	30,54	0,73	0,00	0,29	14,26	3,29	0,00	0,00	0,00	0,00	98,89	81,3
PLAG	49171		50,22	0,00	30,48	0,83	0,00	0,41	14,30	3,36	0,00	0,00	0,00	0,00	99,60	81,0
PLAG	49171		51,08	0,00	29,22	0,83	0,00	0,31	13,10	3,95	0,11	0,00	0,00	0,00	98,61	76,3
PLAG	49171		50,97	0,00	30,72	0,88	0,00	0,44	14,19	3,68	0,00	0,00	0,00	0,00	100,88	79,4
PLAG	49171		49,66	0,00	30,63	0,91	0,00	0,42	14,62	2,95	0,00	0,00	0,00	0,00	99,19	83,2
PLAG	49171		47,03	0,00	32,61	0,59	0,00	0,38	16,56	2,08	0,00	0,00	0,00	0,00	99,25	88,8
PLAG	49171		50,56	0,00	29,99	0,73	0,00	0,43	13,70	3,58	0,16	0,00	0,00	0,00	99,15	78,6
PLAG	49178		62,98	0,00	23,44	0,39	0,00	0,22	4,91	8,77	0,00	0,00	0,00	0,00	100,71	35,9
PLAG	49178		56,86	0,00	26,07	0,44	0,00	0,22	8,48	5,67	1,53	0,00	0,00	0,00	99,29	54,1
PLAG	49178		57,36	0,00	26,38	0,45	0,00	0,27	8,67	6,83	0,00	0,00	0,00	0,00	99,96	55,9
PLAG	49178		60,97	0,00	23,92	0,36	0,00	0,00	5,67	8,20	0,20	0,00	0,00	0,00	99,31	40,3
PLAG	49178		53,29	0,00	28,44	0,56	0,00	0,24	11,29	5,24	0,00	0,00	0,00	0,00	99,07	68,3
PLAG	49178		51,12	0,00	29,95	0,74	0,00	0,28	13,25	4,01	0,00	0,00	0,00	0,00	99,36	76,8

Mineral	Sample#		SiO2	TiO2	Al2O3	FeO	MnO	MgO	CaO	Na2O	K2O	Cl	P2O5	Cr2O3	Total	An
PLAG	49178		53,59	0,00	28,29	0,55	0,00	0,31	11,33	5,17	0,00	0,00	0,00	0,00	99,24	68,7
PLAG	49178		55,60	0,00	27,20	0,45	0,00	0,29	9,77	6,25	0,00	0,00	0,00	0,00	99,56	61,0
PLAG	49178		55,53	0,00	27,46	0,53	0,00	0,22	10,06	5,80	0,00	0,00	0,00	0,00	99,61	63,4
PLAG	49172		47,49	0,00	32,43	0,84	0,00	0,31	15,87	2,45	0,00	0,00	0,00	0,00	99,39	86,6
PLAG	49172		47,70	0,17	32,36	0,81	0,00	0,29	16,25	2,35	0,00	0,00	0,00	0,00	99,92	87,4
PLAG	49172		50,37	0,00	30,71	0,65	0,00	0,29	13,89	3,71	0,00	0,00	0,00	0,00	99,61	78,9
PLAG	49172		49,07	0,00	31,41	0,74	0,00	0,40	15,15	3,12	0,00	0,00	0,00	0,00	99,89	82,9
PLAG	49172		48,46	0,00	32,17	0,89	0,00	0,31	15,93	2,66	0,00	0,00	0,00	0,00	100,43	85,7
PLAG	49172		49,62	0,00	31,59	0,80	0,00	0,49	15,04	3,10	0,00	0,00	0,00	0,00	100,64	82,9
PLAG	49172		50,94	0,00	30,87	0,74	0,00	0,30	14,05	3,70	0,00	0,00	0,00	0,00	100,59	79,2
PLAG	49172		48,89	0,00	32,09	0,74	0,00	0,33	15,50	2,73	0,00	0,00	0,00	0,00	100,29	85,0
PLAG	49172		48,81	0,00	31,49	0,80	0,00	0,35	15,40	1,93	1,13	0,00	0,00	0,00	99,91	83,4
PLAG	49174		52,78	0,00	28,25	0,64	0,00	0,32	11,27	5,08	0,09	0,00	0,00	0,00	98,43	68,6
PLAG	49174		53,17	0,00	27,84	0,56	0,00	0,30	10,18	5,89	0,18	0,00	0,00	0,00	98,13	62,6
PLAG	49174		51,30	0,00	29,87	0,71	0,00	0,26	13,12	3,98	0,00	0,00	0,00	0,00	99,25	76,7
PLAG	49174		54,62	0,00	27,36	0,52	0,00	0,28	10,12	5,62	0,00	0,00	0,00	0,00	98,53	64,3
PLAG	49174		55,01	0,00	27,67	0,45	0,00	0,24	10,22	5,90	0,00	0,00	0,00	0,00	99,48	63,4
PLAG	49174		54,59	0,00	27,59	0,55	0,00	0,26	10,24	5,54	0,12	0,00	0,00	0,00	98,89	64,4
PLAG	49174		52,14	0,00	28,74	0,94	0,00	0,46	10,71	5,23	0,27	0,00	0,00	0,00	98,48	66,1
PLAG	49174		56,82	0,00	26,50	0,30	0,00	0,28	8,62	6,65	0,09	0,00	0,00	0,00	99,28	56,1
PLAG	49174		58,95	0,00	24,81	0,43	0,00	0,00	7,20	7,22	0,00	0,00	0,00	0,00	98,61	49,9
PLAG	49127		54,54	0,00	27,93	0,51	0,00	0,00	10,67	5,52	0,00	0,00	0,00	0,00	99,17	65,9
PLAG	49127		54,33	0,00	28,46	0,43	0,00	0,00	10,86	5,53	0,00	0,00	0,00	0,00	99,61	66,3
PLAG	49127		52,35	0,00	29,41	0,65	0,00	0,00	12,50	4,51	0,00	0,00	0,00	0,00	99,41	73,5
PLAG	49127		52,40	0,00	29,14	0,63	0,00	0,00	11,97	4,68	0,00	0,00	0,00	0,00	98,82	71,9
PLAG	49127		50,86	0,00	30,50	0,88	0,00	0,00	13,42	3,83	0,00	0,00	0,00	0,00	99,48	77,8
PLAG	49127		50,98	0,00	29,62	0,74	0,00	0,00	13,16	3,97	0,21	0,00	0,00	0,00	98,68	75,9
PLAG	49127		56,46	0,00	26,64	0,48	0,00	0,00	8,90	6,64	0,24	0,00	0,00	0,00	99,38	56,4
PLAG	49127		59,13	0,00	25,10	0,58	0,00	0,00	7,03	7,51	0,11	0,00	0,00	0,00	99,45	48,0
PLAG	49127		49,60	0,00	30,19	0,63	0,00	0,00	13,99	3,54	0,51	0,00	0,00	0,00	98,47	77,5
PLAG	49127		53,19	0,00	28,72	0,59	0,00	0,00	11,51	4,84	0,00	0,00	0,00	0,00	98,85	70,4
PLAG	49127		55,71	0,00	27,54	0,44	0,00	0,00	10,11	5,74	0,00	0,00	0,00	0,00	99,55	63,8
PLAG	49127		50,40	0,00	30,21	0,70	0,00	0,00	13,94	3,70	0,00	0,00	0,00	0,00	98,94	79,0
PLAG	49123		50,45	0,00	30,92	0,77	0,00	0,00	14,17	3,57	0,00	0,00	0,00	0,00	99,87	79,9
PLAG	49123	rim	51,68	0,00	29,41	0,93	0,00	0,00	12,60	4,23	0,00	0,00	0,00	0,00	98,86	74,9
PLAG	49123		50,86	0,00	30,51	0,67	0,00	0,00	14,00	3,54	0,00	0,00	0,00	0,00	99,59	79,8

Mineral	Sample#		SiO2	TiO2	Al2O3	FeO	MnO	MgO	CaO	Na2O	K2O	Cl	P2O5	Cr2O3	Total	An
PLAG	49123		46,55	0,00	34,35	0,44	0,00	0,00	17,99	1,62	0,00	0,00	0,00	0,00	100,95	91,7
PLAG	49123		46,13	0,00	34,34	0,47	0,00	0,00	18,01	1,46	0,00	0,00	0,00	0,00	100,42	92,5
PLAG	49123		46,23	0,00	34,09	0,41	0,00	0,00	17,67	1,44	0,00	0,00	0,00	0,00	99,84	92,5
PLAG	49123	rim	50,51	0,00	30,30	0,83	0,00	0,00	13,71	3,62	0,00	0,00	0,00	0,00	98,97	79,1
PLAG	49123	rim	54,17	0,00	28,20	1,31	0,00	0,44	11,64	4,87	0,00	0,00	0,00	0,00	100,62	70,5
PLAG	49123	rim	60,36	0,00	24,24	1,51	0,00	0,00	6,53	7,12	0,15	0,00	0,00	0,00	101,04	47,3
PLAG	49123		46,26	0,00	33,14	0,41	0,00	0,00	16,98	1,91	0,00	0,00	0,00	0,00	98,68	89,9
PLAG	49123		51,80	0,00	29,89	0,77	0,00	0,00	13,06	4,08	0,00	0,00	0,00	0,00	99,60	76,2
PLAG	47660		63,27	0,00	22,03	1,07	0,00	0,44	4,36	8,60	0,81	0,00	0,00	0,00	100,59	31,7
PLAG	46743		46,91	0,00	33,24	0,73	0,00	0,00	17,15	1,94	0,00	0,00	0,00	0,00	99,97	89,8
PLAG	46743	rim	53,66	0,00	28,82	1,49	0,00	0,43	11,42	4,66	0,10	0,00	0,00	0,00	100,59	70,6
PLAG	46743	rim	56,89	0,00	26,61	0,67	0,00	0,00	8,85	4,86	2,64	0,00	0,00	0,00	100,54	54,1
PLAG	46743		74,83	0,00	15,70	0,00	0,00	0,00	2,20	7,01	0,12	0,00	0,00	0,00	99,87	23,6
PLAG	46743		59,27	0,00	25,19	0,45	0,00	0,00	7,17	7,37	0,00	0,00	0,00	0,00	99,46	49,3
PLAG	46743		66,58	0,00	19,20	0,00	0,00	0,00	2,52	10,28	0,24	0,00	1,07	0,00	99,89	19,3
PLAG	47648		49,99	0,00	31,09	0,57	0,00	0,00	14,81	3,19	0,00	0,00	0,00	0,00	99,65	82,3
PLAG	47648		50,19	0,00	31,34	0,46	0,00	0,00	14,63	3,15	0,00	0,00	0,00	0,00	99,77	82,3
PLAG	47648	rim	50,72	0,00	30,96	0,59	0,00	0,00	14,36	3,38	0,00	0,00	0,00	0,00	100,01	80,9
PLAG	47648	rim	50,37	0,00	30,78	0,59	0,00	0,00	14,49	3,47	0,00	0,00	0,00	0,00	99,70	80,7
PLAG	47648		51,26	0,00	30,83	0,56	0,00	0,00	14,28	3,71	0,00	0,00	0,00	0,00	100,64	79,4
PLAG	47648		50,77	0,00	30,96	0,50	0,00	0,23	14,35	3,44	0,00	0,00	0,00	0,00	100,26	80,7
PLAG	47648	rim	51,78	0,00	30,74	0,65	0,00	0,00	14,16	3,79	0,00	0,00	0,00	0,00	101,13	78,9
PLAG	47648	rim	50,05	0,00	31,53	0,65	0,00	0,00	14,84	3,09	0,13	0,00	0,00	0,00	100,30	82,2
PLAG	47648		51,24	0,00	30,91	0,47	0,00	0,00	13,95	3,88	0,00	0,00	0,00	0,00	100,46	78,2
PLAG	47648		50,84	0,00	30,81	0,56	0,00	0,00	13,92	3,68	0,00	0,00	0,00	0,00	99,81	79,1
PLAG	47648	rim	53,05	0,48	26,21	2,61	0,00	1,99	12,80	3,90	0,00	0,00	0,00	0,00	101,05	76,6
PLAG	47648	rim	53,60	0,00	28,78	0,96	0,00	0,00	12,33	4,51	0,00	0,00	0,00	0,00	100,18	73,2

Mineral	Sample#		SiO2	TiO2	Al2O3	FeO	MnO	MgO	CaO	Na2O	K2O	Cl	P2O5	Cr2O3	Total	An
							New Caledonia									
PLAG	49225		52,41	0,14	29,40	0,85	0,02	0,29	12,10	4,66	0,08	0,02	0,08	0,00	100,00	71,8
PLAG	49225		52,12	0,05	29,82	0,96	0,04	0,37	12,71	4,41	0,01	0,00	0,10	0,00	100,49	74,2
PLAG	49225		54,10	0,08	28,60	0,57	0,00	0,19	10,91	5,32	0,07	0,02	0,10	0,00	99,88	66,9
PLAG	49225		52,35	0,03	29,10	1,35	0,00	0,21	11,85	4,71	0,01	0,01	0,07	0,09	99,75	71,5
PLAG	49225		50,87	0,06	29,93	1,03	0,01	0,27	13,18	4,21	0,03	0,00	0,07	0,00	99,63	75,7
PLAG	49225		51,21	0,04	30,60	1,03	0,03	0,30	13,47	3,99	0,06	0,00	0,03	0,00	100,74	76,9
PLAG	49225		50,55	0,01	29,78	1,06	0,05	0,23	13,09	4,05	0,01	0,00	0,07	0,06	98,92	76,3
PLAG	49225		53,69	0,03	29,08	0,93	0,00	0,25	11,52	5,06	0,04	0,02	0,12	0,00	100,67	69,3
PLAG	49225		51,39	0,12	29,74	0,92	0,04	0,25	12,71	4,20	0,03	0,03	0,06	0,00	99,47	75,0
PLAG	49225		51,57	0,10	29,37	1,04	0,00	0,32	12,47	4,26	0,00	0,03	0,08	0,00	99,23	74,5
PLAG	49251		48,99	0,00	31,60	0,57	0,06	0,40	14,95	3,14	0,00	0,01	0,05	0,03	99,73	82,7
PLAG	49251		49,89	0,04	30,16	0,65	0,04	0,41	13,77	3,64	0,05	0,04	0,05	0,08	98,81	78,9
PLAG	49251		53,69	0,03	29,08	0,93	0,00	0,25	11,52	5,06	0,04	0,02	0,12	0,00	100,67	69,3

PYX = pyroxene

PLAG = plagioclase

All analyses with totals > 98% are listed.

Only analyses with totals >98.5% were used in Chapters 2 and 3.

Unless otherwise stated, analyses are taken from the core of the mineral grain.

Some plagioclase analyses are from the groundmass.

The presented mineral compositions for both the Tangihua Complex and the Poya terrane were determined from carbon-coated polished thin sections by energy dispersive (EDS) methods using the JOEL JXA-5A electron microprobe housed in the Department of Geology, University of Auckland, and at the University of Clermont-Ferrand

Mineral	Sample#		SiO2	TiO2	Al2O3	FeO	MnO	MgO	CaO	Na2O	K2O	Cl	P2O5	Cr2O3	Total	En	Wo	Fs
							New Zealand											
CPX	49170		48,4	1,6	5,4	9,7	0,3	14,4	19,5	0,8	0,0	0,0	0,0	0,0	100,0	44,7	33,1	22,2
CPX	49170		48,6	1,3	4,9	8,9	0,0	15,6	18,3	0,7	0,0	0,0	0,0	0,0	98,3	42,8	36,4	20,8
CPX	49170		49,7	1,0	4,4	8,5	0,3	16,4	18,1	0,8	0,0	0,0	0,0	0,3	99,5	42,1	38,1	19,8
CPX	49170		48,5	1,2	5,0	10,0	0,3	15,3	17,9	0,7	0,0	0,0	0,0	0,0	99,0	41,4	35,5	23,1
CPX	49170		49,5	0,8	4,3	6,7	0,2	16,4	19,3	0,7	0,0	0,0	0,0	0,8	98,7	45,5	38,7	15,8
CPX	49170	rim	48,6	1,2	4,4	10,4	0,2	14,2	19,3	0,6	0,0	0,0	0,0	0,0	99,0	44,0	32,4	23,6
CPX	49170		49,7	1,0	4,3	7,9	0,0	16,1	19,2	0,7	0,0	0,0	0,0	0,4	99,3	44,4	37,3	18,2
CPX	49170		52,3	0,4	2,4	5,9	0,0	17,3	20,4	0,6	0,0	0,0	0,0	0,5	99,8	46,8	39,6	13,6
CPX	49170		52,5	0,4	2,0	9,6	0,2	18,8	16,1	0,7	0,0	0,0	0,0	0,0	100,4	36,2	42,3	21,5
CPX	49170		50,7	0,6	3,9	6,2	0,0	16,1	21,3	0,7	0,0	0,0	0,0	0,7	100,0	48,9	36,9	14,2
CPX	49170		51,1	0,6	3,2	6,1	0,0	16,8	20,4	0,6	0,0	0,0	0,0	0,8	99,5	47,2	38,8	14,0
CPX	49170		50,6	0,7	3,9	6,2	0,0	16,2	20,3	0,5	0,0	0,0	0,0	1,2	99,5	47,6	37,9	14,4
CPX	49170		46,3	2,7	5,5	15,2	0,3	11,6	17,9	0,9	0,0	0,0	0,0	0,0	100,4	40,1	26,0	33,9
CPX	49182		50,1	0,8	3,6	7,9	0,0	14,4	21,9	0,8	0,0	0,0	0,0	0,0	99,4	49,5	32,6	18,0
CPX	49182		49,0	0,9	3,9	7,8	0,0	14,1	21,9	0,8	0,0	0,0	0,0	0,0	98,4	50,0	32,2	17,8
CPX	49182		48,5	1,2	3,9	10,6	0,3	13,0	20,8	0,7	0,0	0,0	0,0	0,0	99,0	46,8	29,3	24,0
CPX	49182		49,7	0,9	3,8	7,8	0,0	14,3	22,1	0,8	0,0	0,0	0,0	0,0	99,5	50,0	32,4	17,6
CPX	49182		50,3	0,7	3,7	6,5	0,0	15,0	22,4	0,7	0,0	0,0	0,0	0,0	99,3	51,1	34,2	14,7
CPX	49182		50,5	0,8	3,5	8,2	0,0	14,9	21,7	0,7	0,0	0,0	0,0	0,0	100,4	48,5	33,2	18,3
CPX	49171		51,5	0,4	2,9	6,2	0,0	17,3	19,5	0,6	0,0	0,0	0,0	0,5	98,8	45,5	40,2	14,4
CPX	49171		51,8	0,4	2,2	7,6	0,2	18,3	17,8	0,7	0,0	0,0	0,0	0,0	99,0	40,8	41,8	17,4
CPX	49171		51,1	0,6	3,8	6,4	0,0	17,0	20,1	0,8	0,0	0,0	0,0	0,4	100,2	46,2	39,0	14,8
CPX	49171		50,1	0,8	3,7	7,6	0,0	15,9	20,0	0,5	0,0	0,0	0,0	0,2	98,8	46,0	36,5	17,5
CPX	49171		49,7	1,0	5,0	8,5	0,0	17,1	17,8	0,6	0,0	0,0	0,0	0,0	99,5	41,0	39,4	19,6
CPX	49171		50,4	0,6	4,3	6,3	0,0	16,5	19,5	0,5	0,0	0,0	0,0	0,6	98,7	46,1	39,0	14,9
CPX	49171		51,2	0,7	3,5	6,9	0,0	16,4	20,5	0,5	0,0	0,0	0,0	0,3	100,0	46,9	37,4	15,8
CPX	49171		51,1	0,8	3,3	9,1	0,0	17,0	17,4	0,6	0,0	0,0	0,0	0,0	99,1	40,0	39,0	20,9
CPX	49171		48,7	1,4	4,6	11,3	0,2	14,5	18,2	0,6	0,0	0,0	0,0	0,0	99,5	41,4	32,9	25,7
CPX	49171		52,1	0,4	2,3	5,3	0,0	17,0	21,4	0,6	0,0	0,0	0,0	0,4	99,4	48,9	39,0	12,1
CPX	49171		51,1	0,7	3,7	6,6	0,0	17,3	19,5	0,6	0,0	0,0	0,0	0,5	99,9	44,8	39,9	15,3
CPX	49178		49,6	0,7	4,4	7,4	0,0	15,3	20,4	0,7	0,0	0,0	0,0	0,5	99,0	47,3	35,5	17,2
CPX	49178		51,5	0,5	2,8	7,7	0,0	15,8	20,4	0,5	0,0	0,0	0,0	0,0	99,1	46,5	36,0	17,5
CPX	49178		50,4	0,5	1,4	16,5	0,7	13,4	15,7	0,7	0,0	0,0	0,0	0,0	99,3	34,5	29,4	36,1
CPX	49178		50,1	0,6	4,0	8,1	0,2	15,4	20,5	0,5	0,0	0,0	0,0	0,0	99,5	46,6	35,0	18,4
CPX	49178		52,0	0,4	2,1	8,4	0,2	16,6	19,7	0,7	0,0	0,0	0,0	0,0	100,2	44,0	37,2	18,8

Mineral	Sample#		SiO2	TiO2	Al2O3	FeO	MnO	MgO	CaO	Na2O	K2O	Cl	P2O5	Cr2O3	Total			
CPX	49178		50,9	0,6	3,0	7,5	0,0	15,8	21,1	0,8	0,0	0,0	0,0	0,0	99,6	47,5	35,6	16,9
CPX	49178		51,9	0,3	2,2	6,9	0,0	16,9	20,0	0,5	0,0	0,0	0,0	0,0	98,7	45,7	38,7	15,6
CPX	49178		50,4	0,7	3,4	8,9	0,0	15,2	20,6	0,6	0,0	0,0	0,0	0,0	99,7	46,0	34,0	19,9
CPX	49178		49,6	0,6	4,1	9,6	0,3	15,2	19,0	0,6	0,0	0,0	0,0	0,0	98,9	43,3	34,6	22,0
CPX	49172		50,8	0,6	2,3	10,1	0,3	14,9	19,7	0,5	0,0	0,0	0,0	0,0	99,3	44,0	33,3	22,7
CPX	49172		50,6	0,8	2,8	9,8	0,2	15,2	19,8	0,7	0,0	0,0	0,0	0,2	100,2	44,2	34,0	21,9
CPX	49172		49,8	0,9	2,8	11,2	0,3	14,5	18,7	0,7	0,0	0,0	0,0	0,0	99,0	42,1	32,7	25,3
CPX	49172		51,2	0,5	2,4	8,5	0,0	15,6	20,4	0,7	0,0	0,0	0,0	0,0	99,2	45,8	35,2	19,0
CPX	49172		50,3	0,8	3,2	12,2	0,4	15,5	17,2	0,7	0,0	0,0	0,0	0,0	100,1	38,2	34,5	27,2
CPX	49172		48,8	0,0	31,5	0,9	0,0	0,4	15,3	3,1	0,0	0,0	0,0	0,0	99,9	92,5	2,3	5,2
CPX	49172		50,9	0,6	2,8	9,8	0,4	14,7	19,6	0,5	0,0	0,0	0,0	0,0	99,3	44,5	33,4	22,2
CPX	49172		50,9	0,7	2,3	9,9	0,0	14,9	20,0	0,7	0,0	0,0	0,0	0,0	99,5	44,5	33,3	22,2
CPX	49172	rim	49,5	1,0	3,3	10,6	0,2	14,6	19,4	0,7	0,0	0,0	0,0	0,0	99,2	43,5	32,7	23,8
CPX	49172	rim	50,8	0,8	2,7	10,4	0,2	15,4	19,3	0,9	0,0	0,0	0,3	0,0	100,9	42,9	34,1	23,0
CPX	49172		49,2	1,1	3,4	11,5	0,3	14,3	18,6	0,8	0,0	0,0	0,0	0,0	99,0	42,0	32,2	25,9
CPX	49174		50,2	0,5	3,9	6,8	0,0	16,0	20,3	0,7	0,0	0,0	0,0	0,3	98,6	47,1	37,2	15,7
CPX	49174		50,3	0,5	3,8	6,7	0,0	16,1	20,3	0,6	0,0	0,0	0,0	0,3	98,6	47,2	37,3	15,5
CPX	49174		51,2	0,5	2,3	7,8	0,2	16,1	20,2	0,6	0,0	0,0	0,0	0,0	98,9	45,8	36,6	17,6
CPX	49174		51,0	0,5	2,0	8,3	0,2	16,2	19,3	0,6	0,0	0,0	0,0	0,0	98,1	44,1	36,9	19,0
CPX	49174		50,1	0,7	2,3	17,1	0,6	14,0	14,4	0,7	0,0	0,0	0,0	0,0	99,9	31,6	30,7	37,6
CPX	49174		51,7	0,3	1,9	8,0	0,0	17,8	18,1	0,6	0,0	0,0	0,0	0,0	98,3	41,3	40,6	18,1
CPX	49174		51,8	0,3	1,9	7,5	0,0	16,9	19,8	0,6	0,0	0,0	0,0	0,0	98,8	44,8	38,3	16,9
CPX	49174		49,9	0,5	3,7	6,8	0,0	16,2	20,4	0,6	0,0	0,0	0,0	0,3	98,3	46,9	37,4	15,7
CPX	49174		50,1	0,7	3,7	7,8	0,0	15,7	20,2	0,7	0,0	0,0	0,2	0,0	99,1	46,1	35,9	18,0
CPX	47127		51,4	0,5	2,6	7,2	0,2	16,1	20,7	0,0	0,0	0,0	0,0	0,2	98,9	47,0	36,6	16,5
CPX	47127	rim	52,0	0,0	0,4	14,5	0,7	10,6	20,8	0,8	0,0	0,0	0,0	0,0	99,7	45,3	23,1	31,6
CPX	47127		51,0	0,8	3,1	7,6	0,0	15,7	20,1	0,0	0,0	0,0	0,0	0,3	98,5	46,3	36,1	17,6
CPX	47127		51,8	0,5	2,1	7,7	0,0	16,7	19,2	0,0	0,0	0,0	0,0	0,2	98,1	44,0	38,4	17,6
CPX	47127		51,6	0,6	2,6	7,7	0,2	16,2	20,1	0,0	0,0	0,0	0,0	0,0	99,0	45,6	36,9	17,5
CPX	47127	rim	44,8	1,0	1,1	22,1	0,4	11,5	19,1	0,0	0,0	0,0	0,0	0,0	100,0	36,2	21,8	42,0
CPX	49123		51,2	0,7	2,7	9,8	0,3	15,7	19,3	0,0	0,0	0,0	0,0	0,0	99,6	43,1	35,1	21,8
CPX	49123		52,1	0,6	2,2	9,7	0,3	16,3	19,2	0,0	0,0	0,0	0,0	0,0	100,4	42,4	36,1	21,5
CPX	49123	rim	50,4	1,4	3,4	16,5	0,5	15,8	13,4	0,0	0,0	0,0	0,0	0,0	101,3	29,3	34,6	36,1
CPX	49123	rim	51,7	0,7	1,9	15,0	0,4	17,1	13,2	0,0	0,0	0,0	0,0	0,0	100,1	29,2	37,7	33,1
CPX	49123		50,9	0,7	2,7	9,7	0,3	15,6	19,2	0,0	0,0	0,0	0,0	0,0	99,1	43,1	35,1	21,8

Mineral	Sample#		SiO2	TiO2	Al2O3	FeO	MnO	MgO	CaO	Na2O	K2O	Cl	P2O5	Cr2O3	Total			
CPX	49123		51,9	0,6	2,2	9,7	0,3	16,2	19,1	0,0	0,0	0,0	0,0	0,0	99,9	42,4	36,1	21,5
CPX	49123	rim	50,2	1,4	3,4	16,4	0,5	15,7	13,3	0,0	0,0	0,0	0,0	0,0	100,8	29,3	34,6	36,1
CPX	49123		50,1	0,8	3,7	6,9	0,0	15,9	20,5	0,0	0,0	0,0	0,0	0,6	98,5	47,3	36,7	16,0
CPX	49123	rim	52,6	0,7	1,9	13,2	0,4	16,0	15,0	0,0	0,0	0,0	0,0	0,0	99,7	33,9	36,1	29,9
CPX	49123		51,4	0,5	2,6	7,0	0,0	16,2	20,6	0,0	0,0	0,0	0,0	0,4	98,7	47,0	36,9	16,1
CPX	49123	rim	56,2	0,7	2,4	14,5	0,3	13,7	11,6	0,0	0,0	0,0	0,0	0,0	99,4	29,1	34,4	36,5
CPX	49123		51,6	0,6	2,0	10,0	0,2	15,8	18,0	0,0	0,0	0,0	0,0	0,2	98,5	41,1	36,1	22,8
CPX	47660		49,8	1,0	4,7	8,0	0,2	15,6	19,8	0,0	0,0	0,0	0,0	0,0	99,2	45,7	36,0	18,3
CPX	47660		50,0	0,7	4,4	8,3	0,2	16,4	18,8	0,0	0,0	0,0	0,0	0,0	98,9	43,2	37,7	19,1
CPX	47660		51,5	0,6	3,6	8,4	0,3	18,2	16,9	0,0	0,0	0,0	0,0	0,0	99,5	38,8	41,9	19,3
CPX	47660	rim	48,9	1,2	4,6	13,2	0,4	12,9	16,7	0,0	0,6	0,0	0,0	0,0	98,3	39,1	30,1	30,8
CPX	47660	rim	51,2	0,7	6,9	10,4	0,2	11,9	17,2	1,1	0,3	0,0	0,0	0,0	99,8	43,7	30,1	26,3
CPX	47660	rim	49,4	1,0	3,4	13,0	0,4	13,6	18,5	0,0	0,0	0,0	0,0	0,0	99,2	41,0	30,2	28,8
CPX	47660		51,7	0,5	2,6	7,9	0,3	16,5	19,9	0,0	0,0	0,0	0,0	0,0	99,2	45,0	37,2	17,8
CPX	47660	rim	49,6	0,8	3,8	11,9	0,4	13,8	19,3	0,0	0,0	0,0	0,0	0,0	99,6	42,9	30,7	26,5
CPX	47660		50,2	0,9	3,8	10,5	0,2	14,8	19,6	0,0	0,0	0,0	0,0	0,0	100,0	43,7	32,9	23,4
CPX	47666	rim	39,9	1,1	6,9	21,9	0,4	23,8	2,6	1,2	0,0	0,1	0,0	0,0	97,9	5,3	49,3	45,4
CPX	47666		51,7	0,6	2,3	6,6	0,0	16,9	20,5	0,0	0,0	0,0	0,0	0,4	98,9	46,6	38,5	15,0
CPX	47666	rim	47,2	1,8	6,3	10,0	0,0	13,9	20,0	0,0	0,0	0,0	0,0	0,0	99,1	45,6	31,6	22,8
CPX	47666		50,3	0,8	3,8	6,2	0,3	15,3	21,8	0,0	0,0	0,0	0,0	0,9	99,3	50,4	35,4	14,2
CPX	47666	rim	51,5	0,5	2,4	6,0	0,0	16,3	21,3	0,0	0,0	0,0	0,0	0,6	98,6	48,9	37,4	13,7
CPX	47666	rim	46,2	1,7	14,6	9,0	0,0	6,1	14,3	1,4	0,0	0,0	0,0	0,0	93,3	48,7	20,6	30,6
CPX	47643		51,1	0,7	3,5	8,5	0,3	16,6	18,7	0,0	0,0	0,0	0,0	0,0	99,3	42,8	37,9	19,3
CPX	47643		52,5	0,4	2,1	7,2	0,2	18,0	18,9	0,0	0,0	0,0	0,0	0,3	99,6	42,9	40,8	16,3
CPX	47643		52,2	0,4	2,2	6,7	0,0	17,1	20,1	0,0	0,0	0,0	0,0	0,2	99,0	45,7	39,0	15,3
CPX	47643		52,4	0,5	2,3	6,8	0,2	17,7	19,6	0,0	0,0	0,0	0,0	0,3	99,8	44,4	40,1	15,5
CPX	47643		51,4	0,7	3,0	6,6	0,0	15,9	20,8	0,0	0,0	0,0	0,0	0,6	98,9	48,1	36,7	15,2
CPX	47643	rim	51,1	0,7	2,9	6,3	0,0	16,0	21,0	0,0	0,0	0,0	0,0	0,6	98,6	48,5	36,9	14,6
CPX	47643		50,4	0,7	4,1	7,6	0,2	16,4	19,8	0,0	0,0	0,0	0,0	0,2	99,4	45,3	37,3	17,4
CPX	47643		49,9	1,0	4,8	8,5	0,3	15,6	18,6	0,0	0,0	0,0	0,0	0,0	98,7	43,6	36,5	19,9
CPX	47643		53,0	0,3	2,0	7,4	0,3	18,4	18,7	0,0	0,0	0,0	0,0	0,2	100,4	42,0	41,3	16,6
CPX	47643		51,7	0,4	2,6	8,2	0,3	18,0	17,6	0,0	0,0	0,0	0,0	0,3	99,2	40,2	41,1	18,7
CPX	47643	rim	52,9	0,4	2,1	7,2	0,2	17,9	18,8	0,0	0,0	0,0	0,0	0,4	99,9	42,7	40,9	16,4
CPX	47643		50,5	0,8	4,3	7,6	0,0	16,4	19,1	0,0	0,0	0,0	0,0	0,5	99,2	44,3	38,1	17,6
CPX	47661		49,6	1,0	4,8	6,6	0,0	14,8	22,4	0,0	0,0	0,0	0,0	0,7	99,8	51,2	33,8	15,0

Mineral	Sample#		SiO2	TiO2	Al2O3	FeO	MnO	MgO	CaO	Na2O	K2O	Cl	P2O5	Cr2O3	Total			
CPX	47661		50,7	0,9	4,1	6,4	0,0	14,8	22,1	0,0	0,0	0,0	0,0	0,6	99,5	51,0	34,1	14,9
CPX	47661		50,7	0,8	3,3	6,0	0,0	15,2	22,5	0,0	0,0	0,0	0,0	0,5	99,2	51,5	34,8	13,7
CPX	47661		49,9	0,9	4,4	6,9	0,0	14,6	21,7	0,0	0,0	0,0	0,0	0,7	99,0	50,2	33,7	16,1
CPX	kn2		51,9	0,4	1,9	8,0	0,4	16,6	20,1	0,0	0,0	0,0	0,0	0,0	99,2	44,9	37,2	17,9
CPX	kn2	rim	51,0	0,4	3,2	7,9	0,2	15,8	20,7	0,0	0,0	0,0	0,0	0,3	99,4	46,7	35,6	17,7
CPX	kn2		51,6	0,3	2,4	6,1	0,0	17,0	20,4	0,0	0,0	0,0	0,0	0,6	98,3	46,9	39,0	14,1
CPX	kn2		51,3	0,3	2,4	6,2	0,2	17,1	20,3	0,0	0,0	0,0	0,0	0,6	98,3	46,6	39,2	14,2
CPX	kn65		51,5	0,4	2,1	8,4	0,2	16,5	19,5	0,7	0,0	0,0	0,0	0,0	99,3	43,9	37,2	18,9
CPX	kn 49		49,7	1,9	4,1	11,6	0,2	14,1	18,2	0,0	0,0	0,0	0,0	0,1	99,9	41,5	32,1	26,4
CPX	kn 49		50,6	1,3	4,0	8,8	0,1	16,0	18,6	0,1	0,1	0,0	0,0	0,4	99,9	43,0	36,8	20,2
CPX	kn 49		49,6	0,1	30,9	0,6	0,0	0,0	15,3	2,8	0,1	0,0	0,0	0,2	99,6	96,2	0,0	3,8
CPX	kn 49		52,0	0,7	1,9	9,9	0,3	16,9	16,7	0,0	0,0	0,0	0,0	0,1	98,6	38,4	38,8	22,8
CPX	kn 49		51,5	0,8	2,6	7,8	0,3	16,3	19,8	0,0	0,1	0,0	0,0	0,4	99,6	45,1	37,1	17,8
CPX	kn 49		49,8	1,5	3,6	11,5	0,3	14,5	17,5	0,0	0,1	0,0	0,0	0,2	99,2	40,2	33,4	26,5
CPX	kn 49		51,3	1,0	3,7	8,4	0,2	15,8	19,6	0,0	0,1	0,0	0,0	0,5	100,8	44,7	36,1	19,1
CPX	kn 49		50,7	1,6	3,0	12,2	0,3	14,4	18,6	0,0	0,1	0,0	0,0	0,0	100,7	41,2	31,9	27,0
CPX	kn 49		51,6	1,1	3,7	9,2	0,2	16,2	18,9	0,0	0,1	0,0	0,0	0,2	101,3	42,6	36,6	20,8
CPX	47649		49,8	2,0	3,8	11,9	0,3	13,3	20,0	0,0	0,1	0,0	0,0	0,0	101,2	44,3	29,4	26,3
CPX	47649		49,3	1,7	3,5	11,9	0,2	13,7	19,0	0,0	0,1	0,0	0,0	0,1	99,7	42,7	30,7	26,6
CPX	47649		51,3	0,6	1,1	15,7	0,6	14,0	16,0	0,0	0,0	0,0	0,0	0,1	99,6	35,0	30,6	34,3
CPX	47649		49,0	1,8	3,3	11,9	0,3	13,2	19,4	0,0	0,1	0,0	0,0	0,1	99,1	43,6	29,7	26,8
CPX	47649		52,9	0,8	1,7	9,7	0,2	17,0	18,4	0,0	0,1	0,0	0,0	0,2	101,2	40,7	37,7	21,6
CPX	KN34		49,2	1,2	4,2	8,4	0,1	14,1	20,7	0,0	0,1	0,0	0,0	0,2	98,2	47,9	32,6	19,4
CPX	KN34		50,6	0,7	3,0	7,7	0,1	14,9	20,9	0,0	0,0	0,0	0,0	0,2	98,2	48,1	34,1	17,8
CPX	KN34		51,2	0,7	2,4	7,2	0,1	15,6	21,3	0,0	0,0	0,0	0,0	0,3	98,8	48,3	35,3	16,4
CPX	KN34		49,9	1,0	4,2	8,2	0,2	14,6	21,1	0,1	0,1	0,0	0,0	0,3	99,7	48,1	33,3	18,6
CPX	KN34		50,8	1,0	1,8	9,6	0,3	15,1	19,6	0,0	0,0	0,0	0,0	0,0	98,3	44,3	34,1	21,6
CPX	KN34		50,3	0,8	2,8	8,0	0,2	14,7	21,0	0,0	0,1	0,0	0,0	0,2	98,2	48,1	33,7	18,3
CPX	KN34		51,7	0,6	1,7	8,9	0,3	15,7	20,2	0,0	0,0	0,0	0,0	0,2	99,5	45,0	35,1	19,9
CPX	KN34		51,8	0,6	3,0	7,2	0,1	15,7	21,4	0,0	0,1	0,0	0,0	0,4	100,3	48,4	35,5	16,1
CPX	KN34		51,8	0,7	2,6	6,0	0,2	16,2	21,7	0,0	0,1	0,0	0,0	0,2	99,5	49,4	37,0	13,6
CPX	KN34		50,0	1,2	4,3	9,2	0,2	14,4	20,6	0,0	0,0	0,1	0,0	0,1	100,3	46,6	32,6	20,8
CPX	KN34		51,4	0,9	2,7	8,4	0,3	14,9	21,4	0,0	0,1	0,0	0,1	0,1	100,4	47,9	33,4	18,7
CPX	KN78		51,2	1,1	3,7	8,2	0,2	16,0	19,8	0,2	0,1	0,0	0,0	0,5	101,0	45,0	36,4	18,6
CPX	KN78		52,0	0,5	2,1	6,9	0,1	16,6	20,3	0,0	0,1	0,0	0,0	0,3	99,0	46,3	37,9	15,8

Mineral	Sample#		SiO2	TiO2	Al2O3	FeO	MnO	MgO	CaO	Na2O	K2O	Cl	P2O5	Cr2O3	Total			
CPX	KN78		51,3	0,9	2,5	9,6	0,3	17,2	17,2	0,0	0,0	0,0	0,0	0,2	99,2	39,1	39,1	21,8
CPX	KN78		51,6	0,9	2,1	7,6	0,3	17,0	19,0	0,0	0,1	0,0	0,0	0,3	98,8	43,7	38,9	17,4
CPX	KN78		51,7	0,6	2,3	6,6	0,2	16,2	20,4	0,2	0,0	0,0	0,0	0,3	98,6	47,3	37,4	15,2
CPX	47663		51,4	0,8	3,0	12,2	0,4	13,3	17,6	0,2	0,1	0,0	0,0	0,0	99,2	40,9	30,8	28,3
CPX	47663		52,1	0,7	1,7	10,2	0,3	16,4	17,9	0,0	0,0	0,0	0,0	0,0	99,5	40,3	36,8	22,9
CPX	47663		53,3	0,5	1,4	7,7	0,2	18,2	18,2	0,0	0,0	0,0	0,0	0,3	99,9	41,3	41,2	17,5
CPX	47663		51,9	1,2	2,7	11,9	0,3	15,2	18,2	0,1	0,1	0,0	0,0	0,2	101,9	40,3	33,5	26,2
CPX	47663		51,1	1,0	3,5	10,5	0,3	15,2	18,9	0,0	0,1	0,0	0,0	0,1	100,8	42,3	34,1	23,6
CPX	47663		51,2	1,0	3,4	10,4	0,3	15,4	18,9	0,0	0,1	0,0	0,0	0,2	100,9	42,3	34,4	23,3
CPX	47663		53,6	0,6	2,0	7,3	0,2	17,7	19,0	0,0	0,0	0,0	0,0	0,3	100,7	43,2	40,3	16,6
CPX	47663		51,0	1,4	2,3	12,4	0,3	14,3	17,8	0,1	0,1	0,0	0,0	0,1	99,8	40,0	32,2	27,8
CPX	47663		51,2	0,9	3,5	8,5	0,1	16,6	18,3	0,0	0,1	0,0	0,0	0,2	99,6	42,1	38,3	19,7
CPX	47665		47,7	2,0	5,4	7,6	0,2	13,9	21,2	0,0	0,0	0,0	0,0	0,5	98,4	49,8	32,5	17,7
CPX	47665		50,6	1,2	4,5	7,4	0,1	15,1	22,1	0,0	0,1	0,0	0,0	0,2	101,3	49,6	33,8	16,6
CPX	47665		51,6	1,2	3,5	7,6	0,1	15,2	21,9	0,0	0,1	0,0	0,0	0,1	101,4	48,9	34,0	17,1
CPX	47665		51,0	1,4	4,0	6,6	0,2	15,1	21,9	0,0	0,1	0,1	0,0	0,4	100,9	50,2	34,6	15,2
CPX	47665		46,2	2,6	7,7	9,0	0,2	12,9	21,0	0,0	0,1	0,0	0,0	0,1	99,9	49,0	30,1	20,9
CPX	KN94		46,8	2,5	4,7	13,1	0,3	11,9	19,0	0,2	0,1	0,0	0,0	0,1	98,8	43,2	27,0	29,7
CPX	KN94		45,5	3,2	7,4	10,0	0,2	11,9	20,9	0,5	0,1	0,0	0,0	0,0	99,8	48,8	27,8	23,4
CPX	KN94		45,1	3,7	7,7	12,4	0,2	11,2	20,2	0,2	0,0	0,1	0,0	0,0	101,0	46,2	25,6	28,2
CPX	KN94		46,6	3,2	7,3	9,6	0,1	12,4	21,5	0,2	0,0	0,0	0,0	0,1	101,1	49,4	28,5	22,1
CPX	KN94		47,6	2,3	5,8	11,8	0,2	12,5	19,5	0,6	0,0	0,0	0,0	0,0	100,4	44,6	28,5	26,9
CPX	KN94		51,7	1,1	2,9	9,6	0,2	16,2	18,8	0,3	0,0	0,0	0,0	0,1	100,9	42,2	36,3	21,4
CPX	KN94		52,4	0,8	2,6	9,0	0,3	16,3	19,4	0,4	0,0	0,0	0,0	0,2	101,4	43,4	36,5	20,1
CPX	KN94		47,4	2,5	6,6	9,4	0,1	13,1	20,8	0,4	0,1	0,0	0,0	0,2	100,6	48,0	30,3	21,7
CPX	KN116		52,2	0,6	3,3	6,7	0,2	16,9	19,6	0,2	0,0	0,0	0,0	1,0	100,8	45,4	39,0	15,6
CPX	KN116		52,5	0,8	2,7	6,7	0,1	16,9	20,0	0,2	0,0	0,0	0,0	0,5	100,6	45,9	38,7	15,4
CPX	KN116		53,0	0,6	2,0	6,2	0,3	17,2	20,3	0,2	0,1	0,0	0,0	0,4	100,4	46,5	39,4	14,1
CPX	KN116		52,3	0,5	2,6	6,3	0,0	16,8	20,7	0,1	0,1	0,0	0,0	0,6	100,1	47,2	38,4	14,3
CPX	KN116		53,0	0,7	2,3	6,1	0,2	17,1	20,7	0,1	0,0	0,0	0,0	0,7	101,1	47,2	38,9	13,9

Mineral	Sample#		SiO2	TiO2	Al2O3	FeO	MnO	MgO	CaO	Na2O	K2O	Cl	P2O5	Cr2O3	Total			
							New Caledonia											
CPX	49225		51,2	0,6	2,3	10,1	0,3	15,5	19,8	0,7	0,0	0,0	0,2	0,1	100,7	43,6	34,1	22,3
CPX	49225		50,4	0,7	2,2	10,2	0,2	14,8	19,9	0,7	0,0	0,0	0,1	0,0	99,2	44,2	33,0	22,8
CPX	49225		51,3	0,5	2,6	7,0	0,2	16,4	20,8	0,6	0,0	0,0	0,1	0,4	99,9	47,2	37,0	15,8
CPX	49225		51,9	0,6	2,6	7,1	0,2	16,5	20,9	0,7	0,0	0,0	0,2	0,1	100,7	47,0	37,0	16,0
CPX	49225		51,3	0,5	2,3	7,4	0,1	16,0	20,8	0,5	0,0	0,0	0,2	0,0	99,2	46,9	36,2	16,8
CPX	49225		50,0	0,8	2,3	12,1	0,3	14,3	19,0	0,7	0,0	0,0	0,1	0,0	99,6	41,8	31,5	26,7
CPX	49225		50,3	0,7	2,1	12,6	0,3	14,2	18,7	0,9	0,0	0,0	0,1	0,2	100,3	41,1	31,3	27,6
CPX	49225		50,9	0,6	2,5	8,7	0,2	15,2	20,4	0,6	0,0	0,0	0,1	0,2	99,5	46,1	34,4	19,5
CPX	49225		51,6	0,4	2,4	6,7	0,2	16,3	20,9	0,5	0,0	0,0	0,1	0,2	99,3	47,6	37,1	15,3
CPX	49225		50,3	0,8	1,8	14,3	0,4	13,5	17,9	0,5	0,0	0,0	0,1	0,0	99,5	39,3	29,5	31,3
CPX	49251		50,1	0,8	3,8	7,0	0,1	15,9	20,3	0,8	0,0	0,0	0,1	0,6	99,4	47,0	36,8	16,2
CPX	49251		51,4	0,3	2,0	6,9	0,2	17,3	18,7	0,5	0,0	0,0	0,2	0,4	98,0	43,7	40,3	16,0
CPX	49251		49,9	0,7	3,5	6,7	0,1	15,9	20,3	0,6	0,0	0,0	0,1	0,9	98,7	47,3	37,1	15,6
CPX	49251		52,2	0,4	2,2	8,3	0,2	18,1	17,5	0,6	0,0	0,0	0,1	0,2	99,7	39,9	41,2	18,9
CPX	49251		50,5	0,7	3,6	7,3	0,2	16,1	20,0	0,7	0,0	0,0	0,0	0,2	99,2	46,2	37,0	16,7
CPX	49251		50,0	0,7	3,4	6,6	0,2	16,0	20,4	0,6	0,0	0,0	0,1	0,6	98,6	47,5	37,2	15,3
CPX	49251		51,4	0,4	2,5	7,2	0,1	16,5	19,7	0,6	0,0	0,0	0,1	0,4	98,9	45,4	38,1	16,6
CPX	49251		51,5	0,4	2,2	6,5	0,1	17,0	19,7	0,8	0,0	0,0	0,1	0,6	98,8	45,7	39,3	15,1
CPX	49251		50,8	0,5	2,3	6,8	0,2	16,4	20,1	0,6	0,0	0,0	0,2	0,2	98,1	46,4	38,0	15,6
CPX	49251		50,0	0,7	3,6	7,4	0,1	15,8	19,8	0,6	0,0	0,0	0,1	0,2	98,1	46,2	36,7	17,1
CPX	49251		52,4	0,5	1,9	6,6	0,2	17,0	20,0	0,6	0,0	0,0	0,1	0,3	99,5	45,8	39,0	15,2
CPX	49251		49,9	0,7	3,5	6,2	0,1	15,6	21,4	0,6	0,0	0,0	0,1	0,8	99,0	49,5	36,1	14,4

PYX = pyroxene

PLAG = plagioclase

All analyses with totals > 98% are listed.

Only analyses with totals >98.5% were used in Chapters 2 and 3.

Unless otherwise stated, analyses are taken from the core of the mineral grain.

Some plagioclase analyses are from the groundmass.

The presented mineral compositions for both the Tangihua Complex and the Poya terrane were determined from carbon-coated polished thin sections by energy dispersive (EDS) methods using the JOEL JXA-5A electron microprobe housed in the Department of Geology, University of Auckland, and at the University of Clermont-Ferrand using a Comeca ????

Electron Microprobe Data

Orthopyroxene

Appendix 4

Mineral	Sample	SiO2	TiO2	Al2O3	FeO	MnO	MgO	CaO	Na2O	K2O	Cl	P2O5	SO3	Cr2O3	NiO	TOTAL
New Zealand																
OPX	49158	53,00	0,82	1,69	16,96	0,48	19,08	9,52	0,00	0,05	0,02	0,00	0,12	0,00	0,00	101,7
OPX	49158	52,61	0,87	1,84	13,90	0,30	17,29	13,45	0,00	0,02	0,02	0,00	0,00	0,09	0,04	100,4
OPX	49158	51,90	1,36	2,98	13,54	0,40	17,08	15,09	0,00	0,03	0,00	0,00	0,10	0,10	0,02	102,6
OPX	47649	54,57	0,52	1,23	13,79	0,38	20,42	11,44	0,00	0,08	0,03	0,00	0,00	0,02	0,08	102,6
OPX	47649	53,64	0,53	1,58	14,33	0,38	19,26	11,18	0,00	0,00	0,00	0,00	0,00	0,01	0,09	101,0
OPX	47649	51,09	1,15	1,25	13,63	0,32	15,60	16,13	0,00	0,12	0,01	0,00	0,00	0,09	0,05	99,4
OPX	49186	52,38	0,59	0,74	16,35	0,49	18,78	9,76	0,00	0,05	0,00	0,00	0,10	0,07	0,09	99,4
OPX	49186	52,56	0,43	0,97	13,50	0,38	19,04	12,44	0,00	0,04	0,05	0,00	0,00	0,13	0,06	99,6
OPX	49186	52,03	0,68	1,86	10,66	0,31	18,55	14,65	0,26	0,05	0,01	0,00	0,01	0,08	0,09	99,3
OPX	49186	49,04	1,44	4,38	10,28	0,25	14,30	19,62	0,15	0,02	0,00	0,00	0,05	0,05	0,00	99,6
OPX	47663	53,26	0,29	0,43	23,12	0,75	20,94	1,95	0,00	0,03	0,00	0,00	0,10	0,02	0,08	101,0
OPX	47663	53,53	0,34	0,43	22,61	0,64	21,44	2,00	0,00	0,09	0,00	0,00	0,00	0,02	0,00	101,1
OPX	47663	52,82	0,52	1,15	23,58	0,52	20,34	2,12	0,00	0,03	0,02	0,00	0,00	0,00	0,01	101,1
OPX	47663	51,85	0,54	0,74	23,39	0,72	19,76	2,30	0,00	0,03	0,04	0,00	0,07	0,01	0,00	99,5
OPX	47663	53,67	0,31	0,13	20,23	0,71	21,66	3,27	0,00	0,05	0,02	0,00	0,13	0,01	0,02	100,2
OPX	47663	53,41	0,48	1,04	19,79	0,65	20,97	3,60	0,00	0,09	0,00	0,00	0,00	0,00	0,05	100,1
OPX	49201	41,33	5,71	11,40	16,31	0,16	11,01	10,89	2,76	0,12	0,07	0,00	0,00	0,05	0,18	100,0
OPX	49201	39,46	6,18	11,23	16,88	0,21	9,92	10,93	2,46	0,17	0,06	0,00	0,13	0,00	0,00	97,6
OPX	49201	40,19	6,00	11,24	16,04	0,14	10,54	10,97	2,71	0,16	0,03	0,00	0,05	0,11	0,06	98,3
OPX	49201	40,47	5,90	11,52	15,34	0,22	11,42	10,74	2,59	0,13	0,06	0,00	0,12	0,03	0,00	98,5

Electron Microprobe Data

Olivine

Appendix 5

Sample	SiO2	TiO2	Al2O3	FeO	MnO	MgO	CaO	Na2O	K2O	Cl	P2O5	Cr2O3	Total
					New Zealand								
49182,00	37,70	0,00	0,00	25,00	0,39	36,26	0,28	0,91	0,00	0,00	0,00	0,00	100,54
49182,00	37,09	0,00	0,00	25,52	0,51	35,44	0,31	0,85	0,00	0,00	0,00	0,00	99,72
49182,00	35,77	0,00	0,00	33,10	0,67	29,45	0,32	0,98	0,00	0,00	0,00	0,00	100,29
49182,00	36,30	0,00	0,00	33,59	0,68	29,56	0,40	0,73	0,00	0,00	0,00	0,00	101,26
49182,00	35,16	0,00	0,00	39,53	0,78	24,48	0,40	0,70	0,00	0,00	0,00	0,00	101,06
47666	39,15	0,00	0,29	19,04	0,20	41,05	0,24	0,00	0,00	0,00	0,00	0,00	99,98
47666	38,92	0,00	0,00	18,79	0,30	41,23	0,24	0,00	0,00	0,00	0,00	0,00	99,48
47666	38,41	0,00	0,00	18,75	0,35	40,47	0,26	0,00	0,00	0,00	0,00	0,00	98,24
47666	38,98	0,00	0,00	19,10	0,32	41,10	0,23	0,00	0,00	0,00	0,00	0,00	99,72
47666	38,50	0,00	0,87	17,99	0,29	38,75	0,43	0,00	0,00	0,00	0,00	0,00	96,83
47666	39,51	0,00	0,36	19,13	0,28	41,00	0,35	0,00	0,00	0,00	0,00	0,00	100,63
49143	39,55	0	0	15,57	0,29	43,25	0,26	0	0,02	0,04	0	0	99,29
49143	38,55	0,04	0	18,31	0,24	40,46	0,34	0	0,08	0,02	0	0,05	98,32
49143	37,22	0,03	0	28,93	0,58	32,37	0,34	0	0,08	0	0	0	99,62
49143	37,79	0,01	0	27,89	0,51	33,73	0,37	0	0,08	0,03	0	0	100,46
49143	40,74	0,07	0	14,66	0,22	45,34	0,36	0	0,04	0,03	0	0	101,75
49143	40,62	0	0	14,44	0,27	44,79	0,32	0	0,09	0,03	0	0	100,93
49143	40,55	0	0	13,67	0,17	45,98	0,37	0	0	0	0	0	100,89
49143	39,55	0,00	0,00	15,57	0,29	43,25	0,26	0,00	0,02	0,04	0,00	0,00	99,3
49143	38,55	0,04	0,00	18,31	0,24	40,46	0,34	0,00	0,08	0,02	0,00	0,05	98,3
49143	37,22	0,03	0,00	28,93	0,58	32,37	0,34	0,00	0,08	0,00	0,00	0,00	99,6
49143	37,79	0,01	0,00	27,89	0,51	33,73	0,37	0,00	0,08	0,03	0,00	0,00	100,5
49143	40,62	0,00	0,00	14,44	0,27	44,79	0,32	0,00	0,09	0,03	0,00	0,00	100,9
49143	40,55	0,00	0,00	13,67	0,17	45,98	0,37	0,00	0,00	0,00	0,00	0,00	100,9

Appendix 6 - Magnetite

	MgO	SO2	CaO	TiO2	Cr2O3	FeO	MnO	NiO	CuO	ZnO	SiO2	Al2O3	Total
						New Zealand							
49172	3,89	0,004	0,220	12,72	0,61	70,98	0,26	0,04	0,00	0,04	0,30	4,12	93,18
49172	3,74	0,108	0,196	13,02	0,54	70,74	0,34	0,00	0,03	0,04	0,16	4,02	92,93
49172	3,90	0,000	0,111	13,26	0,40	72,04	0,38	0,03	0,02	0,13	0,20	4,01	94,48
49172	3,93	0,028	0,143	13,30	0,53	71,56	0,27	0,03	0,00	0,06	0,15	3,95	93,96
49172	3,85	0,038	0,155	13,27	0,34	71,86	0,30	0,05	0,00	0,08	0,15	3,93	94,02
49172	3,91	0,038	0,172	13,41	0,32	71,57	0,33	0,04	0,06	0,04	0,14	3,92	93,96
49172	3,82	0,000	0,194	13,19	0,30	72,33	0,27	0,04	0,00	0,08	0,17	4,03	94,42
49164	4,28	0,046	0,175	12,97	0,54	70,80	0,33	0,04	0,00	0,08	0,40	4,06	93,72
49164	3,84	0,012	0,116	13,67	0,31	72,00	0,34	0,02	0,02	0,06	0,16	4,04	94,61
49164	3,83	0,000	0,151	13,17	0,44	71,21	0,30	0,00	0,03	0,01	0,19	4,03	93,36
49164	3,95	0,016	0,175	12,94	0,42	70,85	0,29	0,09	0,00	0,09	0,36	3,96	93,13

Appendix 7 - Pyrite

	Mg	S	Ca	Ti	Cr	Fe	Mn	Ni	Cu	Zn	Si	Al	Total
						New Zealand							
49172	0,02	38,66	0,00	0,04	0,00	58,75	0,02	0,47	0,52	0,00	0,04	0,00	98,52
49172	0,01	37,60	0,20	0,04	0,03	57,79	0,02	0,56	1,21	0,10	0,22	0,08	97,86
49172	2,49	0,02	0,00	7,33	0,27	53,56	0,21	0,04	0,02	0,03	0,07	2,07	66,11
49172	2,45	0,00	0,00	7,44	0,25	53,32	0,25	0,00	0,00	0,01	0,08	2,10	65,90
49172	0,00	37,90	0,00	0,06	0,05	59,04	0,03	0,43	0,74	0,00	0,03	0,01	98,29
49172	0,00	37,57	0,00	0,05	0,04	59,35	0,05	0,27	0,26	0,03	0,14	0,08	97,83
49172	0,24	27,81	0,42	0,46	0,02	45,89	0,04	0,37	0,46	0,01	6,48	1,66	83,88
49164	0,00	37,90	0,03	0,17	0,02	58,27	0,01	0,43	0,07	0,00	0,31	0,12	97,32
49164	0,00	38,77	0,00	0,04	0,05	58,67	0,03	0,30	0,43	0,04	0,03	0,00	98,35
49164	0,04	37,54	0,04	0,05	0,00	59,42	0,02	0,22	0,22	0,00	0,16	0,01	97,72
49164	0,39	33,69	0,57	0,19	0,00	53,22	0,00	0,31	0,91	0,00	2,75	0,83	92,86
49164	0,02	38,09	0,00	0,04	0,00	58,94	0,04	0,36	0,72	0,01	0,06	0,02	98,29

Appendix 8 and 9
Whole Rock Geochemistry Data

A collection of over 120 samples from the Tangihua Complex and 35 samples from the Poya terrane have been analysed for major oxides and trace elements. From these analyses, 34 Tangihua Complex samples and 17 Poya terrane samples with total volatile content < 4wt% were chosen for REE analyses. Samples were selected on the basis of location and freshness. All samples with LOI > 4wt% were discarded for discussion within this thesis and in published papers, however, the entire set of data is given in Appendices 1a-d.

External surfaces of fresh rocks were removed by splitting and the samples split into chips, which were then ground to a powder in a tungsten carbide ring grinder. H2O+, H2O- and CO2 were determined by gravimetry, the remaining major oxides and trace elements were determined by XRF (after Norrish and Chappell, 1977) at the University of Auckland, New Zealand. Major oxide compositions were determined on glass fusion disks, whereas trace element content was determined using powder pellets containing a borric acid flux. Analytical precision was controlled using standard samples and duplicate measurements. The precision (2θ) of the major oxide determinations is generally less than 2%, and less than 5% for the trace elements (at ten times the detection limit of 1-2 ppm). All analyses were undertaken using uniform calibration conditions and are reported in diagrams on a 100%, volatile free basis.

Rare earth element (REE) abundances, Rb, Sr, Ba, Y, Zr, Nb, Cs, Ta, Th, U, Hf, Nb, La and Ce, were determined by Inductively Coupled Plasma Mass Spectroscopy (ICP-MS) at the Laboratoire de Geodynamique des Chaînes Alpines (LGCA – ESA5025), Université Joseph Fourier, Grenoble, France, following the procedure of Barrat *et al.*, 1996. The precision (2θ) for ICP-MS analyses is generally better than 5% for all REE and trace elements. In some case the precision may range up to10% for the elements analysed, specifically for Zr and Hf, due chemical complexing in solution, however, Zr values were confirmed with XRF analyses, and appear to be correct.

									ARC SAMPLES								CALC-ALKALINE SAMPLES	
Sample#	49212	49211	49191	47660	47644	47654	47656	49181	49204	49189	47643	49112	49162	49162	49206	49172	49130	49207
rock type	dol	basalt	basalt	dol dyke	dol	dol	matrix	dol	basalt	basalt	dol	glass	glass	glass	glass	glass	basalt	bas clast
location	Cape MVD	Cape MVD	Hihi Beach	Ahipara	Cable Bay	Ahipara	Ahipara	Whirinakei	Bergan pt	Maungamuka	Coopers bch	flat top	Tongariro	Tongariro	north?	ahipara	Waihui	Hooper pt
	Tangihua	Tangihua	Tangihua	Tangihua	Tangihua	Tangihua	Tangihua	Tangihua	Tangihua	Tangihua	Tangihua	Tangihua	Tangihua	Tangihua	Tangihua	Tangihua	Tangihua	Tangihua
wt.%																		
SiO2	50,98	49,94	51,96	50,79	52,02	50,55	52,09	47,91	50,84	49,08	50,64	49,78	56,23	51,4	41,24	52,23	48,21	53,42
TiO2	0,86	1,04	1,07	1,09	1,12	1,21	1,07	1,09	1,03	1,49	1,39	1,02	1,47	1,42	0,50	1,63	0,99	1,01
A1203	16,33	15,17	14,35	15,53	14,98	15,23	13,58	18,18	17,04	15,19	15,13	14,4	14,45	13,42	3,01	14,19	16,20	17,94
Fe203	9,95	11,33	10,88	10,24	10,97	10,60	9,30	8,80	10,26	11,14	11,28	10,63	13,16	11,94	19,38	11,96	10,93	8,23
MnO	0,16	0,17	0,18	0,17	0,18	0,17	0,15	0,15	0,14	0,18	0,18	0,18	0,19	0,18	0,26	0,21	0,19	0,16
MgO	6,39	6,33	6,34	6,06	6,02	6,00	6,62	5,55	5,47	5,67	6,32	3,9	4,23	3,82	30,87	3,69	7,64	4,15
CaO	10,39	10,54	9,58	7,00	10,40	8,54	8,42	11,42	13,66	10,36	10,21	7,23	7,31	6,97	4,28	7,63	11,26	8,95
Na20	2,87	2,76	1,82	4,08	2,01	3,44	3,94	2,53	1,37	3,03	2,34	2,01	2,41	2,09	0,46	3,03	2,06	3,41
K20	0,10	0,17	0,17	1,64	0,15	0,40	0,58	0,61	0,12	0,41	0,22	0,43	0,44	0,33	0,11	0,79	0,71	0,91
P205	0,08	0,09	0,10	0,09	0,10	0,10	0,10	0,10	0,10	0,12	0,13	0,1	0,13	0,12	0,05	0,17	0,19	0,17
LOI	1,33	1,48	0,20	1,07	0,10	0,58	1,16	1,44	0,38	1,83	0,29	0,02	0,22	3,52	0,01	1,34	0,59	1,18
%H2O	0,96	1,41	1,86	1,75	1,48	2,52	2,13	2,50	0,00	1,93	1,38	3,22	2,39	3,71	0,33	3,15	0,79	1,12
Total	100,40	100,41	98,51	99,50	99,53	99,34	99,16	100,28	100,43	100,44	99,50	92,92	102,63	98,92	100,48	100,02	99,76	100,64
Recalculated to 100% using Fe2O3/FeO = 0.15																		
SiO2	52,43	51,73	54,41	53,02	53,63	53,04	54,80	50,13	51,28	51,28	52,29	56,09	56,87	56,70	41,89	55,28	49,48	54,72
TiO2	0,89	1,08	1,12	1,14	1,15	1,27	1,13	1,14	1,04	1,56	1,44	1,15	1,49	1,57	0,51	1,73	1,02	1,03
Al2O3	16,79	15,71	15,03	16,21	15,44	15,98	14,29	19,02	17,19	15,87	15,62	16,23	14,61	14,80	3,06	15,02	16,63	18,38
Fe2O3	1,22	1,40	1,36	1,27	1,35	1,32	1,16	1,10	1,23	1,38	1,39	1,42	1,58	1,57	2,34	1,51	1,33	1,00
FeO	8,12	9,31	9,04	8,48	8,98	8,83	7,76	7,31	8,22	9,24	9,24	9,51	10,56	10,45	15,62	10,05	8,90	6,69
MnO	0,16	0,18	0,19	0,18	0,19	0,18	0,16	0,16	0,14	0,19	0,19	0,20	0,19	0,20	0,27	0,22	0,20	0,16
MgO	6,57	6,56	6,64	6,33	6,21	6,30	6,96	5,81	5,52	5,92	6,53	4,39	4,28	4,21	31,35	3,91	7,84	4,25
CaO	10,69	10,91	10,03	7,31	10,72	8,96	8,86	11,95	13,78	10,82	10,54	8,15	7,39	7,69	4,34	8,08	11,56	9,16
Na2O	2,95	2,86	1,91	4,26	2,07	3,61	4,14	2,65	1,38	3,17	2,42	2,26	2,44	2,31	0,46	3,21	2,11	3,50
K2O	0,10	0,18	0,18	1,71	0,15	0,42	0,61	0,64	0,12	0,43	0,23	0,48	0,45	0,36	0,11	0,84	0,73	0,93
P2O5	0,08	0,09	0,10	0,09	0,10	0,10	0,11	0,10	0,10	0,13	0,13	0,11	0,13	0,13	0,05	0,18	0,20	0,17
Total	100,00	100,00	100,00	100,01	100,00	100,00	99,98	100,00	100,00	99,99	100,01	100,00	100,00	100,00	100,00	100,00	100,00	100,00

								ARC SAMPLES								CALC-ALKALINE SAMPLES	
Sample#	49212	49211	49191	47660	47644	47654	47656	49181	49204	49189	47643	49112	49162	49162	49206	49172	49130	49207
rock type	dol	basalt	basalt	dol dyke	dol	dol	matrix	dol	basalt	basalt	dol	glass	glass	glass	glass	glass	basalt	bas clast
location	Cape MVD	Cape MVD	Hihi Beach	Ahipara	Cable Bay	Ahipara	Ahipara	Whirinakei	Bergan pt	Maungamuka	Coopers bch	flat top	Tongariro	Tongariro	north?	ahipara	Waihui	Hooper pt
	Tangihua	Tangihua	Tangihua	Tangihua	Tangihua	Tangihua	Tangihua	Tangihua	Tangihua	Tangihua	Tangihua	Tangihua	Tangihua	Tangihua	Tangihua	Tangihua	Tangihua	Tangihua
Traces elements (ppm)																		
Ba	31,99	16,59	47,53	66,78	26,12	40,86	21,87	54,49	22,53	23,24	22,14	77,35	61,72	66,77	45,15	88,56	289,09	283,61
Rb	0,67	1,34	1,91	20,38	1,98	4,46	4,72	9,11	1,14	5,61	1,85	10,80	8,30	8,96	0,83	14,36	15,34	32,88
Sr	120,32	157,49	106,96	68,58	96,14	141,75	100,34	174,30	55,67	101,67	99,75	160,92	142,84	145,19	166,36	128,69	321,50	257,81
Ta	0,07	0,07	0,08	0,08	0,11	0,10	0,12	0,09	0,18	0,10	0,13	0,10	0,15	0,00	0,07	0,26	0,27	0,37
Th	0,19	0,18	0,18	0,12	0,15	0,13	0,13	0,12	0,30	0,15	0,16	0,32	0,41	1,23	0,23	0,33	2,58	3,22
Zr	41,85	48,04	53,02	57,19	58,12	57,90	54,06	57,01	49,48	80,61	81,30	68,45	96,77	99,84	45,05	114,75	64,52	76,30
Nb	0,67	0,78	0,85	0,78	0,94	0,99	1,04	1,03	1,16	1,16	1,22	0,81	1,52	2,42	0,65	2,38	4,60	4,93
Y	20,68	24,23	25,53	22,91	24,76	24,61	21,89	24,22	24,58	30,53	28,23	25,39	32,87	34,28	18,23	38,71	20,45	20,52
Hf	1,47	1,69	1,77	1,69	1,73	1,78	1,65	1,81	1,76	2,28	2,23	1,96	2,75	0,00	1,35	3,28	2,00	2,38
V	270,18	356,91	318,12	321,31	322,86	321,22	292,96	276,02	311,96	380,84	328,94	300,95	357,22	362,58	118,94	373,03	308,51	200,80
Cr	114,24	113,66	121,02	77,53	64,44	77,23	256,34	132,46	146,46	93,87	92,89	42,64	26,94	21,24	1328,2	16,02	183,62	131,45
Ni	52,85	46,33	55,91	45,34	32,24	40,20	56,28	45,33	57,30	33,26	46,19	23,85	16,55	16,16	919,95	9,46	88,06	40,99
Co	44,27	47,81	45,89	33,39	40,77	33,97	82,81	44,44	51,75	36,97	40,04	0,00		0,00		0,00	50,60	41,72
U	0,07	0,07	0,07	0,05	0,06	0,08	0,21	0,08	0,18	0,12	0,06	0,13	0,33	0,00	0,08	0,13	0,66	1,15
Sc	34,36	42,58	38,35					27,03	39,41			36,04	34,31	38,34	26,86	35,79	38,39	30,23
Cu	57,84	64,48	58,63	65,28	69,11	32,36	93,07	58,29	10,38	47,24	52,05	74,52	49,82	47,71	8,69	41,86	41,18	37,23
Zn	45,76	80,55	71,03	61,98	62,12	69,01	58,57	55,75	49,39	71,19	69,26	84,49	101,37	100,65	103,97	97,04	72,41	77,14
Pb	0,11	0,72	0,17	0,24	0,44	1,30	0,70	0,05	1,30	0,48	0,63	1,72	2,19	3,66	0,31	1,00	4,73	10,03
Ga	17,44	18,03	16,66					18,28	20,30			14,76	18,01	17,52	4,82	18,70	17,96	19,66
Cs	0,01	0,02	0,33	0,25	0,14	0,05	0,03	0,00	0,27	0,08	0,05	0,61	0,38	0,00	0,08	0,32	0,24	3,38
La	1,87	2,01	2,38	1,91	2,30	2,19	2,51	1,92	3,24	2,58	2,76	2,59	3,14	2,84	1,83	4,32	10,29	9,68
Ce	6,07	6,64	7,87	6,03	7,20	7,00	7,46	6,75	8,86	8,66	8,95	7,78	10,02	11,20	5,28	13,12	23,64	23,09
Pr	1,09	1,22	1,43	1,04	1,23	1,21	1,23	1,27	1,25	1,51	1,55	1,31	1,69	0,00	0,88	2,18	3,11	2,96
Nd	6,19	7,07	8,15	5,74	6,63	6,54	6,44	7,30	6,87	8,11	8,16	6,86	8,99	0,00	4,47	11,40	13,62	12,03
Sm	2,32	2,81	3,16	2,07	2,32	2,31	2,14	2,85	2,41	2,84	2,77	2,36	3,06	0,00	1,62	3,76	3,46	2,75
Eu	0,90	1,09	1,22	0,78	0,85	0,86	0,86	1,12	0,91	1,06	1,01	0,89	1,14	0,00	0,66	1,40	1,14	0,92
Gd	3,18	3,81	4,18	2,76	3,03	3,04	2,75	3,78	2,73	3,72	3,52	3,24	4,13	0,00	2,26	5,09	3,59	3,03
Tb	0,56	0,67	0,72	0,53	0,58	0,58	0,53	0,66	0,61	0,73	0,68	0,59	0,77	0,00	0,41	0,93	0,57	0,51
Dy	3,59	4,23	4,51	3,54	3,85	3,84	3,49	4,14	3,74	4,77	4,47	3,87	5,22	0,00	2,78	6,03	3,42	3,27
Ho	0,78	0,92	0,97	0,80	0,86	0,86	0,77	0,89	0,84	1,05	0,97	0,88	1,16	0,00	0,62	1,36	0,72	0,72
Er	2,20	2,57	2,70	2,35	2,48	2,43	2,20	2,48	2,43	3,04	2,82	2,50	3,32	0,00	1,84	3,87	1,97	2,03
Tm	0,32	0,38	0,39					0,36	0,38					0,00			0,29	0,30
Yb	2,15	2,48	2,63	2,29	2,42	2,36	2,07	2,35	2,34	2,88	2,73	2,42	3,31	0,00	1,84	3,81	1,85	1,96
Lu	0,34	0,39	0,41	0,36	0,37	0,36	0,32	0,36	0,37	0,45	0,43	0,38	0,51	0,00	0,29	0,59	0,29	0,30

BACK-ARC SAMPLES

Sample#	49164	49123	47664	49183	49194	47652	49186	47645	47651	49174	49188	47649	49116	49159	47659	47648	49201	49177	49137	47662
rock type	glass	basalt	basalt	basalt	dol	basalt	basalt	dol	dol	bas/dol?	basalt	alk-dol	basalt	basalt	basalt	basalt	glass	basalt	basalt	dol? dyke
location	Tongariro	Waihui	Parakau	Peria	Houto	Broadwood	Fern Flat	Cable Bay	Whangapei	Whangapei	Coopers bch	Whangapei	Port Albert	Lovatt rd	Ahipara	Whangapei	Mitimiti	Ponguru	Houto	Ahipara
	Tangihua	Tangihua	Tangihua	Tangihua	Tangihua	Tangihua	Tangihua	Tangihua	Tangihua	Tangihua	Tangihua	Tangihua	Tangihua	Tangihua	Tangihua	Tangihua	Tangihua	Tangihua	Tangihua	Tangihua
wt.%																				
SiO2	50,82	57,05	47,46	49,45	49,27	48,05	48,80	48,69	49,51	52,42	49,27	48,42	47,93	53,15	49,43	53,51	49,14	51,64	57,66	48,50
TiO2	2,24	2,16	2,38	1,30	1,58	1,64	1,80	1,60	1,64	1,77	1,88	1,82	1,65	2,06	1,52	1,77	1,78	2,10	2,07	1,66
A1203	13,58	13,19	13,36	15,08	15,19	15,17	15,27	15,05	13,12	14,95	15,19	15,00	14,34	14,53	14,64	14,54	15,26	15,17	13,71	14,59
Fe203	14,41	11,64	13,28	10,18	11,64	11,11	12,12	10,33	10,15	9,73	12,75	11,25	11,63	12,94	10,92	9,71	11,13	12,46	9,26	11,69
MnO	0,21	0,21	0,23	0,16	0,19	0,19	0,20	0,18	0,19	0,18	0,20	0,14	0,18	0,19	0,19	0,16	0,18	0,23	0,15	0,19
MgO	4,07	3,30	6,78	6,61	6,57	6,58	5,96	6,64	7,51	5,50	5,61	6,46	6,51	4,26	6,63	5,50	5,51	3,67	3,59	6,77
CaO	8,22	7,82	9,87	10,79	9,98	10,75	9,98	10,85	9,97	9,46	10,20	10,35	7,79	8,20	8,70	9,99	10,26	8,15	7,63	9,47
Na20	2,76	2,71	2,28	2,69	0,51	2,76	3,21	2,83	2,34	3,07	2,77	2,65	4,58	3,22	4,29	2,58	2,93	3,44	3,21	3,52
K20	0,27	0,16	0,05	0,30	0,06	0,19	0,19	0,18	2,02	0,12	0,18	0,15	0,31	0,14	0,17	0,21	0,23	0,11	0,10	0,40
P205	0,18	0,18	0,26	0,13	0,14	0,16	0,18	0,16	0,20	0,21	0,20	0,20	0,15	0,21	0,17	0,22	0,21	0,27	0,25	0,20
LOI	0,68	1,08	3,36	0,58	1,93	1,36	0,58	0,58	1,95	1,46	0,39	2,23	1,81	0,40	0,58	0,50	3,10	1,74	0,78	0,49
%H2O	1,66	0,30	0,58	2,99	1,25	1,55	2,04	2,52	0,68	1,07	1,57	0,68	2,67	0,20	2,33	0,40	0,22	1,45	1,18	1,66
Total	99,11	99,80	99,90	100,27	98,31	99,51	100,34	99,61	99,28	99,93	100,20	99,35	99,55	99,50	99,57	99,08	99,95	100,43	99,58	99,14
Recalculated to 100% using Fe2O3/FeO = 0.15																				
SiO2	53,21	58,57	50,06	51,61	52,35	50,25	50,49	50,93	51,70	54,29	50,73	50,72	50,96	54,36	51,65	54,98	51,37	53,71	59,56	50,54
TiO2	2,35	2,22	2,51	1,36	1,68	1,71	1,86	1,67	1,71	1,83	1,94	1,91	1,75	2,11	1,59	1,82	1,86	2,18	2,14	1,73
Al2O3	14,22	13,54	14,09	15,74	16,14	15,86	15,80	15,74	13,70	15,48	15,64	15,71	15,25	14,86	15,30	14,94	15,95	15,78	14,16	15,20
Fe2O3	1,79	1,42	1,67	1,26	1,47	1,38	1,49	1,29	1,26	1,20	1,56	1,40	1,47	1,57	1,36	1,19	1,38	1,54	1,14	1,45
FeO	11,97	9,48	11,12	8,43	9,82	9,22	9,95	8,58	8,41	8,00	10,42	9,35	9,81	10,50	9,06	7,92	9,23	10,28	7,59	9,67
MnO	0,22	0,22	0,24	0,17	0,20	0,20	0,21	0,19	0,20	0,19	0,21	0,15	0,19	0,19	0,20	0,16	0,19	0,24	0,15	0,20
MgO	4,26	3,39	7,15	6,90	6,98	6,88	6,17	6,95	7,84	5,70	5,78	6,77	6,92	4,36	6,93	5,65	5,75	3,82	3,71	7,05
CaO	8,61	8,03	10,41	11,26	10,60	11,24	10,32	11,35	10,41	9,80	10,50	10,84	8,28	8,39	9,09	10,26	10,73	8,48	7,88	9,87
Na2O	2,89	2,78	2,41	2,81	0,54	2,89	3,32	2,96	2,44	3,18	2,85	2,78	4,87	3,29	4,48	2,65	3,07	3,58	3,32	3,67
K2O	0,28	0,16	0,05	0,31	0,06	0,20	0,20	0,19	2,11	0,12	0,19	0,16	0,33	0,14	0,18	0,22	0,24	0,11	0,10	0,42
P2O5	0,19	0,18	0,27	0,14	0,15	0,17	0,19	0,17	0,21	0,22	0,21	0,21	0,16	0,21	0,18	0,23	0,22	0,28	0,26	0,21
Total	99,99	100,00	99,99	99,99	100,00	100,00	99,99	100,00	100,00	100,01	100,01	100,00	100,00	100,00	100,00	100,01	100,00	100,00	100,01	100,00

BACK-ARC SAMPLES

Sample#	49164	49123	47664	49183	49194	47652	49186	47645	47651	49174	49188	47649	49116	49159	47659	47648	49201	49177	49137	47662
rock type	glass	basalt	basalt	basalt	dol	basalt	basalt	dol	dol	bas/dol?	basalt	alk-dol	basalt	basalt	basalt	basalt	glass	basalt	basalt	dol? dyke
location	Tongariro	Waihui	Parakau	Peria	Houto	Broadwood	Fern Flat	Cable Bay	Whangapei	Whangapei	Coopers bch	Whangapei	Port Albert	Lovatt rd	Ahipara	Whangapei	Mitimiti	Ponguru	Houto	Ahipara
	Tangihua	Tangihua	Tangihua	Tangihua	Tangihua	Tangihua	Tangihua	Tangihua	Tangihua	Tangihua	Tangihua	Tangihua	Tangihua	Tangihua	Tangihua	Tangihua	Tangihua	Tangihua	Tangihua	Tangihua
Traces elements (ppm)																				
Ba	27,91	40,73	23,80	26,51	13,51	18,85	30,70	27,66	61,17	16,56	18,84	17,75	384,77	33,35	18,55	30,69	37,79	293,15	28,40	46,56
Rb	2,51	3,72	0,62	3,63	0,38	1,70	2,18	1,61	9,62	0,40	2,10	1,51	2,61	1,92	2,59	2,13	2,21	1,39	0,36	1,95
Sr	86,40	92,23	117,77	143,24	101,32	122,19	206,22	106,50	82,74	117,36	160,77	120,90	141,34	171,79	79,04	130,42	138,40	333,06	170,57	105,48
Ta	0,17	0,17	0,14	0,16	0,17	0,17	0,20	0,24	0,22	0,24	0,24	0,26	0,23	0,27	0,29	0,33	0,44	0,29	0,33	0,35
Th	0,13	0,15	0,18	0,18	0,17	0,17	0,23	0,15	0,21	0,25	0,30	0,24	0,30	0,35	0,26	0,28	0,30	0,49	0,36	0,34
Zr	119,64	115,39	82,91	78,88	103,03	102,97	116,56	68,35	122,17	134,86	113,77	135,39	98,11	135,18	103,23	126,00	130,07	152,42	153,83	122,90
Nb	1,04	1,23	1,51	1,82	2,08	2,12	2,57	2,78	2,86	3,23	3,26	3,33	3,41	3,43	3,54	3,99	4,09	4,14	4,28	4,63
Y	44,90	47,87	37,41	32,17	32,66	32,09	36,53	31,80	39,00	36,86	43,70	39,48	40,57	48,42	36,85	46,30	43,67	50,27	54,75	41,83
Hf	3,22	4,19	3,07	2,80	2,79	2,77	3,04	1,91	3,33	3,40	3,44	3,48	2,82	4,57	3,60	4,26	4,26	4,46	4,42	4,24
V	452,49	450,10	382,87	314,63	317,62	324,39	354,47	314,70	365,99	321,77	378,60	343,79	339,53		315,45	333,61	333,87	349,53	337,25	325,43
Cr	16,88	15,03	173,53	181,18	252,14	210,81	115,93	191,71	233,49	116,51	31,37	224,58	193,06		239,74	191,97	133,18	5,34	35,47	247,38
Ni	13,47	16,33	96,13	59,20	58,07	57,12	42,13	50,53	55,75	42,25	31,05	63,92	71,31		56,56	81,13	42,95	6,41	32,44	77,29
Co	50,57	49,81	48,22	42,83	39,75	36,18	36,35	36,34	35,27	33,59	46,58	39,76	47,73	37,48	43,71	52,65	52,44	36,77	45,56	44,44
U	0,06	0,58	0,08	0,13	0,07	0,08	0,09	0,05	0,09	0,10	0,15	0,11	0,12	0,15	0,11	0,39	0,13	0,18	0,15	0,18
Sc		41,71	36,72	40,46							40,93		44,30		40,05	38,97	36,17	31,95	28,87	41,26
Cu	43,44	38,08	50,91	65,24	47,70	53,64	49,60	48,79	41,87	22,61	45,95	52,79	56,90		48,37	49,48	53,84	43,34	40,67	22,30
Zn	100,94	110,07	114,37	80,77	70,18	70,27	79,90	73,19	58,00	67,00	103,38	78,64	86,00		80,20	88,60	89,77	111,15	78,91	85,89
Pb	0,79	0,91	0,37	0,63	0,69	0,59	0,80	0,74	0,28	0,26	0,51	0,66	0,65	1,24	0,32	0,64	0,73	1,22	0,43	0,31
Ga		20,44	20,77	17,58							20,41		17,13		16,35	18,34	19,33	21,96	19,30	17,18
Cs	0,11	0,15	0,01	0,09	0,03	0,11	0,14	0,08	0,03	0,00	0,01	0,07	0,05		0,18	0,06	0,04	0,05	0,00	0,04
La	2,99	14,73	3,22	3,08	3,46	3,55	4,10	3,83	4,48	4,69	5,12	4,79	4,85	5,54	4,72	6,04	5,44	7,00	6,90	5,75
Ce	11,15	19,49	10,56	10,02	11,15	11,39	12,76	11,95	14,09	14,37	17,46	14,97	13,80	17,06	14,30	18,17	16,68	21,85	21,02	17,11
Pr	2,08	23,79	1,86	1,73	1,90	1,93	2,14	1,97	2,35	2,36	3,08	2,47	2,00	2,86	2,33	2,95	2,74	3,56	3,38	2,76
Nd	11,52	27,10	10,10	9,13	10,04	10,07	11,03	10,16	12,32	12,03	16,98	12,61	11,30	14,72	11,94	14,84	14,12	17,88	16,44	13,93
Sm	4,09	30,44	3,44	3,08	3,33	3,33	3,55	3,36	4,12	3,81	6,66	4,06	3,96	4,82	3,79	4,69	4,53	5,63	4,98	4,39
Eu	1,46	28,55	1,27	1,15	1,17	1,21	1,24	1,19	1,33	1,30	2,40	1,38	1,41	1,64	1,34	1,55	1,53	1,89	1,60	1,49
Gd	5,35	30,37	4,77	4,15	4,21	4,22	4,54	4,17	5,23	4,73	7,91	5,09	4,44	6,30	4,95	5,90	5,78	7,03	6,49	5,63
Tb	0,99	31,76	0,91	0,79	0,80	0,80	0,82	0,79	0,98	0,85	1,27	0,96	0,97	1,18	0,93	1,11	1,08	1,28	1,23	1,06
Dy	6,76	30,88	6,01	5,14	5,21	5,13	5,62	5,14	6,26	5,75	7,71	6,18	5,58	7,68	6,04	7,29	6,96	8,23	8,18	6,87
Ho	1,50	30,71	1,32	1,12	1,13	1,12	1,24	1,13	1,36	1,26	1,64	1,35	1,28	1,67	1,30	1,59	1,49	1,81	1,84	1,49
Er	4,31	30,52	3,82	3,20	3,29	3,17	3,52	3,16	3,78	3,60	4,51	3,84	3,65	4,81	3,75	4,60	4,32	5,13	5,27	4,31
Tm		0,75	0,56	0,47							0,66		0,55	0,73	0,54	0,67	0,63	0,76	0,79	0,62
Yb	4,19	29,07	3,61	3,00	3,09	3,04	3,39	2,90	3,51	3,44	4,38	3,63	3,41	4,57	3,49	4,27	4,05	4,89	5,02	3,98
Lu	0,63	29,42	0,57	0,47	0,47	0,46	0,52	0,45	0,53	0,52	0,67	0,56	0,53	0,71	0,54	0,66	0,62	0,75	0,78	0,62

Whole Rock Chemistry Data — New Zealand

					BACK-ARC SAMPLES						
Sample#		47665	49164	49135	49219	49193	49172	49117	49201	49193g	49193g
rock type		basalt	glass	glass	glass	glass	glass	glass	glass	glass	glass
location		Repeater st	Tongariro	Houto	Te Paki	nr houto	ahipara	port albert	mitimiti	nr houto	nr houto
		Tangihua	Tangihua	Tangihua	Tangihua	Tangihua	Tangihua	Tangihua	Tangihua	Tangihua	Tangihua
wt.%											
SiO2		51,55	50,82	46,68	51,19	48,31	52,47	48,52	49,14	47,53	47,53
TiO2		1,57	2,24	1,84	1,97	2,03	1,61	1,69	1,78	1,98	1,98
A1203		14,64	13,58	13,84	14,46	14,96	14,01	14,46	15,26	14,63	14,63
Fe203		10,57	14,41	11,11	12,91	11,6	11,59	11,65	11,13	11,28	11,28
MnO		0,17	0,21	0,18	0,17	0,19	0,17	0,21	0,18	0,21	0,21
MgO		5,26	4,07	6,34	6,22	5,23	3,66	6,98	5,51	4,85	4,85
CaO		10,19	8,22	10,14	9,97	9,97	7,65	10,21	10,26	8,93	8,93
Na20		2,41	2,76	1,52	2,57	2,79	3,01	2,92	2,93	1,98	1,98
K20		0,07	0,27	0,57	0,19	0,31	0,3	0,22	0,23	0,34	0,34
P205		0,13	0,18	0,2	0,22	0,24	0,17	0,16	0,21	0,23	0,23
LOI		2,23	0,68	3,61	0,03	1,05	2,75	1,75	3,10	2,31	2,31
%H2O		0,78	1,66	3,8	3,28	3,53	2,56	0,88	0,22	5,44	5,44
Total		99,57	99,10	99,83	103,18	100,21	99,95	99,65	99,95	99,71	99,71
Recalculated to 100% using Fe2O3/FeO = 0.15											
SiO2		53,90	53,21	51,04	51,85	51,06	56,04	50,54	51,37	52,25	52,25
TiO2		1,64	2,35	2,01	1,99	2,15	1,72	1,76	1,86	2,18	2,18
Al2O3		15,31	14,22	15,13	14,64	15,81	14,96	15,06	15,95	16,08	16,08
Fe2O3		1,31	1,79	1,45	1,56	1,46	1,47	1,44	1,38	1,47	1,47
FeO		8,77	11,98	9,64	10,38	9,73	9,82	9,63	9,23	9,84	9,84
MnO		0,18	0,22	0,20	0,17	0,20	0,18	0,22	0,19	0,23	0,23
MgO		5,50	4,26	6,93	6,30	5,53	3,91	7,27	5,75	5,33	5,33
CaO		10,65	8,61	11,09	10,10	10,54	8,17	10,64	10,73	9,82	9,82
Na2O		2,52	2,89	1,66	2,60	2,95	3,21	3,04	3,07	2,18	2,18
K2O		0,07	0,28	0,62	0,20	0,33	0,32	0,23	0,24	0,37	0,37
P2O5		0,14	0,19	0,22	0,22	0,25	0,18	0,17	0,22	0,25	0,25
Total		100,00	100,00	100,00	100,00	100,00	100,00	100,00	100,00	100,00	100,00

Whole Rock Chemistry Data — New Zealand

			BACK-ARC SAMPLES								
Sample#		47665	49164	49135	49219	49193	49172	49117	49201	49193g	49193g
rock type		basalt	glass	glass	glass	glass	glass	glass	glass	glass	glass
location		Repeater st	Tongariro	Houto	Te Paki	nr houto	ahipara	port albert	mitimiti	nr houto	nr houto
		Tangihua	Tangihua	Tangihua	Tangihua	Tangihua	Tangihua	Tangihua	Tangihua	Tangihua	Tangihua
Traces elements (ppm)											
Ba		27,13	27,91	101,55	26,24	49,40	38,14	265,14	37,79	104,92	125,03
Rb		0,13	2,51	7,06	3,82	2,89	4,24	1,28	2,21	4,13	4,74
Sr		105,75	86,40	429,96	112,11	154,91	126,99	179,54	138,40	197,44	199,84
Ta		0,39	0,17	0,32	0,31	0,42	0,00	0,27	0,44	0,35	0,00
Th		0,34	0,13	0,26	0,29	0,30	-0,70	0,28	0,30	0,29	0,38
Zr		158,61	119,64	152,22	161,39	176,44	115,84	113,55	130,07	172,45	172,67
Nb		5,03	1,04	3,86	3,99	4,28	3,59	3,55	4,09	4,20	5,16
Y		53,64	44,90	43,18	45,42	48,65	40,85	37,43	43,67	47,15	49,25
Hf		5,38	3,22	4,04	4,08	4,58	0,00	2,95	4,26	4,39	0,00
V		390,04	452,49	320,38	360,47	350,19	377,56	345,52	333,87	348,69	348,69
Cr		67,98	16,88	210,20	192,61	54,36	7,52	213,63	133,18	54,95	54,95
Ni		42,56	13,47	73,57	56,53	36,97	7,89	68,63	42,95	37,09	37,09
Co		41,65	50,57	0,00		0,00	0,00	0,00	52,44	0,00	0,00
U		0,15	0,06	0,14	0,26	0,14	0,14	0,12	0,13	0,13	-0,11
Sc		43,26		39,26	43,64	36,61	31,80	46,44	36,17	38,57	38,57
Cu		49,86	43,44	54,57	59,40	49,88	40,99	59,57	53,84	49,04	49,04
Zn		83,41	100,94	93,88	97,10	99,29	96,85	89,36	89,77	97,81	97,81
Pb		1,03	0,79	0,70	0,76	0,82	1,19	0,66	0,73	0,81	2,84
Ga		19,53		16,79	18,87	19,32	19,77	20,68	19,33	17,35	17,35
Cs		0,00	0,11	0,06	0,11	0,04	0,00	0,02	0,04	0,06	0,00
La		6,35	2,99	5,23	5,66	5,96	3,70	4,60	5,44	5,72	5,79
Ce		19,94	11,15	16,47	17,24	18,60	15,11	13,61	16,68	17,89	23,16
Pr		3,33	2,08	2,72	2,84	3,09	0,00	2,25	2,74	2,96	0,00
Nd		17,38	11,52	14,04	14,28	15,80	0,00	11,51	14,12	15,19	0,00
Sm		5,60	4,09	4,48	4,70	5,13	0,00	3,76	4,53	4,91	0,00
Eu		1,86	1,46	1,56	1,59	1,68	0,00	1,45	1,53	1,65	0,00
Gd		7,27	5,35	6,00	6,13	6,76	0,00	5,22	5,78	6,45	0,00
Tb		1,37	0,99	1,08	1,11	1,19	0,00	0,91	1,08	1,16	0,00
Dy		8,82	6,76	7,09	7,18	7,74	0,00	5,84	6,96	7,43	0,00
Ho		1,92	1,50	1,55	1,56	1,69	0,00	1,30	1,49	1,64	0,00
Er		5,44	4,31	4,38	4,55	4,87	0,00	3,67	4,32	4,69	0,00
Tm		0,81					0,00		0,63		0,00
Yb		5,09	4,19	4,19	4,42	4,68	0,00	3,45	4,05	4,53	0,00
Lu		0,80	0,63	0,64	0,68	0,73	0,00	0,53	0,62	0,70	0,00

Sample#	7303	7304	7307	7846	7847	7847	7852	9294	9294	9370	14635	23221	23223	23224	26409	26412
rock type	diorite	andesite	basalt	basalt	basalt	basalt	nephenelite	teschenite		pbasalt	basalt					
location	Tiriwhiriı	Tokatoka	Mititai	Whakahara	Arapohe	Arapohe	Maungarahu	Hughes, 66	Okarahura	Briggs, 69	Briggs, 69	Briggs, 69	Briggs, 69	Briggs, 69	Briggs, 69	Briggs, 69
wt.%																
SiO2	51,86	49,34	50,59	48,73	48,79	48,79	43,90	48,82	48,82	49,70	47,63	49,04	50,01	50,52	48,96	48,74
TiO2	0,77	0,90	0,89	1,03	0,91	0,91	1,98	1,83	1,83	1,48	1,54	0,97	1,19	1,31	1,29	1,00
A1203	15,57	16,19	17,25	17,10	15,40	15,40	11,76	15,25	15,25	15,51	14,80	16,96	17,90	16,15	18,80	17,96
Fe203	8,41	10,06	9,16	11,90	10,36	10,36	11,55	11,15	11,15	10,47	11,51	10,84	11,55	12,63	10,63	10,85
MnO	0,16	0,16	0,18	0,18	0,17	0,17	0,17	0,21	0,21	0,16	0,18	0,27	0,19	0,21	0,17	0,19
MgO	7,69	6,38	4,80	5,47	9,49	9,49	12,70	5,66	5,66	5,69	5,95	6,33	4,33	4,63	4,05	4,96
CaO	8,38	9,97	6,64	10,05	10,96	10,96	10,34	7,50	7,50	11,01	8,69	12,37	10,55	9,80	10,82	11,15
Na20	2,55	2,08	4,60	2,62	1,95	1,95	2,95	4,81	4,81	2,11	3,92	2,39	3,12	3,21	2,99	2,66
K20	1,06	0,74	1,56	1,01	0,70	0,70	1,47	0,23	0,23	0,36	0,15	0,67	0,84	0,92	1,17	0,65
P205	0,17	0,18	0,22	0,17	0,14	0,14	0,76	0,20	0,20	0,12	0,13	0,19	0,22	0,23	0,31	0,17
LOI	1,56	1,74	0,96	0,39	0,50	0,50	0,30	0,32	0,32	1,74	1,46	0,10	0,40	0,60	0,30	0,69
%H2O	1,07	1,64	2,88	0,99	0,30	0,30	1,28	3,28	3,28	1,36	3,61	0,30	0,20	0,20	0,59	0,69
Total	99,26	99,39	99,74	99,64	99,65	99,65	99,17	99,27	99,27	99,69	99,57	100,44	100,49	100,41	100,09	99,71
Recalculated to 100% using Fe2O3/FeO = 0.15																
SiO2	54,08	51,87	53,20	50,12	49,81	49,81	45,45	51,55	51,55	51,95	50,94	49,49	50,58	51,29	49,82	50,05
TiO2	0,80	0,95	0,94	1,06	0,93	0,93	2,05	1,93	1,93	1,55	1,65	0,98	1,20	1,33	1,31	1,03
Al2O3	16,24	17,02	18,14	17,59	15,72	15,72	12,18	16,10	16,10	16,21	15,83	17,12	18,10	16,39	19,13	18,44
Fe2O3	1,04	1,26	1,15	1,46	1,26	1,26	1,42	1,40	1,40	1,30	1,46	1,30	1,39	1,53	1,29	1,33
FeO	6,96	8,39	7,64	9,71	8,39	8,39	9,49	9,34	9,34	8,69	9,77	8,68	9,27	10,18	8,58	8,84
MnO	0,17	0,17	0,19	0,19	0,17	0,17	0,18	0,22	0,22	0,17	0,19	0,27	0,19	0,21	0,17	0,20
MgO	8,02	6,71	5,05	5,63	9,69	9,69	13,15	5,98	5,98	5,95	6,36	6,39	4,38	4,70	4,12	5,09
CaO	8,74	10,48	6,98	10,34	11,19	11,19	10,71	7,92	7,92	11,51	9,29	12,48	10,67	9,95	11,01	11,45
Na2O	2,66	2,19	4,84	2,69	1,99	1,99	3,05	5,08	5,08	2,21	4,19	2,41	3,16	3,26	3,04	2,73
K2O	1,11	0,78	1,64	1,04	0,71	0,71	1,52	0,24	0,24	0,38	0,16	0,68	0,85	0,93	1,19	0,67
P2O5	0,18	0,19	0,23	0,17	0,14	0,14	0,79	0,21	0,21	0,13	0,14	0,19	0,22	0,23	0,32	0,17
Total	99,99	99,99	99,99	100,00	100,02	100,02	99,99	99,99	99,99	100,02	100,00	99,99	100,01	100,00	99,99	100,00
Traces elements (ppm)																
Ba	538,41	342,71	595,43	406,93	32,60	306,67	763,01	29,29	96,57	21,00	20,43	351,23	361,53	367,45	585,55	260,44
Rb	38,44	20,74	94,90	29,90	1,68	20,27	36,72	1,36	6,17	4,08	6,94	17,33	16,54	20,11	31,37	13,64
Sr	320,16	304,71	670,47	301,37	101,60	252,61	1160,29	101,79	404,21	155,66	116,90	388,88	347,34	318,09	426,86	328,68
Th	4,41	3,94	5,90	2,42	0,00	2,76	8,67	0,00	0,02	0,84	0,04	3,16	2,11	3,39	5,14	0,61
Zr	114,54	104,23	135,21	93,86	80,02	83,60	186,64	79,80	165,91	94,88	106,55	79,44	101,55	108,04	121,09	81,29
Nb	4,32	3,95	5,43	3,54	1,81	4,04	78,56	2,10	4,31	2,52	2,92	4,31	4,93	5,18	7,05	4,17
Y	20,24	22,82	29,05	25,55	30,67	19,61	29,23	30,91	48,79	35,21	39,82	31,59	27,14	29,71	27,54	24,16
V	208,53	290,53	203,96	348,63	297,13	291,65	209,01	298,71	326,32	346,30	339,34	277,07	341,58	396,71	289,79	329,33
Cr	473,80	226,00	84,17	46,08	246,17	565,11	467,95	247,85	120,22	99,78	132,83	137,53	23,64	19,70	24,74	57,04
Ni	146,86	71,99	35,97	26,62	76,94	180,79	371,49	76,35	58,75	44,35	59,23	87,80	21,71	24,23	18,73	34,47
U	0,96	1,65	0,01	1,57	0,38	0,67	3,57	0,00	0,00	1,15	0,24	2,05	1,89	2,35	2,24	0,45
Sc	28,71	34,47	21,47	38,58	40,83	40,48	20,99	46,39	35,58	40,68	37,65	34,67	26,09	35,71	25,31	33,65
Cu	54,14	64,59	47,63	112,54	54,85	74,78	62,65	55,55	7,19	57,00	57,35	180,69	129,25	129,82	130,72	115,92
Zn	71,43	73,11	78,69	74,29	78,70	75,02	102,30	77,85	106,89	84,87	88,66	84,32	82,61	95,54	74,63	80,71
Pb	8,79	5,92	8,51	4,38	2,91	8,16	5,59	1,24	3,71	1,32	0,91	7,13	8,29	8,29	5,79	3,96
Ga	18,37	18,57	19,57	20,69	17,72	16,36	18,10	18,03	18,57	19,11	16,56	18,98	20,70	20,14	21,14	19,21
La	13,06	12,71	16,00	9,86	3,58	9,91	48,45	0,13	4,49	2,54	2,49	12,73	8,86	10,21	16,79	9,04
Ce	30,28	25,64	33,71	20,94	6,99	20,63	78,61	10,09	24,60	14,54	13,17	19,39	19,47	21,86	35,71	19,83

26413	26721	26723	38239	38240	38241	38242	38542	38243	38243	38256	39493	39497	40475	40483	40485	40511
			?	altered???							basalt	basalt	pbasalt	pbasalt	pbasalt	pbasalt
Briggs, 69	Briggs, 69	Briggs, 69	Larsen, 87	Larsen, 87	Larsen, 87	Larsen, 87	Larsen, 87	Larsen, 87	Larsen, 87	Larsen, 87	Larsen, 87	Larsen, 87	Martin, 88	Arden, 88	Arden, 88	Arden, 88
49,52	49,89	49,61	50,51	52,15	49,15	51,27	49,71	50,88	50,88	48,16	51,07	49,98	51,66	52,41	52,32	49,54
1,21	1,20	1,03	1,07	1,39	1,44	1,62	1,57	1,68	1,68	1,83	2,09	1,19	1,15	1,16	1,05	2,00
17,18	17,59	18,95	14,80	15,50	14,87	14,64	14,70	14,63	14,63	14,93	13,29	14,65	14,63	15,24	13,35	14,51
11,48	11,24	10,58	10,62	9,28	11,15	12,16	11,59	12,49	12,49	10,83	13,58	11,15	11,07	11,14	11,67	12,34
0,19	0,18	0,17	0,16	0,13	0,16	0,19	0,19	0,21	0,21	0,19	0,19	0,18	0,18	0,17	0,20	0,20
5,14	4,76	3,87	5,89	4,50	6,06	4,96	5,80	5,58	5,58	6,17	4,49	6,33	6,00	4,84	7,12	6,39
11,08	10,59	10,98	9,70	9,62	10,52	9,04	10,08	9,86	9,86	11,14	8,15	8,87	8,44	8,61	9,63	11,07
2,99	2,97	3,04	2,00	2,42	2,22	2,59	2,65	2,56	2,56	2,19	2,53	3,05	2,65	2,95	1,84	2,31
0,94	0,95	0,69	0,12	0,14	0,07	0,30	0,16	0,11	0,11	0,05	0,11	0,61	0,70	0,25	0,04	0,04
0,24	0,25	0,18	0,09	0,12	0,12	0,14	0,13	0,15	0,15	0,17	0,16	0,08	0,11	0,10	0,11	0,22
0,10	0,40	0,69	0,30	2,59	2,31	1,75	1,75	0,20	0,20	2,41	2,02	0,93	0,39	0,29	0,68	0,10
0,30	0,10	0,30	1,18	1,34	1,35	1,07	1,07	1,28	1,28	1,35	1,54	2,51	2,62	2,34	1,56	0,89
100,37	100,10	100,11	96,43	99,19	99,42	99,71	99,40	99,65	99,65	99,43	99,21	99,54	99,59	99,50	99,57	99,61
50,04	50,59	50,52	53,72	55,22	51,85	53,50	52,02	52,41	52,41	50,84	54,06	52,54	54,03	54,65	54,32	50,79
1,22	1,22	1,05	1,14	1,47	1,52	1,69	1,64	1,73	1,73	1,93	2,21	1,25	1,20	1,21	1,09	2,05
17,36	17,84	19,30	15,74	16,41	15,69	15,28	15,38	15,07	15,07	15,76	14,07	15,40	15,30	15,89	13,86	14,88
1,38	1,36	1,28	1,34	1,17	1,40	1,51	1,44	1,53	1,53	1,36	1,71	1,39	1,38	1,38	1,44	1,50
9,21	9,05	8,55	8,96	7,80	9,34	10,07	9,63	10,21	10,21	9,07	11,41	9,30	9,19	9,22	9,62	10,04
0,19	0,18	0,17	0,17	0,14	0,17	0,20	0,20	0,22	0,22	0,20	0,20	0,19	0,19	0,18	0,21	0,21
5,19	4,83	3,94	6,26	4,76	6,39	5,18	6,07	5,75	5,75	6,51	4,75	6,65	6,28	5,05	7,39	6,55
11,20	10,74	11,18	10,32	10,19	11,10	9,43	10,55	10,16	10,16	11,76	8,63	9,32	8,83	8,98	10,00	11,35
3,02	3,01	3,10	2,13	2,56	2,34	2,70	2,77	2,64	2,64	2,31	2,68	3,21	2,77	3,08	1,91	2,37
0,95	0,96	0,70	0,13	0,15	0,07	0,31	0,17	0,11	0,11	0,05	0,12	0,64	0,73	0,26	0,04	0,04
0,24	0,25	0,18	0,10	0,13	0,13	0,15	0,14	0,15	0,15	0,18	0,17	0,08	0,12	0,10	0,11	0,23
100,00	100,02	99,98	100,01	99,99	100,00	100,02	100,00	99,98	99,98	99,99	100,01	99,99	100,01	100,00	100,00	100,00
377,82	350,51	293,59	128,19		32,46	39,37	49,02	26,03	40,84	31,41	42,39	168,80	93,89	58,35	45,26	39,64
20,62	20,01	12,38	2,42		0,53	1,70	2,84	1,98	1,64	1,08	1,11	8,57	11,51	3,85	0,00	0,06
372,60	360,05	353,83	106,61		139,30	102,42	119,64	101,78	123,77	139,95	98,32	144,33	131,38	127,14	102,85	139,19
2,27	3,96	1,10	0,00		0,00	0,00	0,00	0,85	0,70	0,00	0,46	0,00	0,10	0,00	0,28	0,00
100,22	104,87	85,32	72,22		90,66	79,93	107,28	80,12	117,43	141,11	129,89	67,38	80,13	75,38	69,66	159,22
5,44	6,04	4,02	1,79		2,96	2,32	2,63	1,80	2,76	4,89	2,56	1,86	2,57	2,21	1,99	5,06
27,05	26,93	24,67	30,56		32,91	30,96	46,56	30,39	40,82	56,62	49,99	29,42	28,35	29,28	28,22	47,75
356,57	315,23	332,19	325,62		356,25	298,57	408,79	299,07	338,03	341,17	452,36	314,74	324,49	329,71	299,07	330,30
45,04	42,08	31,83	49,59		98,02	247,34	34,82	250,20	53,45	240,07	20,38	163,22	77,77	32,10	100,51	149,23
36,36	33,48	22,65	41,12		48,57	77,41	29,78	75,57	34,04	433,11	17,56	66,13	40,52	24,87	59,29	60,22
2,14	2,00	0,78	0,00		1,09	1,38	0,05	0,69	0,00	1,59	1,14	0,16	0,00	0,09	1,80	0,00
27,07	28,64	30,79	37,59		41,12	43,73	40,63	44,31	39,02	38,46	32,47	38,62	39,86	39,31	36,12	37,21
126,79	124,41	411,42	61,32		66,98	56,47	50,27	55,50	48,95	66,55	38,87	54,30	61,34	39,27	17,81	55,92
81,56	80,00	85,92	77,58		110,99	79,43	102,96	79,56	82,57	99,09	113,75	74,92	87,35	68,65	79,70	98,26
4,79	7,47	6,24	2,38		2,49	2,29	2,99	1,85	2,21	2,36	3,50	1,09	2,70	2,42	2,61	3,37
20,38	21,01	20,59	18,45		17,94	17,38	19,66	17,37	20,16	18,91	21,68	17,66	16,12	18,36	16,76	20,38
10,94	11,11	8,29	1,75		3,49	1,02	0,00	4,84	5,38	8,43	6,59	2,35	3,22	2,75	4,40	5,98
23,66	28,56	19,39	10,36		13,50	6,70	12,78	11,27	13,08	18,40	12,17	9,79	9,26	11,24	7,43	18,64

All Remaining Data — New Zealand — Appendix 8

40554	40554	40555	40556	40557	40559	40560	43504	43539	43541	38239	47341	47342	47643	47644	47645	47648
pbasalt	pbasalt	pbasalt	pbasalt	pbasalt	pbasalt	pbasalt	basalt	diorite	dyke	basalt	basalt	basalt	basalt	basalt	basalt	basalt
Arden, 88	Arden, 88	Arden, 88	Arden, 88	Arden, 88	Arden, 88	Arden, 88	Arden, 88	Hansen, 91	Hansen, 91	Soffe, 86	Thompson,	Thompson,	This study	This study	This study	This study
47,94	47,94	50,70	51,81	48,55	49,68	50,15	49,75	49,81	49,90	53,00	60,63	57,51	50,64	52,02	48,69	53,51
1,77	1,77	2,35	1,46	1,83	1,81	2,28	1,25	1,23	1,77	1,11	0,58	0,69	1,39	1,12	1,60	1,77
14,71	14,71	13,80	14,42	14,56	14,79	13,59	14,92	15,28	14,83	15,61	16,30	16,46	15,13	14,98	15,05	14,54
10,95	10,95	14,14	10,94	11,61	10,77	14,71	10,71	10,40	12,29	11,15	6,09	7,00	11,28	10,97	10,33	9,71
0,20	0,20	0,20	0,17	0,20	0,17	0,20	0,17	0,18	0,19	0,17	0,10	0,12	0,18	0,18	0,18	0,16
6,61	6,61	4,11	5,70	6,87	6,28	4,48	7,04	6,98	6,98	6,20	3,28	4,62	6,32	6,02	6,64	5,50
9,37	9,37	7,01	9,67	10,41	10,38	7,47	11,06	11,21	8,54	10,06	6,90	8,56	10,21	10,40	10,85	9,99
3,80	3,80	3,57	2,30	2,24	2,10	3,22	2,15	1,92	2,67	2,07	3,02	2,65	2,34	2,01	2,83	2,58
0,20	0,20	1,19	0,31	0,07	0,13	0,52	0,15	0,15	0,17	0,12	1,54	1,24	0,22	0,15	0,18	0,21
0,19	0,19	0,18	0,14	0,20	0,20	0,16	0,10	0,10	0,17	0,09	0,11	0,13	0,13	0,10	0,16	0,22
0,96	0,96	1,21	1,56	1,55	2,04	1,75	0,29	0,20	0,29	1,00	0,69	0,20	0,29	0,10	0,58	0,50
2,70	2,70	1,07	1,17	1,74	0,97	1,07	1,76	1,57	1,86	0,00	0,40	0,20	1,38	1,48	2,52	0,40
99,42	99,42	99,53	99,63	99,82	99,31	99,59	99,35	99,04	99,67	100,58	99,65	99,38	99,50	99,53	99,61	99,08
50,57	50,57	52,80	54,00	50,83	52,10	52,52	51,63	51,69	51,74	53,75	61,85	58,46	52,29	53,63	50,93	54,98
1,87	1,87	2,45	1,52	1,92	1,90	2,39	1,30	1,28	1,84	1,13	0,59	0,70	1,44	1,15	1,67	1,82
15,52	15,52	14,37	15,03	15,24	15,51	14,23	15,48	15,86	15,38	15,83	16,63	16,73	15,62	15,44	15,74	14,94
1,37	1,37	1,75	1,36	1,45	1,34	1,83	1,32	1,28	1,52	1,35	0,74	0,85	1,39	1,35	1,29	1,19
9,17	9,17	11,69	9,05	9,65	8,96	12,23	8,82	8,57	10,11	8,97	4,93	5,65	9,24	8,98	8,58	7,92
0,21	0,21	0,21	0,18	0,21	0,18	0,21	0,18	0,19	0,20	0,17	0,10	0,12	0,19	0,19	0,19	0,16
6,97	6,97	4,28	5,94	7,19	6,59	4,69	7,31	7,24	7,24	6,29	3,35	4,70	6,53	6,21	6,95	5,65
9,88	9,88	7,30	10,08	10,90	10,89	7,82	11,48	11,63	8,85	10,20	7,04	8,70	10,54	10,72	11,35	10,26
4,01	4,01	3,72	2,40	2,35	2,20	3,37	2,23	1,99	2,77	2,10	3,08	2,69	2,42	2,07	2,96	2,65
0,21	0,21	1,24	0,32	0,07	0,14	0,54	0,16	0,16	0,18	0,12	1,57	1,26	0,23	0,15	0,19	0,22
0,20	0,20	0,19	0,15	0,21	0,21	0,17	0,10	0,10	0,18	0,09	0,11	0,13	0,13	0,10	0,17	0,23
99,98	99,98	100,00	100,02	100,01	100,01	100,01	100,00	99,99	99,99	100,00	99,99	100,00	100,01	100,00	100,00	100,01
26,86	19,95	33,12	35,64	31,10	50,84	35,13	31,92	20,27	30,76		428,00	357,00	32,00	46,00	54,00	37,00
1,29	5,29	5,42	5,75	0,28	1,49	4,49	1,82	2,13	1,45		53,00	43,00	2,00	2,00	3,00	2,00
101,81	114,92	104,97	132,44	164,17	141,59	96,15	118,43	102,42	131,00		264,00	299,00	119,00	110,00	130,00	132,00
0,44	0,00	0,77	0,00	0,00	1,29	0,00	0,65	2,09	0,00		6,00	6,00	0,00	0,00	0,00	0,00
79,71	141,21	137,83	100,71	150,69	157,62	136,53	82,83	80,64	122,25		106,00	105,00	97,00	74,00	121,00	153,00
1,78	4,51	2,40	2,99	4,80	5,63	2,62	2,22	1,89	3,22		4,00	4,00	2,00	2,00	4,00	5,00
30,64	43,21	54,62	35,39	45,66	73,39	52,06	31,08	31,14	46,31		17,00	17,00	34,00	28,00	39,00	49,00
297,02	341,05	440,04	390,59	331,18	349,61	551,81	309,41	298,94	371,16		143,00	189,00	329,00	323,00	315,00	334,00
249,45	224,76	4,43	113,19	190,03	178,02	11,51	208,72	250,03	233,66		79,00	144,00	93,00	64,00	192,00	192,00
76,13	87,87	11,21	54,47	75,99	112,38	20,60	68,25	76,57	79,72		10,00	20,00	54,00	36,00	62,00	81,00
0,00	1,69	0,46	0,66	0,36	1,57	0,90	0,00	0,00	2,03		2,00	2,00	1,00	1,00	1,00	0,00
41,74	39,74	39,93	42,08	34,57	37,33	36,20	46,86	41,95	47,78		22,00	29,00	39,00	37,00	42,00	39,00
54,29	58,43	12,13	57,28	53,11	57,09	41,82	64,72	55,81	57,15		25,00	33,00	58,00	79,00	54,00	49,00
78,97	88,56	66,16	91,65	76,26	113,47	89,52	78,77	80,59	99,01		61,00	59,00	87,00	77,00	77,00	89,00
2,31	1,59	2,68	3,39	1,91	2,68	1,26	2,46	1,55	2,52		11,00	8,00	2,00	3,00	1,00	2,00
16,32	17,81	23,97	19,40	20,33	19,30	23,51	17,47	17,61	18,66		17,00	16,00	18,00	18,00	19,00	18,00
1,90	3,31	2,36	4,48	5,87	14,10	3,75	4,42	0,00	3,14		16,00	15,00	1,00	3,00	6,00	6,00
12,22	23,74	17,35	15,21	20,30	29,50	16,42	8,26	12,12	17,50		28,00	23,00	16,00	7,00	16,00	24,00

All Remaining Data — New Zealand — Appendix 8

47649	47651	47652	47654	47655	47656	47658	47659	47660	47661	47662	47662	47663	47664	47665	49134	49134
basalt	basalt	basalt	basalt	basalt	basalt	basalt	basalt	basalt	basalt	basalt	basalt	basalt	basalt	basalt	basalt	basalt
This study	This study	This study	This study	This study	This study	This study	This study	This study	This study	This study	This study	This study	This study	This study	This study	This study
48,42	49,51	48,05	50,55	47,64	52,09	48,47	49,43	50,79	43,84	48,50	49,34	48,76	47,46	51,55	44,18	44,18
1,82	1,64	1,64	1,21	0,99	1,07	0,24	1,52	1,09	0,37	1,66	1,61	1,51	2,38	1,57	1,56	1,56
15,00	13,12	15,17	15,23	16,14	13,58	29,30	14,64	15,53	10,49	14,59	14,88	13,96	13,36	14,64	14,07	14,07
11,25	10,15	11,11	10,60	9,22	9,30	1,81	10,92	10,24	9,15	11,69	12,05	11,45	13,28	10,57	13,49	13,49
0,14	0,19	0,19	0,17	0,17	0,15	0,03	0,19	0,17	0,14	0,19	0,21	0,18	0,23	0,17	0,12	0,12
6,46	7,51	6,58	6,00	6,13	6,62	1,21	6,63	6,06	16,41	6,77	7,31	6,42	6,78	5,26	3,82	3,82
10,35	9,97	10,75	8,54	9,81	8,42	14,76	8,70	7,00	11,82	9,47	9,85	8,29	9,87	10,19	4,09	4,09
2,65	2,34	2,76	3,44	2,74	3,94	2,51	4,29	4,08	0,69	3,52	2,41	3,27	2,28	2,41	0,33	0,33
0,15	2,02	0,19	0,40	0,55	0,58	0,03	0,17	1,64	0,01	0,40	0,72	0,96	0,05	0,07	0,65	0,65
0,20	0,20	0,16	0,10	0,08	0,10	0,02	0,17	0,09	0,02	0,20	0,18	0,13	0,26	0,13	0,13	0,13
2,23	1,95	1,36	0,58	1,13	1,16	0,20	0,58	1,07	3,65	0,49	0,49	1,92	3,36	2,23	9,99	9,99
0,68	0,68	1,55	2,52	4,98	2,13	0,99	2,33	1,75	2,81	1,66	1,66	2,30	0,58	0,78	6,26	6,26
99,35	99,28	99,51	99,34	99,57	99,16	99,55	99,57	99,50	99,39	99,14	100,72	99,15	99,90	99,57	98,69	98,69
50,72	51,70	50,25	53,04	51,42	54,80	49,36	51,65	53,02	47,58	50,54	50,60	51,91	50,06	53,90	54,37	54,37
1,91	1,71	1,71	1,27	1,07	1,13	0,24	1,59	1,14	0,40	1,73	1,65	1,61	2,51	1,64	1,92	1,92
15,71	13,70	15,86	15,98	17,42	14,29	29,84	15,30	16,21	11,39	15,20	15,26	14,86	14,09	15,31	17,31	17,31
1,40	1,26	1,38	1,32	1,18	1,16	0,22	1,36	1,27	1,18	1,45	1,47	1,45	1,67	1,31	1,97	1,97
9,35	8,41	9,22	8,83	7,90	7,76	1,46	9,06	8,48	7,88	9,67	9,81	9,67	11,12	8,77	13,18	13,18
0,15	0,20	0,20	0,18	0,18	0,16	0,03	0,20	0,18	0,15	0,20	0,22	0,19	0,24	0,18	0,15	0,15
6,77	7,84	6,88	6,30	6,62	6,96	1,23	6,93	6,33	17,81	7,05	7,50	6,83	7,15	5,50	4,70	4,70
10,84	10,41	11,24	8,96	10,59	8,86	15,03	9,09	7,31	12,83	9,87	10,10	8,83	10,41	10,65	5,03	5,03
2,78	2,44	2,89	3,61	2,96	4,14	2,56	4,48	4,26	0,75	3,67	2,47	3,48	2,41	2,52	0,41	0,41
0,16	2,11	0,20	0,42	0,59	0,61	0,03	0,18	1,71	0,01	0,42	0,74	1,02	0,05	0,07	0,80	0,80
0,21	0,21	0,17	0,10	0,09	0,11	0,02	0,18	0,09	0,02	0,21	0,18	0,14	0,27	0,14	0,16	0,16
100,00	100,00	100,00	100,00	100,01	99,98	100,02	100,00	100,01	100,01	100,00	99,99	100,00	99,99	100,00	100,00	100,00
36,00	85,00	27,00	53,00	47,00	30,00		33,00	80,00	36,00	47,00	47,00	49,00	21,00	29,00	811,00	813,00
2,00	13,00	2,00	5,00	8,00	7,00		3,00	24,00	7,00	2,00	2,00	7,00	0,00	1,00	17,00	17,00
143,00	102,00	147,00	165,00	222,00	141,00		81,00	80,00	242,00	108,00	108,00	155,00	116,00	124,00	993,00	979,00
0,00	0,00	0,00	1,00	0,00	0,00		0,00	0,00	0,00	0,00	0,00	0,00	1,00	0,00	2,00	0,00
156,00	146,00	120,00	79,00	70,00	75,00		124,00	68,00	133,00	145,00	145,00	111,00	195,00	103,00	132,00	129,00
5,00	5,00	4,00	2,00	2,00	2,00		4,00	2,00	5,00	5,00	5,00	3,00	6,00	3,00	3,00	3,00
47,00	47,00	39,00	29,00	25,00	27,00		38,00	28,00	40,00	43,00	43,00	38,00	59,00	40,00	42,00	41,00
344,00	366,00	324,00	321,00	263,00	293,00		315,00	321,00	311,00	325,00	325,00	339,00	383,00	390,00	427,00	425,00
225,00	233,00	211,00	77,00	231,00	256,00		240,00	78,00	256,00	247,00	247,00	123,00	174,00	68,00	17,00	16,00
78,00	59,00	66,00	46,00	63,00	66,00		57,00	52,00	83,00	77,00	77,00	47,00	96,00	43,00	16,00	15,00
0,00	2,00	1,00	0,00	0,00	0,00		0,00	0,00	1,00	0,00	0,00	0,00	0,00	2,00	0,00	0,00
37,00	49,00	40,00	42,00	37,00	42,00		40,00	39,00	39,00	41,00	41,00	36,00	37,00	43,00	42,00	40,00
56,00	39,00	58,00	31,00	40,00	118,00		48,00	68,00	58,00	22,00	22,00	63,00	51,00	50,00	59,00	57,00
92,00	62,00	76,00	84,00	89,00	80,00		80,00	60,00	88,00	86,00	86,00	84,00	114,00	83,00	107,00	106,00
2,00	2,00	3,00	3,00	2,00	2,00		2,00	1,00	2,00	2,00	2,00	2,00	2,00	3,00	2,00	4,00
20,00	17,00	20,00	16,00	20,00	12,00		16,00	17,00	16,00	17,00	17,00	18,00	21,00	20,00	13,00	13,00
6,00	4,00	5,00	2,00	0,00	2,00		3,00	1,00	5,00	4,00	4,00	4,00	7,00	1,00	1,00	1,00
19,00	24,00	16,00	10,00	8,00	13,00		16,00	9,00	16,00	19,00	19,00	14,00	30,00	15,00	7,00	7,00

49112	49121	49135	49162	49180	49138	49158	49172	49193	49193	49195	49127	49189	49116	49117	49136	49177
basalt	basalt	basalt	basalt	basalt	basalt	basalt	basalt	basalt	basalt	basalt	basalt	basalt	basalt	basalt	basalt	basalt
This study	This study	This study	This study	This study	This study	This study	This study	This study	This study	This study	This study	This study	This study	This study	This study	This study
49,78	48,28	46,68	51,40	48,71	49,02	48,95	52,47	47,53	48,77	48,27	47,56	49,08	47,93	48,52	49,11	51,64
1,02	1,40	1,84	1,42	1,69	1,49	1,77	1,61	1,98	1,57	1,49	1,89	1,49	1,65	1,69	1,88	2,10
14,40	14,32	13,84	13,42	13,64	15,43	14,37	14,01	14,63	14,70	14,45	14,42	15,19	14,34	14,46	14,05	15,17
10,63	10,28	11,11	11,94	13,24	9,93	11,09	11,59	11,28	11,63	10,85	12,26	11,14	11,63	11,65	11,39	12,46
0,18	0,19	0,18	0,18	0,21	0,13	0,16	0,17	0,21	0,18	0,21	0,27	0,18	0,18	0,21	0,18	0,23
3,90	5,07	6,34	3,82	6,13	5,34	6,06	3,66	4,85	5,79	6,43	5,22	5,67	6,51	6,98	6,58	3,67
7,23	8,01	10,14	6,97	9,61	10,40	9,70	7,65	8,93	10,29	9,42	9,51	10,36	7,79	10,21	10,51	8,15
2,01	1,41	1,52	2,09	2,47	2,09	2,56	3,01	1,98	3,03	3,95	2,51	3,03	4,58	2,92	2,66	3,44
0,43	0,43	0,57	0,33	0,12	0,06	0,13	0,30	0,34	0,26	0,28	0,27	0,41	0,31	0,22	0,12	0,11
0,10	0,14	0,20	0,12	0,14	0,13	0,17	0,17	0,23	0,14	0,14	0,14	0,12	0,15	0,16	0,21	0,27
5,05	4,34	3,61	3,52	3,45	3,22	3,05	2,75	2,31	1,93	1,90	1,89	1,83	1,81	1,75	1,75	1,74
4,69	5,07	3,80	3,71	0,67	1,90	1,53	2,56	5,44	1,83	2,86	3,41	1,93	2,67	0,88	1,16	1,45
99,42	98,94	99,83	98,91	100,07	99,14	99,54	99,95	99,71	100,12	100,24	99,35	100,44	99,57	99,66	99,61	100,43
56,09	54,47	51,04	56,71	51,39	52,62	52,08	56,04	52,25	51,15	51,06	51,15	51,28	50,95	50,54	51,31	53,71
1,15	1,58	2,01	1,57	1,78	1,60	1,88	1,72	2,18	1,65	1,58	2,03	1,56	1,75	1,76	1,96	2,18
16,23	16,16	15,13	14,81	14,39	16,56	15,29	14,96	16,08	15,42	15,29	15,51	15,87	15,24	15,06	14,68	15,78
1,42	1,38	1,45	1,57	1,66	1,27	1,40	1,47	1,47	1,45	1,37	1,57	1,38	1,47	1,44	1,42	1,54
9,51	9,21	9,64	10,46	11,09	8,46	9,36	9,82	9,84	9,68	9,11	10,46	9,24	9,81	9,63	9,45	10,28
0,20	0,21	0,20	0,20	0,22	0,14	0,17	0,18	0,23	0,19	0,22	0,29	0,19	0,19	0,22	0,19	0,24
4,39	5,72	6,93	4,21	6,47	5,73	6,45	3,91	5,33	6,07	6,80	5,61	5,92	6,92	7,27	6,88	3,82
8,15	9,04	11,09	7,69	10,14	11,16	10,32	8,17	9,82	10,79	9,96	10,23	10,82	8,28	10,63	10,98	8,48
2,26	1,59	1,66	2,31	2,61	2,24	2,72	3,21	2,18	3,18	4,18	2,70	3,17	4,87	3,04	2,78	3,58
0,48	0,49	0,62	0,36	0,13	0,06	0,14	0,32	0,37	0,27	0,30	0,29	0,43	0,33	0,23	0,13	0,11
0,11	0,16	0,22	0,13	0,15	0,14	0,18	0,18	0,25	0,15	0,15	0,15	0,13	0,16	0,17	0,22	0,28
100,00	100,00	100,00	100,01	100,01	100,00	100,00	100,00	100,00	100,00	100,01	100,00	99,99	99,98	99,99	99,99	100,00
99,00	48,00	115,00	67,00	29,45	28,00	15,00	38,14	125,03	23,70	31,86	184,00	33,47	408,00	269,00	34,00	283,86
11,00	6,00	8,00	9,00	2,31	1,00	3,00	4,24	4,74	4,04	6,66	4,00	6,78	3,00	2,00	3,00	1,61
162,00	255,00	457,00	145,00	107,02	134,00	127,00	126,99	199,84	161,19	112,59	375,00	118,00	144,00	182,00	147,00	348,15
1,00	0,00	1,00	1,00	-0,64	0,00	1,00	-0,70	0,38	1,46	0,16	0,00	0,63	0,00	1,00	1,00	0,67
72,00	114,00	164,00	100,00	109,90	113,00	135,00	115,84	172,67	106,13	104,37	115,00	96,07	113,00	116,00	160,00	184,71
2,00	3,00	5,00	2,00	2,39	3,00	3,00	3,59	5,16	2,77	2,53	2,00	2,56	4,00	5,00	5,00	5,44
26,00	38,00	47,00	34,00	42,90	59,00	48,00	40,85	49,25	37,16	36,29	42,00	36,54	41,00	39,00	47,00	53,81
301,00	311,00	320,00	363,00	371,02	367,00	363,00	377,56	348,69	379,55	311,95	364,00	380,84	340,00	346,00	339,00	349,53
43,00	133,00	210,00	21,00	93,28	132,00	130,00	7,52	54,95	118,57	170,33	74,00	93,87	193,00	214,00	227,00	5,34
24,00	47,00	74,00	16,00	61,06	29,00	75,00	7,89	37,09	45,96	54,89	44,00	39,50	71,00	69,00	83,00	6,41
0,00	0,00	0,00	0,00	0,65	0,00	0,00	0,14	-0,11	1,38	-0,76	2,00	1,98	1,00	0,00	0,00	1,11
36,00	45,00	39,00	38,00	35,39	43,00	35,00	31,80	38,57	37,48	38,41	36,00	39,63	44,00	46,00	41,00	31,95
75,00	49,00	55,00	48,00	53,35	62,00	52,00	40,99	49,04	51,89	56,95	11,00	51,22	57,00	60,00	51,00	43,34
84,00	83,00	94,00	101,00	97,64	96,00	90,00	96,85	97,81	87,08	75,88	45,00	86,16	86,00	89,00	89,00	111,15
3,00	2,00	2,00	4,00	2,47	2,00	2,00	1,19	2,84	2,90	3,30	2,00	1,38	2,00	3,00	2,00	2,86
15,00	16,00	17,00	18,00	19,31	19,00	19,00	19,77	17,35	19,40	18,09	20,00	18,43	17,00	21,00	21,00	21,96
2,00	5,00	4,00	3,00	1,51	3,00	5,00	3,70	5,79	1,36	4,11	2,00	3,02	4,00	2,00	4,00	5,96
7,00	15,00	25,00	11,00	13,94	12,00	21,00	15,11	23,16	17,11	14,84	17,00	16,22	12,00	17,00	17,00	26,25

49126	49163	49192	49178	49174	49181	49172	49171	49193	49170	49182	49182	49159	49188	49125	49185	49187
basalt	basalt	basalt	basalt	basalt	basalt	basalt	basalt	basalt	basalt	basalt	basalt	basalt	basalt	basalt	basalt	basalt
This study	This study	This study	This study	This study	This study	This study	This study	This study	This study	This study	This study	This study	This study	This study	This study	This study
49,39	50,29	48,11	49,58	52,42	47,91	52,23	53,66	48,31	47,75	49,32	50,65	53,15	49,27	51,88	48,75	51,17
1,91	1,04	1,48	0,93	1,77	1,09	1,63	0,97	2,03	1,32	1,41	1,08	2,06	1,88	2,83	3,01	1,40
15,36	14,64	14,53	15,73	14,95	18,18	14,19	15,12	14,96	14,15	17,01	15,58	14,53	15,19	13,54	13,52	14,81
11,75	10,27	11,00	9,48	9,73	8,80	11,96	7,29	11,60	10,86	11,98	9,60	12,94	12,75	14,62	15,68	10,58
0,22	0,16	0,19	0,16	0,18	0,15	0,21	0,14	0,19	0,20	0,19	0,16	0,19	0,20	0,25	0,24	0,18
4,69	6,54	6,59	6,01	5,50	5,55	3,69	4,63	5,23	7,66	4,28	7,00	4,26	5,61	4,18	5,01	6,93
9,23	7,27	7,75	6,56	9,46	11,42	7,63	9,76	9,97	10,31	9,94	10,61	8,20	10,20	7,99	7,48	10,97
2,82	4,87	5,77	5,97	3,07	2,53	3,03	2,37	2,79	2,39	3,24	2,64	3,22	2,77	3,47	4,17	1,43
0,14	0,19	0,08	0,30	0,12	0,61	0,79	0,41	0,31	0,34	1,14	0,19	0,14	0,18	0,11	0,22	0,07
0,16	0,10	0,16	0,08	0,21	0,10	0,17	0,08	0,24	0,10	0,33	0,10	0,21	0,20	0,19	0,35	0,13
1,63	1,62	1,62	1,52	1,46	1,44	1,34	1,32	1,05	0,95	0,59	0,49	0,40	0,39	0,20	0,20	0,20
2,59	3,05	2,87	3,70	1,07	2,50	3,15	4,70	3,53	3,72	0,59	1,86	0,20	1,57	0,10	1,38	1,28
99,90	100,05	100,14	100,03	99,93	100,28	100,01	100,44	100,21	99,76	100,00	99,94	99,50	100,20	99,35	100,02	99,13
52,18	53,23	50,81	52,76	54,29	50,13	55,28	57,22	51,06	50,72	50,44	52,35	54,36	50,73	53,06	50,22	52,90
2,02	1,10	1,56	0,99	1,83	1,14	1,73	1,03	2,15	1,40	1,44	1,12	2,11	1,94	2,89	3,10	1,45
16,23	15,49	15,35	16,74	15,48	19,02	15,02	16,12	15,81	15,03	17,40	16,10	14,86	15,64	13,85	13,93	15,31
1,48	1,29	1,38	1,20	1,20	1,10	1,51	0,92	1,46	1,37	1,46	1,18	1,57	1,56	1,78	1,92	1,30
9,85	8,63	9,22	8,01	8,00	7,31	10,05	6,17	9,73	9,16	9,72	7,87	10,50	10,42	11,87	12,82	8,68
0,23	0,17	0,20	0,17	0,19	0,16	0,22	0,15	0,20	0,21	0,19	0,17	0,19	0,21	0,26	0,25	0,19
4,95	6,92	6,96	6,39	5,70	5,81	3,91	4,94	5,53	8,14	4,38	7,24	4,36	5,78	4,28	5,16	7,16
9,75	7,69	8,18	6,98	9,80	11,95	8,08	10,41	10,54	10,95	10,17	10,97	8,39	10,50	8,17	7,71	11,34
2,98	5,15	6,09	6,35	3,18	2,65	3,21	2,53	2,95	2,54	3,31	2,73	3,29	2,85	3,55	4,30	1,48
0,15	0,20	0,08	0,32	0,12	0,64	0,84	0,44	0,33	0,36	1,17	0,20	0,14	0,19	0,11	0,23	0,07
0,17	0,11	0,17	0,09	0,22	0,10	0,18	0,09	0,25	0,11	0,34	0,10	0,21	0,21	0,19	0,36	0,13
99,99	99,99	100,01	99,99	100,01	100,00	100,01	100,01	100,00	99,99	100,02	100,02	100,00	100,01	100,01	99,99	100,02
62,00	40,00	20,10	95,46	44,01	71,08	88,12	58,56	67,76	46,48	564,52	35,47		36,46	42,00	57,15	38,95
2,00	2,00	3,09	3,54	0,60	10,15	15,34	4,41	2,69	4,77	24,80	2,51		1,75	0,00	3,03	0,88
194,00	67,00	31,60	77,73	134,77	181,78	129,23	252,21	155,52	127,78	413,04	142,53		167,44	127,00	191,84	143,86
0,00	0,00	-0,09	-0,60	-0,12	-0,44	1,31	0,72	0,26	-0,91	5,36	-0,60		0,78	0,00	0,87	0,24
113,00	80,00	116,35	55,53	151,36	69,71	115,31	68,16	173,90	75,13	128,15	72,98		133,90	165,00	221,06	98,29
2,00	2,00	3,49	2,14	4,32	1,90	3,37	1,57	5,26	2,18	7,72	2,15		4,08	3,00	6,14	3,03
44,00	30,00	38,04	23,42	42,64	25,80	40,11	23,74	49,95	28,85	32,06	28,37		46,34	60,00	67,52	35,47
332,00	285,00	307,11	299,67	321,77	276,02	373,03	245,34	350,19	318,36	364,64	291,05		378,60	418,00	470,97	295,72
47,00	139,00	215,49	96,54	116,51	132,46	16,02	69,33	54,36	289,45	35,13	189,32		31,37	2,00	20,39	257,75
29,00	55,00	60,73	43,15	48,58	45,33	9,46	44,41	36,97	113,63	29,39	78,59		31,05	7,00	32,10	96,54
1,00	0,00	1,02	-0,61	0,49	0,25	-0,89	-0,35	1,32	0,93	1,99	0,94		1,57	1,00	1,93	0,65
38,00	32,00	36,85	34,60	35,81	27,03	35,79	30,67	36,61	37,45	28,45	35,71		40,93	40,00	41,56	37,04
11,00	72,00	54,75	7,13	13,60	58,29	41,86	50,44	49,88	59,88	141,65	62,95		45,95	9,00	18,55	74,34
49,00	71,00	82,56	47,72	71,97	55,75	97,04	64,82	99,29	78,74	88,46	71,09		103,38	77,00	109,54	78,34
2,00	2,00	2,55	1,95	2,32	1,54	2,91	2,79	1,92	2,27	6,61	2,85		1,34	2,00	1,94	2,64
21,00	17,00	19,49	15,24	19,26	18,28	18,70	12,88	19,32	15,48	21,94	16,48		20,41	24,00	22,82	18,89
3,00	1,00	4,84	2,47	3,76	1,66	3,31	1,75	4,85	1,41	18,97	2,74		2,96	3,00	7,95	5,30
15,00	11,00	19,84	3,85	19,55	12,92	16,42	9,27	22,16	11,49	36,54	9,56		15,80	26,00	29,12	13,33

Sample#	49220	49222	49225	49229	49223	49237	49239	49241	49242	49245	49251	49252	49253	49259
rock type	basalt	basalt	basalt	basalt	basalt	basalt	basalt	alk-dolerite	basalt	basalt	basalt	basalt	basalt	basalt
location	Poya terrane	Poya terrane	Poya terrane	Poya terrane	Poya terrane	Poya terrane	Poya terrane	Poya terrane	Poya terrane	Poya terrane	Poya terrane	Poya terrane	Poya terrane	Poya terrane
wt.%														
SiO2	49,07	48,20	47,50	48,07	48,33	48,44	48,38	47,04	49,37	48,15	48,60	48,11	50,34	50,01
TiO2	1,36	1,45	1,31	1,27	1,25	1,24	1,34	3,09	1,71	1,30	1,35	1,31	1,25	1,67
A1203	13,91	14,36	15,33	13,48	13,11	13,86	13,94	11,90	13,63	13,84	16,61	13,72	15,04	14,72
Fe203	11,99	11,55	10,94	11,57	11,38	12,17	12,50	19,36	12,61	12,57	9,61	12,63	9,57	12,36
MnO	0,21	0,24	0,25	0,17	0,17	0,20	0,23	0,39	0,21	0,19	0,16	0,20	0,16	0,16
MgO	7,79	6,85	7,50	6,30	6,28	7,83	7,92	5,41	6,74	7,55	5,80	7,33	8,03	8,15
CaO	9,35	12,24	10,69	12,91	14,87	10,56	10,76	7,62	11,13	9,69	11,25	10,94	8,50	6,41
Na20	2,78	2,14	3,24	2,88	0,88	2,84	2,48	3,04	2,72	3,00	3,11	2,39	3,49	2,98
K20	0,78	0,19	0,92	0,03	0,01	0,68	0,12	0,18	0,37	0,86	0,16	0,18	0,72	3,33
P205	0,12	0,12	0,14	0,12	0,11	0,10	0,10	0,26	0,14	0,10	0,13	0,11	0,10	0,15
LOI	0,39	0,39	0,20	0,29	0,19	0,29	0,29	0,10	0,39	0,29	1,16	0,68	0,19	0,10
%H2O	1,95	1,95	2,05	2,90	3,65	2,15	2,05	1,67	1,28	2,72	2,13	2,52	3,10	0,10
Total	99,70	99,68	100,07	100,00	100,23	100,36	100,12	100,05	100,31	100,26	100,07	100,12	100,48	100,14
Recalculated to 100% using Fe2O3/FeO = 0.15														
SiO2	50,95	50,04	49,04	50,18	50,66	50,01	50,04	48,70	50,62	50,08	50,66	50,21	52,25	50,59
TiO2	1,41	1,51	1,35	1,33	1,31	1,28	1,39	3,20	1,75	1,35	1,41	1,37	1,30	1,69
Al2O3	14,44	14,91	15,83	14,07	13,74	14,31	14,42	12,32	13,97	14,39	17,31	14,32	15,61	14,89
Fe2O3	1,48	1,43	1,34	1,44	1,42	1,49	1,54	2,38	1,54	1,56	1,19	1,57	1,18	1,49
FeO	9,88	9,52	8,96	9,59	9,47	9,97	10,26	15,91	10,26	10,38	7,95	10,46	7,88	9,92
MnO	0,22	0,25	0,26	0,18	0,18	0,21	0,24	0,40	0,22	0,20	0,17	0,21	0,17	0,16
MgO	8,09	7,11	7,74	6,58	6,58	8,08	8,19	5,60	6,91	7,85	6,05	7,65	8,33	8,24
CaO	9,71	12,71	11,04	13,48	15,59	10,90	11,13	7,89	11,41	10,08	11,73	11,42	8,82	6,48
Na2O	2,89	2,22	3,34	3,01	0,92	2,93	2,56	3,15	2,79	3,12	3,24	2,49	3,62	3,01
K2O	0,81	0,20	0,95	0,03	0,01	0,70	0,12	0,19	0,38	0,89	0,17	0,19	0,75	3,37
P2O5	0,12	0,12	0,14	0,13	0,12	0,10	0,10	0,27	0,14	0,10	0,14	0,11	0,10	0,15
Total	100,00	100,00	100,00	99,99	100,00	100,00	99,99	100,01	99,99	100,00	100,00	100,00	100,01	100,00

Sample#	49220	49222	49225	49229	49223	49237	49239	49241	49242	49245	49251	49252	49253	49259
rock type	basalt	basalt	basalt	basalt	basalt	basalt	basalt	alk-dolerite	basalt	basalt	basalt	basalt	basalt	basalt
location	Poya terrane	Poya terrane	Poya terrane	Poya terrane	Poya terrane	Poya terrane	Poya terrane	Poya terrane	Poya terrane	Poya terrane	Poya terrane	Poya terrane	Poya terrane	Poya terrane
Traces elements (ppm)														
Ba	1983,03	118,70	63,50	26,49	13,38	121,84	143,52	49,47	54,98	55,21	6,17	33,67	55,37	392,63
Rb	12,61	2,19	13,20	0,48	0,11	12,08	24,10	1,52	3,70	0,63	3,30	2,22	15,21	86,34
Sr	201,00	125,38	85,38	55,86	39,93	200,19	427,35	147,97	164,14	113,69	260,73	181,94	75,17	40,09
Ta	0,38	0,30	0,18	0,33	0,31	0,36	0,37	0,69	0,38	0,35	0,18	0,32	0,27	0,37
Th	0,40	0,30	0,07	0,33	0,30	0,37	0,39	0,66	0,34	0,35	0,13	0,32	0,28	0,39
Zr	67,65	66,61	31,57	76,56	74,45	64,72	74,67	179,01	95,00	59,56	91,59	57,03	66,93	85,50
Nb	5,32	3,91	1,95	4,30	3,84	5,15	5,56	9,52	5,01	4,67	2,35	4,41	3,76	5,30
Y	23,21	23,72	24,44	26,26	24,93	25,27	31,30	50,97	30,89	21,99	30,51	24,95	19,96	26,37
Hf	1,88	1,93	1,32	2,02	2,01	1,82	2,07	4,88	2,59	1,66	2,40	1,70	1,94	2,46
V	376,09	356,14	267,85	314,77	296,45	336,71	341,77	439,51	376,43	350,18	286,71	365,34	277,57	330,38
Cr	176,60	255,39	377,68	294,45	282,02	213,53	182,06	1,63	19,33	175,55	211,49	184,75	298,59	256,14
Ni	78,89	83,58	99,70	89,07	74,72	100,58	94,18	20,03	36,85	94,98	73,09	99,02	126,53	91,41
Co	46,48	51,41	49,95	57,94	55,76	54,36	59,07	54,63	49,52	45,82	48,57	51,88	46,64	48,05
U	0,11	0,09	0,07	0,11	0,08	0,10	0,10	0,19	0,10	0,10	0,06	0,08	0,14	0,13
Sc	48,98	50,91	47,10	54,12	48,83	48,97	46,19	38,47	46,07	49,39	40,29	55,35	34,62	39,05
Cu	138,36	131,50	29,81	62,53	120,99	147,26	162,17	112,24	140,02	150,23	62,71	203,95	120,59	145,33
Zn	75,35	136,97	68,43	83,96	73,90	79,03	94,92	145,18	86,34	76,86	72,51	95,11	67,09	86,28
Pb	0,59	1,68	0,51	2,55	1,01	2,22	0,66	0,49	0,77	1,18	0,56	3,01	0,92	0,66
Ga	19,56	19,28	14,60	16,03	20,33	16,80	17,45	28,14	19,40	17,30	18,14	17,38	15,25	16,34
Cs	0,39	0,32	0,50	0,13	0,28	0,43	1,98	0,09	0,07	0,03	0,10	0,25	0,63	3,56
La	4,59	4,28	2,78	5,02	4,08	4,52	4,71	9,08	5,13	3,93	2,98	3,87	3,49	5,21
Ce	11,70	10,94	8,60	12,75	11,04	11,60	12,53	25,53	14,10	10,12	9,66	10,06	9,91	15,12
Pr	1,71	1,68	1,45	1,90	1,73	1,74	1,94	3,95	2,21	1,50	1,66	1,59	1,58	2,35
Nd	8,25	8,26	7,61	9,28	8,69	8,41	9,52	19,53	10,95	7,25	8,74	7,85	7,97	11,68
Sm	2,54	2,59	2,59	2,83	2,75	2,56	3,05	5,88	3,46	2,25	2,96	2,53	2,50	3,49
Eu	0,94	1,10	1,03	1,06	1,04	1,00	1,20	2,06	1,32	0,88	1,15	1,00	1,02	1,36
Gd	5,18	3,36	3,40	3,56	3,43	3,40	4,06	7,34	4,38	2,94	3,95	3,32	3,05	4,52
Tb	0,58	0,60	0,62	0,65	0,63	0,61	0,74	1,33	0,78	0,53	0,74	0,61	0,54	0,73
Dy	3,81	3,88	4,01	4,10	4,01	3,98	4,84	8,44	5,04	3,52	4,87	4,08	3,45	4,65
Ho	0,83	0,86	0,88	0,89	0,86	0,87	1,06	1,82	1,09	0,77	1,07	0,88	0,73	0,95
Er	2,37	2,42	2,45	2,52	2,45	2,50	3,05	5,10	3,02	2,20	3,03	2,54	2,03	2,63
Tm														
Yb	2,26	2,28	2,26	2,34	2,29	2,35	2,87	4,77	2,80	2,07	2,84	2,36	1,84	2,30
Lu	0,35	0,36	0,34	0,35	0,34	0,36	0,43	0,72	0,42	0,32	0,43	0,36	0,27	0,33

Sample#	49112	49117	49121	49135	49162	49164	49172	49193	49201	49219
V-SMOW	6,4	6,4	6,4	6	6,2	6,5	6,1	6	5,7	6,4
duplicates	6,2		6,3	6						

ANALYTICAL METHODS

Oxygen isotopic analyses of Tangihua Comples glasses were done at the Institute of Geological and Nuclear Sciences, Wellington, New Zealand by Dr. K. Faure.

Prior to extraction of oxygen, samples and standards were placed in an oven for 48 hours at 150'C to remove absorebed and loosely bound water. Samples, still hot, were quickly places in the sample chamber and evacualted to minimize re-aborbtion of moisture. Oxygen was extracted from the glass using a CO2 laser and BrF5, similar to the method discribed by Sharp (1990). Samples were left over night in a BrF5 atmosphere (5 kpa) and then pre-treated repeatedly with BrF5, prior to extraction, until CO2 blank values were <0.1 micromoles. All sampples were normalised to the quartz standard NBS 28 (assuming a value of +9.6") with one standard analyzed for every four samples. All values are reported relative to VSMOW and reproducibility is generally better than 0.2".

Sample#	49211 arc	49164 glass	49183 bab	49186 bab	47648 bab	47662 bab
87/86 Sr	0,703611	0,702993	0,703197	0,703489	0,702951	0,702683
err.	0,00002	0,000011	0,00001	0,000011	0,000012	0,00001
143/144 Nd	0,513059	0,513052	0,513062	0,513057	0,513064	0,513043
err.	0,000008	0,000005	0,000007	0,000007	0,000008	0,000007
ENd	0,80563673	0,79783395	0,8134395	0,80368603	0,8153902	0,77637631

*** All data corrected to 85 Ma

ANALYTICAL METHODS

The preperation for radiogenic isotope analyses was done at the Institut Dolomieu, LGCA, Universite Joseph Fourier, France. The analyses were done at the Universite de Toulousse, France.

Approximately 0.1g of powdered sample was firstly leached in acid to remove alteration products and then attacked using HCl and Hf to isolate the trace and rare earth elements. Secondly the samples were put through seperation columns to isolate Sr and Nd. Sr seperation required the addition of 4N, 1.5N and 6N HCl, H2O and amonium citrate, which isolates both Sr and Rb, a second column (μSr) used 1.5N HCl to eliminate Rb. A separate column was used to separate Nd, which used 0.3N HCl.

$^{40}Ar/^{36}Ar$ Dating Methods

$^{40}Ar/^{36}Ar$ dating on whole rock and plagioclase separates was carried out at the University of Michigan, USA, by Dr. C. Hall. The samples were irradiated for 30 hr in location L67 of the Phoenix-ford Memorial reactor. All ages are calculated relative to interlaboratory standard MMHb-1 with an assumed K-Ar age of 520.4 Ma (Samson and Alexander, 1987). Samples totalling about 0.5-1 mg were placed in individual 2 mm diameter wells in a copper tray and step-heated for 60 seconds using a defocussd Coherent INNOVA model 70 continuous Ar ion laser with a maximum power output of 5 W. Ar isotopes were measured with a VG1200S mass spectrometer and all analyses were performed using a Daly detector in analog mode with an effective gain of approximately 10^4. Mass discrimination was monitored daily by measuring the $^{40}Ar/^{36}Ar$ ratio of about 4.5×10^{-9} mlSTP of atmospheric Ar. Fusion system blanks were subtracted from all sample gas fractions and blanks were monitored frequently, typically every fifth sample fraction. Typical blank values at masses 36 to 40 were $1x10^{-13}$, $1.3x10^{-13}$, $5x10^{-14}$, $1x10^{-13}$, and $5x10^{-12}$ mlSTP respectively.

RESUME

De nouvelles données analytiques en éléments majeurs, en éléments traces et en isotopes des laves basaltiques du Complexe ophiolitique de Tangihua (Nouvelle Zélande) sont présentées afin de développer un nouveau modèle sur la genèse de ce complexe et une nouvelle interprétation de l'évolution tectonique de la Nouvelle Zélande au Crétacé.

L'essentiel du complexe de Tangihua est constitué par des formations volcaniques d'affinité tholéiitique à calco-alcaline. Le plagioclase (An66-87) est le minéral primaire le plus fréquent suivi du clinopyroxène (En31-52 Fs10-33 Wo 28-45, Mg# = 61), de l'orthopyroxène et de la magnétite. L'olivine, la biotite et la hornblende sont rares. Les assemblages minéralogiques issus des altérations de basse température correspondent à trois phases : une phase initiale marquée par la précipitation de zéolites sodiques, une phase transitoire riche en zéolites potasiques, sodiques et calciques, et une phase de très basse température (T<50°C) potassique et calcique. Les schémas d'altération dans le complexe de Tangihua suggèrent qu'entre la formation de l'ophiolite et son obduction, l'activité tectonique était faible ou inexistante, ce qui a permis le développement de l'altération océanique. Les datations par la méthode $^{40}Ar/^{39}Ar$ confirment la formation de l'ophiolite vers 100 Ma et révélent un épisode majeur d'altération vers 30 Ma qui probablement correspond à l'âge de l'obduction du complexe.

Chimiquement, les laves montrent un continuum entre des signatures d'arc et arrière-arc avec des teneurs déprimées en Nb et éléments HFS. Les laves arrière-arc résultent d'une source déprimée et de liquides ayant subit au moins 35% de cristallisation fractionnée, tandis que les laves d'arc résultent d'une source encore plus déprimée et de liquides ayant subit au moins 30% de cristallisation fractionnée. Les rapports élevés LILE/HFSE et LILE/REE suggèrent un enrichissement en LILE par un fluide acqueux lié à la croûte subductée et peut être aussi à des matériaux siliceux fondus.

Les teneurs en éléments traces et les rapports isotopiques $^{87}Sr/^{86}Sr$ et $^{143}Nd/^{144}Nd$ sont typiques des systèmes d'arcs et d'arrière-arcs rencontrés dans le Pacifique SW. Par contre, en Nouvelle Calédonie, l'Unité de Poya qui a longtemps été considérée de même nature (mêmes caractéristiques lithologiques, même âge de formation 80-85 Ma) est en réalité différente du point de vue géochimique révélant une histoire tectonique différente pour ces deux complexes.

La combinaison des contraintes géochimiques et tectoniques suggèrent que le complexe de Tangihua s'est formé soi dans une zone transitionnelle arc - bassin arrière-arc, soit dans une zone de passage entre un volcanisme d'arc et un volcanisme arrière arc. La fin du Crétacé-supérieur, marquée par la fragmentation des marges Est et Sud du Gondwana, a vu le rapprochement et la collision naissante de la dorsale en expansion entre les plaques de Phoenix et du Pacifique. La plaque de Phoenix, petite, légère et ayant à l'origine subi une subduction, a été capturée par la plaque Pacifique, initiant ainsi le rifting entre la plaque Phoenix-Pacifique nouvellement formée, et celle de l'Antarctique W. La mise en place de la dorsale Phoenix-Pacifique et du système de subduction associé, conjugués à l'initiation du rifting dans la mer de Tasman, ont eu pour effet la subduction et la déshydratation partielles de portions de la plaque de Phoenix qui alors ont réagi avec le coin mantellique précédemment déprimé. Le complexe de Tongihua est une des conséquences de tels processus.

ABSTRACT

New major oxide, trace element and isotopic analyses of basaltic lavas from the Tangihua Complex ophiolite, Northland, New Zealand, have led to the development of a new model explaining its generation and a new interpretation of the tectonic setting of New Zealand during the Cretaceous.

The Tangihua Complex basalts are relatively homogeneous, differentiated (Mg#<45) and dominantly tholeiitic with lesser calc-alkaline and minor alkaline affinities. The primary phenocryst assemblage is dominated by plagioclase (An66-87) with lesser amounts of clinopyroxene (En31-52Fs10-33Wo28-45; Mg#=61), orthopyroxene and magnetite whereas olivine, biotite and hornblende are rare.

The pervasive, low-temperature alteration assemblage can be divided into three main phases : an initial phase of Na-rich zeolite precipitation, followed by a transitional cooling phase, characterised by K-, Na- and Ca-rich zeolites, and finally, at <50°C, a period of K- and Ca-dominated alteration. The alteration patterns in the Tangihua Complex suggests that little or no tectonic activity occurred between formation and obduction, enabling a classic seafloor alteration sequence to develop. New 40Ar/39Ar dates from the Tangihua Complex confirm their age of formation is most likley ±100Ma and they have suffered a major episode of alteration at ±30Ma, which most likely corresponds to the age of emplacement of the Northland Allochthon.

Unusually, the lavas reveal a continuum between arc and back-arc chemistries, with a depletion of Nb and HFSE suggesting derivation from a depleted mantle source. Geochemical modelling shows the back-arc lavas have undergone (35% fractional crystallisation of a source depleted by (2-3% and the arc lavas have undergone (30% fractional crystallisation of a source depleted by less than 5%. High LILE/HFSE and LILE/LREE ratios suggest LILE enrichment by a slab-related aqueous fluid and possibly small amounts of a slab-derived silicic melt. The trace element contents and 87Sr/86Sr and 143Nd/144Nd ratios of the Tangihua Complex are typical of arc and back-arc systems found within the SW Pacific. The Poya terrane ophiolite of New Caledonia is the geographically closest ophiolite complex of a similar age to the Tangihua Complex but despite many similarities between the systems, close inspection of the alteration and geochemistry show that the systems are unrelated.

The combined geochemistry and tectonic constraints suggest that the Tangihua Complex formed either in a transitional zone between an arc and a back-arc setting, or in a zone of migration from arc to back-arc volcanism. The end of the Late Cretaceous, and the break-up of the eastern and southern Gondwana margin, saw the approach and incipient collision of the spreading ridge between the Phoenix and Pacific plates. Initially subducted, the small, buoyant, Phoenix plate was captured by the Pacific plate, which led to the initiation of rifting between the newly formed Phoenix-Pacific plate and West Antarctica. Stalling of the Phoenix-Pacific ridge and associated subduction system, in combination with the initiation of rifting in the Tasman Sea, resulted in the partial subduction and dehydration of portions of the Phoenix Plate, which then reacted with the previously depleted mantle wedge. Remnants of the ensuing volcanism include the obducted Tangihua Complex of Northland.

BIBLIOTHÈQUE SCIENCES GRENOBLE UNIVERSITAIRE